VAPOUR-LIQUID EQUILIBRIA AND INFINITE DILUTION ACTIVITY COEFFICIENT MEASUREMENTS OF SYSTEMS INVOLVING DIKETONES

Minal Soni

University of Natal – Durban

2003

Submitted in fulfilment of the academic requirements for the degree Master of Science in Chemical Engineering. All the work presented in this dissertation is original unless otherwise stated and has not (in whole or part) been submitted previously to any tertiary institute as part of a degree.

As the candidate's supervisor, I approve this dissertation for submission

---

Prof. D Ramjugernath

As the candidate's co-supervisor, I approve this dissertation for submission

---

Prof. JD Raal

The financial assistance of the National Research Foundation (NRF) towards this research is hereby acknowledged. Opinions expressed and conclusions arrived at, are those of the author and not necessarily to be attributed to the NRF.

ABSTRACT

Acetylpropionyl (2,3-pentanedione) and diacetyl (2,3-butanedione) are by-products of sugar manufacture. Both diketones have many uses, mainly food related. Vapour-liquid equilibrium data and infinite dilution activity coefficients are required to design purification processes for these chemicals. A review of available experimental methods revealed that the vapour and liquid recirculating still is most appropriate when both isobaric and isothermal VLE are required. The low-pressure dynamic still of Raal and Mühlbauer (1998) used in this study incorporates many features to ensure that measurements are of excellent quality (as demonstrated by Joseph et al., 2001). VLE measurements were made for the following systems:

- Acetone with diacetyl at 30 °C, 40 °C, 50 °C and 40 kPa
- Methanol with diacetyl at 40 °C, 50 °C, 60 °C and 40 kPa
- Diacetyl with 2,3-pentanedione at 60 °C, 70 °C, 80 °C and 40 kPa
- Acetone with 2,3-pentanedione at 50 °C, 30 kPa and 40 kPa

All the systems, except for methanol with diacetyl, displayed close to ideal behaviour. This was expected as they are mixtures of ketones.

Solution thermodynamics allows one to perform data reduction of the measured VLE data to ensure accurate extrapolation and interpolation of the measurements. Furthermore, the quality of the data can be judged using thermodynamic consistency tests. The data were represented by the Gamma-Phi approach to VLE (the preferred method for low-pressure VLE computations). The two-term virial equation of state was used to account for vapour phase non-ideality. Second virial coefficients were calculated by the method of Hayden and O' Connell (1975). The liquid phase non-ideality was accounted for by the Wilson, NRTL or UNIQUAC models.

The best fit models are proposed for each system, as are parameters as functions of temperature for the isobaric data. The data were judged to be of high thermodynamic consistency by the stringent point test (Van Ness and Abbott, 1982) and the direct test (Van Ness, 1995) for thermodynamic consistency. The data sets were rated, at worst, "3" on the consistency index proposed by Van Ness (1995). A rating of "1" is given for a perfectly consistent data set and "10" for an unacceptable data set. For the system acetone with 2,3-pentanedione, isobars at 30 kPa and 40 kPa were measured. The results from the reduction of the 30 kPa set were used to accurately predict the 40 kPa data set.

Infinite dilution activity coefficients were measured by the inert gas stripping method (based on the principle of exponential dilution). In order to specify the appropriate dilutor flask height (to ensure equilibrium is achieved), mass transfer considerations were made. These computations ensured that the gas phase was in equilibrium with the liquid phase at the gas exit point. The following infinite dilution activity coefficients were measured:

- Acetone in diacetyl at 30 °C
- Methanol in diacetyl at 40 °C
- Diacetyl in 2,3-pentanedione at 60 °C
- Acetone in 2,3-pentanedione at 50 °C

The ketone mixtures, once again, displayed close to ideal behaviour.

ACKNOWLEDGEMENTS

I wish to thank the following people for their contribution to my work:

- My supervisor, Professor Deresh Ramjugernath, who was undeterred by a mediocre undergraduate student. The opportunities he has provided for me to learn, have prepared me for my future endeavours, which he is responsible for as well.
- My co-supervisor Professor JD Raal. His generosity with his time, wealth of knowledge and his enthusiasm for my work were most appreciated.
- My parents, Shanta and Vijay. As with so much in my life, my post-graduate studies were only possible through their selfless sacrifices, support and encouragement.
- Prathieka, Roger and Kasuren. Their invaluable contributions to my work are as appreciated as their friendship.
- My colleagues and friends Scott, Tyrone, Warren, Yash, Alex, Ildephonse, Ranjeetha, Natasha, Nick and the rest of the School of Chemical Engineering post-graduate students.
- The staff at the School of Chemical Engineering workshop, in particular Mr. Les Henwood for his expertise and patience.
- Glassblower, Peter Siegling, for constructing the dynamic VLE still and dilutor flask used in this study.
- My friends and family. Their support and assistance will not be forgotten.
- Illovo, for generously supplying the diacetyl and 2,3-pentanedione used in this work.
- The National Research Foundation (NRF), for funding this project.
- NRF and Sasol, for financial assistance in 2002 and 2003 (respectively).

CONTENTS

LIST OF FIGURES

LIST OF TABLES

NOMENCLATURE

Units are SI unless otherwise stated.

A	Gas chromatograph peak area (Eqs. 5-14 to 5-17)
B_{ii}	Pure component second virial coefficient (Eq. 3.50)
B_{ij}	Cross second virial coefficient (Eq. 3.50)
C_P	Heat capacity at constant pressure (refer to Section 3.4)
C_V	Heat capacity at constant volume (refer to Section 3.4)
C_i^L	concentration of solute in the bulk liquid phase (refer to Figure D-1)
C_i^G	concentration of solute in the gas bubble (refer to Figure D-1)
$C_{i,s}{}^L$	concentration of solute in liquid phase of the boundary layer (refer to Figure D-1)
$C_{i,s}{}^G$	concentration of solute in vapour phase of the boundary layer (refer to Figure D-1)
D	Volumetric flow rate (refer to Figure 5-1 and Eqs. 5-14 to 5-17)
D_{ij}^L	Liquid phase diffusion coefficient (required in Eq. D-14 to calculate the mass transfer coefficient)
D_{ij}^G	Gas phase diffusion coefficient (refer to Section D.2.1)
d_b	Diameter of the bubble
f	pure component fugacity (Eq.3.22)
$\hat{f}_i$	Fugacity of species i in solution (Eq. 3.25)
G	Gibbs energy (refer to Section 3.3)
g	Gravitational acceleration (required by Eq. D-9 to calculate the terminal bubble rise velocity)
H	Enthalpy (refer to Section 3.3)
h	Bubble rise height (required in Eqs. D-8 and D-20)
k_L	Mass transfer coefficient (refer to Section D.1.2)
M	Molecular mass
$\overline{M}_i$	Partial molar property of species i in solution (refer to Section 3.3)
m	mass
N	Number of moles of solute (Eqs. 5-14 to 5-17)
Nu	Nusselt number (required for the mass transfer coefficient correlation – Section D.1.2)
n	Number of moles of solute (refer to Section 5.2.1)
P	Pressure
P'	Parachor (refer to Section 3.7.2.1.3)

Pe	Peclet number (required for the mass transfer coefficient correlation – Section D.1.2)
Q	Heat (Eq. 3-1)
R	Universal gas constant
R'	Mean radius of gyration [Å] (refer to Section 3.7.2.1.3)
R_b	Radius of the bubble (required in Eqs. D-8 and D-20)
Re	Reynolds number (Eq. D-12)
S	Entropy (Eq. 3-2)
T	Temperature
t	time
U	Internal energy (Eq. 3-1)
u^{t}	Bubble terminal rise velocity (required in Eqs. D-8 and D-20)
V	Molar volume (Eq. 3-1)
W	Work (Eq. 3-1)
x	liquid mole fraction
y	vapour mole fraction
Z	Compressibility factor (Eq. 3.28)
Φ	Correction term for vapour-phase non-ideality (GammD-Phi approach to VLE, refer to Section 3.11.4 and Eqs. 3-83, 3.84 and 3.85)
Γ	Integration constant (Eqs. 3-20 and 3.63)
ϕ	Pure component fugacity coefficient (Eqs. 3.24 and 3.34)
$\hat{\phi}_i$	Fugacity coefficient of species i in solution (Eqs. 3.26, 3.33 and 3.51)
γ	Activity coefficient (Eqs. 3.64 and 3.66)
η	viscosity [cP]
μ	Chemical potential (Different from the dipole moment, refer to Eq. 3-11)
μ_D	Dipole moment [debye] (Different from the chemical potential, refer to Section 3.7.2.1.2)
ω	acentric factor (refer to Section 3.7.1)
ρ	density

Superscripts

0	Pitzer correlation parameter (refer to section 3.7.1)
1	Pitzer correlation parameter (refer to section 3.7.1)
E	Excess property ($M^E = M\text{-}M^{i.d.}$, refer to Section 3.8)
exp	Experimental value (refer to Section 3.13.1)

i.d.	Property value for an ideal solution (refer to Section 3.8)
∞	Property value at infinitely dilute concentration (Eq. 5-1)
i.g.	Property value for an ideal gas (refer to section 3.4)
L	Liquid phase property
R	Residual property ($M^R = M\text{-}M^{i.g.}$) refer to section 3.5
rev	Property value for a reversible process (Eq. 3-4)
sat	Property value at saturation (e.g. P^{sat} is the pure component saturation pressure) refer to Section 3.6
t	Total system property (Eq. 3-6)
V	Vapour phase property

Subscript

0	Initial value of a property (Eqs. 5-14 to 5-17)
i	Property of species *i*
G	Gas phase property (refer to Figure 5-1)
sol	Solute property (Eq. 5-1)
S	Solvent property (Eq. 5-2)
C	Critical property (refer to Section 3.7.1)
r	Reduced property (refer to Section 3.7.1)

CHAPTER 1

INTRODUCTION

Acetylpropionyl (2,3-pentanedione) and diacetyl (2,3-butanedione) are by-products of sugar manufacture. Diacetyl's main use is as a flavour component in beer, wine and dairy products. 2,3-Pentanedione also has many food related uses ranging from flavouring to being a starting material for antioxidants. It is a biodegradable solvent, a polymerization inhibitor and a starting material for pharmaceutical intermediates. Extractive distillation is being considered as a separation technique for purification of both diketones, thus VLE data and infinite dilution activity coefficients are required for the considered systems.

It is essential that the VLE data used to design separation processes be accurately measured. This is however, a costly and time-consuming exercise. Many examples of successful separation processes, designed from VLE measurements (or extrapolation or interpolation of data), are available in literature. It is, however, a case study of the design of a fractionating column, described as a "major blunder" by Palmer (1987), which best highlights the importance of accurate VLE data and the careful theoretical treatment of the data.

The Monsanto Company of Texas designed a fractionator to remove water from a solvent. The number of bubble-cap trays in the column was specified based on a set of VLE data. The resulting column was described as marginally operable at four times the design reflux. Furthermore, losses were reported to be 20 times the design value and the annual unexpected costs were in excess of $100 000 (in 1964). Two causes for the problems experienced were identified (Martin, 1964). The first was poor tray efficiency, which is unrelated to this project. The second cause (more relevant to this study) was found to be the VLE data. The deficiencies were as follows:

- Data were not measured in the dilute region.
  The dilute region is of considerable importance when high purity chemicals are required as this is usually the most expensive part of the process (Raal and Mühlbauer, 1998).
- Activity coefficients were extrapolated from excess Gibbs energy models.
  These models often fail to account for molecular interactions at infinite dilution (Alessi et al., 1991). It is, however, at times necessary to rely on such methods. It was found in the case study of Palmer (1987) that a more sophisticated model than the one used in

the original design gives a satisfactory result. The true infinite dilution activity coefficient eventually revealed that the choice of separation process was questionable.

A proper phase equilibrium study will have avoided a costly mistake and it is, therefore, understandable why much effort is made to refine VLE measurement techniques. Focus must also be placed on the theoretical treatment of VLE data, which features largely in a phase equilibrium study, as it is impractical to measure data for every possible chemical combination and at every condition of pressure, temperature and composition. Proper treatment of the data enables one to predict VLE at various conditions and for multi-component systems from only binary measurements. Experimental data are also important for the development of models and predictive techniques (such as the UNIFAC method described in Chapter 3). The case study highlights that both experimental and theoretical methods are fundamental parts of a phase equilibrium study. It more importantly stresses that both methods are of little use if they are improperly applied.

The experience of the Monsanto Company serves as a cautionary example for others. This study was, therefore, approached with the lessons of the example in mind. It is only possible to understand the applicability of the various experimental and theoretical techniques by undertaking a thorough review of the available methods. These reviews were, therefore, the starting point of this study and were used to make informed decisions to achieve the following objectives:

- Measurement of isobaric VLE by the most accurate method.
- Measurement of isothermal VLE by the most accurate method.
- Using thermodynamic principles to judge the quality of the data.
- Thermodynamic treatment of the data so that accurate VLE can be predicted at unmeasured conditions.
- Measurement of the infinite dilution activity coefficient by the most appropriate method.

Thus, separation processes for systems with diacetyl and 2,3-pentanedione can be confidently designed based on the results of this study.

CHAPTER 2

VAPOUR-LIQUID EQUILIBRIUM AT LOW PRESSURE - EXPERIMENTAL METHODS

The use of vapour-liquid equilibrium data in the separation industry is well established. This chapter will present the results of a review of recent journal articles to determine the popular experimental methods for the measurement of low-pressure VLE. Only a brief description of each of the popular methods will be presented. Extensive reviews of VLE apparatus are available in the excellent texts of Hala et al. (1957), Raal and Mühlbauer (1998) and the publications of Malanowski (1982), Abbott (1986) and Joseph et al. (2002).

Abbott (1986) presents a review of low pressure VLE publications made between the years 1976 and 1985 in order to gauge the trends of that decade. The journals reviewed by Abbott were:

- *Fluid Phase Equilibria*
- *The Journal of Chemical and Engineering Data*
- *The Journal of Chemical Thermodynamics*

The publications of the above-mentioned journals represent only part of the actual number of data sets measured as some data sets remain unpublished due to confidentiality issues. Furthermore, many data sets may have been published in other journals. Abbott (1986) however, reports that the 300 relevant articles published in the three journals are large enough in number to be a representative sample. Selected results of Abbott's review are:

- A large increase in the number of isothermal sets measured over the decade as compared to isobars (mainly P-x sets from static cells).
- An increase in the number of isothermal sets measured using recirculating stills.
- A slow increase in publication rates.

Abbott suggests that the increase in the number of isothermal measurements could be due to the awareness of the theoretical advantages of isothermal sets (discussed in Chapter 3) or the

time-saving modifications made to the static methods, such as the multi-cell cluster assembly introduced by Maher and Smith (1979).

A similar, though less extensive review, is presented in this chapter. The intent was to gauge the popularity of the various apparatus available for low pressure VLE measurements. Each of the options were considered and are described in order to choose the appropriate method for this study. The three journals considered by Abbott were reviewed for the period September 1999 to September 2002. Articles containing VLE data of the following type were considered (as these were the parameters of the measurements required by this study):

- Non-reacting binary systems.
- Temperature range from 303.15K to 493.15K.
- System pressures up to atmospheric.

It was found that the number of relevant publications during this period in *The Journal of Chemical Thermodynamics* was small compared to the other two journals. It was, therefore excluded from the review. A total of 110 articles of interest were found during the three year period, presenting 439 data sets. The classification of the types apparatus used to measure the data and the percentage of data sets measured using each of the methods is shown in Table 2-1. A discussion of each method will be presented shortly. The level of detail of each category was influenced by the results of Table 2-1.

Table 2-1 Classification (according to apparatus type) of low pressure VLE data sets published in the considered journals during the review period

Apparatus used	Percentage data sets
Recirculating stills	66
Static cells	19
Flow-type	7
Headspace Chromatography	5
Other	3

Recirculating methods remain the most convenient way of measuring isobaric data. The latter type of data are of considerable importance in the analysis of distillation columns (Raal and Mühlbauer, 1998). As in the case of Abbott's study it was noticed that the number of isotherms and isobars per system was more or less constant. On average more isotherms are measured per system compared to isobars per system, as multiple isotherms enable one to determine the temperature dependence of certain parameters (see Chapter 3). Abbott (1986) shows that isothermal measurements were more popular at that time than isobaric

measurements. The study presented in this work reveals that isothermal measurements now only constitute 46% of the data sets measured. It is interesting to note that 34% of the isothermal sets were measured using recirculating stills. The latter observation was made by Abbott but not quantified, so it is not possible to comment much further on this statistic. Most static apparatuses produce only *P-x* data, which excludes the possibility of testing for thermodynamic consistency (see Chapter 3). *P-x-y* data may be obtained from recirculating apparatus and consistency tests can be performed on this data. The discussion that follows describes each of the types of apparatus shown in Table 2-1 with particular focus on recirculating stills.

2.1 Recirculating Stills

Recirculating methods allow for accurate and rapid measurement of vapour-liquid equilibria. Malanowski (1982) states that all circulation methods have in common the principle of the continuous separation of vapour evolved from a liquid phase under steady-state conditions and recirculation of the vapour phase. Malanowski (1982) also lists the following criteria that a recirculating still should satisfy:

- Simplicity in its design.
- Small samples required.
- Design should ensure accurate pressure and temperature measurements.
- Steady-state should be achieved rapidly if an equilibrium parameter (such as composition or pressure) is changed.
- The vapour should not be allowed to partially condense on the temperature sensor, neither should there be overheating in the vicinity of the sensor.
- Liquid droplets should not be allowed to be entrained in the vapour phase.
- The circulated vapour should be well mixed with the liquid phase to maintain uniform composition.
- The composition and flow of the circulated stream should be steady.
- The apparatus should contain no dead-volume where the test chemicals may accumulate.
- Sampling and introducing material to the still should be accomplished without interruption of boiling.

The recirculating stills are required to provide liquid and vapour samples that are representative of the equilibrium concentrations. Moreover, the apparatus is required to

precisely measure the boiling temperature of the test mixture (ebulliometry). It was apparent to those who pioneered the development of the recirculating still that simply noting the temperature of a thermometer immersed in a boiling liquid is not indicative of the true boiling temperature. The surface tension of the liquid prevents the formation of small vapour bubbles, and this coupled with the hydrostatic head experienced by the liquid at the bottom of the vessel results in the liquid being slightly superheated (Hala et al., 1957). Placement of the temperature sensor in the vapour space is not a solution as measurement of condensation temperature of the vapour phase is only equal to the boiling temperature for samples of extremely high purity.

Circulation stills may be classified as follows:

- Recirculation of the vapour and liquid phase.
- Recirculation of the vapour phase only.

Vapour recirculation methods will be described briefly and methods that circulate both the vapour and liquid phases will be discussed in detail as this is the preferred method.

2.1.1 Vapour and liquid recirculation stills

The modern vapour and liquid recirculation still represents the evolution of the recirculating still. Its history dates back to the early part of the 20th century and is punctuated by the introduction of many innovative modifications that have endured to feature in the modern still. The development of the VLE still is very closely linked to the development of the ebulliometer (apparatus used to accurately measure the boiling temperature of a substance). The discussion will, therefore, begin with the development of the ebulliometer. Several hundred papers have been published proposing modifications to the VLE still. Not mentioning every one of them should be taken as an indication of how numerous they are and not of their significance. Some of these features (such as measures taken to reduce flashing in the boiling chamber) will be highlighted when the following designs are discussed:

- The still presented by Malanowski (1982).
- Fischer LABODEST VLE still.
- The still presented by Raal and Mühlbauer (1998) for the measurement of low pressure VLE data.

The design of Malanowski (1982) has been described as a modern VLE still of "good design" by Abbott (1986). It is, therefore, appropriate that the features of the still be discussed. The review of journal articles (discussed earlier in this chapter) revealed the commercially available Fischer LABODEST VLE still to be most popular and it will be discussed briefly. Finally, the design presented by Raal and Mühlbauer (1998) will be described as it incorporates many of the novel features presented in the following section.

2.1.1.1 The development of the recirculation still

The discussion begins by describing the early ebulliometers as they provide the base design for the VLE still. The Cottrell pump is very much a central feature of vapour and liquid recirculation stills. The ebulliometer presented by Cottrell (1919) is, therefore, a good starting point.

2.1.1.1.1 The Cottrell pump

Cottrell (1919) introduced an ebulliometer that featured a thermal lift pump (Cottrell pump). Vapour bubbles formed in the boiling chamber (A) (see Figure 2-1) entrain slugs of liquid, which travel up the Cottrell tube (B). Part of the superheated liquid vaporises and the temperature drops to the equilibrium value (Hala et al., 1957). The vapour is condensed by a condenser (C) and the liquid flows over a thermometer (D), which is placed in the vapour space. As the apparatus was presented as an ebulliometer, no provision was made for sampling of the phases.

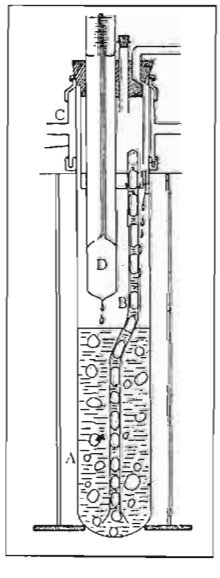

Figure 2-1: Cottrell ebulliometer (Cottrell, 1919): A - Boiling tube; B - Cottrell tube; C - Condenser; D- Thermometer

Washburn and Read (1919) developed the idea of the Cottrell pump further and presented an ebulliometer that featured the two phase mixture splashing over the thermometer. The purpose of the Washburn still was to investigate the boiling point elevation of various solutes. The boiling chamber (A) (see Figure 2-2) is unchanged, the Cottrell pump (B) branches into multiple arms and the mixture squirts onto the thermometer (D). The vapour is condensed in the condenser (C) and returned to the boiling chamber. The purpose of the sheath (F) is to prevent the cold condensate from flowing over the thermometer. Also included is a capillary (E) so that the liquid may be sampled. Hala et al. (1957) report that the Washburn apparatus was still in use at that time.

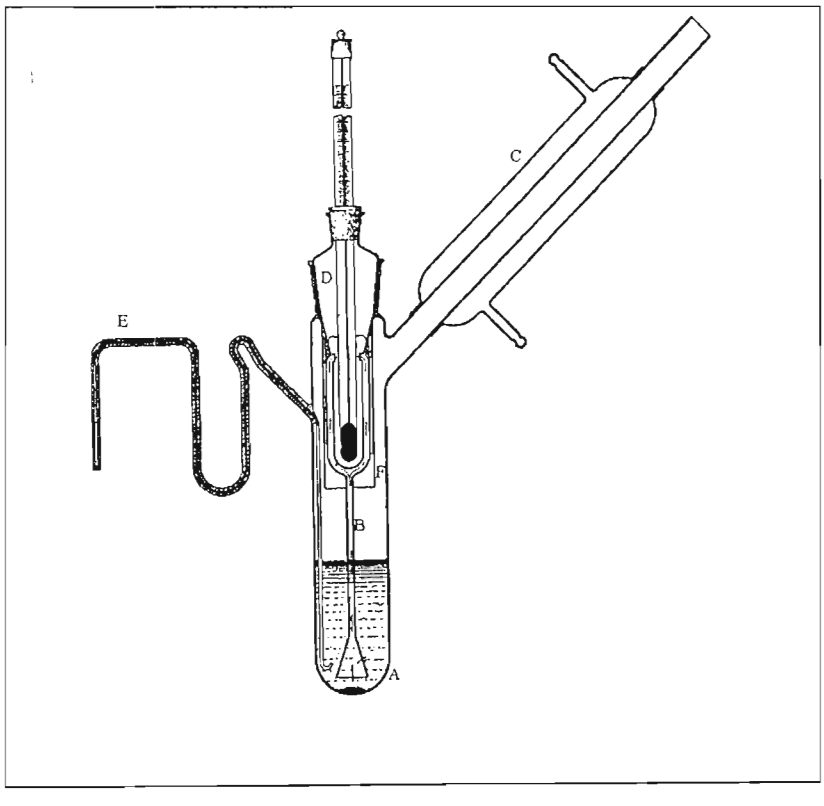

Figure 2-2: Washburn ebulliometer (Washburn and Read, 1919): A - Boiling tube; B - Cottrell tube; C - Condenser; D - Thermometer; E - Sampling tube; F - Sheath

2.1.1.1.2 The Świętoslawski ebulliometer

Świętosławski presented many different ebulliometer designs incorporating the Cottrell pump. The ebulliometer presented in 1929 (Figure 2-3) was the most popular (Hala et al., 1957). A feature of note is the thimble or thermowell (D) into which the thermometer is inserted. The vapour and liquid mixture exits the Cottrell pump (B) and splashes onto the thimble (D) fitted with a spiral to break the liquid run-off. Also included in the design is a condensate drop counter (E). The latter allows for the boiling intensity to be measured

(through the drop rate). An appropriate boiling intensity may be found for a test mixture by noting the effect of boiling intensity (hence the drop rate) on the temperature measured. Hala et al. (1957) give the example of water, which was found to yield constant values for the boiling temperature for drop rates between 8-25 drops per minute for a particular Święstosławski-type ebulliometer.

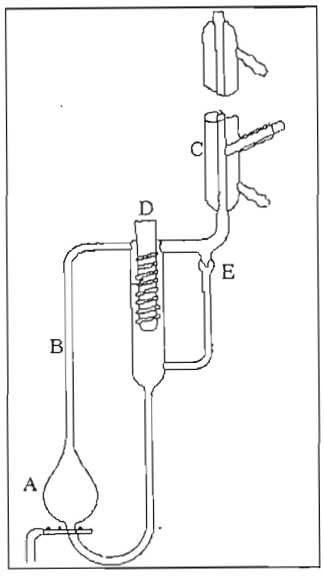

Figure 2-3: Święstosławski ebulliometer (Hala et al., 1957): A - Boiling chamber; B - Cottrell tube; C - Condenser; D - Thermowell; E - Drop counter

Boiling intensities below 8 drops per minute provide insufficient heat in this example and values greater than 25 drops per minute provide too much superheat for the equilibrium value to be obtained. The region where the temperature remains constant is referred to as the "plateau region." Discussion of the plateau region may be found in Kneisl et al. (1989) as well as briefly in the "Experimental Procedure" chapter of this work. Hala et al. (1957) suggest that the superheat in the boiling chamber may be lowered by increasing the activity on the wall of the chamber. This is achieved by providing nucleation sites for vapour bubble formation in the form of ground glass. The Święstosławski apparatus does not allow for the sampling of the equilibrium vapour or liquid. It is, therefore, an ebulliometer but does highlight some of the features of the modern VLE still. Many modern VLE stills are in fact described as "modified Święstosławski" stills.

2.1.1.1.3 Vapour condensate and liquid sampling

The first still to allow for sampling of the vapour condensate and liquid was presented by Lee (1931) (illustration not shown in this work). The apparatus, discussed in detail by Joseph

(2001), discharges the liquid and vapour mixture onto a thermometer using a Cottrell pump. The vapour condensate is collected and may be sampled by cessation of the boiling. Liquid samples are taken from the boiling chamber, which is not indicative of the equilibrium liquid composition. The disengaged liquid splashing onto the thermowell should, in fact, be sampled (Raal and Mühlbauer, 1998).

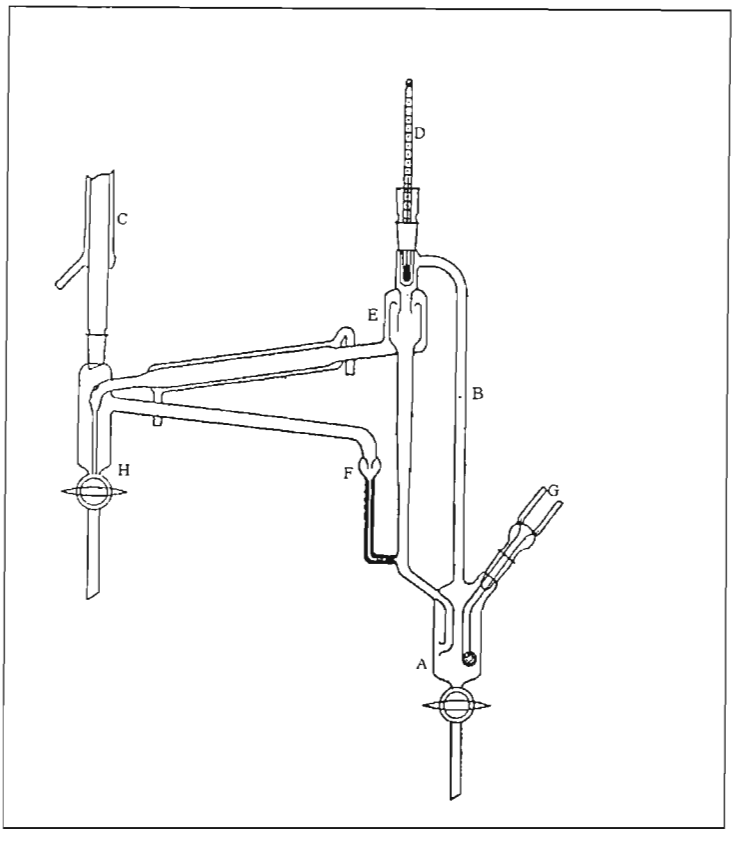

Figure 2-4: Gillespie Still (Gillespie, 1946): A - Boiling chamber; B - Cottrell tube; C - Condenser; D - Thermometer; E - Disengagement chamber; F - Drop counter; G - Internal heater; H - Vapour sample chamber

The apparatus of Gillespie (1946) (Figure 2-4) is a more satisfactory still. Sampling may be done without interrupting the boiling and the still features a disengagement chamber (E) which has proved very popular. Heat input to the boiling chamber is provided by a heating spiral wrapped around the reboiler and a heated platinum wire (G) immersed in the chamber. The latter serves to promote the formation of vapour bubbles and thereby reduces the superheat (Hala et al., 1957). The vapour-liquid mixture splashes onto the thermometer and enters the disengagement chamber (E) where the vapour flows upwards to the condenser (C). The vapour sample is collected in a sampling chamber (H) and the overflow is returned to the reboiler after passing through a drop counter (F). Like the still of Lee (1931), the Gillespie still samples the liquid in the boiling chamber. This, as mentioned before, is not acceptable.

Many modifications were made to the Gillespie still, the most significant by Brown (1952). The liquid leaving the disengagement chamber is allowed to accumulate in a liquid sampling point and the overflow is directed to the boiling chamber. Thus the issue of equilibrium liquid sampling is properly addressed. The still maintains the other features of the Gillespie still and an illustration is, therefore, not shown in this work.

2.1.1.1.4 The packed equilibrium chamber

Raal and Mühlbauer (1998) express concern regarding the use of only a Cottrell pump to attain equilibrium. The contact time of the liquid with the vapour phase in the Cottrell pump is likely to be insufficient for the phases to be in equilibrium. Mass transfer may be improved by using a longer Cottrell tube (to improve contact time) such as the spiral type used by Ellis (Hála et al., 1957) and featured in the Fischer LABODEST still. Use of a packed equilibrium chamber in conjunction with a Cottrell pump is another interesting feature.

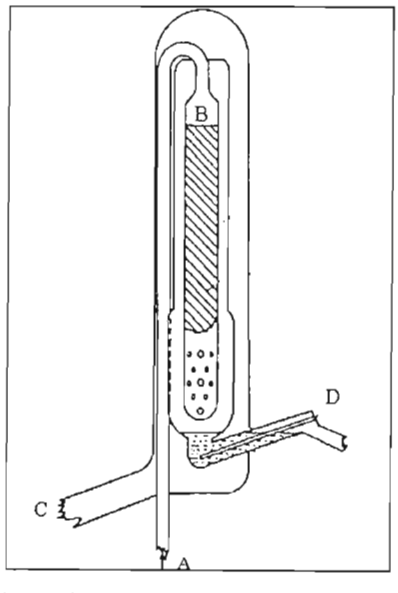

Figure 2-5: Packed equilibrium chamber (Yerazunis et al., 1964): A - Cottrell tube; B - Packed chamber; C - Vapour to condenser; D - Thermowell

A packed equilibrium column was used by Heertjes (1960) to measure VLE data. The idea was extended to the Świętosławski-type recirculating still by Yerazunis et al. (1964). The central feature of the latter design was the equilibrium chamber (shown in Figure 2-5). The vapour and liquid mixture is forced to flow downward through a bed of ¼ in. glass helices (B). The packed bed provides enhanced interfacial contact between the phases and equilibrium may be achieved more rapidly. The liquid collects in a liquid trap containing a thermowell (D) for temperature measurement. The disengaged vapour is allowed to flow

upward and around the equilibrium chamber to provide a thermal barrier. The use of the vapour as thermal lagging was first used by Rose and Williams (1955). Yerazunis et al. (1964) state that the still gives thermodynamically consistent data in a fairly short period of time (30-45 minutes).

2.1.1.1.5 Other significant modifications

- Raal and Mühlbauer (1998) advocate the use of a vacuum jacketed equilibrium chamber in order to minimise heat losses. This was first introduced by Altsheler et al. (1951). It is very much a feature of the modern VLE still (see the designs of Malanowski (1982) and Raal and Mühlbauer (1998) described shortly).
- The importance of stirring in the sample collection chambers was stressed by Dvořák and Boublik (1963) for systems of high relative volatility.

2.1.1.2 The still of Malanowski

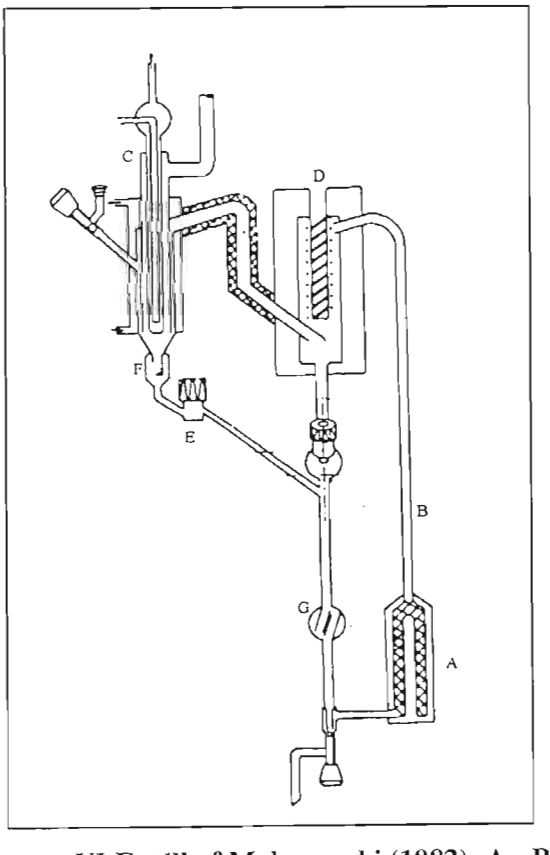

Figure 2-6: Low pressure VLE still of Malanowski (1982): A - Boiling chamber; B - Cottrell tube; C - Condenser; D - Thermowell; E - Vapour sample chamber; F - Drop counter; G - Mixing chamber

The apparatus presented by Malanowski (1982) (see Figure 2-6) uses the Świętosławski ebulliometer as a base for its design due to its high accuracy. The walls of the boiling chamber (A) are activated with sintered glass, which promotes vapour bubble formation (as used in the Świętosławski ebulliometer). The vapour and liquid mixture is forced through the Cottrell pump (B) and splashes onto the thermowell where equilibrium is established. The equilibrium chamber is contained within a vacuum jacket to minimise heat losses. The disengaged liquid collects in the liquid sample point and the vapour is directed to the condenser (C) through a heated tube (to prevent partial condensation). The vapour condensate collects in a sample point (E) after passing through a drop counter. The overflow from both the vapour and liquid sample points are mixed in a mixing chamber (G). This ensures that the fluid returning to the reboiler is of uniform concentration and composition and is necessary to reduce pressure fluctuations. The Malanowski still requires that equilibrium be achieved using only the Cottrell pump. Joseph et al. (2002) express reservations of relying on the Cottrell pump alone to achieve equilibrium in a single pass.

2.1.1.3 The Fischer LABODEST VLE still

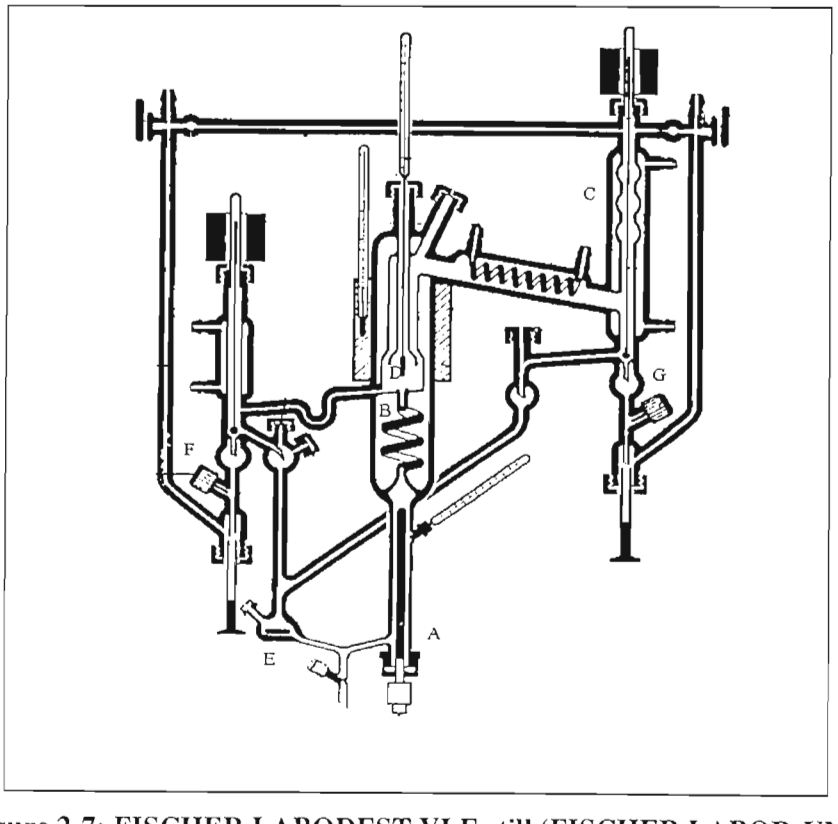

Figure 2-7: FISCHER LABODEST VLE still (FISCHER LABOR-UND VERFAHRENSTECHNIK catalogue): A - Heater; B - Spiral Cottrell tube; C - Condenser; D - Thermometer; E - Mixing chamber; F - Liquid sample point; G - Vapour sample point

The unusual feature of this still is the spiral tube that serves as a Cottrell pump. This type of thermal lift pump was featured in the Ellis still (Hála et al., 1957). Yu et al (1999) and Li et al (1995) make use of inclined Cottrell pumps as the longer travel of the tube assists in attaining equilibrium. Heat is supplied to the liquid by a heater (A) and the two-phase mixture is forced up the spiral tube (B). The apparatus does not make use of the more conventional design of Gillespie where the Cottrell tube empties its contents at the top of the equilibrium chamber. The mixture splashes onto the thermometer (D), which is located immediately above the exit of the Cottrell pump.

The equilibrium liquid is directed to a mixing chamber (E) through the liquid return tube (shown to the left of the Cottrell pump). The vapour rises through the equilibrium chamber, is condensed and also directed to the mixing chamber (E). The magnetic stirrer bar ensures that the liquid entering the boiling chamber is of uniform concentration and temperature to avoid flashing as the colder volatiles come into contact with the hot liquid return. Provisions are made to take appropriate equilibrium liquid and vapour samples (F and G respectively). As in the case of the Malanowski (1982) still, the Fischer LABODEST still relies on only the Cottrell pump to achieve equilibrium between the liquid and vapour phases.

2.1.1.4 Low pressure VLE still of Raal and Mühlbauer (1998)

The still (see Figure 2-8) employs a packed equilibrium chamber (A), a feature originally used in the design of Yerazunis et al. (1964). A mixture is heated in the boiling chamber by means of a cartridge heater (internal heater) (B) and by nichrome wire wrapped around the boiling chamber (external heater) as in the Gillespie type still (Hala et al, 1957). The external heater compensates for heat losses to the environment and the internal heater is used to control the boiling. The cartridge sits in a glass sheath which has the surface exposed to the liquid activated with powdered glass in order to promote vapour bubble formation. The vapour-liquid mixture travels up the Cottrell pump (C), which is vacuum-jacketed, and into an annular space which houses 3 mm stainless-steel wire mesh packing. The purpose of the vacuum jacket around the Cottrell pump is to prevent the superheated mixture from transferring heat to the packed chamber. It should be noted that unlike the design of Yerazunis et al. (1964), the packing is readily accessible and may be changed for a more inert type should it be required by the system.

The two-phase mixture travels downwards through the packing where equilibrium is achieved and the temperature measured (the thermowell is embedded in the packing). The mixture then

exits through small holes at the bottom of the packed chamber where the phases separate. The liquid phase collects in a sampling chamber (D) and the overflow is directed to the reboiler through a liquid return line (E). The equilibrium vapour rises past the packed chamber to serve as thermal lagging as advocated by Rose and Williams (1955). To further prevent heat losses, the entire equilibrium chamber is contained in a vacuum jacket (F) as seen in the still of Altsheler (Hala et al, 1957).

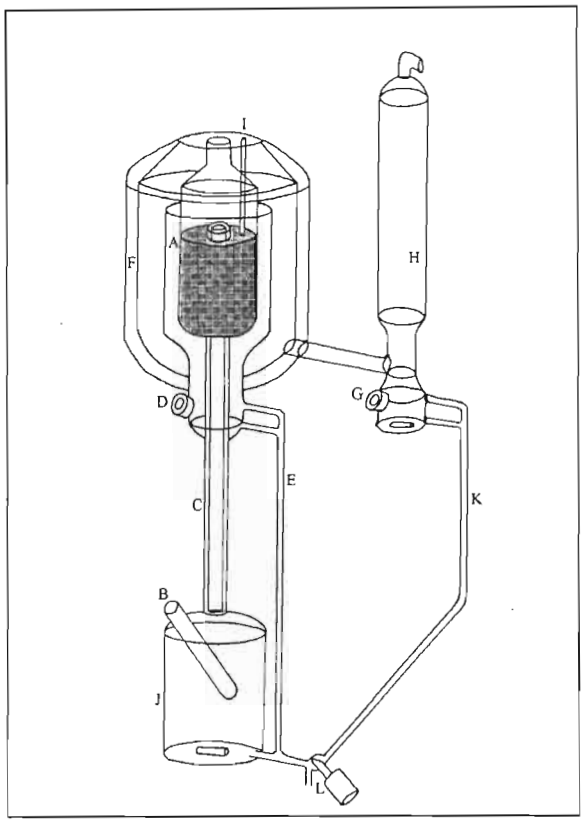

Figure 2-8: Low-pressure recirculating VLE still of Raal and Mühlbauer (1998): A – Packed equilibrium chamber; B – Heater cartridge; C – Vacuum jacketed Cottrell pump; D – Liquid sample point; E – Liquid return line; F – Vacuum jacket for equilibrium chamber; G – Vapour sample point; H – Condenser; I – Thermowell; J – Boiling chamber; K – Vapour return line; L – Drain valve

The vapour then enters a condenser (H) and the condensate collects in a sampling chamber (G) that contains a magnetic stirrer bar. The importance of stirring in the sample chambers had been stressed by Dvorak and Boublik (1963). Both the liquid and vapour sampling chambers allow for sampling through septa without interrupting the boiling, which is a standard feature of the modern VLE still. The overflow of the vapour sample chamber is directed to the reboiler through a tube that feeds into the liquid return leg through a capillary to reduce flashing. The flashing is a result of the cold vapour sample (rich in the volatile component) coming into contact with the hot liquid sample (rich in the non-volatile

component). Also of note is the magnetic stirrer bar in the boiling chamber, which also serves to reduce flashing.

The design of Raal and Mühlbauer (1998) is compact and robust. It incorporates many of the novel features from previous designs. Unlike the Malanowski and Fischer LABODEST stills, it does not rely on just the Cottrell pump for the liquid and vapour phases to reach equilibrium. The still is straightforward to operate and is in fact used in an undergraduate practical. Numerous data sets of excellent quality were measured by Joseph et al. (2001) and were shown to be thermodynamically consistent by the stringent point and direct tests of Van Ness et al. (1982) and Van Ness (1995) respectively. Discussion of these consistency tests will be presented in the subsequent chapter.

2.1.2 Vapour recirculation stills

The review revealed that while vapour and liquid recirculation methods are very popular, 4.5% of the recent measurements considered employ methods where the vapour phase only is circulated. The vapour phase recirculation methods may be classified as follows:

- Circulation of the vapour condensate.
- Circulation of revaporised vapour condensate.

As the vapour and liquid phase recirculation methods are preferred, only a brief description of vapour phase recirculation methods will be presented in this work. The reader is referred to the texts of Hala et al. (1957), Raal and Mühlbauer(1998) and the publications of Malanowski (1982) and Joseph (2001).

2.1.2.1 Vapour condensate recirculation

All the apparatuses used were described as "modified Othmer-type," the still (Othmer, 1928) being the first vapour still that operated satisfactorily (Hala et al, 1957). Malanowski (1982) reports that more than 150 modifications have been made to the original Othmer design. One of the latest versions of the Othmer still (Othmer, 1948) is shown in Figure 2-9.

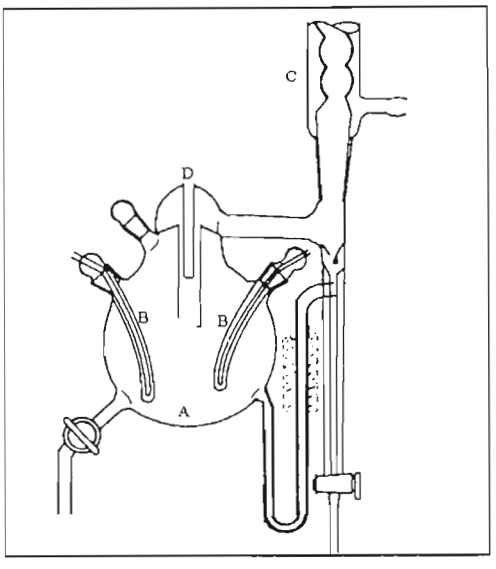

Figure 2-9: Othmer Still (Malanowski, 1982): A -Boiling chamber; B - Immersion heaters; C - Condenser; D - Thermowell

The operation is fairly straightforward. The mixture is brought to a boil in the boiling chamber (A). The vapour is directed to a condenser (C) after passing over a thermowell (D). The condensate is then returned to the boiling chamber. Raal and Mühlbauer (1998) highlight the following concerns:

- Temperature measurement is unsatisfactory.
- Absence of stirring in the boiling chamber.
- The operation of the still is disturbed to obtain samples.
- Possibility of partial condensation on the walls of the boiling chamber, which affects the composition in the still.

Raal and Mühlbauer (1998) conclude that use of the Othmer type still is not advisable for accurate work. Malanowski (1982) report that more satisfactory results may be obtained from vapour condensate recirculation stills that incorporate a Cottrell pump such as that of Scatchard et al. (1938). The latter still is described at length by Joseph (2001). While vapour recirculating stills employing a Cottrell pump are considered more accurate than the Othmer-type, they do require a longer equilibration time (Malanowski, 1982).

2.1.2.2 Revapourised vapour condensate recirculation

The principle of revapourised vapour condensate recirculation may be illustrated by the still presented by Jones et al. (1943) is shown in Figure 2-10.

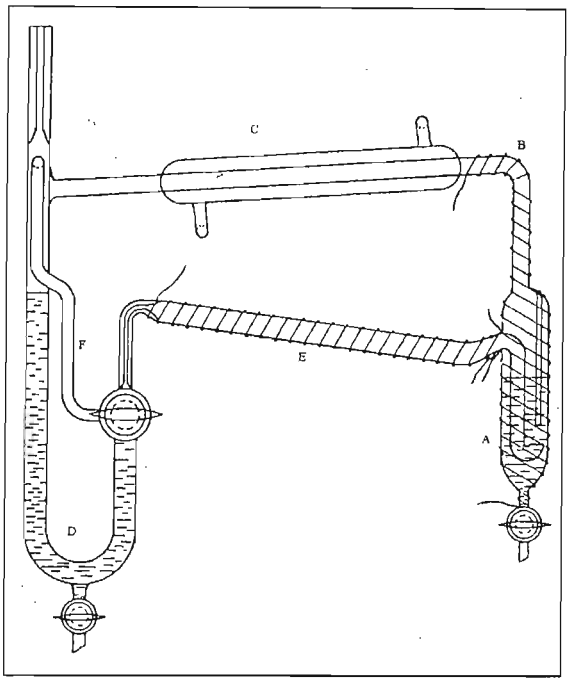

Figure 2-10: Jones Still (Jones et al., 1943): A - Boiling tube; B - Heated line to condenser; C - Condenser; D - Vapour condensate receiver; E - Revapouriser; F - Tube to equalise pressure

Malanowksi (1982) reports that the still produced accurate data and that more than 60 papers were published presenting modifications. The vapour formed in the boiling chamber (A) is directed to the condenser (C) through a heated tube (B) to prevent partial condensation. The condensate collects in (D) before passing through (E) where the condensate is revaporised. The tube (F) serves to equalise pressure across the condensate receiver. Disadvantages of the method reported by Malanowski (1982) and Raal and Mühlbauer(1998) are:

- The heating and cooling loads must be carefully balanced, making the method labour intensive and unstable.
- Equilibration may take several hours.
- The vapour composition is very sensitive to the temperature gradient in the boiling chamber (A).
- Bubbling of the vapour phase through the liquid phase results in pressure drops that compromises the accuracy of the temperature and pressure measurements.

A more recent still based on the circulation of the vapour phase that addresses the above concerns is discussed by Raal (2003). The still features an annular Cottrell pump. The vapour phase is bubbled through the liquid phase to produce rapid equilibration. The reader is referred to this publication for further detail.

2.2 Static methods

A static VLE cell contains a stirred liquid maintained at a constant temperature. Appropriate pressure and composition measurement thus enables one to measure isothermal VLE. The method presents challenges different to those of the recirculation method. It requires the complete evacuation of the cell prior to introducing the liquid mixture (which must also be totally degassed). Abbott (1986) reports that even small amounts of dissolved gas in the test mixture can result in meaningless pressure measurements. Degassing may be achieved through a series of freeze-thawing cycles under vacuum (Maher and Smith, 1979) or by distillation (Gibbs and Van Ness, 1972).

A further difficulty of the static method is proper vapour sampling. At low system pressure the molar hold-up is very small. The sample must also be small so as not to disturb the equilibrium in the cell (Raal and Mühlbauer, 1998). Vapour phase sampling, therefore, is not straightforward. Although methods, such as that of Inoue et al. (1975), do propose vapour sampling, many methods choose to measure temperature, pressure and the liquid phase composition only. This is sufficient as the vapour phase composition may be calculated from *P-x* data (a consequence of the Gibbs-Duhem equation discussed in the next chapter). *P-x* measurement, however, removes the opportunity of thermodynamic consistency testing to judge the quality of the data (also discussed in the next chapter).

Abbott (1986) reports that liquid phase compositions may be established in the following ways:

- Direct sampling of the liquid phase
  The errors introduced using this method are those associated with sample handling.
- Calculated from the overall composition
  Requires that the vapour and liquid volumes be known. The liquid phase composition may be found during the data reduction procedure. Rigorous computation procedures are available such as that of Raal and Ramjugernath (2001).
- Volumetric metering of degassed chemicals
  Developed by Gibbs and Van Ness (1972), who used commercial piston injectors to meter the chemicals. Care must be taken to ensure that the injectors are at a constant known temperature in order to know the mass introduced accurately.

19% of the data sets reviewed were measured by static methods with 50% of those sets being measured with apparatus referred to as Gibbs and Van Ness types (Gibbs and Van Ness, 1972). Due to its popularity, the latter will be described briefly.

Figure 2-11 shows an illustration of the Gibbs and Van Ness (1972) static VLE apparatus. The chemicals are degassed prior to being metered into the cell (A) by refluxing, cooling and evacuating (the degassing flask is not shown). The cell is evacuated through the vacuum line (B) and precise amounts of the test chemicals are transferred into the cell using the piston injectors (C) (only one shown). The mixture is magnetically stirred (D) and allowed to reach equilibrium at which point the pressure is noted (E).

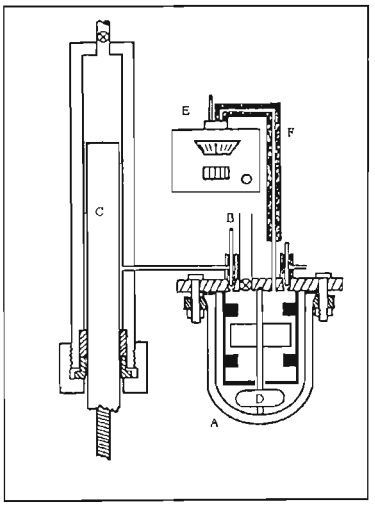

Figure 2-11: Static Cell (Gibbs and Van Ness, 1972): A - Cell; B - Vacuum line; C - Piston injectors; D - Magnetic stirrer; E - Pressure measuring device; F - Heated line to prevent partial condensation

The line leading to the pressure measuring device (F) is heated to ensure no partial condensation. Abbott (1986) reports that a binary system may be measured in a day or two and that the apparatus may be extended to ternary systems by adding a third piston injector. Abbott also reports that the method is also suitable for the measurement of vapour-liquid-liquid equilibrium.

A modern example of the static cell is presented by Raal and Mühlbauer (1998). The glass cell (see Figure 2-12) shows two time-saving developments:

- The static cell cluster

Maher and Smith (1979) developed an apparatus that consisted of 15 static cells connected to a common manifold. Multiple data points may be measured simultaneously.

- The degassing condenser

  The freeze-thawing cycles as used by Maher and Smith (1979) are time-consuming. Degassing may also be accomplished by gently boiling the mixture in a cell fitted with a condenser. The possibility of losing volatiles must be considered, the cell (Figure 2-12) therefore, includes a liquid sample point.

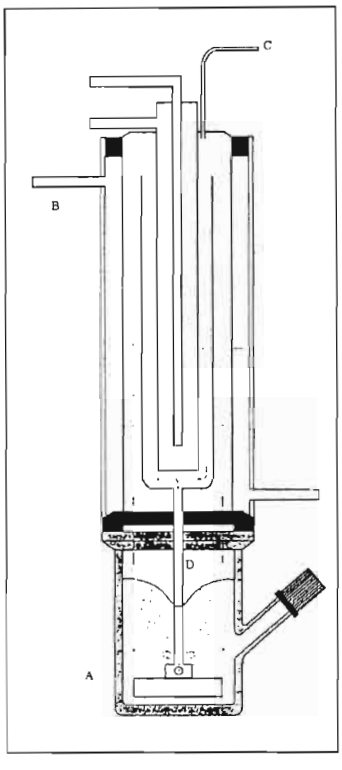

Figure 2-12: Individual unit of a static cell cluster (Raal and Mühlbauer, 1998): A, Stirred cell, B, Degassing condenser; C, Vapour line to manifold; D, Draft tube

The stirred cell (A) is attached to the degassing condenser (B) using a silicone gasket and the vapour is directed to the manifold (not shown) through line (C). Note the use of a draft tube (D). The vapour is circulated in the condenser and returned to the liquid surface by the draft induced by the magnetic stirrer. Raal and Mühlbauer (1998) report that equilibrium is achieved in a few hours and six points may be obtained in a day. Data for the system cyclohexane with ethanol presented by the authors, showed good agreement with literature.

2.3 Flow-type apparatus

The flow-type apparatus resembles that used in the inert gas stripping method (discussed in chapter 4). An inert gas is bubbled through a constant temperature binary mixture and the vapour phase entrained in the exit stream and analysed. The method involves a calculation procedure that relates the partial pressure to the peak areas of the respective components. Like the inert gas stripping method the following two assumptions are made:

- The gas solubility in the liquid is negligible.
- The vapour phase correction is assumed to be negligible.

7% of the data sets considered in this study were measured using the flow method. A description of the experiment as well as the calculation procedure may be found in the publication of Miyamoto et al. (2000). Ovečková et al. (1991) also report good results using a method based on the variation of the liquid composition. The reader is referred to these publications for further detail.

2.4 Headspace chromatography

Weidlich and Gmehling (1985) describe an apparatus that produces isothermal *x-y* data. The method uses headspace chromatography and a calculation procedure that requires knowledge of the initial amounts of liquid. As the method does not make pressure measurements, the authors confirm thermodynamic consistency by the area test of Redlich and Kister (1948). This test is shown to be lacking as a test for consistency in the next chapter. The data were used to extend the UNIFAC method for predicting activity coefficients by group contribution (discussed briefly in the next chapter). A significant number of data sets (5%) were measured using this apparatus. The reader is referred to the publication of Weidlich and Gmehling (1985) for further detail.

2.5 Other Methods

A small number of data sets were measured using apparatus that cannot be classified in the sections above. These methods will not be described in this work. References are given to texts that adequately describe these apparatus:

1. Flow Still – Hala et al (1957).
2. Semi-micro method – Raal and Mühlbauer (1998) and Hala et al (1957).

2.6 Conclusion of the review

The vapour and liquid recirculating still is a refined method that offers the following advantages:

- It is capable of accurately and rapidly measuring both isothermal and isobaric data. This flexibility is a considerable advantage as it satisfies the requirements of both theoretical and practical applications.
- The integrity of the data may be checked by recent stringent methods of thermodynamic consistency testing such as that of Van Ness (1995).
- Operation of a modern still is not a complicated exercise. A still of similar construction to that of Raal and Mühlbauer (1998) (described earlier) has been used as a successful teaching tool in the under-graduate Thermodynamics course.
- The still yields *P-T-x-y* by direct measurement and the total composition of the feed to the still need not be known.
- No degassing of the chemicals is required as in the case of static methods.

Areas of concern expressed by Abbott (1986) were:

- The attainment of true equilibrium.
- Minimisation of the pressure fluctuations.
- Determination of the true equilibrium temperature.
- Determination of the true equilibrium vapour composition.

Abbot does mention, however, that good data may be measured with a still of good design. The still presented by Malanowski (1982) is described as such by Abbott. It is designed such that the above mentioned concerns are addressed. It also conforms to the criteria a recirculating still should satisfy (see Section 2.1). The low-pressure apparatus of Raal and Mühlbauer (1998) is of similar construction to the Malanowski still. Moreover, it features a packed equilibrium chamber, which ensures that the still does not rely on only the Cottrell pump to achieve equilibrium. It was for these reasons and considering the excellent data of Joseph et al. (2001) that the still of Raal and Mühlbauer (1998) was chosen for use in this study.

CHAPTER 3

SOLUTION THERMODYNAMICS

The accurate measurement of vapour-liquid equilibria (VLE) is a time consuming and difficult exercise. The large number of chemical combinations and conditions (of temperature, pressure and composition) that data may be required for makes measurement of all possible systems impractical. Through the analysis of VLE measurements using thermodynamic principles, one is able to reduce the data to sets of parameters. The parameters and their origins shall be discussed in detail shortly as it is necessary to introduce certain concepts first. Appropriate use of the parameters can predict VLE at unmeasured conditions of P, T and composition. Further, multi-component VLE may be predicted from the constituent binary sets. Thermodynamics, therefore, extends the applicability of accurate VLE measurements. It will also be shown later in this chapter how thermodynamics may be used to judge the quality of measured VLE using consistency tests. An overview of the chapter is shown in Figures 3-1, 3-2, 3-3 and 3-4.

Solution thermodynamics has been discussed in detail by many authors, such as Van Ness and Abbott (1982), Smith et al. (1996) and Perry and Green (1998). The objective of this chapter is to briefly introduce the theory that is essential to data reduction of low pressure VLE. Concepts such as equilibrium and the criteria for equilibrium will be discussed, as well as expressions that describe VLE for the following cases:

- The vapour behaves as an ideal gas and the liquid as an ideal solution (Raoult's Law).
- The vapour behaves as an ideal gas and the liquid phase non-ideality is accounted for (Modified Raoult's Law).
- Both the liquid and vapour phases are assumed to display non-ideal behaviour (Gamma-Phi and the Phi-Phi representations).

Although this chapter is concerned with the application of thermodynamics to phase equilibrium, a number of concepts must first be explained in order to understand the development of the above-mentioned formulations. An appropriate starting point of this chapter would be the first law of thermodynamics.

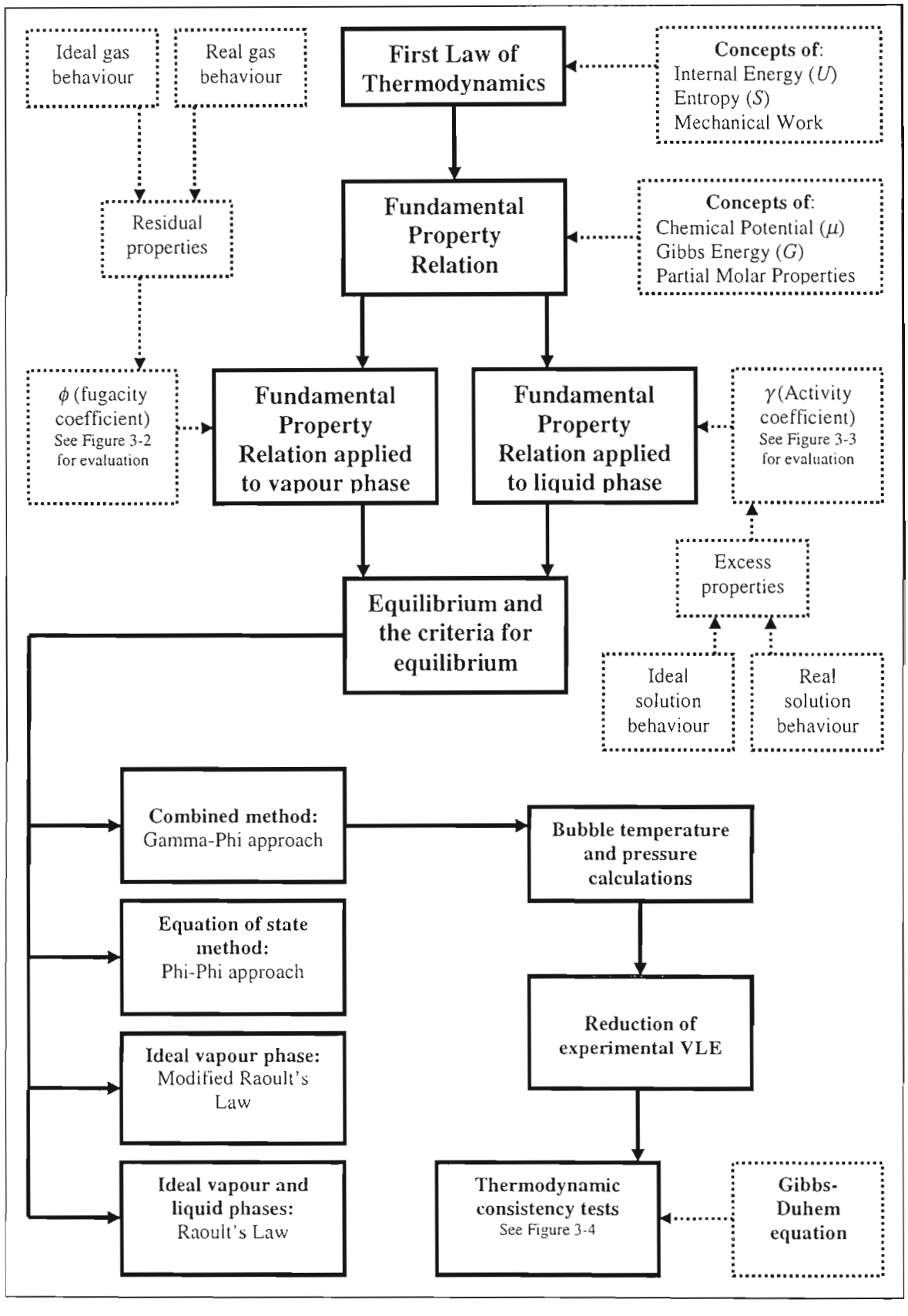

Figure 3-1: Block diagram to show an overview of solution thermodynamics as applied to low pressure vapour-liquid equilibrium

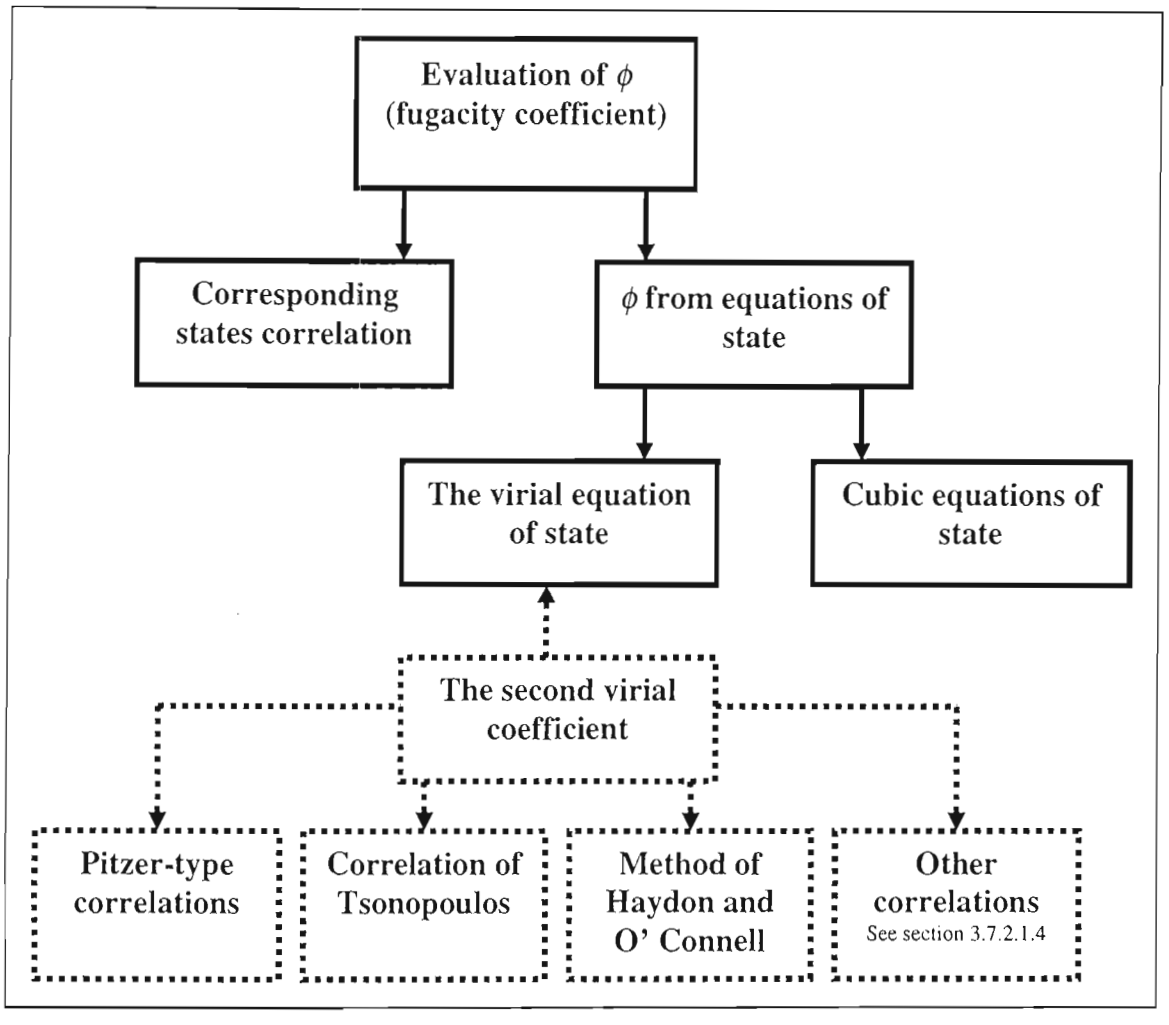

Figure 3-2: Block diagram to show how the fugacity coefficient can be evaluated for low pressure vapour-liquid equilibrium

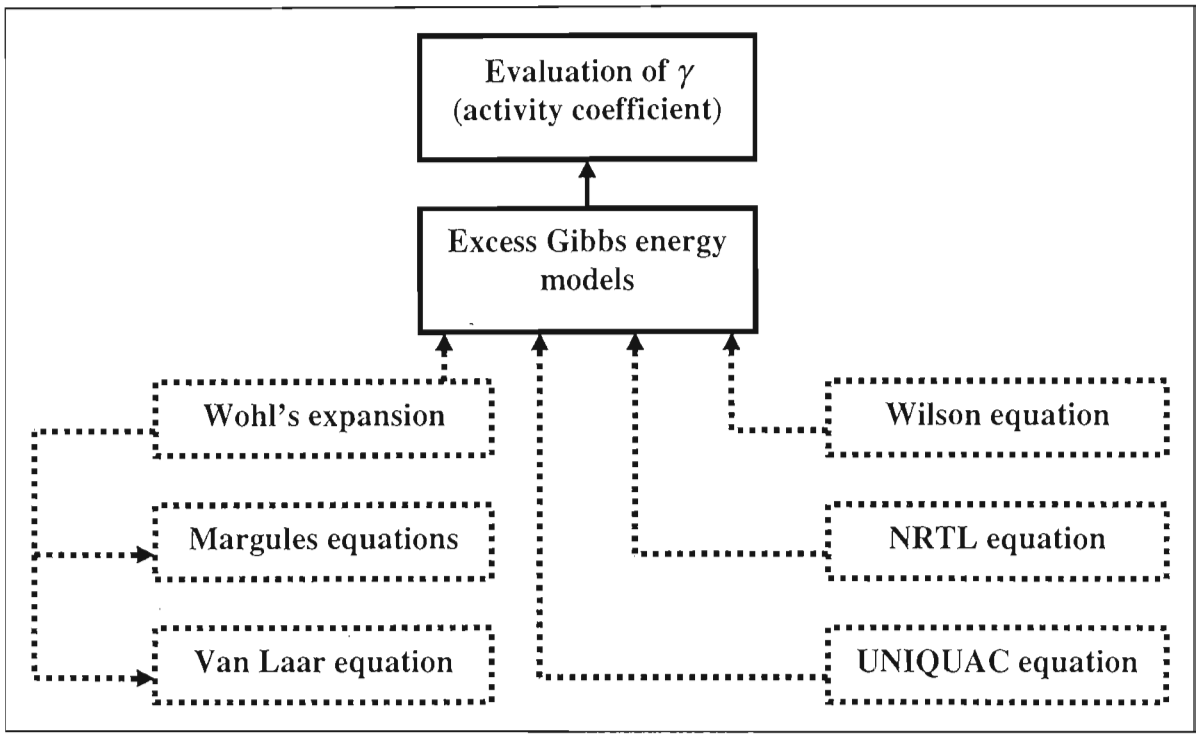

Figure 3-3: Block diagram to show how the activity coefficient can be evaluated for use in the Gamma-Phi approach to vapour-liquid equilibrium

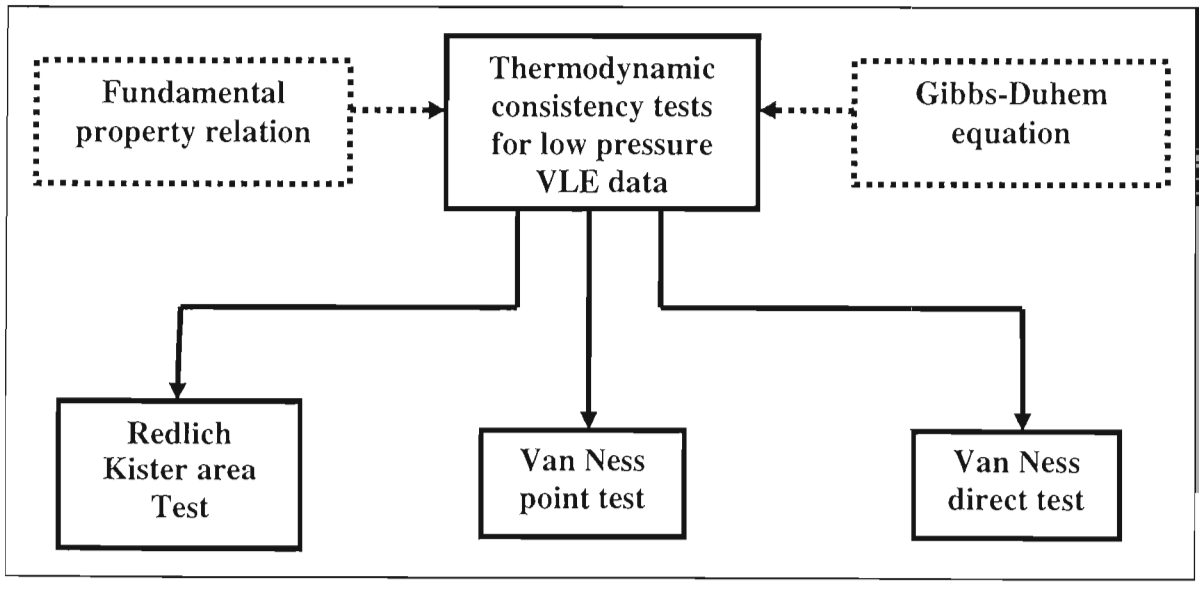

Figure 3-4: Block diagram to show the thermodynamic consistency tests available for low pressure vapour-liquid equilibrium

3.1 Internal energy (U) and the first law of thermodynamics

To understand what internal energy is, the following must be defined:

- Open system
  Mass and energy transfer to and from the system's surrounding are allowed
- Closed system
  Only energy transfer to and from the system's surrounding is allowed
- Isolated system
  Neither mass nor energy may be transferred to or from the system's surrounding

An isolated system may not be affected by its surrounding. It does however undergo measurable internal changes (such as temperature and pressure). The system eventually reaches a static state and is judged to be in internal equilibrium (Perry and Green, 1998). The internal energy is a form of energy that exists for systems in a state of internal equilibrium.

The first law of thermodynamics states that *the total energy of a system and its surrounding remains constant.* When applied to a closed (constant mass) system, the energy change of the system must be exactly compensated by the energy change in the surrounding. The energy changes are either through the transfer of heat or by doing work. The first law is therefore expressed by Eq. 3-1:

$$dU' = dQ + dW \tag{3-1}$$

3.2 Entropy (S) and the second law of thermodynamics

The concept of reversibility is required to understand the definition of entropy (S). A process that proceeds such that the system is never more than just differentially displaced from equilibrium is said to be reversible. The system may be brought to its original state by an infinitesimal change in external conditions. The entropy exists for any system in internal equilibrium and for a reversible process the total entropy may be calculated from:

$$dS' = \frac{dQ_{rev}}{T} \tag{3-2}$$

The second law of thermodynamics states that *the entropy change of any system and its surroundings, considered together resulting from any real process is positive, approaching zero when the process approaches reversibility.*

This may be written as:

$$dS^t \geq \frac{dQ}{T} \tag{3-3}$$

Eq. 3-3 shall be used later in the developing the criteria for phase equilibrium. Reversible work may be calculated from the following equation that results from the definition of mechanical work:

$$dW_{rev} = -PdV^t \tag{3-4}$$

3.3 The fundamental property relation

The fundamental property relation provides the basis for solution thermodynamics (Van Ness and Abbott, 1982). All equations relating properties of pressure-volume-temperature (*PVT*) systems are derived from it. Before deriving the relation, the chemical potential (μ) and Gibbs energy (G) must be introduced.

Eqs. 3-1, 3-2 and 3-4 may be combined to give:

$$dU^t = TdS^t - PdV^t \tag{3-5}$$

which is valid for a closed system containing a single phase undergoing a reversible process and no chemical reaction.

The use of total properties is abandoned. A total property (M^t) for a system containing n number of moles is given by:

$$M^t\left(T, P, n_1, n_2, \ldots\right) = nM \tag{3-6}$$

The following may be written for a non-reacting closed system undergoing any type of process (i.e. reversible or irreversible):

$$d(nU) = Td(nS) - Pd(nV) \tag{3-7}$$

where $n = n_1+n_2+n_3+\ldots$

Two cases are now considered, firstly for a closed system where $nU = function(nS, nV)$ the following may be shown from Eq. 3-7:

$$\left(\frac{\partial(nU)}{\partial(nS)}\right)_{nV,n} = T \text{ and } \left(\frac{\partial(nU)}{\partial(nV)}\right)_{nS,n} = -P$$

Secondly for an open system where $nU = function(nS, nV, n_1, n_2, n_3, \ldots)$ combining the above results with the definition of the chemical potential (μ):

$$\mu_i \equiv \left(\frac{\partial(nU)}{\partial n_i}\right)_{nS,nV,n_j}$$

The following may be obtained for an open system and where $n_i = x_i n$:

$$d(nU) = Td(nS) - Pd(nV) + \sum_i \mu_i d(x_i n)$$

This may be written as:

$$\left(dU - TdS + PdV - \sum_i \mu_i dx_i\right)n + \left(U - TS + PV - \sum_i \mu_i x_i\right)dn = 0$$

Since n and dn are independent and arbitrary, therefore:

$$dU = TdS - PdV + \sum_i \mu_i dx_i \tag{3-8}$$

$$U = TS - PV + \sum_i \mu_i x_i \tag{3-9}$$

It is at this stage that the Gibbs energy (G) and Enthalpy (H) may be introduced:

$$G \equiv U + PV - TS = H - TS$$

where $H \equiv U + PV$

$$d(nG) = -nSdT + nVdP + \sum_i \mu_i dn_i \tag{3-10}$$

Eq. 3-10 is the fundamental property relation for a single fluid of constant or variable mass and constant or variable composition (open system). Eq. 3-10 may also be written in terms of the enthalpy, a form useful later for the development of consistency tests:

$$d\left(\frac{nG}{RT}\right) = \frac{nV}{RT}dP + \frac{nH}{RT^2}dT + \sum_i \frac{\mu_i}{RT}dn_i \tag{3-11}$$

By introducing the idea of a partial molar property:

$$\overline{M}_i \equiv \left(\frac{\partial(nM)}{\partial n_i}\right)_{T,P,n_j}$$

The chemical potential may be shown to be related to the Gibbs energy through:

$$\mu_i = \left(\frac{\partial(nG)}{\partial n_i}\right)_{T,P,n_j} \equiv \overline{G}_i \tag{3-12}$$

Smith et al. (1996) show summability of the partial molar property, which shall be used extensively later in the chapter:

$$nM = \sum_i n_i \overline{M}_i$$

Smith et al. (1996) also derive the Gibbs-Duhem equation, which applies a constraint on how partial molar properties may change with a change in T and P. This equation shall be used to develop thermodynamic consistency tests for measured data later in this chapter. The general form is given by:

$$\left(\frac{\partial M}{\partial P}\right)_{T,x} dP + \left(\frac{\partial M}{\partial T}\right)_{P,x} dT - \sum_i x_i d\overline{M}_i = 0$$

The form of the Gibbs-Duhem equation used in developing thermodynamic consistency tests is:

$$\frac{V}{RT} dP + \frac{H}{RT^2} dT = \sum_i x_i d\frac{\overline{G}_i}{RT} \tag{3-13}$$

3.4 The ideal gas state

The ideal gas equation is given by:

$$PV^{ig} = RT \tag{3-14}$$

Eq. 3-14 describes the behaviour of imaginary molecules of zero volume that do not interact (Perry and Green, 1998). It is used as a standard to compare real gas behaviour through residual properties (discussed shortly).

By introducing the following heat capacities:

Constant pressure: $C_P \equiv \left(\frac{\partial H}{\partial T}\right)_P$

Constant volume: $C_V \equiv \left(\frac{\partial U}{\partial T}\right)_V$

The following may be shown:

$$dH = C_P dT \tag{3-15}$$

$$dS = \frac{C_P}{T} dT - \frac{R}{P} dP \tag{3-16}$$

A feature of the ideal gas model is that the total pressure is given by the sum of the partial pressures (hence $P_i = x_i P$). Gibbs theorem for a mixture of ideal gases follows from the ideal gas model, and states:

The partial molar property, other than the volume, of the constituent species in an ideal gas mixture is equal to the corresponding molar property of the species as a pure gas at the mixture temperature and the partial pressure in the mixture.

Gibbs theorem may be expressed as:

$$\overline{M}_i^{ig}(T,P) = M_i^{ig}(T,P_i) \tag{3-17}$$

Considering Gibbs theorem and applying Eqs. 3-15 and 3-16 at constant temperature:

$$\overline{H}_i^{ig} = H_i^{ig} \tag{3-18}$$

$$\overline{S}_i^{ig} = S_i^{ig} - R\ln y_i \tag{3-19}$$

The value for the Gibbs energy for an ideal gas is found by combining Eqs. 3-10, 3-18 and 3-19 and integrating to yield:

$$G_i^{ig} = \Gamma(T) + RT\ln P \tag{3-20}$$

The chemical potential for an ideal gas may be derived using Eqs. 3-12 and 3-20:

$$\mu_i^{ig} = \Gamma(T) + RT\ln y_i P \tag{3-21}$$

Γ is an integration constant and is a function of temperature only.

The significance of Eq. 3-20 will become apparent when residual properties are discussed.

3.5 Fugacity and the fugacity coefficient

This section deals with the departure of real gas behaviour from the ideal gas state. The ideal gas equation is used to define residual properties. These are basically the difference between the property value of a real fluid and an ideal fluid:

$$M^R \equiv M - M^{ig}$$

The ideal gas model serves as a standard to which the behaviour of real gases may be compared. The value for the Gibbs energy of a real fluid is written as:

$$G_i \equiv \Gamma(T) + RT \ln f_i \tag{3-22}$$

where the fugacity (f) replaces the pressure (P) in Eq. 3-20. The units for the fugacity are the same as those for pressure. Eq. 3-22 together with:

$$f_i^{ig} = P \tag{3-23}$$

completes the definition of the fugacity. Further for a pure species the fugacity coefficient is defined:

$$\phi_i \equiv \frac{f_i}{P}$$

and

$$G_i^R = G_i - G_i^{ig} = RT \ln \phi_i \tag{3-24}$$

A similar expression may be derived for species in solution using the chemical potential:

$$\mu_i = \Gamma_i(T) + RT \ln \hat{f}_i \tag{3-25}$$

where $\hat{f}_i$ is the fugacity of species i in solution. Combining Eq. 3-21 and 3-25:

$$\overline{G}_i^R = \mu_i - \mu_i^{ig} = RT \ln \hat{\phi}_i \tag{3-26}$$

where the fugacity coefficient of species i in solution is defined as: $\hat{\phi}_i \equiv \frac{\hat{f}_i}{y_i P}$ and for an ideal gas:

$$\hat{f}_i^{ig} = y_i P \tag{3-27}$$

The fugacity of species i in an ideal gas mixture is therefore equal to its partial pressure. As shown later, when the fugacity of each species in solution is the same the system is in chemical equilibrium.

The fugacity coefficient is evaluated using the compressibility factor (Z). The latter compares the ideal gas molar volume (V^{ig}) with the true molar volume (V):

$$Z = \frac{V}{V^{ig}} = \frac{PV}{RT} \tag{3-28}$$

We may write Eq. 3-11 in terms of residual properties, and considering Eq. 3-26:

$$d\left(\frac{nG^R}{RT}\right) = \frac{nV^R}{RT}dP + \frac{nH^R}{RT^2}dT + \sum_i \ln\hat{\phi}_i dn_i \tag{3-29}$$

$$\text{where } \ln\hat{\phi}_i = \left(\frac{\partial\left(nG^R/RT\right)}{\partial n_i}\right)_{P,T,n_j} \tag{3-30}$$

At constant T and composition

$$\frac{nG^R}{RT} = \int_0^P \frac{nV^R}{RT}dP \tag{3-31}$$

since $V^R = V - \frac{RT}{P}$ and considering Eq. 3-29

$$\frac{nG^R}{RT} = \int_0^P (nZ - n)\frac{dP}{P} \tag{3-32}$$

Eqs. 3-30 and 3-32 together yield:

$$\ln\hat{\phi}_i = \int_0^P (\overline{Z}_i - 1)\frac{dP}{P} \tag{3-33}$$

where $\bar{Z}_i = \left[\frac{\partial(nZ)}{\partial n_i}\right]_{P,T,n_j}$

The fugacity coefficient of a pure component is given by:

$$\ln\phi = \int_0^P (Z-1)\frac{dP}{P} \tag{3-34}$$

The fugacity coefficient for a pure species (Eq. 3-34) and the fugacity coefficient for a species in solution (Eq. 3-33) may then be calculated once an appropriate expression for the compressibility factor is proposed. These expressions are discussed in the next section.

3.6 Evaluating the liquid fugacity of a pure component

The essential role of the liquid fugacity of a pure component in phase equilibria will become apparent in the section describing the combined (or Gamma-Phi) method for describing VLE later in this chapter. Eq. 3-10 applied to a closed system containing a pure liquid evaporating at constant temperature and pressure reduces to $dG = 0$ and considering Eq. 3-22 for both the liquid and vapour phase:

$$G_i^L - G_i^V = RT\ln\frac{f_i^L}{f_i^V} = 0 \tag{3-35}$$

The above implies that:

$$f_i^L = f_i^V = f_i^{sat} \tag{3-36}$$

and considering the definition of the fugacity

$$\phi_i^L = \phi_i^V = \phi_i^{sat} \tag{3-37}$$

These relationships are used to derive an expression for the fugacity of a compressed liquid. The derivation is done in two parts (Raal and Mühlbauer, 1998):

- The fugacity of the saturated liquid is calculated from:

$$f_i^L = f_i^{sat} = \phi_i^{sat} P_i^{sat} \tag{3-38}$$

- The isothermal fugacity change in going from the saturated pressure to a higher pressure is derived from Eq. 3-11:

$$G_i^L - G_i^{sat} = \int_{P_i^{sat}}^{P} V_i^L dP \tag{3-39}$$

The liquid molar volume (V_i^L) is a weak function of pressure and considering Eqs. 3-35 and 3-39 together:

$$f_i^L = \phi_i^{sat} P_i^{sat} \exp \frac{V_i^L \left(P - P_i^{sat}\right)}{RT} \tag{3-40}$$

The exponential term is referred to as the Poynting correction factor and may be neglected for low pressure computations as its contribution is negligible (Smith et al., 1996). The liquid molar volume may be calculated from appropriate equations of state (discussed later in the chapter) or from the Rackett equation (Smith et al., 1996) or modification thereof:

$$V_i^L = V_{Ci} Z_{Ci}^{(1-T_r)^{0.2857}} \tag{3-41}$$

The reduced temperature (T_r) is defined in the section describing corresponding states correlations.

3.7 Evaluation of the fugacity coefficient

The expressions for the compressibility factor may either be in the form of correlations of *PVT* data or obtained analytically from equations of state. Corresponding states correlations shall be discussed briefly in this section as well a more detailed description of evaluating the fugacity coefficient from equations of state.

3.7.1 Corresponding states correlations and the fugacity coefficient

The corresponding states theorem is based on the observation that data for different fluids display uniformity when the thermodynamic coordinates (T and P) are expressed in a reduced

form (Van Ness and Abbott, 1982). The two-parameter version is a simple case that states for all pure fluids the compressibility factor is the same at the same values of reduced temperature (T_r) and reduced pressure (P_r), where

$$T_r \equiv \frac{T}{T_C} \text{ and } P_r \equiv \frac{P}{P_C}$$

and

$$Z = Z(T_r, P_r) \text{ for all fluids}$$

The critical pressure and temperature for many chemicals are given in Reid et al. (1988). Methods of estimating P_C and T_C when data is not available are also discussed in the text and shall be briefly described in the Discussion chapter.

Equations described in terms of the reduced parameters are referred to as generalised as they apply to all gases. The two parameter correlation represents the behaviour of simple fluids (Ar, Kr and Xe), however, a third parameter is necessary to extend the applicability of the method. The accentric factor (ω) was introduced by Pitzer (Pitzer and Brewer, 1961) and is defined as:

$$\omega \equiv -1.0 - \log\left(P_r^{sat}\right)_{T_r=0.7}$$

The accentric factor may therefore be calculated from only P_C, T_C and a vapour pressure measurement at $T_r = 0.7$. The correlation for the compressibility factor is:

$$Z = Z^0 - \omega Z^1 \tag{3-42}$$

where Z^0 and Z^1 are functions of T_r and P_r.

Substituting Eq. 3-42 into Eq. 3-34 and writing the result in reduced form:

$$\phi = \left(\phi^0\right)\left(\phi^1\right)^{\omega} \tag{3-43}$$

where

$$\ln\phi^0 \equiv \int_0^{P_r} \left(Z^0 - 1\right)\frac{dP_r}{P} \text{ and } \ln\phi^1 \equiv \int_0^{P_r} Z^1 \frac{dP_r}{P}$$

The values of ϕ^0 and ϕ^1 may be obtained from tables such as those presented by Lee and Kesler (1975). The tabulated data may also be represented graphically and can be found in Lee and Kesler (1975), Perry and Green (1998) and Smith et al. (1996).

The Pitzer type correlations are given for pure components only, it is however possible to obtain properties for mixtures. This is done through the use of pseudo-parameters (defined for a mixture):

$$T_{pC} = \sum_i x_i T_{Ci}$$

$$P_{pC} = \sum_i x_i P_{Ci}$$

$$\omega_{pC} = \sum_i x_i \omega_{Ci}$$

Although these parameters are used to obtain properties for the mixture, they have no physical significance for the mixture and the correlations are not suitable for highly polar substances (Van Ness and Abbott, 1982). Although the correlation for only the fugacity coefficient is discussed in this work, Pitzer-type correlations are available for other properties (such as the reduced enthalpy). The reader is referred to the texts of Smith et al. (1996) and the publication of Lee and Kesler (1975) for further detail.

3.7.2 Equations of state and the fugacity coefficients

As stated earlier the fugacity coefficient may be evaluated analytically from equations of state using Eq. 3-33. The Pitzer type correlations are developed for a class of substances, which means that accuracy may be compromised for specific compounds. Further, they are limited to non-polar chemicals. The method for determining fugacity coefficients from the virial equation of state and cubic equations of state shall be described.

3.7.2.1 The virial equation of state

The virial equation of state has its theoretical basis in statistical mechanics. At constant temperature and composition, the compressibility factor may be considered a function of molar density $(\rho \equiv 1/V)$ and can be represented by a Taylor series expansion (Van Ness and Abbott, 1982):

$$Z = Z_0 + \sum_{m=1}^{\infty} W_m (\rho - \rho_0)^m \tag{3-44}$$

$$\text{where } W_m \equiv \frac{1}{m!}\left(\frac{\partial^m Z}{\partial \rho^m}\right)_{T,y,\rho_0}$$

Z_0 and ρ_0 are measured at a reference state, which is chosen to be a real gas at zero pressure in this case, therefore $Z_0 = 1$ and $\rho_0 = 0$. The virial equation in density, referred to as the Leiden form after the first worker to cite the equation (Prausnitz et al., 1986), is now written as:

$$Z = 1 + \sum_{m=1}^{\infty} W_m \rho^m \tag{3-45}$$

$$\text{where } W_m \equiv \frac{1}{m!}\left(\frac{\partial^m Z}{\partial \rho^m}\right)_{T,y,\rho_0=0}$$

We define the virial coefficients B, C, etc.:

$$B \equiv W_1 = \left(\frac{\partial Z}{\partial \rho}\right), \quad C \equiv W_2 = \left(\frac{\partial^2 Z}{\partial \rho^2}\right), \quad \cdots$$

The composition dependencies of B, C, etc. are given (exactly by statistical mechanics) by the following (Van Ness and Abbott, 1982):

$$B = \sum_i \sum_j y_i y_j B_{ij} \tag{3-46}$$

$$\text{and } C = \sum_i \sum_j \sum_k y_i y_j y_k C_{ijk}, \quad \cdots$$

B_{ii} and B_{jj} are pure component properties which may be calculated from correlations (to be discussed shortly). The evaluation of B_{ij} (=B_{ji}), the cross coefficient (a mixture property), shall also be discussed in due course. The exact composition dependence for mixtures shown in Eq. 3-46 is a particularly attractive feature of the virial equation of state.

The virial equation may be written in pressure (taking the real gas at zero pressure to be the reference state once again):

$$Z = 1 + \sum_{m=1}^{\infty} W'_m P^m \tag{3-47}$$

$$\text{where } W'_m \equiv \frac{1}{m!}\left(\frac{\partial^m Z}{\partial \rho^m}\right)_{T,y,\rho_0=0}$$

The expansion in pressure (Eq. 3-47) is referred to as the Berlin form after the first worker to cite the equation (Prausnitz et al., 1986). Analogous to the expansion in density, the following may be defined:

$$B' \equiv W'_1 = \left(\frac{\partial Z}{\partial \rho}\right) = \frac{B}{RT}, \quad C' \equiv W'_2 = \left(\frac{\partial^2 Z}{\partial \rho^2}\right) = \frac{C - B^2}{(RT)^2}, \quad \cdots$$

Eqs. 3-45 and 3-47 are infinite series and reduce to the ideal gas equation if all the terms in the summation are neglected. For systems at low pressure it is sufficient to consider just one term from the summation (Perry and Green, 1998) and the two-term virial equation of state is given by:

$$Z = 1 + \frac{BP}{RT} \tag{3-48}$$

It follows that:

$$\overline{Z}_i = 1 + \left(\frac{\partial (nB)}{\partial n_i}\right)_{T,n_j} \frac{P}{RT} \tag{3-49}$$

Considering Eqs. 3-33, 3-47 and 3-49, we evaluate the fugacity coefficient for a binary mixture from:

$$\ln\hat{\phi}_i = \frac{P}{RT}\left(B_{jj} + y_j^2\delta_{12}\right) \tag{3-50}$$

$$\text{where } \delta_{12} \equiv 2B_{12} - B_{11} - B_{22}$$

For a multi-component mixture:

$$\ln\hat{\phi}_k = \frac{P}{RT}\left[B_{kk} + \frac{1}{2}\sum_i\sum_j y_i y_j\left(2\delta_{ik} - \delta_{ij}\right)\right] \tag{3-51}$$

$$\text{where } \delta_{ij} \equiv 2B_{ij} - B_{ii} - B_{jj}$$

$$\text{and } \delta_{ik} \equiv 2B_{ik} - B_{ii} - B_{kk}$$

The applicability of the two-term virial equation of state is up to about 5bar. Many methods are available for calculating second virial coefficients, three of the most popular methods are briefly discussed:

3.7.2.1.1 Pitzer-type correlation

Prausnitz et al. (1986) explains how the Pitzer-type correlation may be used to calculate second virial coefficients. The method is briefly described in this section. Eqs. 3-42 and 3-48 together yield:

$$B_{ij} = \frac{RT_{Cij}}{P_{Cij}}\left(B^{(0)} + \omega_{ij}B^{(1)}\right) \tag{3-52}$$

The values for B^0 and B^1 are represented by:

$$B^{(0)} = 0.083 - \frac{0.422}{T_r^{1.6}} \quad \text{and} \quad B^{(1)} = 0.139 - \frac{0.172}{T_r^{4.2}} \text{ Smith et al. (1996)}$$

or

$$B^{(0)} = 0.1445 - \frac{0.330}{T_r} - \frac{0.1385}{T_r^2} - \frac{0.0121}{T_r^3}$$

$$\text{and } B^{(1)} = 0.073 + \frac{0.46}{T_r} - \frac{0.50}{T_r^2} - \frac{0.097}{T_r^3} - \frac{0.0073}{T_r^8} \quad \text{Pitzer and Curl (1957)}$$

Combining rules (for T_C, P_C and ω) have been proposed by Prausnitz (1986) so that the cross virial coefficient may be evaluated. The reader is referred to this text for the combining rules. The method is limited to systems where the two-term virial equation of state is valid. It is also unable to handle systems containing polar or associating molecules.

3.7.2.1.2 Correlation of Tsonopoulos

The empirical correlation of Tsonopoulos (1974) is a modification of the Pitzer-Curl correlation for calculating second virial coefficients (Pitzer and Curl, 1957). Tsonopoulos (1974) presents expressions applicable to both non-polar (where the dipole moment is zero) and polar chemicals such as ketones, aldehydes, alcohols, etc.

For **non-polar compounds** Tsonopoulos presents the following modifications to the Pitzer-Curl correlations (shown in the previous section) based on experimental data available at that time:

$$B^{(0)} = \left(B^{(0)}\right)_{Pitzer-Curl} - \frac{0.000607}{T_r^8}$$

$$\text{and } B^{(1)} = 0.0637 + \frac{0.331}{T_r^2} - \frac{0.432}{T_r^3} - \frac{0.008}{T_r^8}$$

The virial coefficient is given by Eq. 3-52.

For **polar but non-hydrogen bonding chemicals** (such as ketones and acetaldehydes), Tsonopoulos modifies Eq. 3-52 by including a third term to the conventional Pitzer-Curl equation. The following equation is for the case of a pure component:

$$B = \frac{RT_C}{P_C}\left(B^{(0)} + \omega_{ij} B^{(1)} + B^{(2)}\right) \tag{3-53}$$

where $B^{(3)} = \frac{a}{T_r^6}$ and a is a function of the reduced dipole moment $\left(\mu_r = \frac{10^5 \mu_D^2 P_C}{T_C^2} \right)$.

Expressions for a in terms of μ_r are available for different classes of chemicals in Tsonopoulos (1974). Values for the dipole moment (μ_D) of several chemicals may be found in McClellan (1974) or calculated using molecular mechanics (by simulation software such as CS Chem3D Ultra v6.0, CambridgeSoft.com).

Hydrogen bonding polar compounds are made up of molecules that tend to associate with each other through hydrogen bonds (dimerisation). The latter makes the polar contribution to the second virial coefficient more complicated (Tsonopolous, 1974). The second virial coefficient may be calculated from Eq. 3-52, however $B^{(2)}$ is now given by:

$$B^{(2)} = \frac{a}{T_r^6} - \frac{b}{T_r^8}$$

The parameter a was chosen to be constant by Tsonopoulos (1974) and b was expressed in terms of μ_r. The reader is referred to the publication for more suggested values for a and b.

Although Eq. 3-42 shows how pure component second virial coefficients may be calculated, the method may be extended to cross virial coefficients (and hence mixtures) using combining rules (as mentioned in the previous section). Tsonopoulos (1974) suggests combining rules and the reader is therefore referred to this publication once again for these rules.

3.7.2.1.3 Hayden and O' Connell method

The method described by Hayden and O' Connell (1975) does not offer the simplicity of the Pitzer-type correlations. It is, however, an accurate predictive method that requires only critical properties and molecular parameters that may be estimated from the molecular structure. As the method consists of many equations, the discussion presented in this work will include only the most relevant. The reader is referred to the publication of Hayden and O' Connell (1975) for more detail. The text of Prausnitz et al. (1980) presents the equations such that it may readily be written in the form of a computer program.

The second virial coefficient is made up of different types of intermolecular forces (Hayden and O' Connell, 1975). For compounds that do not experience non-classical interactions (such as hydrogen bonding):

$$B_{total} = B_{free} + B_{metastable} + B_{bound} \tag{3-54}$$

The terms $B_{metastable}$ and B_{bound} describe molecular pairs that are in a bound or metastably bound state. The molecules may be in a bound state despite experiencing only classical interactions such as non-polar repulsion and attraction. The metastable and bound terms are combined and an analytical expression in terms of temperature and reduced dipole moment may be found in Hayden and O' Connell (1975).

The Pitzer-type equations show that a third parameter (such as the acentric factor) is sufficient to describe the properties of non-polar fluids. In order to calculate B_{free} (the contribution from interactions when the distance between molecules is large), the method instead makes use of the mean radius of gyration as a quantity to describe non-sphericity of non-polar forces. Its use is preferred over the accentric factor as the latter is affected by complexing interactions (such as association) which the method attempts to account for as well. The cases of non-polar substances, polar non-associating chemicals and polar associating chemicals are considered separately for expressing B_{free} for pure components. This ensures that cross virial coefficients are calculated more accurately for mixtures where both components may not be classified as non-polar for example.

For **non-polar substances** the effect of non-polar non-sphericity on B_{free} was considered by Hayden and O' Connell (1975). The authors present an analytical expression for B_{free} based on the hydrocarbon data available at that time (such as principle moments of inertia and critical properties). The second virial coefficient may then be calculated from Eq. 3-54.

The effect of large dipole moments on the critical properties was accounted for when calculating B_{free} for **polar non-associating compounds.** The reader is referred to Hayden and O' Connell (1975) for detail on how this may be achieved using angle averaging. The authors present an analytical expression for B_{free} based on data available at that time for halogenated and oxygenated substances that do not associate. The second virial coefficient may be then calculated from Eq. 3-54.

Hayden and O 'Connell (1975) describe the second virial coefficient of **polar associating compounds** (such as alcohols and carboxylic acids) by the following equation:

$$B_{total} = B_{free} + B_{metastable} + B_{bound} + B_{chem} \tag{3-55}$$

B_{chem} is the contribution of the chemical interactions (hydrogen bonding) to the second virial coefficient. Hayden and O' Connell (1975) present an expression for B_{chem} by correlating the association contribution to the second virial coefficient as an equilibrium constant (Nothnagel et al., 1973). The authors also account for the effect of association on the critical properties. Further detail may be found in the publication. The other terms in Eq. 3-55 may be evaluated as before.

Combining rules are used to calculate cross virial coefficients as in the previous methods. These rules were developed by Hayden and O' Connell (1975) and were based on available data at the time and may be found in their publication. The method requires the following data:

- Critical pressure and temperature
  References of sources for P_C and T_C are given in the "Corresponding states correlation and the fugacity coefficient" section.
- Mean radius of gyration
  May be estimated from the parachor (P') (Hayden and O' Connell, 1975):

$$P' = 50 + 7.6R' + 13.75R'^2$$

  The parachor may be estimated by a group contribution method as given in Reid et al. (1988).
- Dipole moment
  References of sources for dipole moments are given in the "Correlation of Tsonopoulos" section.
- Solvation and association parameters
  These values may be found in Prausnitz et al. (1980).

In general, the method yields results not significantly better than the correlation of Tsonopoulos (1974). It is however better capable of predicting values for pure chemicals and mixtures that associate (Hayden and O' Connell, 1975). The Hayden and O' Connell method is suited for complex molecules where no data are available and is popular in VLE calculations.

3.7.2.1.4 Other methods

Other methods of estimating second virial coefficients include:

- Black (1958)
- O' Connell and Prausnitz (1967) or the "extended Pitzer" method
  Unlike the Pitzer-type, which is generalised, this method uses some empirical parameters for complex molecules.
- Kreglewski (1969)
- Nothnagel et al. (1972)
  Predicts values from a correlation that fits virial coefficient data.

These methods will not be discussed in this work and the reader is referred to the above-mentioned publications. A comparison of results of the various methods may be found in Hayden and O 'Connell (1975). The Hayden and O' Connell and Tsonopoulos methods were shown to be more accurate.

3.7.2.2 Cubic equations of state

Cubic equations of state are able to accurately describe *PVT* behaviour over a large range of temperature and pressure without becoming overly complicated (Van Ness and Abbott, 1982). The equations are cubic with respect to molar volume and are the simplest polynomial type equations able to represent both liquid and vapour behaviour (Smith et al., 1996). All the cubic equations of state have the general form:

$$P = \frac{RT}{V-b} - \frac{a(V-\eta)}{(V-b)(V^2+\delta V+\varepsilon)} \tag{3-56}$$

The parameters b, a, δ, η and ε are functions of temperature and composition.

The first cubic equation of state was the Van der Waals equation (Smith et al., 1996) and is the simplest non-trivial case of Eq. 3-56 (the trivial case being the ideal gas law):

$$P = \frac{RT}{V-b} - \frac{a}{V^2} \tag{3-57}$$

The Redlich-Kwong equation (Redlich and Kwong, 1949) is another example of a cubic equation of state:

$$P = \frac{RT}{V-b} - \frac{a}{T^{1/2}V(V+b)} \tag{3-58}$$

$$a = \frac{0.42748R^2T_C^{2.5}}{P_C} \quad \text{and} \quad b = \frac{0.08664RT_C}{P_C}$$

The reader is referred to the text of Smith et al. (1996) and Redlich and Kwong (1949) for further details about Eq. 3-58 and how the expressions for *a* and *b* are derived. The parameters *a* and b may be evaluated for mixtures using mixing rules. Unlike the virial equation of state (for which the exact composition dependence of the parameters is known), mixing rules must be proposed for the cubic equations of state (Perry and Green, 1998). The following are the common mixing rules for the Redlich Kwong equation:

$$a = \sum_i \sum_j y_i y_j a_{ij} \quad \text{and} \quad b = \sum_i y_i b_i$$

The Redlich Kwong equation does not often yield accurate results for VLE calculations (Perry and Green, 1998). A modification of Eq. 3-58 called the Soave Redlich Kwong (SRK) equation (Soave, 1972) is one of two popular methods that gives more satisfactory results for VLE calculations. The Peng Robinson (PR) equation (Peng and Robinson, 1976) is the second preferred expression. The SRK and PR equations were developed specifically for VLE calculations. The applicability of the equations was, however, limited by inadequate empirical mixing rules. The class of theoretically based mixing rules introduced by Wong and Sandler (1992) extended the application of cubic equations of state. The mixing rules, SRK and PR equations will not be described, as the virial equation of state is sufficiently accurate for low pressure VLE calculations. The reader is referred to the before mentioned publications for further detail.

3.8 Excess properties and the activity coefficient

The ideal gas model was used to compare the behaviour of real gases through the residual properties. For the liquid phase, the ideal solution serves the same purpose and the comparison is done through excess properties (the difference between real and ideal solution behaviour). The molar Gibbs energy is written as:

$$\overline{G}_i^{id} \equiv G_i + RT \ln x_i \tag{3-59}$$

The following may also be written for an ideal solution:

$$\mu_i^{id} = \Gamma_i(T) + RT \ln \hat{f}_i^{id} \tag{3-60}$$

Eqs. 3-22, 3-59 and 3-60 together show that:

$$\hat{f}_i^{id} = x_i f_i \tag{3-61}$$

The definition of excess properties is analogous to that of residual properties:

$$M^E \equiv M - M^{id} \tag{3-62}$$

For a real fluid the molar Gibbs energy is given by:

$$\overline{G}_i = \Gamma_i(T) + RT \ln \hat{f}_i \tag{3-63}$$

and

$$\overline{G}_i^E = \overline{G}_i - \mu_i^{id} = RT \ln \gamma_i \tag{3-64}$$

where $\gamma_i \equiv \dfrac{\hat{f}_i}{x_i f_i}$ is the activity coefficient of species i in solution. For an ideal solution $\gamma_i = 1$.

The fundamental excess property relation is given by:

$$d\left(\frac{nG^E}{RT}\right) = \frac{nV^E}{RT}dP + \frac{nH^E}{RT^2}dT + \sum_i \frac{\overline{G}_i^E}{RT}dn_i \tag{3-65}$$

It can be seen from Eqs. 3-64 and 3-65 that:

$$\ln \gamma_i = \left(\frac{\partial\left(nG^E / RT\right)}{\partial n_i}\right)_{P,T,n_j} \tag{3-66}$$

The activity coefficient may therefore be calculated from proposed expressions for the excess Gibbs energy. This is an essential requirement for the Gamma-Phi representation of VLE (discussed later in this chapter).

3.9 Excess Gibbs energy models and the activity coefficient

Evaluating activity coefficients from Eq. 3-66 requires that an expression for the excess Gibbs energy must be known. Many such expressions have been proposed, however, the following equations are the most popular:

- Wohl's expansion (Margules and Van Laar)
- Wilson
- NRTL
- UNIQUAC

Each of the above shall be briefly discussed for the case of binary mixtures. In many cases only binary parameters are necessary to calculate multi-component VLE. These methods are sufficiently complicated that the computations are best made using a computer program. The reader is referred to Prausnitz et al. (1986) for details on the computer techniques. When temperature is constant the models represent the excess Gibbs energy as a function of composition and pressure. The effect of pressure is usually ignored at no expense of accuracy for low pressure computations (Prausntiz et al., 1986). The models also include adjustable parameters which may be temperature dependant and are determined from experimental isothermal data discussed in detail later in this chapter. It is not strictly correct to assume temperature independence of model parameters if isobaric data are available (Prausnitz et al., 1986). The assumption is only valid in the case of an athermal mixture, i.e. where the components mix isothermally and isobarically without the evolution or absorption of heat. For practical applications the assumption can be made if the temperature range is small. Prausnitz et al. (1986) present a data set measured for the system n-propanol + water at atmospheric pressure that is well represented by the Van Laar equation. Once the adjustable parameters have been determined activity coefficients (and hence VLE data) may be both interpolated and extrapolated for unmeasured compositions. Adjustable parameters can also be fixed using infinite dilution activity coefficients and (in the case of systems that display a miscibility gap) from mutual solubility data (Prausnitz et al., 1986).

3.9.1 Wohl's expansion

The Wohl expansion expresses the excess Gibbs energy as a power series in terms of effective volume fractions (z_1 and z_2). The general form is given by:

$$\frac{G^E}{RT(x_1q_1 + x_2q_2)} = 2a_{12}z_1z_2 + 3a_{112}z_1^2z_2 + 3a_{122}z_1z_2^2 + 4a_{1112}z_1^3z_2 + 4a_{1222}z_1z_2^3 + 6a_{1122}z_1^2z_2^2 + \ldots \quad (3\text{-}67)$$

where

$$z_1 \equiv \frac{x_1q_1}{x_1q_1 + x_2q_2} \quad \text{and} \quad z_2 \equiv \frac{x_2q_2}{x_1q_1 + x_2q_2}$$

q and a are two types of parameters. The q's are effective volumes of a pure component and for non-polar mixtures it may be assumed the that the ratio of the q's is the same as the ratio of liquid molar volumes. The significance of the a's (the interaction coefficients) is similar to that of the virial coefficients (Prausnitz et al., 1986). Many models have been derived from Wohl's expansion; two very popular expressions (viz. the Margules and Van Laar) shall be discussed briefly.

3.9.1.1 Margules equation

The Margules equation assumes that the molecular size of the constituent chemicals of a binary mixture are the same ($q_1 = q_2$). If the terms greater than the fourth power are neglected and when Eq. 3-66 is applied to Wohl's expansion the four-suffix Margules equation is obtained:

$$\ln\gamma_1 = A'_M x_2^2 + B'_M x_2^3 + C'_M x_2^4 \quad (3\text{-}68)$$

$$\ln\gamma_2 = \left(A'_M + \frac{3}{2}B'_M + 2C'_M\right)x_1^2 - \left(B'_M + \frac{8}{3}C'_M\right)x_1^3 + C'_M x_1^4 \quad (3\text{-}69)$$

where

$$A'_M = q(2a_{12} + 6a_{112} - 3a_{122} + 12a_{1112} - 6a_{1122})$$

$$B'_M = q(6a_{122} - 6a_{112} - 24a_{1112} - 8a_{1222} + 24a_{1122})$$
$$C'_M = q(12a_{1112} + 12a_{1222} - 18a_{1122})$$

Setting C'_M to zero and removing the fourth order composition term reduces the method to the three-suffix Margules equation. The two-suffix form is obtained by truncating the composition dependence at the second order term and setting B'_M and C'_M to zero. Prausnitz et al. (1986 lists the following features of the Margules equation:

- Despite being derived from a simplification that suggests the molar volumes are similar, the three-suffix version gives good representation of many systems where this is not so.
- The four-suffix form is most applicable when many precise data points are available.
- The two and three suffix versions are most useful for smoothing data sets containing only a few points and are useful for interpolation.
- An additional advantage of the three-suffix model is that it is capable of representing maxima and minima in activity coefficient plots (although these are rare).

3.9.1.2 Van Laar equation

The Van Laar equation is also a special case of the Wohl expansion. We consider the case of the constituents of the binary system being "not chemically dissimilar" but having different molar volumes. Prausntiz et al. (1986) quotes benzene with iso-octane as an example. All the interaction parameters except the binary parameter (a_{12}) may be neglected and the Wohl expansion reduces to:

$$\frac{G^E}{RT} = \frac{2a_{12}x_1x_2q_1q_2}{x_1q_1 + x_2q_2} \tag{3-70}$$

Applying Eq. 3-66 to find the expressions for the activity coefficients:

$$\ln\gamma_1 = \frac{A_{VL}}{\left(1 + \frac{A_{VL}}{B_{VL}}\frac{x_1}{x_2}\right)^2} \quad \text{and} \quad \ln\gamma_2 = \frac{B_{VL}}{\left(1 + \frac{B_{VL}}{A_{VL}}\frac{x_2}{x_1}\right)^2}$$

where $A_{VL} = 2q_1a_{12}$ and $B_{VL} = 2q_2a_{12}$. Despite the derivation suggesting that the Van Laar equation is suitable for simple, non-polar liquids, it has been found to represent some complex

systems well (Prausnitz et al., 1986). The method is popular as it offers the advantages of being flexible yet comparatively mathematically simple.

3.9.2 The Wilson model

The Wilson equation like the NRTL and UNIQUAC equations (discussed shortly) can not be derived from the Wohl expansion. It is based on the notion that the interactions between molecules depend primarily on local concentrations, which are expressed as volume fractions (Walas, 1985). The derivation of the Wilson equation is presented by Prausnitz et al. (1986). The excess Gibbs energy is expressed as:

$$\frac{G^E}{RT} = -x_1 \ln(x_1 + x_2\Lambda_{12}) - x_2 \ln(x_2 + x_1\Lambda_{21})$$

The expressions for the activity coefficients obtained from Eq. 3-66 are:

$$\ln\gamma_1 = -\ln(x_1 + x_2\Lambda_{12}) + x_2\left(\frac{\Lambda_{12}}{x_1 + x_2\Lambda_{12}} - \frac{\Lambda_{21}}{x_2 + x_1\Lambda_{21}}\right)$$

$$\ln\gamma_2 = -\ln(x_2 + x_{12}\Lambda_{21}) + x_1\left(\frac{\Lambda_{12}}{x_1 + x_2\Lambda_{12}} - \frac{\Lambda_{21}}{x_2 + x_1\Lambda_{21}}\right)$$

where

$$\Lambda_{12} = \frac{V_2}{V_1}\exp\left(-\frac{\lambda_{12} - \lambda_{11}}{RT}\right)$$

$$\Lambda_{21} = \frac{V_1}{V_2}\exp\left(-\frac{\lambda_{21} - \lambda_{22}}{RT}\right)$$

As seen in the equations above, the Wilson equation has two adjustable parameters viz. (λ_{12}-λ_{11})and (λ_{21}-λ_{22}). The Wilson model is considered to be superior to other models such as the Van Laar and Margules expressions (Raal and Mühlbauer, 1998). For accurate computations the temperature dependence of the adjustable parameters may not be ignored, although they are fairly temperature insensitive over a modest temperature range (Prausnitz et al., 1986). The

Wilson equation may therefore be applied to isobaric data if the temperature range is not extensive. The model can be applied to multi-component systems using parameters from the constituent binary systems. The Wilson equation is not, however, able to predict liquid immiscibility or extrema in the activity coefficients (Prausnitz et al., 1986). A modification to the equation, discussed by Walas (1985), referred to as the T-K Wilson equation is able to predict limited miscibility. The reader is referred to this text for more detail.

3.9.3 The NRTL equation

The NRTL (Non-random two liquid) equation is a two cell theory (Walas, 1985). In a binary system it is assumed that the liquid is made up of two types of cells, viz. molecules of species 1 at the centre of molecules of species 1 and 2 and molecules of species 2 similarly surrounded by both species of the binary (Renon and Prausnitz, 1968). The expression for G^E and the activity coefficients are:

$$\frac{G^E}{RT} = x_1 x_2 \left(\frac{\tau_{21} G_{21}}{x_1 + x_2 G_{21}} + \frac{\tau_{12} G_{12}}{x_2 + x_1 G_{12}} \right)$$

$$\ln \gamma_1 = x_2^2 \left[\tau_{21} \left(\frac{G_{21}}{x_1 + x_2 G_{21}} \right)^2 + \left(\frac{\tau_{12} G_{12}}{(x_2 + x_1 G_{12})^2} \right) \right]$$

$$\ln \gamma_2 = x_1^2 \left[\tau_{12} \left(\frac{G_{12}}{x_2 + x_1 G_{12}} \right)^2 + \left(\frac{\tau_{21} G_{21}}{(x_1 + x_2 G_{21})^2} \right) \right]$$

where

$$G_{ij} = \exp(-\alpha_{ij} \tau_{ji})$$

$$\tau_{ji} = \frac{g_{ji} - g_{ii}}{RT}$$

The NRTL equation has 3 adjustable parameters, viz. (g_{12}-g_{11}), (g_{21}-g_{22}) and α_{12} ($=\alpha_{21}$). The adjustable parameter α_{12} is an indication of the non-randomness of the mixture and is equal to zero for a completely random mixture (Renon and Prausnitz, 1968). α_{12} was originally

suggested (by Renon and Prausnitz (1968)) to have a value of between 0.1 and 0.47 depending on the nature on the constituent chemicals. Walas (1985) states that activity coefficients are relatively insensitive to values α_{12} between 0.1 and 0.5 and in some cases a value of -1 produces results similar to those produced using 0.3. Walas (1985) further suggests that a value of 0.3 be used for non-aqueous mixtures and 0.4 for aqueous mixtures. Raal and Mühlbauer (1998) and Joseph (2001) suggest that it is best to determine α_{12} than to use a fixed value. Like the Wilson equation, the NRTL model may also be used for multi-component mixtures using binary parameters (Walas, 1985). It has the advantage over the Wilson equation in that it can be applied to liquid-liquid equilibria.

3.9.4 The UNIQUAC equation

The UNIQUAC (Universal quasi-chemical) equation, like the Wilson and NRTL models, is also based on the concept of local concentration. The NRTL and Wohl expansion type equations are expressions more suitable for excess enthalpy rather than the excess Gibbs energy (Abrams and Prausnitz, 1975). The NRTL equation also has the disadvantage of being expressed in terms of three adjustable parameters. The model stipulates that the excess Gibbs energy is composed of two parts (Walas, 1985), viz. the configurational or combinatorial part and the residual part. The configurational part is the contribution due to the differences in sizes and shapes of molecules. It attempts to describe the entropic contribution (Prausnitz et al. (1986). The residual part is the contribution due to energetic interactions between molecules that are responsible for enthalpy of mixing. The equation requires volume and surface factors (r and q) which are obtained by crystallographic measurements (Walas, 1985). These factors may also be obtained from group contributions. Prausnitz (1980) lists values for many substances and the method for obtaining parameters by group contribution may be found in Raal and Mühlbauer (1998). When the appropriate simplifying assumptions are made the UNIQUAC equation reduces to the Margules, Van Laar, Wilson and NRTL equations (Abrams and Prausnitz, 1975). The following is the expression for the excess Gibbs energy:

$$G^E = G^E(configurational) + G^E(residual)$$

$$\frac{G^E(configurational)}{RT} = x_1 \ln\frac{\Omega_1}{x_1} + x_2 \ln\frac{\Omega_2}{x_2} + \frac{Z}{2}\left(q_1 x_1 \ln\frac{\theta_1}{\Omega_1} + q_2 x_2 \ln\frac{\theta_2}{\Omega_2}\right)$$

$$\frac{G^E(residual)}{RT} = -q_1' x_1 \ln\left(\theta_i' + \theta_2'\xi_{21}\right) - q_2' x_2 \ln\left(\theta_2' + \theta_1'\xi_{12}\right)$$

$$\Omega_i = \frac{x_i r_i}{x_i r_i + x_j r_j}$$

$$\theta_i = \frac{x_i q_i}{x_i q_i + x_j q_j}$$

$$\theta'_i = \frac{x_i q'_i}{x_i q'_i + x_j q'_j}$$

$$\xi_{ij} = \exp\left(-\frac{u_{ij} - u_{ii}}{RT}\right)$$

The activity coefficients are found from:

$$\ln \gamma_i = \ln \gamma_i (configurational) + \ln \gamma_i (residual)$$

$$\ln \gamma_i (configurational) = \ln \frac{\Omega_i}{x_i} + \frac{z}{2} q_i \ln \frac{\theta_i}{\Phi_i} + \Phi_j \left(l_i - \frac{r_i}{r_j} l_j \right)$$

$$\ln \gamma_i (residual) = -q'_i \ln\left(\theta'_i + \theta'_j \xi_{ji}\right) + \theta'_j q'_i \left(\frac{\xi_{ji}}{\theta'_i + \theta'_j \xi_{ji}} - \frac{\xi_{ij}}{\theta'_j + \theta'_i \xi_{ij}} \right)$$

$$l_i = \frac{z}{2}(r_i - q_i) - (r_i - 1)$$

The equations presented in this section are for a modified version of the original UNIQUAC expression. q' has special values for water and alcohols, whereas in the original formulation $q = q'$. The UNIQUAC equation has the advantages of the previous models (predicting immiscibility and activity coefficient extrema) and is also superior in representing mixtures of widely different molecular sizes (Walas, 1985). The equation is applicable to a large range of non-electrolyte chemicals, both polar and non-polar. Although the method only has two adjustable parameters it produces good representations in most cases except where the data are highly precise and plentiful (Prausnitz et al., 1986). The UNIQUAC equation is the basis of the UNIFAC method, a group contribution method for predicting activity coefficients. The group

contribution method divides a molecule into functional groups and molecule-molecule interactions are considered to be weighted sums of the group-group interactions (Prausnitz et al., 1986). The group contributions are derived from experimental results of binary systems. The method has been successfully used to design distillation columns where experimental multi-component data were not available (Prausnitz et al., 1986). The reader is referred to the works of Fredenslund et al. (1975), Fredenslund et al. (1977a) and Fredenslund et al. (1977b) for more detail about the UNIFAC method.

3.10 Equilibrium and the criteria for equilibrium

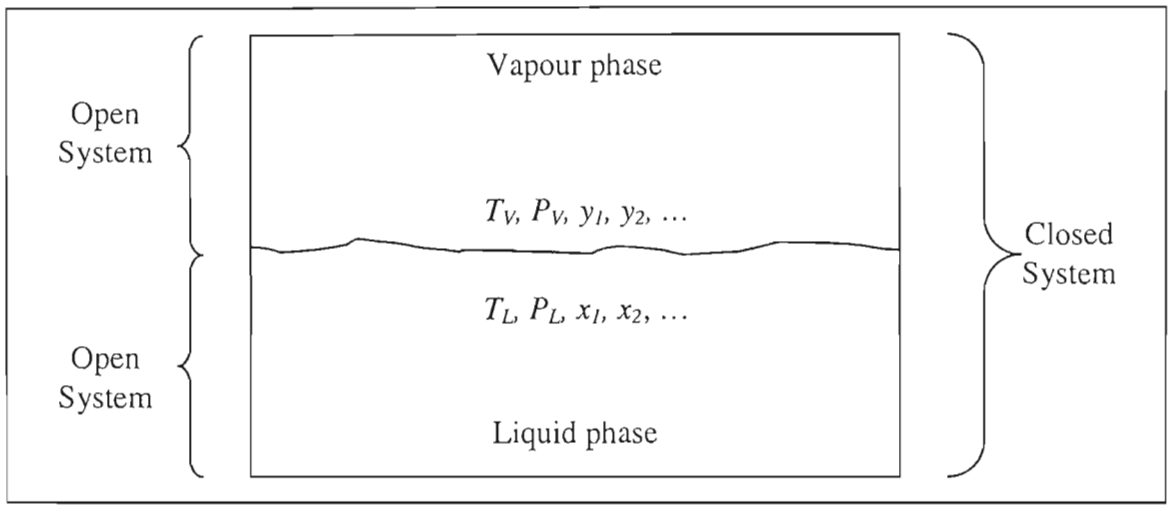

Figure 3-5: Illustration of a liquid and its vapour together constituting a closed system

Consider a mixture of chemicals contained within a closed system (see Figure 3-5). The total system is regarded as closed as no mass transfer is allowed through the boundary. The chemicals separate into a vapour and a liquid phase and the constituent chemicals distribute into each phase. The vapour and liquid are each regarded as open systems as both mass and energy may be transferred across the boundary of the phases. Figure 3-5 therefore represents two open systems, which together make a closed system.

The system is said to have achieved thermal equilibrium when the temperatures (T_1 and T_2) are the same in each phase (Perry and Green, 1998). Mechanical equilibrium requires that the pressures (P_1 and P_2) be the same in each phase. Chemical equilibrium requires that the chemical potentials of each species in both phases be the same, i.e. $\mu_i^L = \mu_i^V$. The criterion is readily extended to systems containing more than two phases.

In order to prove the criterion for phase equilibrium to be true we must consider the first and second laws of thermodynamics together. For a system in mechanical and thermal equilibrium but not in a state of phase equilibrium, the changes occurring in the system are irreversible and bring the system closer to equilibrium (Perry and Green, 1998). When Eqs. 3-1 and 3-3 are combined:

$$dU^t - dW - TdS^t \leq 0 \tag{3-71}$$

Substituting Eq. 3-4 (the expression for mechanical work) into Eq. 3-71 to yield an expression valid for both reversible and irreversible work:

$$dU^t + PdV^t - TdS^t \leq 0 \tag{3-72}$$

At constant T and P the following result is obtained:

$$d\left(U^t + PV^t - TS^t\right)_{T,P} \leq 0 \text{ or } dG^t_{T,P} \leq 0$$

The above equation shows that all irreversible processes occur in a direction such that the total Gibbs energy decreases. The equilibrium state is therefore achieved when the system is in the state of minimum total Gibbs energy. At equilibrium the differential changes experienced by the system do not affect the total Gibbs energy and hence $dG^t_{T,P} = 0$.

We write the fundamental property relation (Eq. 3-10) for the liquid and vapour phases:

$$d(nG)^L = -(nS)^L dT + (nV)^L dP + \sum_i \mu_i^L dn_i^L \tag{3-73}$$

$$d(nG)^V = -(nS)^V dT + (nV)^V dP + \sum_i \mu_i^V dn_i^V \tag{3-74}$$

The total Gibbs energy is found using Eq. 3-5 combined with Eqs. 3-73 and 3-74 and taken at constant T and P (Perry and Green, 1997):

$$dG^t_{T,P} \equiv d(nG)_{T,P} = \sum_i \mu_i^L dn_i^L + \sum_i \mu_i^V dn_i^V = 0 \tag{3-75}$$

since $dn_i^L = -dn_i^V$

$$\sum_i \left(\mu_i^L - \mu_i^V\right) dn_i = 0 \tag{3-76}$$

Smith et al. (1996) arrive at Eq. 3-76 by combining Eqs. 3-73 and 3-74, which together form a closed system. Combining the result with Eq. 3-7 then yields Eq. 3-76.

dn_i is an arbitrary quantity, therefore, it follows that $\mu_i^L = \mu_i^V$ and the chemical potential of each species must be the same in each phase for the system to judged in phase equilibrium. The prerequisite for phase equilibria to be attained is that both thermal and mechanical equilibrium be achieved first. Raal and Muhlbauer (1998) present the proof that temperature and pressure must be the same in each phase for phase equilibrium to occur.

The chemical potential has been shown to play an important role in phase equilibrium. It is, however, an inconvenient quantity to work with as it is defined in terms of internal energy and entropy (absolute values of neither are known), (Van Ness and Abbott, 1982). The chemical potential also approaches negative infinity as P and x_i tend to zero. It is preferred to work in terms of fugacity for these reasons. The equivalent criteria (in terms of fugacity) for phase equilibrium may be found by substituting Eq. 3-25 for the chemical potential. The result is that the fugacity of species i must be the same in each phase, i.e.:

$$\hat{f}_i^L = \hat{f}_i^V \tag{3-77}$$

3.11 Expressions describing vapour-liquid equilibrium

Solution thermodynamics may be used to develop equations that relate temperature, pressure, liquid phase composition and vapour phase composition for a system in phase equilibrium. The criterion for phase equilibrium shown in Eq. 3-77 may be applied to the following cases:

- The non-ideal behaviour of both the vapour and liquid phases are neglected (Raoult's Law).
- The non-ideal behaviour of the vapour phase is neglected but the liquid phase non-ideality is accounted for through the activity coefficient and hence excess Gibbs energy models (modified Raoult's Law).

- The vapour and liquid phase departure from ideal behaviour is accounted for through the fugacity coefficient calculated from an equation of state (Phi-Phi or equation of state method).
- The vapour phase non-ideality is accounted for through the fugacity coefficient (usually using an equation of state) and the liquid phase non-ideal behaviour through the activity coefficient and hence excess Gibbs energy models (Gamma-Phi or combined method).

Each of the above-mentioned expressions are only valid if the assumptions used to derive them are true. Raoult's law for example is the most limited expression, as it is the simplest. It may therefore, only be applied to low pressure data where the vapour phase correction is close to 1. The equation, however, does not yield realistic results in general and is used mainly as a standard to judge real system behaviour (Perry and Green, 1998). The applicability of the other equations shall be discussed shortly. By specifying two variables, either P or T and x_i or y_i, one is able to calculate the unspecified variables. For example, calculating P and y_i from specified T and x_i using any of the four expressions mentioned above is referred to as a bubble pressure calculation. It is required that other information be available too, such as the pure component saturated vapour pressures and adjustable parameters for the excess Gibbs energy model or equation of state. These parameters may be obtained by regressing experimental data using procedures such as the bubble pressure calculation. The bubble pressure and temperature calculations are discussed in the section that follows, as is the data regression technique using these calculation procedures. A brief derivation of each expression describing VLE and their applicability is given below.

3.11.1 Raoult's law

We first consider the simplest VLE case where the vapour may be described by the ideal gas law and the liquid is assumed to behave as an ideal solution. The resulting equation is referred to as Raoult's Law and may be used to predict VLE from only pure component vapour pressure data. It does, however, have severely limited application due to its simplicity. Raoult's law may be derived by substituting Eqs. 3-27 and 3-61 into Eq. 3-77 (the criterion for phase equilibrium):

$$y_i P = x_i P_i^{sat} \tag{3-78}$$

Raoult's law is primarily as a standard for comparison with real VLE behaviour (Perry and Green, 1998).

3.11.2 Modified Raoult's law

If the vapour phase is considered to be an ideal gas and the liquid phase non-ideality is accounted for through the activity coefficient, the modified Raoult's Law is obtained. From the definition of the activity coefficient we obtain that $\hat{f}_i^L = x_i \gamma_i f_i$. Substituting the latter and Eq. 3-27 (vapour phase fugacity of a species in an ideal gas mixture) into Eq. 3-77 yields:

$$y_i P = x_i \gamma_i P_i^{sat} \tag{3-79}$$

The modified Raoult's law provides more realistic VLE and is most applicable for low pressure computations (where the vapour phase deviation from ideal gas behaviour is not too large). If the activity coefficient is assumed to be independent of pressure, γ_i may be calculated from the excess Gibbs energy models discussed earlier.

3.11.3 Equation of state approach

The equation of state approach is preferred for systems at elevated pressure (Perry and Green, 1998). The vapour phase non-ideality at these conditions, therefore, may not be ignored. Both the vapour and liquid-phase deviations from ideal behaviour are accounted for using an equation of state. This requires the equation of state to be able to accurately represent both liquid and vapour properties, particularly the volumetric behaviour of liquids (Perry and Green, 1998). The Soave-Redlich-Kwong and Peng-Robinson equations of state, as well as the Wong-Sandler mixing rules (referred to earlier in this chapter) were specifically developed for use in the equation of state approach. A fugacity coefficient is defined for both the liquid and vapour phases and application of Eq. 3-77 yields:

$$x_i \hat{\phi}_i^L = y_i \hat{\phi}_i^V \tag{3-80}$$

As the fugacity coefficients are function of T, P and composition the calculations are best performed using a computer program. Details of the calculation procedure will not be discussed in this work and may be found in the texts of Smith et al. (1996), Van Ness and Abbott (1982), Raal and Mühlbauer (1998) and Perry and Green (1998).

3.11.4 The Gamma-Phi approach

The Gamma-Phi approach to VLE allows one to correct for vapour phase non-ideality using an equation of state as in the method described above. The liquid phase departure from ideal behaviour is accounted for through the activity coefficient (hence excess Gibbs energy models). This is the preferred method for data measured at low pressure (Perry and Green, 1998), the equation of state may therefore be a simple type, such as the virial equation. The definition of the fugacity coefficient in solution for the vapour phase yields:

$$\hat{f}_i^V = y_i \hat{\phi}_i P \tag{3-81}$$

For the liquid phase we write from the definition of the activity coefficient:

$$\hat{f}_i^L = x_i \gamma_i f_i^L \tag{3-82}$$

The significance of the pure component liquid phase fugacity (f_i^L) given by Eq. 3-40 is now apparent. Applying the criterion for phase equilibrium (Eq. 3-77) to Eqs. 3-81 and 3-82 yields the Gamma-Phi representation of VLE:

$$x_i \gamma_i P_i^{sat} = y_i \Phi_i P \tag{3-83}$$

where

$$\Phi_i \equiv \frac{\hat{\phi}_i}{\hat{\phi}_i^{sat}} \exp\left[-\frac{V_i^L \left(P - P_i^{sat}\right)}{RT} \right] \tag{3-84}$$

The exponential term is the reciprocal of the Poynting correction factor (Eq. 3-40) and can be ignored for low pressure computations (Smith et al., 1996). Φ_i may be calculated from the fugacity coefficients. Evaluation of the fugacity coefficient by various methods was discussed elsewhere in this chapter. We choose for example the two-term virial equation of state to obtain:

$$\Phi_i = \exp\left[\frac{\left(B_{ii} - V_i\right)\left(P - P_i^{sat}\right) + P y_j^2 \delta_{ij}}{RT} \right] \tag{3-85}$$

where $\delta_{ij} \equiv 2B_{ij} - B_{ii} - B_{jj}$ and the second virial coefficients may be evaluated as before. VLE calculations using the Gamma-Phi method are discussed in the section that follows.

3.12 VLE calculations from the Gamma-Phi approach

The following types of calculations may be performed based on the Gamma-Phi representation of VLE:

- Bubble pressure
  Given T and x_i, one calculates P and y_i.
- Bubble temperature
  Given P and x_i, one calculates T and y_i.
- Dew pressure
  Given T and y_i, one calculates P and x_i.
- Dew temperature
  Given P and y_i, one calculates T and x_i.

Due to the implicit dependence of the following relationships on T, P, x_i and y_i the calculations are iterative:

$$\Phi_i = \Phi(T, P, y_1, y_2, \ldots)$$

$$\gamma_i = \gamma(T, x_1, x_2, \ldots)$$

$$P_i^{sat} = P_i^{sat}(T)$$

Note the pressure dependence is ignored in the expression for the activity coefficient (for reasons discussed previously). The procedures for the bubble pressure and temperature calculations are shown in Figures 3-6 and 3-7 (as these procedures were used in this work). The dew pressure and temperature calculations are discussed by Smith et al. (1996). Setting the Φ_i's to 1 reduces Eq. 3-83 to the modified Raoult's law, and setting both the Φ_i's and γ_i's to 1 reduces the equation to Raoult's law. The procedures (shown in Figures. 3-6 and 3-7) are therefore readily applied to both Raoult's law and the modified Raoult's law by making these simplifications. The calculation procedure for the equation of state (Phi-Phi) method can not be derived from Figures 3-6 and 3-7 but may also be found in Smith et al. (1996).

3.12.1 Bubble pressure

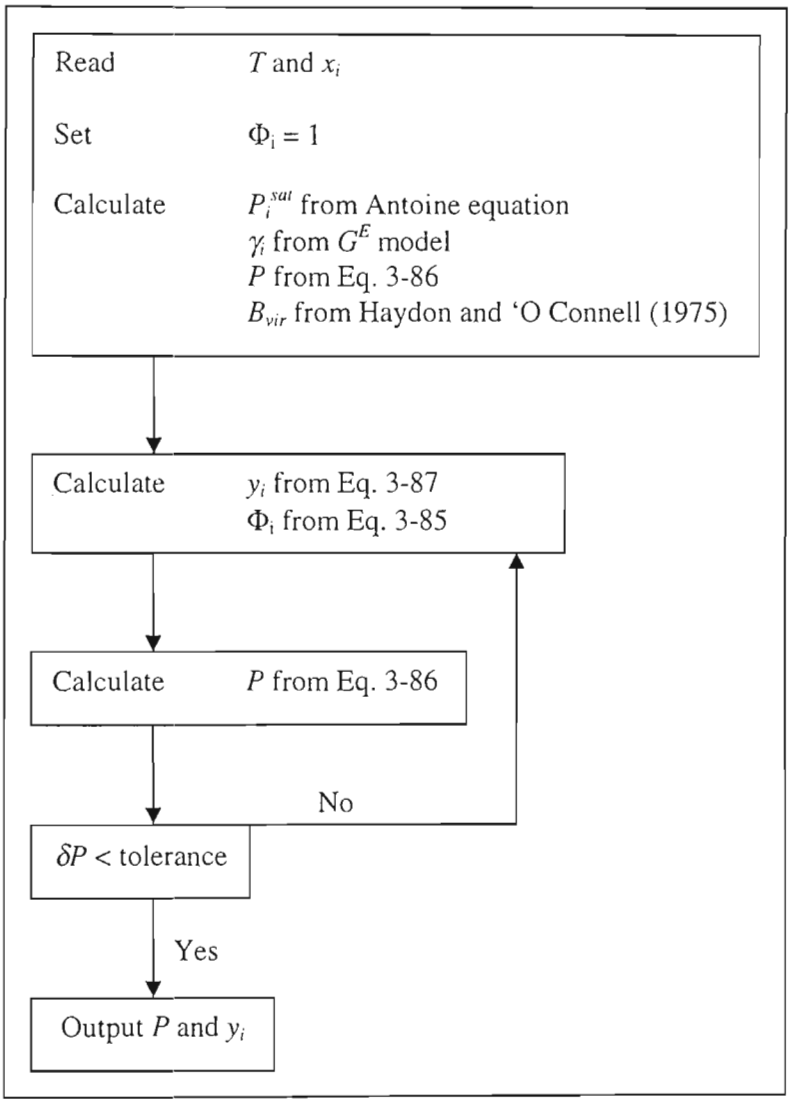

Figure 3-6: Block diagram to show the bubble pressure calculation from the Gamma-Phi representation of VLE (Smith et al., 1996)

The following equations result from Eq. 3-83 and are required for the bubble pressure calculation:

$$P = \sum_i \frac{x_i \gamma_i P_i^{sat}}{\Phi_i} \tag{3-86}$$

$$y_i = \frac{x_i \gamma_i P_i^{sat}}{\Phi_i P} \tag{3-87}$$

3.12.2 Bubble temperature

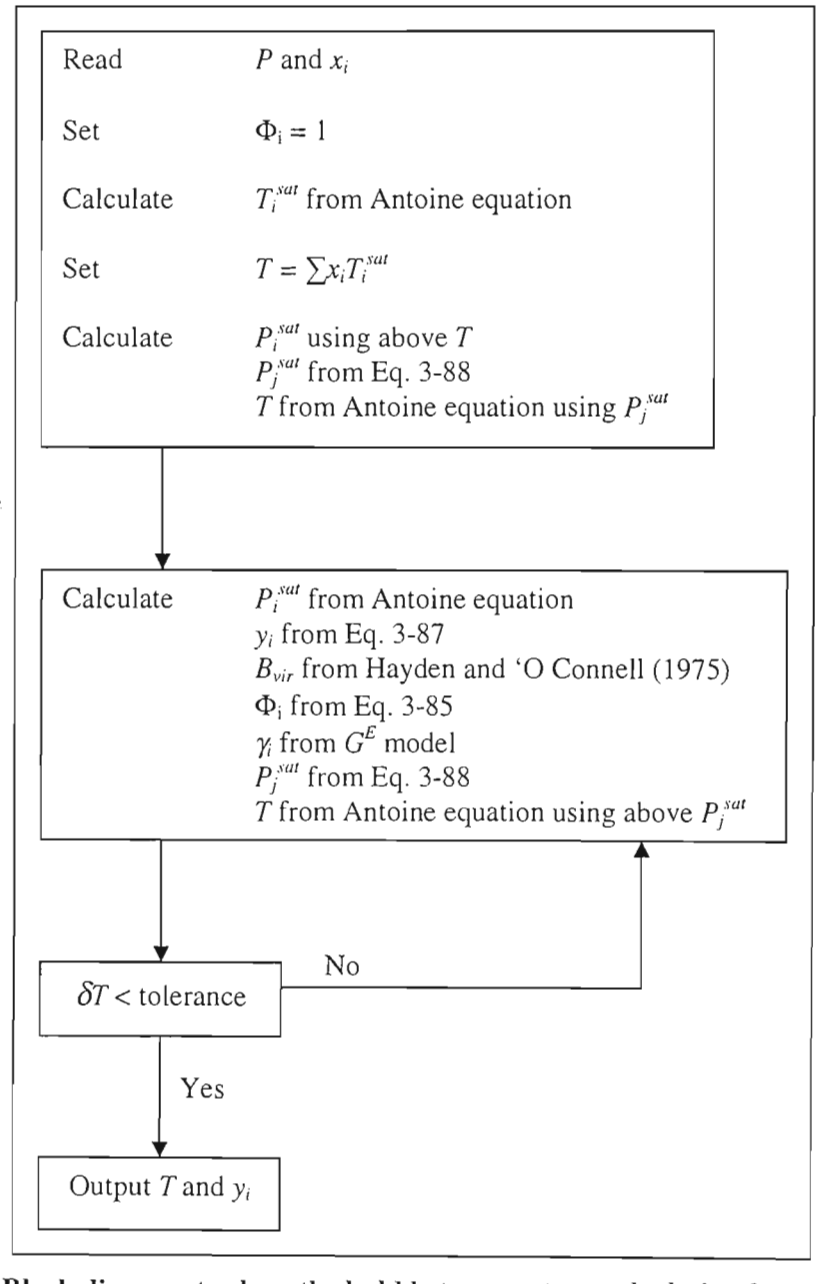

Figure 3-7: Block diagram to show the bubble temperature calculation from the Gamma-Phi representation of VLE (Smith et al., 1996)

The following equation (resulting from Eq. 3-83) together with Eqs. 3-86 and 3-87 are required for the bubble temperature calculation (Figure 3-7):

$$P_j^{sat} = \frac{P}{\sum_i \left(\frac{x_i \gamma_i}{\Phi_i} \right) \left(\frac{P_i^{sat}}{P_j^{sat}} \right)} \tag{3-88}$$

3.13 Data reduction using the Gamma-Phi approach (Model dependent method)

The calculation procedures described in the previous section may only be used to perform VLE calculations if the adjustable parameters (such as those for the Gibbs excess models) are known. The parameters can be evaluated from experimental data. By performing data reduction, one correlates the experimental data to the proposed models. The resulting set of parameters may be used for interpolating or extrapolating data within reason (discussed in the "Excess Gibbs energy and the activity coefficient" section). The bubble pressure and temperature calculations are an integral part of data reduction as shown in Figure 3-8. The reduction of both isothermal and isobaric binary VLE data is discussed briefly:

3.13.1 Isothermal data

Isothermal measurements may be obtained from either static cells or recirculating-type VLE stills (discussed in the previous chapter under experimental techniques for VLE measurement). The experiments are made at constant temperature and by varying the composition of the chemicals one obtains the following experimental data:

- Static cell - experiment temperature, total pressure for various compositions and the corresponding equilibrium liquid composition (T, P_i and x_i).
- Recirculating-type still - experiment temperature, total pressure for various compositions and the corresponding equilibrium liquid **and** vapour compositions (T, P_i, y_i and x_i).

Although data from static cell measurements appears to be missing y_i, a consequence of the Gibb-Duhem equation (Eq. 3-13) is that only three variables need to be measured and the fourth may be calculated during the data reduction procedure. This excludes the possibility of testing for thermodynamic consistency using the Gibbs-Duhem equation (discussed shortly). The procedure using a bubble pressure calculation (shown in Figure 3-8) is iterative and involves making initial guesses for the model parameters. The primary residuals (difference between experimental and values calculated from the model) are defined:

$$\delta y_i \equiv y_i^{\exp} - y_i^{calculated}$$

$$\delta P_i \equiv P_i^{\exp} - P_i^{calculated}$$

The above are referred to as primary residuals as all other residuals (such as $\delta\gamma$) may be written in terms of δP and δy (Van Ness and Abbott, 1982).

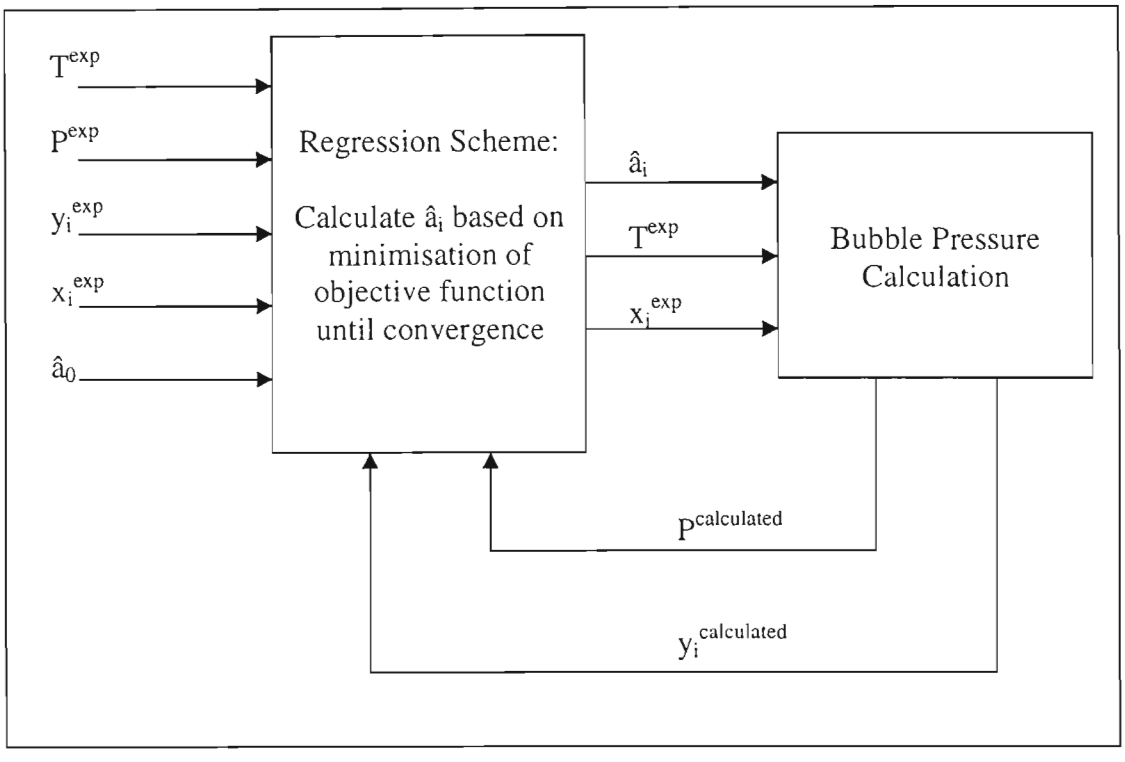

Figure 3-8: Block diagram to show how a bubble pressure calculation may be used to reduce experimental data

The residuals form the basis for the data reduction as an objective function written in terms of δP and δy is minimised. Figure 3-8 shows a set of initial guess adjustable parameters yielding values for P and y_i. The objective function is then minimised and a new set of parameters are calculated by a non-linear regression scheme. The method of Marquardt was used in this work (Marquardt, 1963). The procedure is repeated until a set of parameters within an acceptable tolerance is converged upon. A perfectly consistent data set should yield exactly the same parameters regardless of the objective used (Van Ness and Abbott, 1982). Van Ness and Abbot (1982) suggest that an objective function in terms of pressure yields the best results:

$$S = \sum (\delta P)^2 \tag{3-89}$$

This is consistent with the work of Joseph (2001). The method of data reduction requires that a number of excess Gibbs energy models are fitted to experimental data until the model that yields no systematic discrepancies is found (i.e. the fit does not show a positive or negative bias). This is referred to as Barker's method (1953) and is a model dependent method. The term

"model dependent" refers to the use of an excess Gibbs energy model. The Phi-Phi method (equation of state approach) also requires that adjustable parameters be solved for. The procedure shown in Figure 3-8 is analogous for the equation of state approach.

As discussed in the excess Gibbs energy section, the adjustable parameters obtained from isothermal data are true constants i.e. they apply throughout the concentration range for an isotherm. This is not so for an isobaric set (see section on excess Gibbs energy models). Data reduction of multiple isotherms yields the temperature dependence of the adjustable parameters (refer to Discussion chapter in this thesis).

3.13.2 Isobaric data

Isobaric VLE data are used in many practical applications (the design of distillation columns for example), (Prausnitz et al., 1986). They may be reduced in a similar way to isothermal data if the temperature dependence of the adjustable parameters is neglected (Van Ness and Abbott, 1982). As discussed in the excess Gibbs energy model section this is only true of a special class of systems that mix athermally (also discussed previously). Isobaric data may nevertheless be well represented by models such as the Van Laar and Wilson equations (which show relative insensitivity to temperature over a small range). The data reduction method is as shown in Figure 3-8 except that the bubble pressure calculation is replaced with a bubble temperature calculation and the pressure residual is replaced with the temperature residual:

$$\delta T_i \equiv T_i^{\exp} - T_i^{calculated}$$

and the objective function suggested by Van Ness and Abbott (1982) is:

$$S = \sum (\delta T)^2 \tag{3-90}$$

3.14 Data reduction using model independent methods

Methods based on Eq. 3-83 that do not assume models for the excess Gibbs energy may be used to reduce VLE data. Two such examples are those that use the coexistence equation for two-phase equilibria and the indirect model-free method of Mixon et al. (1965). Neither method will be discussed in detail, the reader is referred to the texts of Van Ness and Abbott (1982), Raal and Mühlbauer (1998) and the publication of Sayegh and Vera (1980).

Briefly the coexistence equation uses the fact that the fugacity of each species in solution is related through the Gibbs-Duhem equation to develop the coexistence equation for two-phase equilibria (Van Ness and Abbott, 1982). The equation cannot be applied to multi-component systems, neither does it apply to systems that exhibit azeotropes (Joseph, 2001).

The indirect method makes no assumption of the form of the excess Gibbs energy and uses a numerical algorithm. It requires an initial fit of an empirical expression (or set of expressions) to the P-x data such that points may be accurately interpolated (Van Ness and Abbott, 1982). The method may be applied to multi-component systems and those that exhibit azeotropes, but is not preferred due to the complex nature of the calculation procedures (Joseph, 2001).

3.15 Thermodynamic consistency tests

Solution thermodynamics allows one to judge the quality of measured VLE data. Some measurement techniques produce data with systematic errors (positive or negative bias to any correlating equation). The Gibbs-Duhem equation (Eq. 3-13) gives the constraint to how partial molar properties change with pressure and temperature. It is the basis for many consistency tests including the following, which shall be briefly described in this section:

- Area test - Herrington (1947) and Redlich and Kister (1948)
- Point test - Van Ness and Abbott (1982)
- Direct test – Van Ness (1995)

Consistency tests such as those of Kojima et al. (1990) are reviewed by Joseph (2001) and the reader is referred to this text. Before discussing the above tests, the Gibbs-Duhem equation must be derived in the form used by the tests. The summability of partial molar properties written for the activity coefficient for one mole of a binary system is:

$$\left(\frac{G^E}{RT}\right) = x_1 \ln \gamma_1 + x_2 \ln \gamma_2$$

It follows that

$$d\left(\frac{G^E}{RT}\right) = x_1 d \ln \gamma_1 + x_2 d \ln \gamma_2 + \ln \frac{\gamma_1}{\gamma_2} dx_1 \qquad (3\text{-}91)$$

The fundamental excess property relation for one mole of a binary mixture is given by

$$d\left(\frac{G^E}{RT}\right)=\frac{V^E}{RT}dP-\frac{H^E}{RT^2}dT+\ln\frac{\gamma_1}{\gamma_2}dx_1 \tag{3-92}$$

Van Ness (1995) rewrites Eq. 3-92:

$$\frac{d\left(G^E/RT\right)}{dx_1}=\ln\frac{\gamma_1}{\gamma_2}+\varepsilon \tag{3-93}$$

where

$$\varepsilon\equiv\varepsilon_T+\varepsilon_P$$

$$\varepsilon_T\equiv\frac{H^E}{RT^2}\frac{dT}{dx_1}\quad\text{and}\quad\varepsilon_P\equiv\frac{V^E}{RT}\frac{dP}{dx_1}$$

For isothermal data $\varepsilon_T = 0$ and for the isobaric case $\varepsilon_P = 0$

The Gibbs-Duhem equation for excess properties results from Eqs. 3-91 and 3-92:

$$x_1\frac{d\ln\gamma_1}{dx_1}+x_2\frac{d\ln\gamma_2}{dx_1}-\varepsilon=0 \tag{3-94}$$

Consistent data should conform to both Eqs. 3-93 and 3-94.

3.15.1 Area test

The area test was proposed by Redlich and Kister (1948). It has been a very popular test due to its simplicity. It is, however, a necessary condition that consistent data pass the area test but not a sufficient one (Van Ness, 1995). The limitations of the area test will be discussed briefly after the equation is developed.

The summability of partial molar properties may be written for experimental values of the activity coefficient to yield the experimental values of the excess Gibbs energy:

$$\left(\frac{G^E}{RT}\right)^{exp} \equiv x_1 \ln \gamma_1^{exp} + x_2 \ln \gamma_2^{exp}$$

Differentiating:

$$\frac{d\left(G^E / RT\right)^{exp}}{dx_1} = x_1 \frac{d \ln \gamma_1^{exp}}{dx_1} + \ln \gamma_1^{exp} + x_2 \frac{d \ln \gamma_2^{exp}}{dx_1} - \ln \gamma_2^{exp}$$

Adding ε - ε to the right-hand side and integrating over the composition range yields:

$$\int_0^1 d\left(\frac{G^E}{RT}\right)^{exp} = \int_0^1 \left(\ln \frac{\gamma_1^{exp}}{\gamma_2^{exp}} + \varepsilon \right) dx_1 + \int_0^1 \left(x_1 \frac{d \ln \gamma_1^{exp}}{dx_1} + x_2 \frac{d \ln \gamma_2^{exp}}{dx_1} - \varepsilon \right) dx_1 \qquad (3\text{-}95)$$

$\left(\frac{G^E}{RT}\right)^{exp} = 0$ at $x_1 = 0$ and $x_1 = 1$, and considering the Gibbs-Duhem equation (Eq. 3-94):

$$\int_0^1 \left(\ln \frac{\gamma_1^{exp}}{\gamma_2^{exp}} + \varepsilon \right) dx_1 = 0 \qquad (3\text{-}96)$$

To perform the test, one plots $\left(\ln \frac{\gamma_1^{exp}}{\gamma_2^{exp}} + \varepsilon \right)$ against x_1. ε is often and incorrectly ignored when applying the area test to both isothermal and isobaric data sets (Van Ness, 1995). The graph that results crosses the x-axis such that the integral may be broken into two areas, i.e. above the x-axis (a_1) and below the x-axis (a_2). Eq. 3-96 requires that $a_1 - a_2 = 0$ although in general it is acceptable that $\frac{a_1 - a_2}{a_1 + a_2} \leq 10\%$ (Van Ness, 1995).

Van Ness (1995) expresses concern over the use of the area test. Eq. 3-96 is derived on the presumption that the data are consistent. Further, ε being neglected is a satisfactory approximation for isothermal data, but in the case of isobaric data the excess enthalpy (heat of mixing) is often a significant quantity. It is also possible that the second integral on the right-hand side of Eq. 3-95 may be non-zero and thus provide a compensating effect to make the first integral fall within the 10% discrepancy required by the test.

Van Ness (1995) highlights a serious concern regarding the area test and pressure measurement. As mentioned earlier, determining experimental values for T, P, x_i and y_i is an over-specification of the VLE problem and the potential of inconsistency of P with y_i exists. Van Ness (1995) states that a test should check for consistency of measured P with y_i. From the Gamma-Phi representation of VLE (Eq. 3-83) it is apparent that the determination of $\frac{\gamma_1^{exp}}{\gamma_2^{exp}}$ (as required by the area test) does not require the experimental pressure. Van Ness (1995) concludes that the area test merely confirms that the pure component vapour pressure ratio is appropriate for the set of y_1-x_1.

3.15.2 Point test

Van Ness and Abbott (1982) discuss a method of testing the consistency of experimental pressure with vapour composition using data reduction. The procedure requires that the regression be performed using Barker's method (discussed earlier) and only the pressure residual in the objective function. The latter ensures that the pressure residual scatters about zero (Van Ness, 1982). Systematic errors are transferred to the vapour composition residual, which scatters about zero for consistent data. The following are required to perform the test:

- The excess Gibbs energy model must be flexible enough to allow the pressure residual to scatter about zero.
- The pure component vapour pressures must be measured carefully as incorrect values introduce systematic errors in δy_i.

It is further suggested that the average absolute deviation of δy_i be less than 0.01 (Fredenslund et al., 1977b and Danner and Gess, 1990).

3.15.3 Direct test

The area test is based on $\ln\left(\gamma_1^{exp}/\gamma_2^{exp}\right)$ and was found to be lacking as a consistency test. The residual $\delta\ln\left(\gamma_1/\gamma_2\right)$ is the basis of the direct test. Writing Eq. 3-93 and 3-94 for the experimental value of the excess Gibbs energy and combining them yields:

$$\frac{d\left(G^E/RT\right)^{exp}}{dx_1} = \ln\frac{\gamma_1^{exp}}{\gamma_2^{exp}} + \varepsilon + x_1\frac{d\ln\gamma_1^{exp}}{dx_1} + x_2\frac{d\ln\gamma_{21}^{exp}}{dx_1} - \varepsilon \qquad (3\text{-}97)$$

The excess Gibbs energy residual results when Eq. 3-97 is subtracted from Eq. 3-93:

$$\frac{d\left(\delta G^E / RT\right)}{dx_1} = \delta \ln \frac{\gamma_1}{\gamma_2} - \left(x_1 \frac{d \ln \gamma_1^{\exp}}{dx_1} + x_2 \frac{d \ln \gamma_2^{\exp}}{dx_1} - \varepsilon \right) \tag{3-98}$$

When an isothermal or isobaric data set is reduced using the following objective function $S = \sum_i \delta \frac{G^E}{RT}$ the excess Gibbs energy residual scatter about zero and Eq. 3-98 becomes:

$$\delta \ln \frac{\gamma_1}{\gamma_2} = x_1 \frac{d \ln \gamma_1^{\exp}}{dx_1} + x_2 \frac{d \ln \gamma_2^{\exp}}{dx_1} - \varepsilon \tag{3-99}$$

The Gibbs-Duhem equation (Eq. 3-94) requires that the right-hand side of Eq. 3-99 be equal to zero and the left-hand side is a measure of the deviation of the experimental data from the Gibbs-Duhem equation (Van Ness, 1995). The direct test, therefore, requires that the residual $\delta \ln \frac{\gamma_1}{\gamma_2}$ for thermodynamically consistent data, scatters about zero when the data are reduced subject to the objective function $S = \sum_i \delta \frac{G^E}{RT}$. Van Ness (1995) suggests a scale based on the root mean square (RMS) of the residual $\delta \ln \frac{\gamma_1}{\gamma_2}$ to judge the quality of experimental data. A value of "1" is assigned to data of the highest quality and 10 for a highly unsatisfactory set (see Table 3-1).

Table 3-1: Consistency Index for VLE data (Van Ness, 1995)

Index	RMS $\delta\ln(\gamma_1/\gamma_2)$	
1	>0	≤0.025
2	>0.025	≤0.050
3	>0.050	≤0.075
4	>0.075	≤0.100
5	>0.100	≤0.125
6	>0.125	≤0.150
7	>0.150	≤0.175
8	>0.175	≤0.200
9	>0.200	≤0.225
10	>0.225	

CHAPTER 4

ACTIVITY COEFFICIENTS AT INFINITE DILUTION – EXPERIMENTAL METHODS

Alessi et al. (1991) define the dilute region for a binary mixture in the following way: "*When a given molecule of type 1 does not find around itself other molecules of type 1 with which it can interact so that the only interaction will be with molecules of type 2.*" It is, therefore, important to begin by explaining how properties at such an abstract condition can be measured. Alessi et al. (1991) show that the activity coefficient of some binary systems actually reaches the value at infinite dilution at a small (though finite) concentration. The extent of the infinite dilution region is due to size or interaction energy differences. The authors state that it is not possible to quantitatively predict the region. Qualitatively, for a mixture of similar hydrocarbons the region is approximately less than 1% (mole percent). For associating species, the dilute region is very much smaller (as low as 10^{-4} mole fraction). Considering this phenomenon, the dilute region for a binary mixture can now be regarded as a state sufficiently dilute that solute-solute interactions can be ignored. Experiments to obtain infinite dilution activity coefficients can, therefore, be performed using mixtures at a finite concentration. The resulting infinite dilution activity coefficients are of considerable use (discussed in Chapter 9).

Raal and Muhlbauer (1998) present a review of experimental techniques for the measurement of infinite dilution activity coefficients (γ^{∞}). The following are listed as the principal methods:

- Inert gas stripping
- Differential ebulliometry
- Differential static
- Gas chromatography

Another extensive review may be found in Moollan (1995) where particular attention is paid to the gas chromatography method. Each of the above-mentioned methods will be discussed with particular focus on the inert gas stripping technique, as this was the method used in this study.

4.1 Inert gas stripping technique

The inert gas stripping technique is based on exponential dilution. The principle of exponential dilution will be explained. Its application to the measurement of infinite dilution activity coefficients will be discussed thereafter.

4.1.1 Exponential dilution

Fowlis and Scott (1963) used the exponential dilution method for GC detector calibration. A constant flow of inert gas is allowed to flow through a flask containing the calibrant fluid. The concentration of fluid in the exit stream will be observed to decrease exponentially as the solute is desorbed from the liquid into the gas bubbles. The method can be extended to gas phase calibration and much discussion is available in the publication of Ritter and Adams (1976).

4.1.2 The apparatus of Leroi et al. (1977)

Leroi et al. (1977) presented an apparatus and procedure to measure infinite dilution activity coefficients using the principle of exponential dilution. The central feature is the dilutor flask (Figure 4-1).

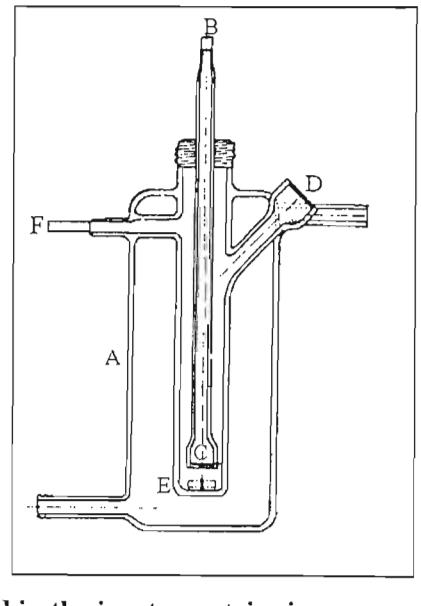

Figure 4-1: Dilutor cell used in the inert gas stripping apparatus of Leroi et al. (1977) for measuring infinite dilution activity coefficients. A - Water jacket; B - Gas inlet; C - Fritted disk gas dispersion device; D - Provision for solute introduction to cell; E - Magnetic stirrer bar; F - Gas outlet

The glass cell constructed from Pyrex contains the dilute mixture and is contained in a water jacket (A) to allow for isothermal operation. The gas enters the dilutor through a glass tube in the middle of the cell (B). The tube ends near the bottom of the cell in a fine porosity fritted disk (C) to produce a fine stream of bubbles. Provision is made (D) for introducing the small quantity of solute required by way of a 10μl syringe. The contents of the cell are stirred by means of a magnetic stirrer.

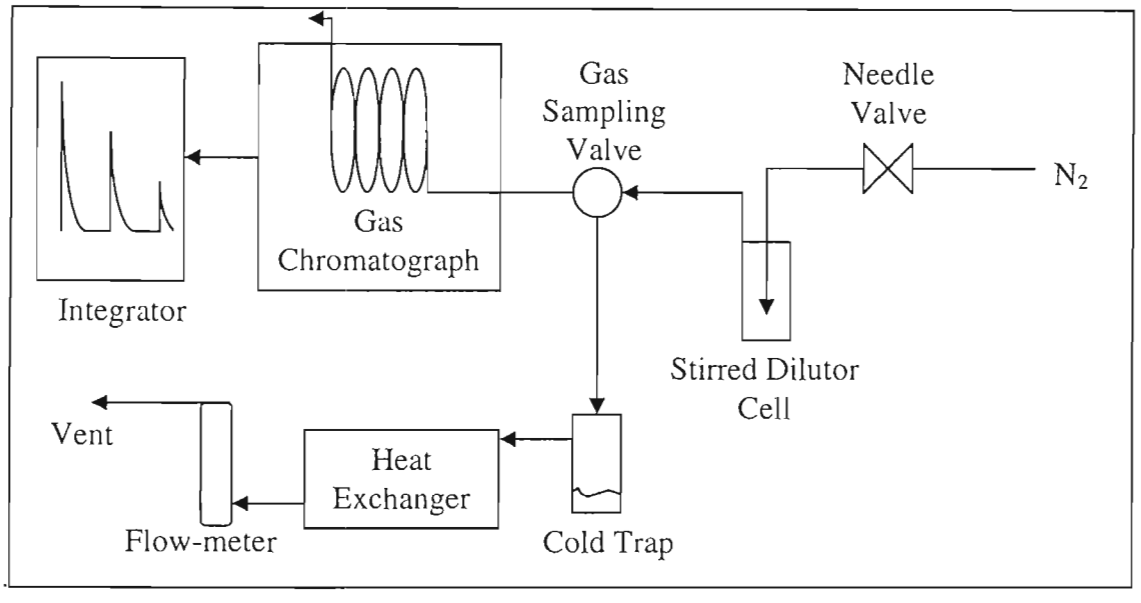

Figure 4-2: Flow Diagram of the inert gas stripping apparatus of Leroi et al. (1977) for measuring infinite dilution activity coefficients

A flow diagram of the inert gas stripping apparatus is shown if Figure 4-2. The flow of inert gas (helium in this case) is regulated with a needle valve prior to being introduced into the cell. The exit stream then enters a GC sampling valve through heated lines. The heating ensures that none of the stripped chemicals condense. The valve operates in two modes:

1. Vent

The stripping gas flows through a sample loop and is directed to a condensation trap. The stripped components are thus removed. The gas is then brought back to ambient temperature in a heat exchanger and the flow-rate measured with a soap bubble flow-meter and vented to the atmosphere.

2. Sample

Carrier gas from the GC is allowed to flow through the sample loop and the sample is analysed. The stripping gas bypasses the sample loop in this mode of operation and is vented.

Some modifications have been proposed to the inert gas stripping technique, mainly relating to the design of the dilutor flask. The method has, however, remained largely unchanged since the original apparatus of Leroi et al. (1977).

4.1.3 Mass transfer considerations and the capillary dispersion device

The inert gas stripping technique requires that the bubble size be minimised in order to maximise mass transfer into the bubble so that equilibrium can be achieved. Richon et al. (1980) presented a dilutor cell designed on the basis of mass transfer considerations in the cell. The authors demonstrate the sensitivity of the method to bubble size in order to find the appropriate bubble rise height (and hence the length of the cell). A similar calculation procedure was used to design the cell used in this study and may be found in Appendices D. The dilutor flask of Richon et al. (1980), shown in Figure 4-3 introduces the gas through capillaries (B) rather than a fritted disk. The authors observed the bubbles to be larger when using the fritted disk (consistent with the observations in this study).

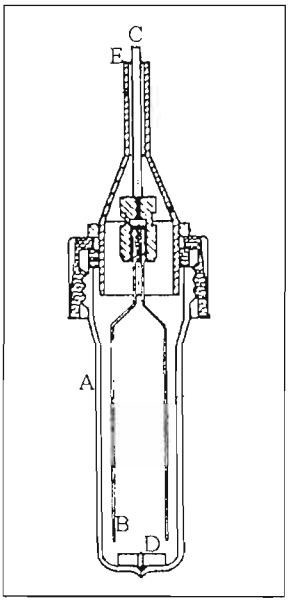

Figure 4-3: Dilutor cell used in the inert gas stripping apparatus of Richon et. al (1980) for measuring infinite dilution activity coefficients. A - Water jacket; B - Capillaries to act as gas dispersion device; C - Gas inlet; D, Magnetic stirrer bar; E - Gas outlet

4.1.4 Pre-saturation of the stripping gas (double cell technique)

Doležal et al. (1981) provide a comparison between the conventional method of Leroi et al. (1977) as described above and one that pre-saturates the inert gas with the solvent prior to entering the dilutor flask (see Figure 4-4). The gas is first directed through a cell (A) of identical design to the dilutor flask (B), containing pure solvent. The solvent saturated gas then enters the

dilutor flask containing the solute in dilute concentration in the solvent. The pre-saturation method is also known as the double cell technique (DCT) and is advised when studying systems containing high volatility solvents.

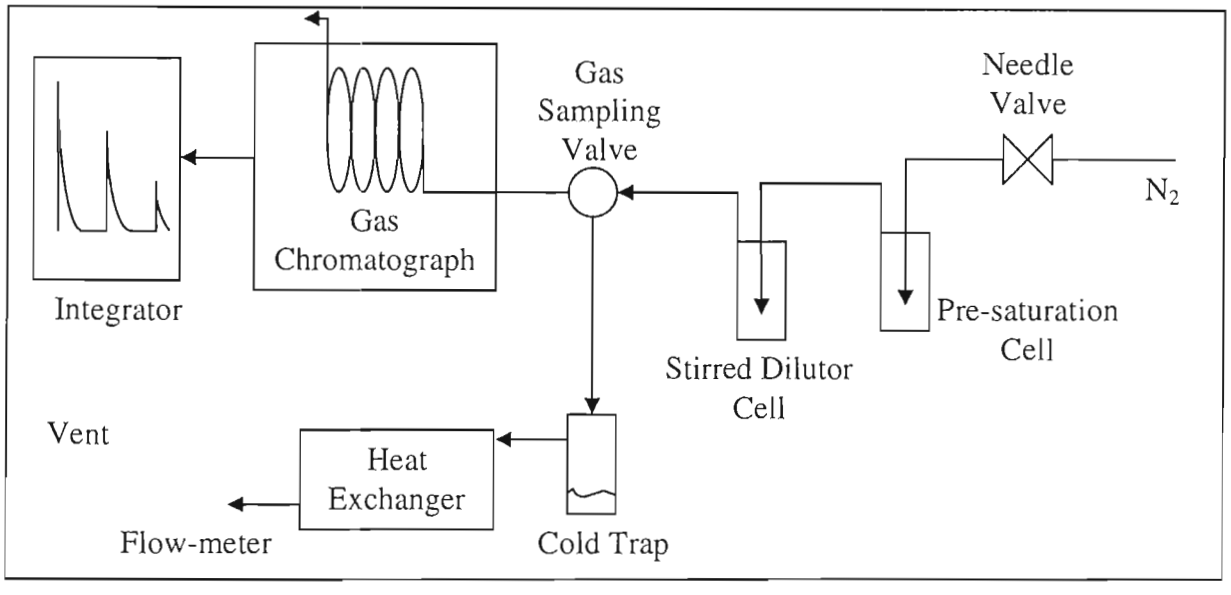

Figure 4-4: Flow diagram of apparatus of the inert gas stripping double cell technique for measuring infinite dilution activity coefficients as introduced by Doležal et al. (1981)

Bao and Han (1995) present an overall scheme suggesting when the use of the single cell technique (SCT) or DCT are most appropriate (see Figure 4-5). The authors advocate the use of the DCT when measuring systems of multiple solutes in a solvent. The infinite dilution activity coefficient of each solute in the solvent can be measured in a single experiment.

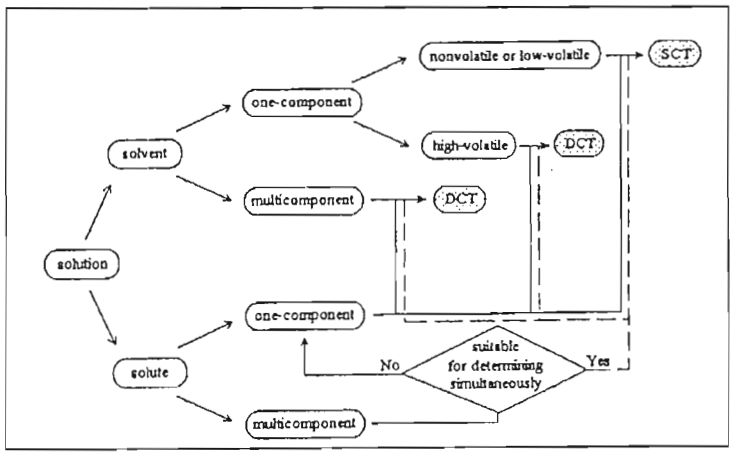

Figure 4-5: Overall scheme given by Bao and Han (1995) for choosing the double or single cell technique for inert gas stripping as used to measure infinite dilution activity coefficients

4.1.5 Viscous or foaming mixtures

Richon et al. (1985) propose a cell design to measure limiting activity coefficients of viscous or foaming mixtures. The apparatus is designed to handle mixtures of viscosity up to 1000 cP (compared to 50 cP of the conventional method). The development of such an apparatus is due to the requirement for the retention of aroma in food. The latter ensures that processed food maintains its best sensory qualities. Measurement of the retention aroma requires the infinite dilution activity coefficient of various substrates in food be measured. The mixtures contain high concentrations of proteins, carbohydrates or polyols, all of which require that the design of the cell be revised. The inert gas enters the dilutor flask (shown in Figure 4-6) through the bottom of the cell and is distributed into the liquid through capillaries (A). The cell features an Archimedes screw (B) to circulate the liquid, a foam breaker (C) and a bladed screw (D) to prevent liquid rotation. Richon et al. (1985) also present mass transfer considerations for the cell design.

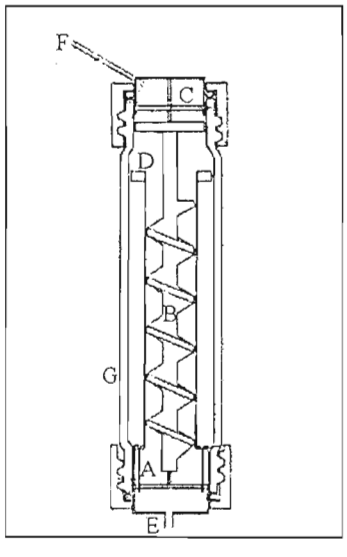

Figure 4-6: Dilutor cell designed for measuring infinite dilution activity coefficients of viscous and foaming mixtures (Richon et al., 1985) A - Capillary dispersion device; B - Archimedes screw; C - Foam breaking device; D - Bladed screw; E - Gas inlet; F - Gas outlet; G - Water jacket

4.1.6 Liquid phase analysis

Hradetzky et al. (1990) describe a method where the remaining liquid is analysed rather than the gas exit stream from the cell. The method is suggested for systems with low volatility solutes and therefore increases the range of applicability of the inert gas stripping method. Wobst et al. (1992) also advocate the use of liquid phase analysis. The authors present a comparison of the gas phase and liquid phase sampling, and show the latter to have improved precision.

4.1.7 Exponential saturation

Hovorka and Dohnal (1999) propose the method of exponential saturation for the measurement of limiting activity coefficients. The apparatus (Figure 4-7) consists of two cells, a pre-saturation cell (A) containing the pure solute and a cell containing a known amount of solvent (B). The inert gas is first saturated with solute and then allowed to bubble through the solvent. The concentration of solute in the second cell will increase with time and the saturation of solvent in the exit stream is monitored. The infinite dilution activity coefficients may be calculated from equations formulated by the authors. The exponential saturator (EXPSAT) is suited for the determination of large limiting activity coefficients. Further details are available in the publication of Dohnal and Hovorka (1999).

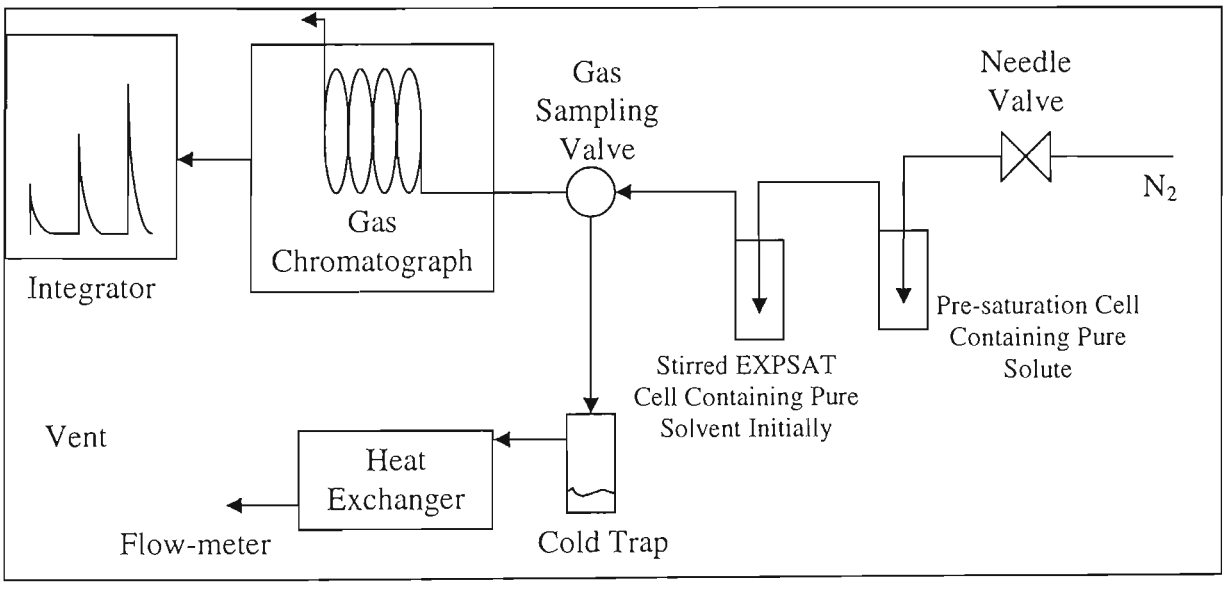

Figure 4-7: Flow diagram of the EXPSAT apparatus for measuring infinite dilution activity coefficients (modification of the inert gas stripping technique) used by Hovorka and Dohnal (1999)

4.1.8 Other applications of the inert gas stripping technique

- Infinite dilution Henry's constants

  Richon and Renon (1980) extended the method to the measurement of infinite dilution Henry's constants. Henry's constants characterise the solubility of gases and are important data for oil recovery problems. The cell employs capillaries for gas distribution and also features baffles.
- Partition coefficients at infinite dilution

The versatility of the method was further shown by Legret et al. (1983), where the authors present a method for measuring partition coefficients at infinite dilution. Such data is useful for the pipe line design and tertiary oil recovery.

- Measurement of vapour-liquid equilibria

  Yet another application of the inert gas stripping technique was described by Ovečková et al. (1991) and Miyamoto et al. (2000). The method was used to produce isothermal VLE measurements. The procedure of Ovečková et al. (1991) involves the measurement of the liquid phase composition whereas Miyamoto et al. (2000) measure the composition of the exit gas stream.

4.1.9 Pros and cons of the inert gas stripping method

Advantages:

- Requires area ratios therefore, the GC detector need not be calibrated as it is reasonable to assume that the response is linear for a low range of solute concentration.
- Multiple solutes may be studied in a single experiment.
- May be used to measure infinite dilution activity coefficients for systems with high volatility solvents.

Disadvantages:

- Good gas-liquid contact is essential for accurate results.
- Requires high purity solutes.
- Measurements are problematic for systems with low volatility solutes. Richon et al. (1980) noted difficulty in measuring systems containing solutes with more than 9 carbons due to low volatility.

4.2 Differential ebulliometry

Gautreaux and Coates (1955) present exact relationships for the activity coefficient ratio $\left(\gamma_i^L / \gamma_i^V\right)^\infty$ given the following sets of data:

1. Isobaric (T-x_i) data
2. Isobaric (T-y_i) data
3. Isothermal (P-x_i) data
4. Isothermal (P-y_i) data

Static and ebulliometer type apparatus can be used to measure isobaric T-x_i and isothermal P-x_i data. These two cases are therefore of interest. Differential ebulliometry requires that a set of ebulliometers be connected to a pressure manifold. The pressure in each ebulliometer is therefore the same. The boiling point difference between the pure solvent and dilute mixtures may then be measured. It is imperative in the method that the liquid concentration be accurately known as discussed by Raal and Muhlbauer (1998) and Raal (2000). Values for infinite dilution activity coefficient may then be calculated from the measured T-x_i data. Infinite dilution activity coefficients of the solvent may be found by repeating the procedure with dilute mixtures of solvent in solute.

The differential ebulliometry method is suitable for systems of low relative volatility. It is, however, problematic for systems containing viscous or nearly non-volatile components. Systems with limited mutual solubility are also unsuitable for measurement by this method.

Advantage:

- Does not require the assumption of a G^E model or composition analysis.

Disadvantage:

- Best suited for systems of low relative volatility.

4.3 Differential static method

Alessi et al (1986) made use of a Gibbs and Van Ness (1972) type static cell to measure isothermal P-x_i data. The equation of Gautreaux and Coates (1955) may then be used to calculate values for the infinite dilution activity coefficient. The cell containing the degassed solvent is allowed to reach equilibrium. A small, precise quantity of degassed solute is then introduced and the pressure difference at equilibrium is noted. According to Raal and Muhlbauer (1998) the accuracy is limited to the accuracy of the quantity of solute introduced. The accuracy is also dramatically affected by the thoroughness of degassing.

Advantage:

- Suitable for measurement of systems with large volatility or partial miscibility.

Disadvantage:

- Requires high purity, degassed solvents and is time-consuming.
- Vapour hold-up must be accounted for (Raal and Ramjugernath, 2001).

4.4 Gas liquid chromatography (GLC)

Measurement of the infinite dilution activity coefficient by gas chromatography is best suited to systems of volatile solutes in low volatility solvents. The principle of gas chromatography is explained by Letcher (1978). Briefly, the process involves the distribution of the solvent between two phases, viz., a mobile phase and a solvent stationery phase. In the case of GLC the liquid stationery phase is coated onto an inert solid support and packed into a column. The mobile phase is an inert gas that flows through the bed of support and solvent. A small quantity of solute is injected into the inlet of the column and is carried through by the mobile phase. A detector is placed at the other end of the column where the eluted solute is observed.

During solute elution a proportion of the solute remains in the mobile phase and part of it dissolves in the stationery phase such that the two phases are in equilibrium. As the equilibrium zone moves further along the column, solute from the mobile phase on the leading edge dissolves into the stationery phase. At the same time, solute from the lagging edge desorbs into the mobile phase and equilibrium is set up again. The rate of solute elution is dependent on the conditions of the experiment (such as mobile phase flow rate) and also properties of the solute and solvent. The infinite dilution activity coefficient may be determined from measurement of the retention time of a solute during a GLC experiment and through use of a plate theory that assumes the column is divided into many theoretical plates. A detailed discussion may be found in Moollan (1995) and Letcher (1978).

Advantages:

- Rapid method that allows one to study many solutes at once. All that is required is that the peaks separate during elution.
- Sample purity is not critical as the pure solute may be separated during elution.
- It is the preferred method for reactive systems as retention times are generally small.

Disadvantage:

- Solvents are required to be of low volatility.
- For a binary system, only the infinite dilution activity coefficient of the solute in the solvent can be found.

CHAPTER 5

INFINITE DILUTION ACTIVITY COEFFICIENTS FROM THE INERT GAS STRIPPING TECHNIQUE - THEORY

The dilute region is typically the area of most interest in a purification process. Often the most amount of effort is expended in purifying a chemical from 95% to 99+%. It is, therefore, essential that the behaviour of the chemicals in the dilute region be understood. Besides the traditional requirement of data in the dilute region for purification, Alessi et al. (1991) gives the following applications:

- Application to environmental problems. E.g. the abatement of pollution from absorption towers.
- Application to the production of polymers. Devolatisation is represented by the removal of the last molecule of monomer or solvents from the polymer.
- Application to the manufacture of products for human consumption (packaging of food and pharmaceuticals).

The system usually displays its greatest departure from ideal behaviour in the infinitely dilute concentration range. Raal and Mühlbauer (1998) state that the infinite dilution activity coefficients are the most accurate characterisation of system behaviour in the dilute region. These limiting activity coefficients have important practical and theoretical uses:

- Screening for potential azeotropes (Palmer, 1987).
- Screening of liquid extraction solvents (Palmer, 1987).
- Screening of extractive distillation solvents (Perry and Green, 1998).
- Provides theoreticians with information about solute-solvent interactions in the absence of solute-solute interactions (Howell et al., 1989).
- Prediction of binary data, which in turn are used to predict multi-component VLE data (Howell et al., 1989).
- Prediction of retention times and selectivity in chromatographic columns (Howell et al., 1989).

Methods to predict the value of the infinite dilution activity coefficient are available in literature. These methods employ group contribution techniques (e.g. UNIFAC model) or extensions of regular solution theory (e.g. MOSCED). The reader is referred to the publication of Howell et al. (1989) as these methods will not be reviewed in this study.

Leroi et al. (1977) described how the infinite dilution activity coefficient may be determined from the inert gas stripping method described in Chapter 4. The following assumptions are made:

- The solubility of the inert gas in the liquid is negligible.
- The vapour phase is ideal.

These are satisfactory approximations for low pressure computations. The modified Raoult's law is applicable and Eq. 3-79 can be written in terms of the solute:

$$x_{sol}\gamma_{sol}^{\infty}P_{sol}^{sat} = y_{sol}P \tag{5-1}$$

For the solvent where $x_S \rightarrow 1$:

$$P_S^{sat} = y_S P \tag{5-2}$$

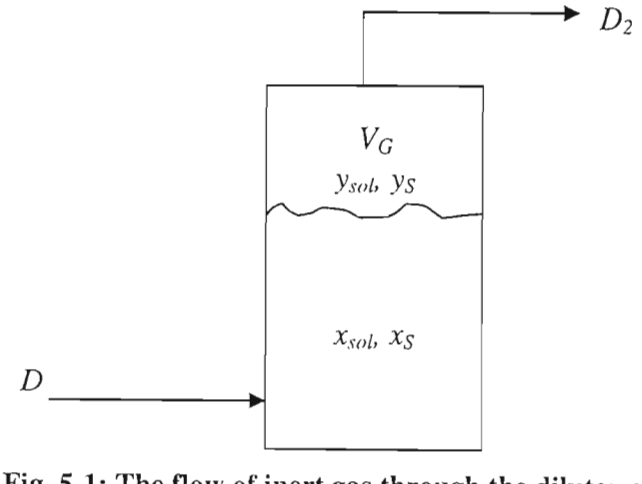

Fig. 5-1: The flow of inert gas through the dilutor cell

Fig. 5-1 shows the pure inert gas entering the dilutor cell, which contains a dilute solution of solute in solvent at constant temperature and total pressure. The volumetric flow D_2 is different from the inlet flow (D) as the exit stream contains the entrained organics.

The following material balance:

$$Accumulation = Input - Output$$

is applied to the solute

$$\frac{dn}{dt} = -y_{sol}\frac{PD_2}{RT} \tag{5-3}$$

For solvent

$$\frac{dN}{dt} = -y_S\frac{PD_2}{RT} \tag{5-4}$$

D_2 may be obtained from the overall material balance:

$$D_2 = D - \frac{RT}{P}\left(\frac{dn}{dt} + \frac{dN}{dt}\right) \tag{5-5}$$

Combining Eq. 5-1 with 5-3 and Eq. 5-2 with 5-4:

$$\frac{dn}{dt} = -x_{sol}\gamma_{sol}^{\infty}P_{sol}^{sat}\frac{D_2}{RT} \tag{5-6}$$

$$\frac{dN}{dt} = -P_S^{sat}\frac{D_2}{RT} \tag{5-7}$$

By substituting Eqs. 5-6 and 5-7 into Eq. 5-5, D_2 can now be found from:

$$D_2 = \frac{D}{1 - x_{sol}\gamma_{sol}^{\infty}\dfrac{P_{sol}^{sat}}{P} - \dfrac{P_S^{sat}}{P}} \tag{5-8}$$

The mole fraction of the solute (x_{sol}) in the liquid can be expressed in one of two ways:

- Leroi et al. (1977) used the following approximation when calculating x_{sol}, as the amount of solute in the liquid is small:

$$x_{sol} = \frac{n}{n+N} \approx \frac{n}{N} \tag{5-9}$$

- Duhem and Vidal (1978) used a more appropriate expression:

$$x_{sol} = \frac{n}{N\left(1+\frac{V}{RT}\frac{P_{sol}^{sat}\gamma_{sol}^{sat}}{N}\right)} \tag{5-10}$$

Equations can be formulated to calculate infinite dilution activity coefficients based on either the approximation 5-9 or Eq. 5-10. Each formulation will be discussed briefly.

5.1 Formulation from the assumptions of Leroi et al. (1977)

The following are the basic differential equations obtained if the approximation shown in Eq. 5-9 is assumed to be valid:

$$\frac{dn}{dt} = -\frac{n}{N}\gamma_{sol}^{\infty}\frac{P_{sol}^{sat}}{RT}\frac{D}{1-\frac{n}{N}\gamma_{sol}^{\infty}\frac{P_{sol}^{sat}}{P}-\frac{P_S^{sat}}{P}} \tag{5-11}$$

$$\frac{dN}{dt} = -\frac{P_S^{sat}}{RT}\frac{D}{1-\frac{n}{N}\gamma_{sol}^{\infty}\frac{P_{sol}^{sat}}{P}-\frac{P_S^{sat}}{P}} \tag{5-12}$$

Leroi et al. (1977) further assumed that the term $\frac{n}{N}\gamma_{sol}^{\infty}\frac{P_{sol}^{sat}}{P}$ can be neglected. The following two cases are considered:

- The solvent is non-volatile.
  Leroi et al. (1977) considers a solvent having vapour pressure less than 1mmHg to be non-volatile. If this assumption is valid, N is constant and the differential Eq. 5-11 can be solved.
- The solvent is volatile.
  N is not constant for a volatile solvent and Eqs. 5-11 and 5-12 must be solved together.

5.1.1 Non-volatile solvent

The solution of Eq. 5-11 is:

$$\ln\frac{n}{n_0} = -\frac{D}{RT}\frac{P_{sol}^{sat}}{N}\gamma_{sol}^{\infty}t \tag{5-13}$$

If the gas chromatograph detector response is linear (i.e. the number of moles is directly proportional to the peak area) eq. 5-13 becomes:

$$\ln\frac{A}{A_0} = -\frac{D}{RT}\frac{P_{sol}^{sat}}{N}\gamma_{sol}^{\infty}t \tag{5-14}$$

The infinite dilution activity coefficient can be found from the measurement of the peak area as a function of time if the assumptions used to derive 5-14 are valid.

5.1.2 Volatile solvent

Solving the set of differential equations 5-11 and 5-12 yields the following expression valid for a volatile solvent:

$$\ln\frac{A}{A_0} = \left(\frac{\gamma_{sol}^{\infty}P_{sol}^{sat}}{P_S^{sat}} - 1\right)\ln\left(1 - \frac{P}{P - P_S^{sat}}\frac{DP_S^{sat}}{N_0RT}t\right) \tag{5-15}$$

5.2 Formulation using the Duhem and Vidal (1978) correction

Equations for calculating the infinite dilution activity coefficient for volatile and non-volatile solvents can be derived using the expression for x_{sol} shown in Eq. 5-10 and assuming that $\frac{n}{N}\gamma_{sol}^{\infty}\frac{P_{sol}^{sat}}{P}$ can not be neglected. Duhem and Vidal (1978) state that the assumptions made by Leroi et al. (1977) are especially not valid if the infinite dilution activity coefficient is large.

5.2.1 Non-volatile solvent

Duhem and Vidal (1978) consider the case of a non-volatile solvent and obtain the following expression by integrating Eq. 5-11.

$$\ln\frac{A}{A_0} = -\frac{D}{RTN\left(1+\frac{V_G}{RT}\frac{P_{sol}^{sat}\gamma_{sol}^{\infty}}{N}\right)}\frac{P_{sol}^{sat}}{1-\frac{\tilde{n}}{N\left(1+\frac{V_G}{RT}\frac{P_{sol}^{sat}\gamma_{sol}^{\infty}}{N}\right)}\frac{\gamma_{sol}^{\infty}P_{sol}^{sat}}{P}}\gamma_{sol}^{\infty}t \qquad (5\text{-}16)$$

Where

$$\tilde{n} = \frac{n-n_0}{\ln\frac{n}{n_0}}$$

The formulation introduces V_G (the volume of the vapour space) into the equations. Bao et al. (1993) obtain V_G from:

$$V_G = V_{cell} - \frac{m_S}{\rho_S}$$

The authors showed improved results using Eq. 5-16 rather than Eq. 5-14, especially for systems having large infinite dilution activity coefficients such as the benzene + water system. Duhem and Vidal (1978) refer to the following term in Eq. 5-17 as a "corrective term":

$$1-\frac{\tilde{n}}{N\left(1+\frac{V_G}{RT}\frac{P_{sol}^{sat}\gamma_{sol}^{\infty}}{N}\right)}$$

The term requires that the quantity of solute in the test mixture be known. Duhem and Vidal (1978) show that neglecting the corrective term yields satisfactory results.

5.2.2 Volatile solvent

Bao and Han (1995) present the solution of the differential Equations 5-11 and 5-12 if Eq. 5-10 is used to calculate x_{sol} (as advocated by Duhem and Vidal, 1978).

$$\ln\frac{A}{A_0} = \left(\frac{1}{1+\dfrac{\gamma_{sol}^{\infty} P_{sol}^{sat} V_G}{N_0 RT}} \frac{\gamma_{sol}^{\infty} P_{sol}^{sat}}{P_S^{sat}} - 1 \right) \ln\left(1 - \frac{P_S^{sat}}{P - P_S^{sat}} \frac{PD}{N_0 RT} t \right) \qquad (5\text{-}17)$$

It should be noted that the corrective term is neglected in Eq. 5-17 (see Section 5.2.1).

Eqs. 5-14, 5-15, 5-16 or 5-17 may be used to calculate values for the infinite dilution activity coefficient when applied appropriately (i.e. the assumptions are valid). It is required that the initial amount of solvent be known, the solute peak areas are then recorded as a function of time. Since the equations are written in terms of area ratios, detector calibration is unnecessary if the detector response is linear. All the other required parameters are readily available (such as pure component vapour pressure) or measurable (such as inert gas flow rate.).

Bao and Han (1995) show the formulation of the equations for the double cell technique (DCT). The method is discussed in the experimental review section. The gas introduced into the dilutor cell is first saturated with the solvent and this must be accounted for in the derivation. The method is preferred for systems containing volatile solvents. As the technique was not part of this study the reader is referred to Bao and Han (1995) and Doležal et al. (1981) for further detail. Doležal and Holub (1985) consider the case where the vapour phase may not be considered to be ideal. The systems considered in this study, however, were not highly non-ideal at the experimental conditions, as may be seen from the results of the vapour-liquid equilibria study. The reader is once again referred to the latter publication for details of how the vapour phase non-ideality may be accounted for.

CHAPTER 6

VAPOUR-LIQUID EQUILIBRIUM – APPARATUS AND EXPERIMENTAL PROCEDURE

The vapour and liquid recirculating still of Raal and Mühlbauer (1998) for low-pressure VLE measurements was used in this project. The features of the still and a description can be found in Chapter 2. The following will be discussed in this chapter:

- Pressure control.
  The measurements were made at sub-atmospheric pressures. The method for maintaining the reduced pressure in the still will be discussed.
- Calibration of the pressure transducer.
- Calibration of the temperature sensor.
- Calibration of the gas-chromatograph (GC) detector response.
  Phase compositions were measured using a GC. It is necessary to calibrate the response of the GC detector.
- Experimental procedure for the measurement of isobaric and isothermal VLE.

6.1 Description of the experimental apparatus

A flow diagram of the experimental apparatus is shown in Figure 6-1. The condenser of the glass VLE still is connected to a ballast flask. The ballast flask serves to reduce pressure fluctuations and to trap condensable chemicals should the condenser fail. A KNF vacuum pump-controller unit is used to evacuate the still and to maintain a constant pressure. The vacuum pump draws incondensable gases from the VLE still until the measured pressure reaches the controller set-point. Once the set-point pressure has been achieved the controller shuts off the vacuum pump. It is nearly impossible to make the VLE still perfectly leak-tight and small leaks in the apparatus will cause the pressure to rise. The pump starts up again when the measured pressure exceeds the set-point. A needle valve installed between the vacuum pump and the VLE still is used to throttle the flow through the pump to ensure that pressure fluctuations are minimised. The system pressure is maintained constant to ±0.05kPa. The reading from the pressure transducer must be calibrated. The calibration procedure is explained in Section 6.3. It is required to vent the still in the course of some experiments to raise the

pressure (the reasons are given in Sections 6.6 and 6.7). To ensure that no moisture is brought into the still, air is introduced through a bed of desiccating crystal when the vent valve is opened.

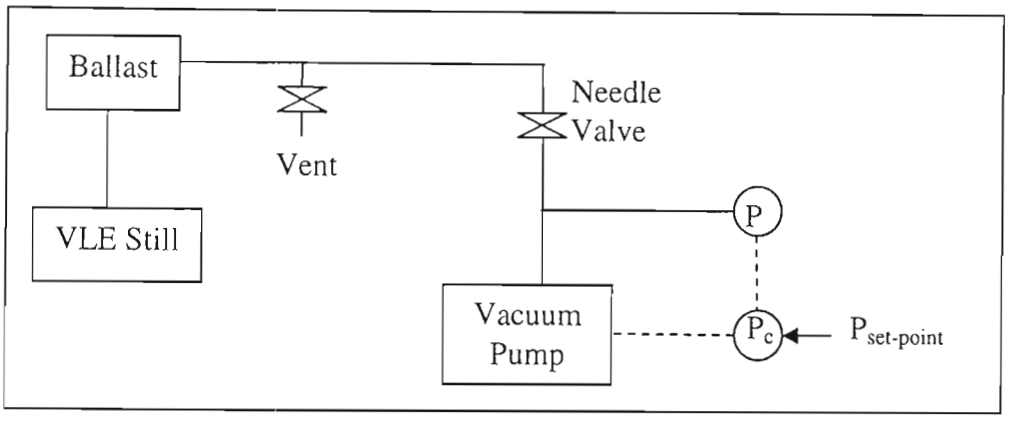

Figure 6-1: Block diagram of the dynamic VLE apparatus for low-pressure measurements P, Pressure transducer; P_C Pressure controller

6.2 Cleaning the still

VLE measurements are made with high purity chemicals. It is, therefore essential that the still be thoroughly cleaned. The still was run with acetone at atmospheric pressure (to allow maximum operating temperature for the chemical) for twenty minutes. The acetone wash was repeated until a gas chromatography trace of the fluid drained out of the still showed no significant peaks other than acetone. To avoid acetone contamination the still was then dried by setting the pressure in the still to its minimum value and allowing the residual acetone to be flashed off. No traces of acetone were noted in the GC analysis of subsequent samples.

6.3 Pressure calibration

A KNF vacuum pump-controller unit (type NC800) is used for pressure control. The pressure display on the controller was calibrated with a mercury manometer and a Vaisala electronic barometer (model PTB100A). It should be noted that the barometer is NIST (National Institute of Standards and Technology) traceable. The controller was allowed to control about various set-points and the transducer response to the actual pressure was noted. The relationship was found to be linear and is shown in Figure 6-2. The accuracy of the pressure calibration is readily confirmed by repeating the procedure and was done periodically. Pressure measurement is estimated to be accurate to ±0.05 kPa.

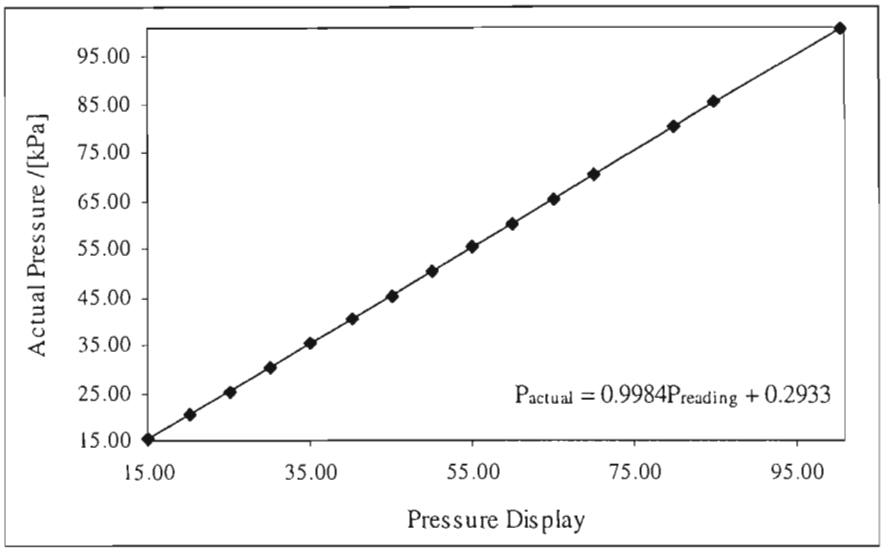

Figure 6-2: Plot to show the linear relationship of actual pressure with pressure displayed on KNF pressure controller used in the VLE apparatus

6.4 Temperature calibration

The resistance of the Pt-100 sensor in the equilibrium chamber of the VLE still is displayed by a Eurotherm temperature display unit. The sensor was calibrated in situ by running the still isobarically with a highly pure chemical and noting the actual boiling temperature of the chemical as predicted by the vapour pressure correlation available in Reid et al [1988]. The linear relationship is shown in Figure 6-3. 99.9% n-hexane was used in this study. The accuracy of the temperature measurement is estimated to be ±0.02°C.

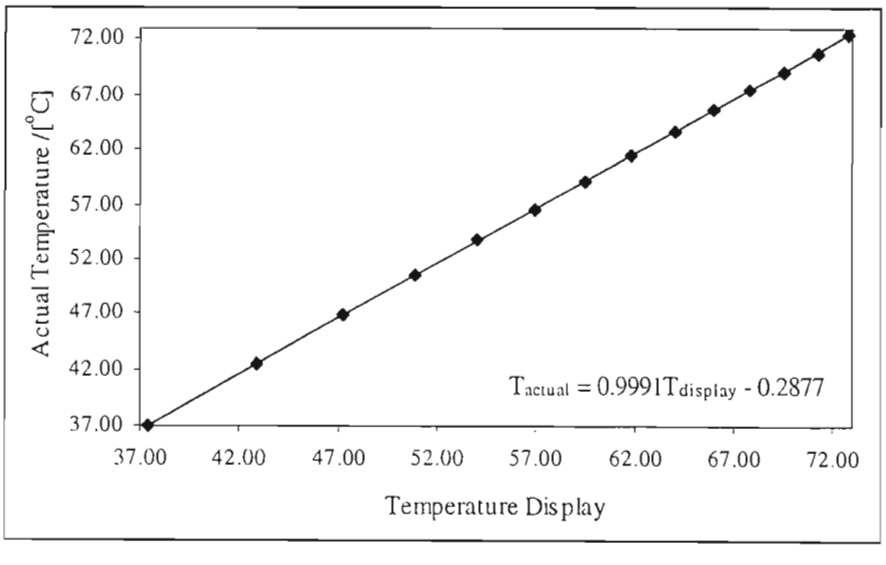

Figure 6-3: Plot to show the linear relationship of actual temperature of Pt-100 sensor (placed in the packing of the equilibrium chamber) with Eurotherm display

6.5 Gas Chromatograph Detector Calibration

Two gas chromatographs were used to analyse samples drawn from the VLE still due to availability. The specification and operating conditions of the GC's are given in Table 6-1. The detector calibration procedure suggested by Raal and Mühlbauer [1998] was used in the study. The procedure is briefly described in the following steps:

1. Samples of each binary system are gravimetrically prepared such that the mole fraction ratios x_1/x_2 and x_2/x_1 range from approximately 0.1 to 1.2.
2. The mixtures are analysed by gas chromatography until the results can be shown to be reproducible and the peak areas of each chemical (A_1 and A_2) are noted.
3. Plots of A_1/A_2 versus x_1/x_2 and A_2/A_1 versus x_2/x_1 are prepared. Examples for the test system (cyclohexane with ethanol) are shown in Figure 6-4 and 6-5.
4. If the detector response is linear, the method requires the reduction of both data sets to straight lines passing through the origin. Furthermore, the reciprocal of the gradient of the graph shown in Figure 6-4 should be approximately equal to the gradient of the graph in Figure 6-5.

All the binary mixtures measured responded linearly and the gradients of A_1/A_2 versus x_1/x_2 were shown to be sufficiently close in value to the reciprocal of the gradient of A_2/A_1 versus x_2/x_1 and can be found in Appendix C. The accuracy of the composition measurement is estimated to be ±0.001 mole fraction.

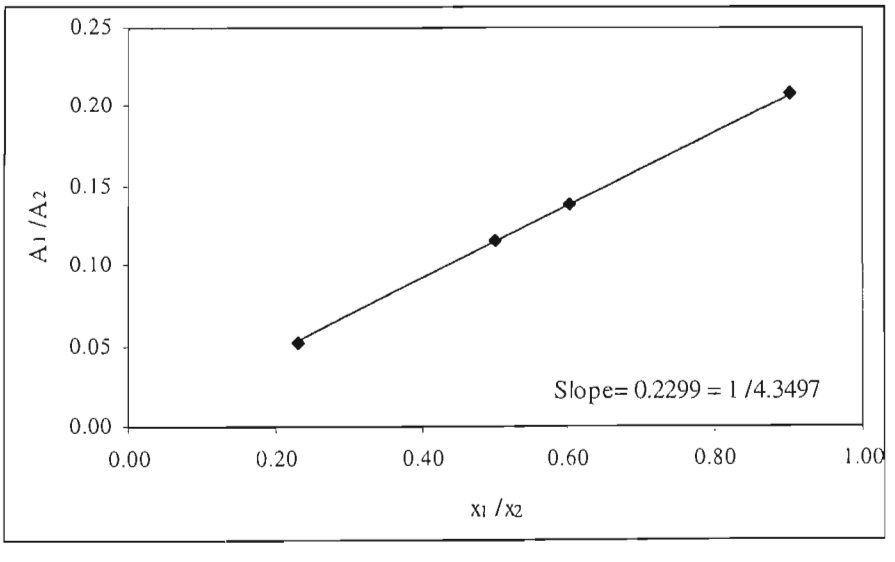

Figure 6-4: Calibration of GC detector response for cyclohexane(1) with ethanol(2)

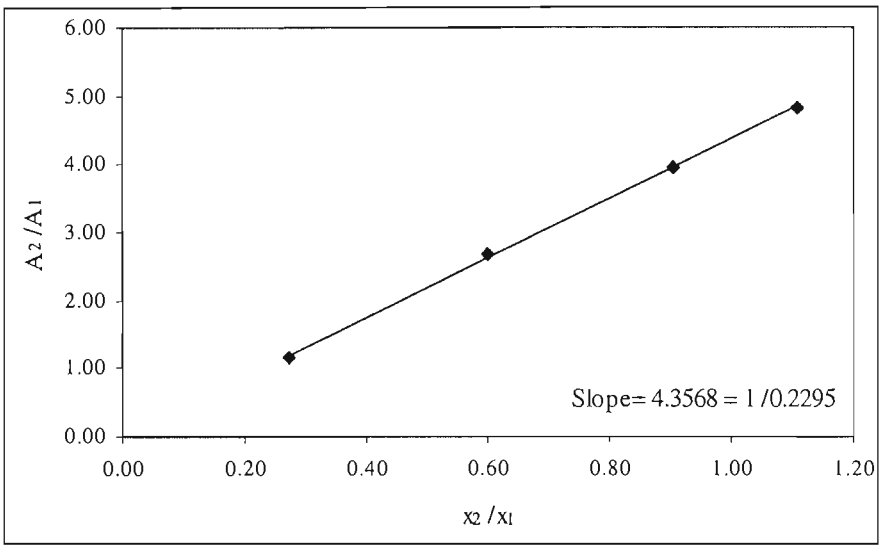

Figure 6-5: Calibration of GC detector response for cyclohexane(1) with ethanol(2)

Table 6-1: Specification and operating conditions of the gas chromatographs used to analyse samples from the VLE experiments

GC	Column	Detector	Operating Conditions		
Shimadzu GC-17A	Capillary column	FID	Acetone	Col	35 °C
	J&W Scientific GS-Q		With	Det	200 °C
			Diacetyl	Inj	200 °C
				Col P	20 kPa
Shimadzu GC-17A	Capillary column	FID	Methanol	Col	35 °C
	J&W Scientific GS-Q		With	Det	200 °C
			Diacetyl	Inj	200 °C
				Col P	20 kPa
Shimadzu GC-17A	Capillary column	FID	Diacetyl	Col	40 °C
	J&W Scientific GS-Q		with	Det	200 °C
			2,3-Pentanedione	Inj	200 °C
				Col P	25 kPa
Chrompack 9000	Capillary column	TCD	Acetone	Col	220 °C
	J&W Scientific GS-Q		with	Det	150 °C
			2,3-Pentanedione	Inj	100 °C

Col – Column temperature; Det – Detector temperature; Inj – Injector temperature; Col P – Column pressure

6.6 Procedure for the measurement of isobaric VLE

The pressure in the still is maintained sub-atmospheric by means of a vacuum pump as explained in Section 6.1. The suction point is at the top of the condenser and the condenser coolant temperature is sufficiently low (approximately -5 °C) to ensure that no volatiles are lost. A KNF vacuum pump /controller unit accepts a set-point and the pressure in the still is controlled about this value. Calibration of the controller display is discussed in section 6.3. The procedure is as follows (and is summarised in Figure 6-6).

1. The still is charged with a pure sample of one of the components of the binary system.
2. The desired pressure set-point is entered into the controller and the still and its contents are brought to this pressure. Coolant is allowed to flow through the jacket of the condenser and the magnetic stirrers in the reboiler and vapour sample point are switched on.
3. The heater external to the reboiler is switched on to compensate for heat losses to the environment and to bring the still contents to a boil.
4. The power input to the internal heater in the reboiler is then varied until the "plateau region" is found. This is the region where the temperature remains constant despite a slight increase or decrease in power input. The plateau region is discussed in detail in Kneisl et al [1989] and briefly in Chapter 2.
5. Samples are drawn periodically from the liquid and vapour sample points using a 1µl GC syringe. The samples are analysed using a gas chromatograph (see Table 6-1) which is situated in the immediate proximity of the still. The volumes removed are small enough to have no significant effect on the still's operation.
6. The still contents are allowed to circulate for 30 minutes to an hour to equilibrate (depending on the chemicals studied). The condensate drop-rate should be sufficiently large to allow good circulation of the volatile components. At this time the temperature should be constant (±0.02K) and the liquid-levels in the liquid and vapour return legs should not be experiencing large fluctuations. Successive samples of the equilibrium vapour and liquid should yield constant values. These values of temperature and composition are taken to be the values at equilibrium for the set-point pressure.
7. A small amount of liquid is drawn from the still and replaced with a pure sample of the second component without disrupting the operation of the still. Steps 4 onwards are repeated until half of the phase diagram is generated.
8. The still is then cleaned and dried (as described in Section 6.2) and steps 1 to 6 are repeated, this time starting with a pure sample of the second component and adding

small quantities of component one to measure successive points. The points starting from opposite ends of the phase diagram should meet without any discontinuity.

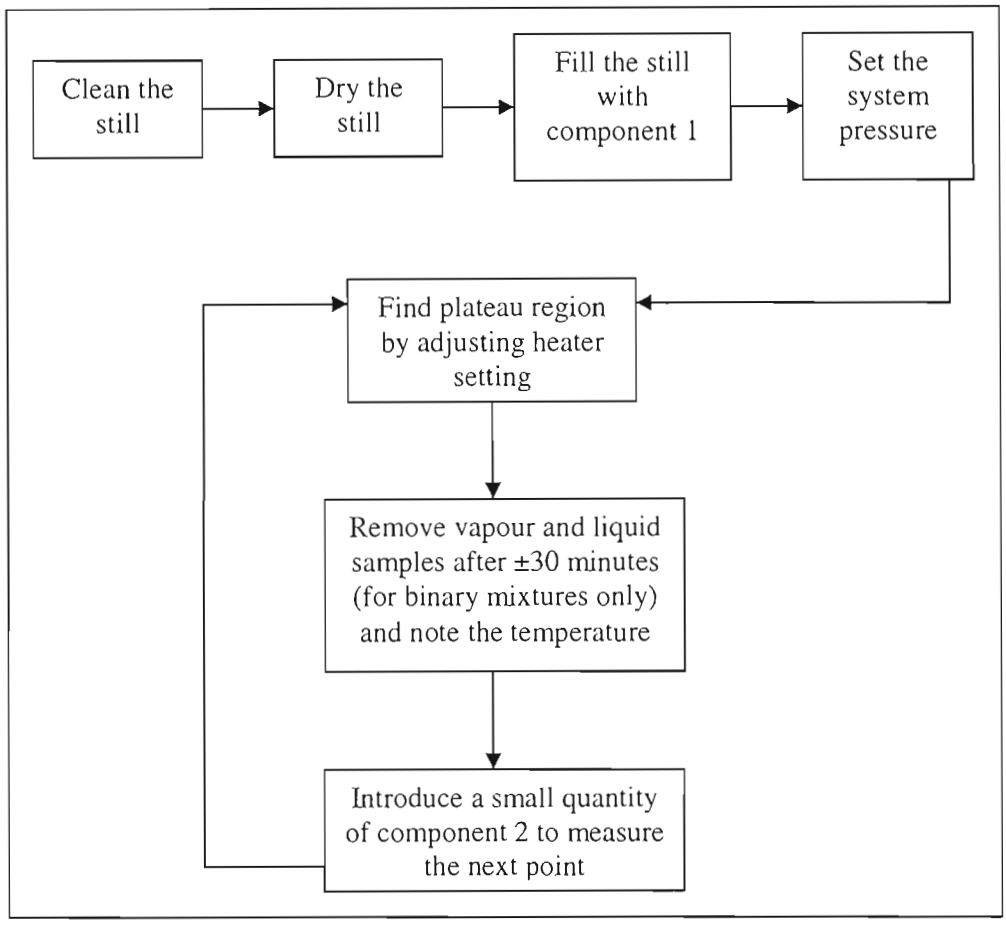

Figure 6-6: Flow diagram to show the procedure used to measure isobaric VLE using a low-pressure vapour and liquid recirculating still

6.7 Procedure for the measurement of isothermal VLE

The ebulliometric total-pressure method introduced by Rogalski and Malanowski (1980) allows one to make isothermal measurements using a recirculating still. The procedure is a slight modification of that used for the isobaric measurements, in that the pressure is adjusted to maintain a constant temperature. If isothermal data at temperature T_i are required:

- The composition of the still contents is once again varied.
- The plateau region for various pressure set-points are found until T_i is achieved for each composition.
- Steps 5 to 8 from the isobaric procedure are then followed (Section 6.6).

It is recommended that the isobaric measurements be made first as the sensitivity and range of the power input and temperature response may be gauged more easily. The temperature control is estimated to be better than 0.1°C. Joseph et al. (2001) measured isothermal VLE of excellent quality by a similar procedure, the manipulation of the system pressure was, however, computer controlled. The procedure used in this study is summarised in Figure 6-7.

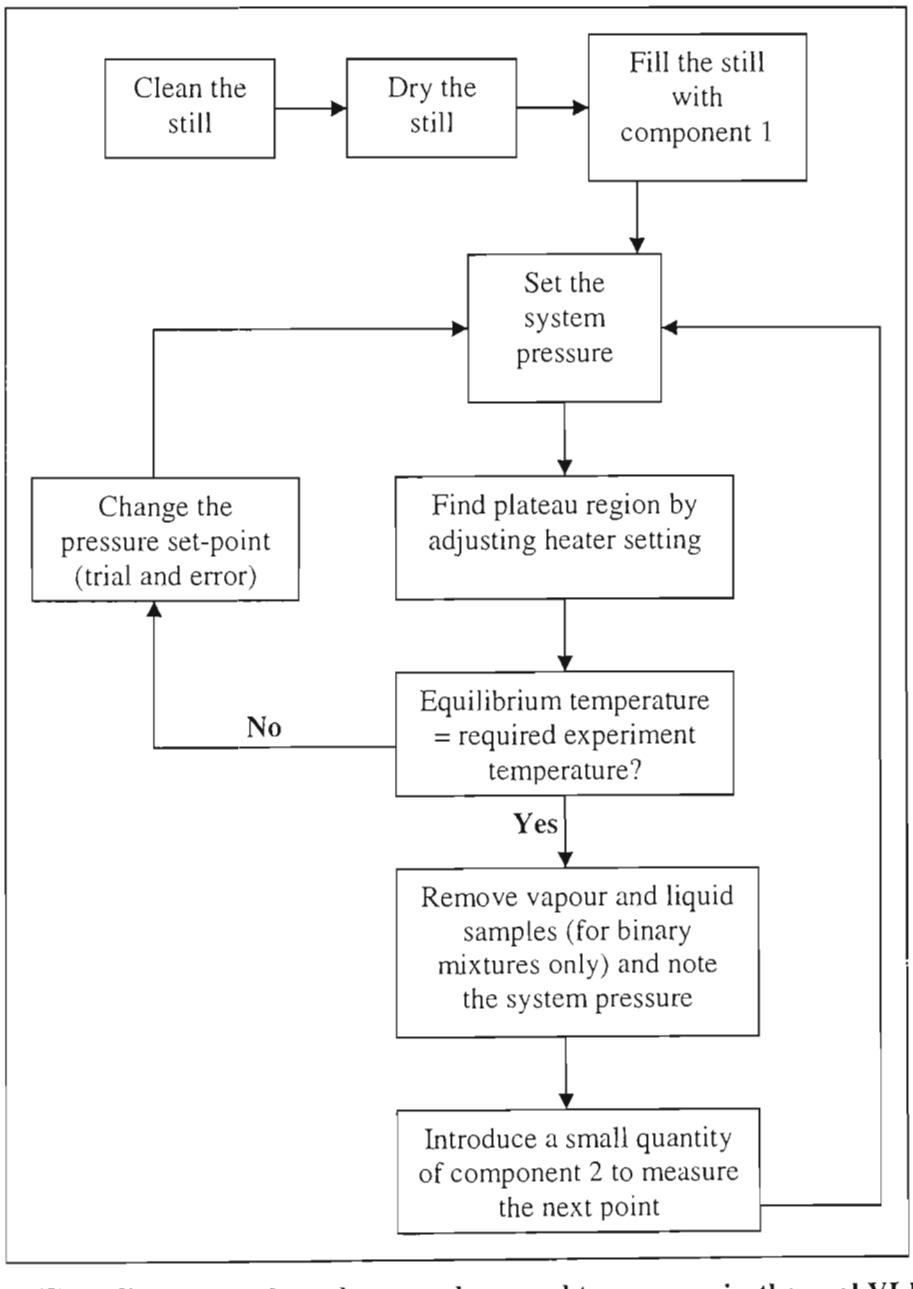

Figure 6-7: Flow diagram to show the procedure used to measure isothermal VLE using a low-pressure vapour and liquid recirculating still

CHAPTER 7

INERT GAS STRIPPING TECHNIQUE – APPARATUS AND EXPERIMENTAL PROCEDURE

In order to ensure that the gas phase exiting the dilutor flask is in equilibrium with the liquid mixture, it is necessary to understand how solute is transferred into the gas bubbles. These mass transfer considerations are discussed in Appendix D and enable one to calculate the appropriate height of the dilutor flask. A number of factors (other than the height) affect the performance of the dilutor flask (the type of dispersion device, for example). The design considerations, the experimental apparatus and the experimental procedure used in this study will be described in this chapter.

7.1 Design of the gas stripping cell

After careful consideration of the literature available on inert gas stripping (described in Chapter 4), the apparatus as described by Leroi et al. (1977) was set up by a previous student (Jourdain, 2000). Jourdain reports results within the range of literature values for the system acetone (solute) in n-heptane (solvent). The experimental apparatus used in this study is for the most part the same. The modifications made were undertaken taking into consideration the systems of interest in this study and the difficulties experienced previously (discussed shortly).

The calculation procedure of Richon et al. (1980) discussed in Appendix D can be used to calculate the bubble rise height required for the gas phase to be in equilibrium with the liquid in the cell. Both the mass transfer of solute to the bubble as well as diffusion of solute into the bubble was considered. A typical plot of the approach to equilibrium as a function of bubble rise height is shown in Figure 7-1 for the system acetone (solute) in 2,3-pentanedione (solvent) under typical experimental conditions. The results of Figure 7-1 were obtained from Eq. D-8 assuming that diffusion of solute into the bubble was fast. The assumption can be tested using Eq. D-17 (Figure 7-2 shows a typical example).

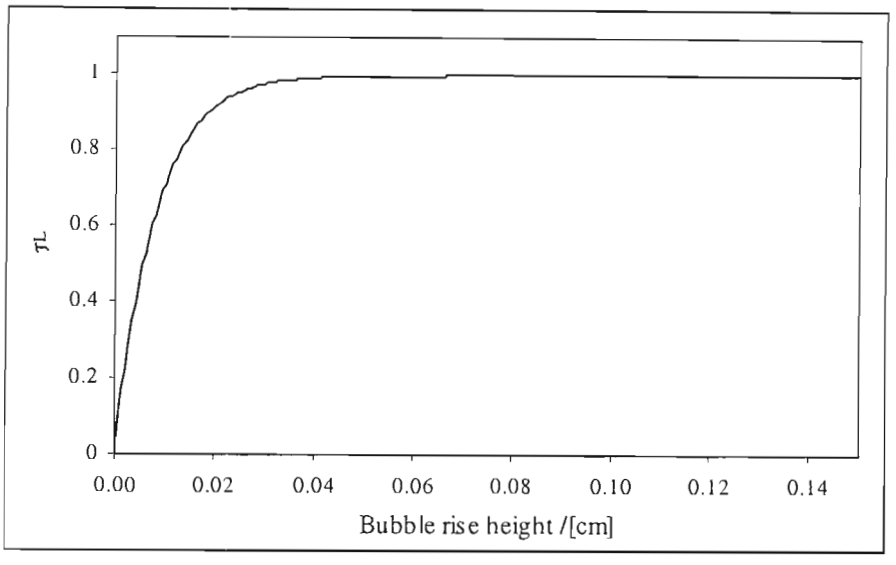

Figure 7-1: Mass transfer rate of solute (acetone) to the gas bubble for the system acetone+2,3-pentanedione (τ_L is the ratio of the mass of solute transferred from the liquid to the film)

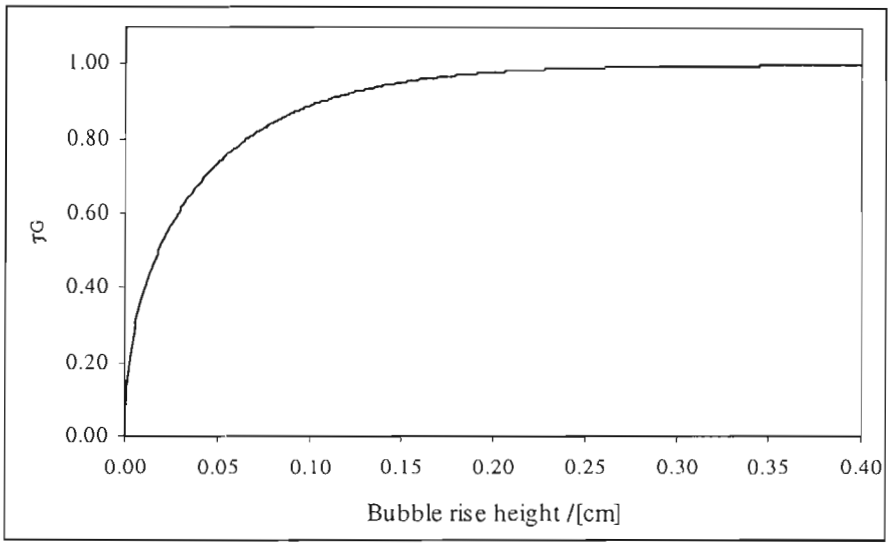

Figure 7-2: Diffusion rate of solute (acetone) in the gas (N_2) bubble for the system acetone+2,3-pentanedione (τ_G is the ratio of the mass of solute in the bubble to the value at equilibrium)

The calculation procedure of Richon et al. (1980) can also be used to judge the sensitivity of the approach to equilibrium on certain experimental conditions. These are presented shortly. Besides choosing the cell height that gives at least the required bubble rise height, the effect of a number of other options must be considered:

- Double or single cell technique

- Type of gas dispersion device
- Stripping gas flow rate
- Liquid viscosity
- Bubble size
- The infinite dilution activity coefficient

7.1.1 Double or single cell technique

As described in Chapter 4 the double cell technique (DCT) was introduced by Dolezal et al. (1981). Whereas the conventional single cell technique (SCT) introduces pure stripping gas, the DCT introduces the stripping gas after its been saturated with solvent. The technique is preferred for systems containing highly volatile solvents or for multi-component systems. Bao and Han (1995) propose a scheme to suggest when the DCT or SCT is most appropriate (see Figure 4-5). The solvents of interest in this study (2,3-pentanedione and diacetyl) can not be classified as highly volatile, therefore the SCT technique was used. Acetone (solute) in methanol (solvent) was chosen to test the method as the SCT was seen as the appropriate technique to study the latter system by Bao and Han (1995).

7.1.2 Type of gas dispersion device

The effectiveness of the dispersion device has a great influence on the accuracy of the results. It is important that the bubble size be minimal in order to achieve good mass transfer and to ensure conditions for the experiment are met. A more detailed discussion of bubble size follows shortly. Further, it is undesirable for the bubbles to be allowed to coalesce. Leroi et al. (1977) introduced the gas through a sintered glass disk. Richon et al. (1980), on the other hand, advocate the use of capillaries as sintered disks can not be made perfectly.

Jourdain (2000) used a sintered disk, in light of a more recent experiment by Li et al. (1993), who report that the smallest bubble sizes were obtained using a sintered disk. Some coalescence was, however, reported by Jourdain and observed by the author of this work. Jourdain suggests that the magnetic stirrer is responsible for the coalescence and recommends modifications that avoid bubbles being introduced into the vortex created by the stirring.

It was decided that the dilutor flask used in this study make use of evenly spaced capillaries as the dispersion device. Ten lengths of $^{1}/_{32}$ in. narrow bore stainless-steel tubing were used to introduce the gas. This was found to be a much more satisfactory method. The bubble size was

improved (smaller diameter) and coalescence was avoided as the bubbles were not directed into the vortex.

7.1.3 Stripping gas flow rate

It is important that sufficient contact time be allowed for the bubbles with the liquid. Among other factors, the gas flow rate plays a large role in determining the contact time. Leroi et al. (1977) used a gas flow rate in the range of 50–150ml /min. Recent studies have, however, used much lower flow rates. Li et al. (1993) investigated the effect of the flow rate on the results obtained. Experiments were conducted using various flow rates until a constant value for the infinite dilution activity coefficient was found. For the system benzene (solute) in water (solvent) the maximum flow rate was 17 ml /min. The value of the ideal flow rate will be system dependent, but the experiments indicate that a low gas stripping flow rate is most appropriate. The inert gas flow rates used in this study were found by reducing the gas flow until constant values for the infinite dilution activity coefficient were obtained.

7.1.4 Liquid viscosity

Richon et al. (1980) describe a procedure for calculating the bubble rise height by considering the transfer of solute to the mass transfer film and into the bubble. The procedure is discussed in Appendix D. Richon found that the influence of viscosity is two-fold. The mass transfer is compromised when the viscosity is high. This is however, compensated for by the bubble rise velocity increasing and the contact time is therefore increased. In fact, Richon also reports that even systems with viscosities as high as 40 cP reach equilibrium after passing through 1 cm of solution.

Solutions having a viscosity greater than 50 cP have been found to be problematic. The main concerns are that the stirring is ineffective and that the liquids tend to foam. Richon et al. (1985) propose a design to address these problems, a brief description of the cell and its applicability is given in the experimental review section.

Performing the calculation using a computer program allows for the code to be generic and therefore applicable to a range of systems. The calculations were performed for all the combinations of chemicals used in this study. The approach to equilibrium was not found to be greatly influenced by viscosity. The latter was therefore not regarded as a limiting factor in this study and the conventional design was deemed adequate.

7.1.5 Bubble size

As mentioned before it is essential that bubble sizes be minimised in order to ensure good mass transfer. Figures 7-3 and 7-4 were obtained from the calculation procedure of Richon et al. (1980) as applied to the system acetone (solute) in 2,3-pentanedione (solvent). The calculations were performed for all the binary systems but the latter binary was chosen as a typical case to serve as an example. Bubble sizes between 2mm and 3mm (diameter) were considered.

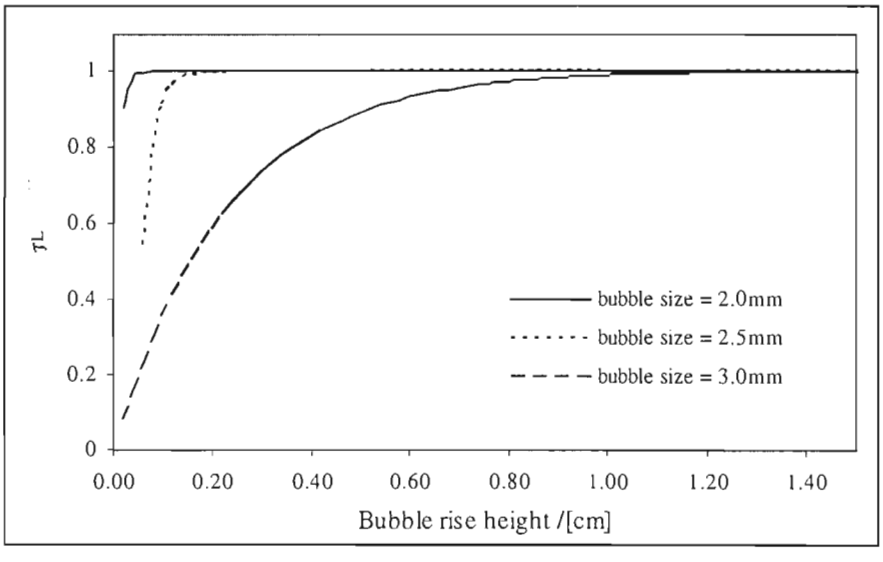

Figure 7-3: The effect of bubble size on the mass transfer rate of solute to the gas bubble for the system acetone+2,3-pentanedione

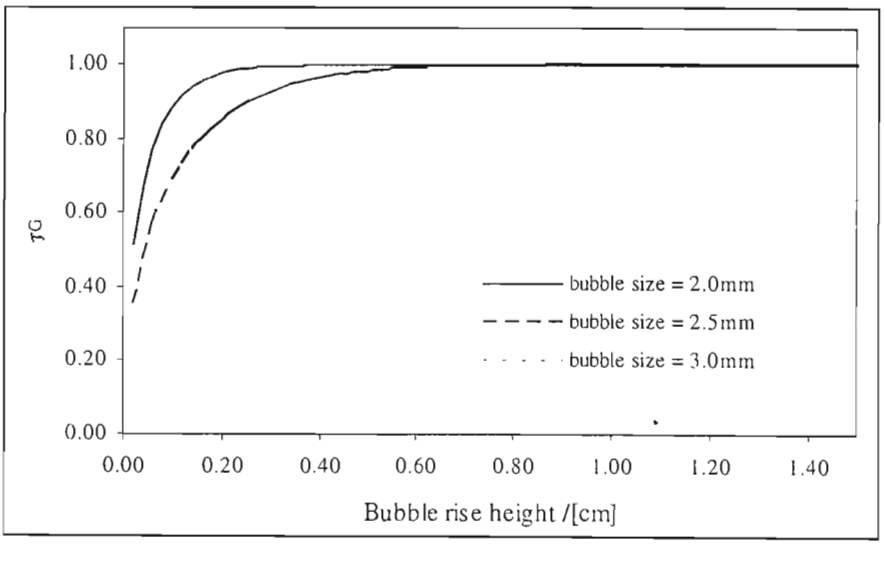

Figure 7-4: The effect of bubble size on the diffusion rate of solute in the gas bubble for the system acetone+2,3-pentanedione

Figure 7-3 shows the effect of bubble size on the rate of mass transfer of solute and Figure 7-4 the influence on the rate of diffusion of solute into the bubble. Although the approach to equilibrium occurs after a fairly short bubble rise height for even 3mm bubbles, both graphs highlight that the approach favours small bubbles. The assumption that diffusion of solute into the bubble is fast is also only valid for small bubble sizes. The bubble size considered when choosing a dispersion device was a diameter of no more than 2.5mm.

7.1.6 The infinite dilution activity coefficient

The design of the cell depends on the value of the infinite dilution activity coefficient. The effect of a large infinite dilution activity coefficient on the rate of solute mass transfer can be seen to be significant in Figure 7-5. The infinite dilution activity coefficient has no effect on solute diffusion (Figure 7-6). It was found that the systems measured in this study did not deviate very much from ideal behaviour. This was taken into consideration in specifying the cell height. The applicability of the cell used in this study is limited by the value of the infinite dilution activity coefficient. Systems such as non-electrolytes in water (discussed by Li et al., 1993) have values of the infinite dilution activity coefficient that are of the order of several thousands and require that the cell height be revised to ensure adequate approach to equilibrium. This is however out of the scope of this study.

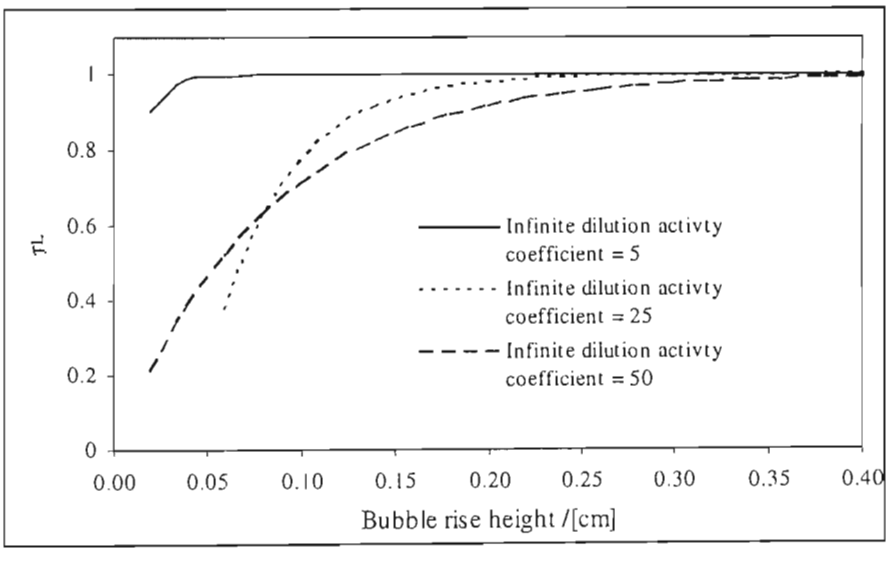

Figure 7-5: The effect of the infinite dilution activity coefficient on the mass transfer rate of solute to the gas bubble for the system acetone+2,3-pentanedione

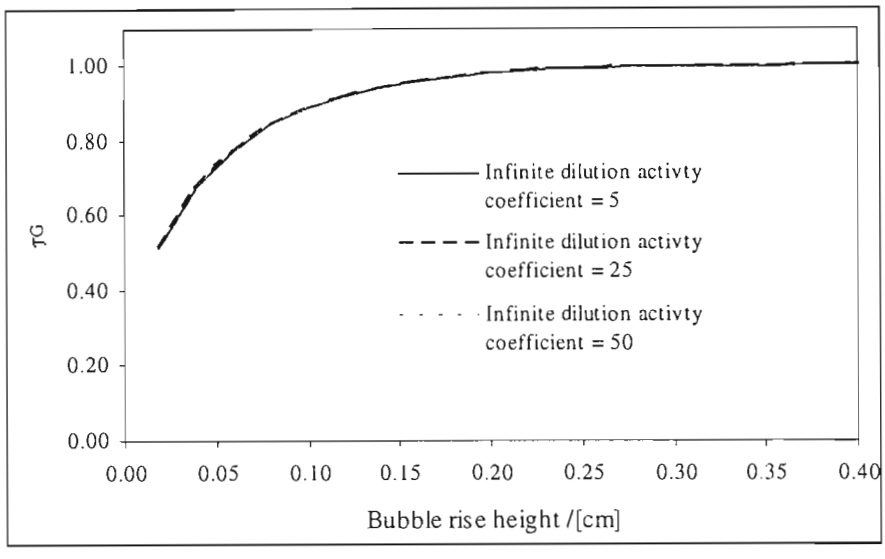

Figure 7-6: The effect of the infinite dilution activity coefficient on the diffusion rate of solute in the gas bubble for the system acetone+2,3-pentanedione

The effects of other parameters were considered, such as the experiment temperature and pressure. The dependence of the infinite dilution activity coefficient on temperature is a separate issue. This section is concerned with the effect of these variables on the approach to equilibrium. Temperatures as high as 50°C were found to have no significant effect. The effect of pressure is generally a non-issue as the cell is essentially open to the atmosphere. Regardless, the sensitivity to cell pressure was also found to be very small.

For all the systems considered in this study, the bubble rise height required for equilibrium was less then 2cm even for large bubble sizes. The height of the dilutor flask was specified such that the bubble rise was approximately 8cm. A description of the cell and its dimensions are given in the experimental procedure section.

7.2 The inert gas stripping apparatus

The experimental apparatus used in this project was similar to that of Leroi et al. (1977), except that the dilutor cell uses capillaries to disperse the gas as proposed by Richon et al. (1980). The apparatus was originally set up by a previous student (Jourdain, 2000) and modified by the author of this work. The original apparatus used a fritted glass disk to disperse the gas. This was changed in favour of capillaries for reasons given in Appendix B and a new dilutor flask was designed.

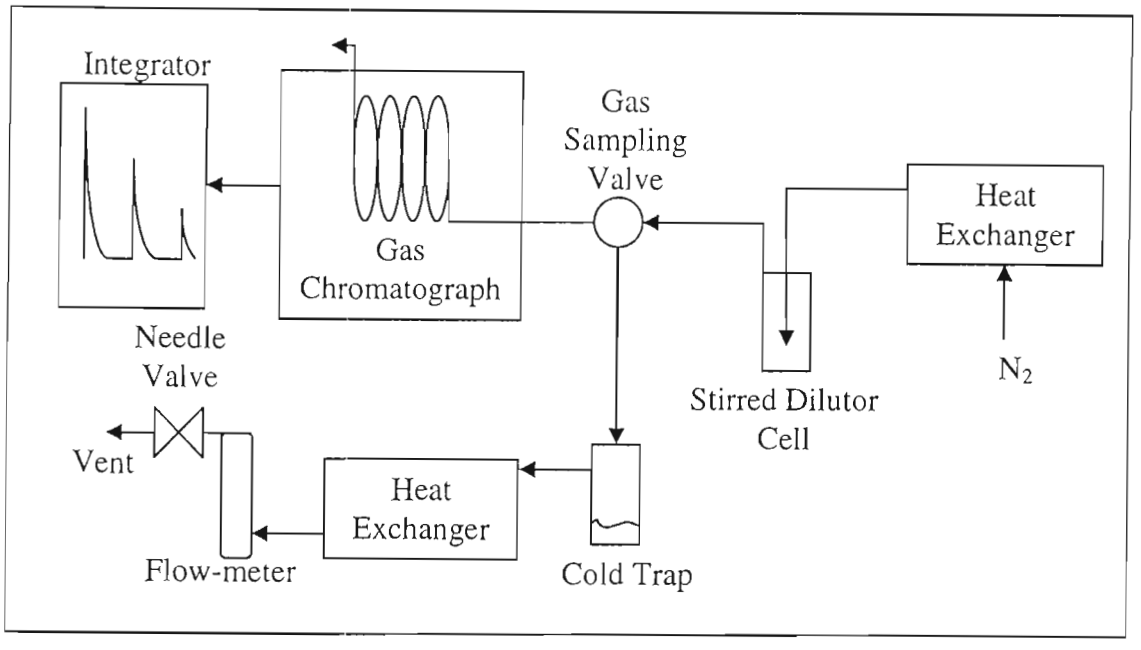

Figure 7-7: Flow diagram of apparatus used to measure infinite dilution activity coefficients by the inert gas stripping method

A flow diagram of the apparatus is shown in Figure 7-7. The inert gas (nitrogen) flows through a coil immersed in a constant temperature bath to bring the gas to the experimental temperature. The heat exchanger is a coil made from 10 m of $^1/_8$ in. stainless-steel tubing. It is immersed in a thermostatted bath. The gas then enters the dilutor flask (Figure 7-8) through 10 lengths of pre-cut $^1/_{32}$ in. stainless tubing (0.005 in. inside diameter). The contents of the flask are stirred by means of a Teflon coated magnetic stirrer-bar. The cell is maintained at the experiment temperature by circulating water through a jacket surrounding the cell. The temperature of the circulating water is controlled with a Julabo water bath controller to within 0.3°C. Temperature is measured with a Class A Pt-100 and the cell pressure measured with a Sensotec TJE pressure transducer Model TJE /713-01-05 (0-25 psia range). A Sensotec (Model GM) display unit was used to read the pressure. The accuracy of the temperature and pressure measurements are estimated to be ±0.03°C and ±0.05 kPa (respectively). The appropriate bubble rise height was calculated as discussed in Appendix B and the cell height was specified accordingly. The stripping gas with entrained solute then flows to a Valco 6-port gas sampling valve through a heated line to prevent condensation. The gas sampling valve has two positions:

- Fill

  The gas is allowed to fill a sample loop and is then vented to the atmosphere. Prior to being vented the condensable components of the gas flow are removed in a cold trap.
- Inject

The sample in the loop is injected into a Varian (model 3300) gas chromatograph (GC) fitted with a flame ionisation detector (FID) for analysis periodically.

The cold trap contains a mixture of acetone and ice. The gas is brought back to ambient temperature in a heat exchanger (a coil of 20 m of $^{1}/_{8}$ in. copper tubing) in a constant temperature bath before being vented. The flow rate of inert gas (free of the entrained components) is then measured (with a soap film flowmeter) and controlled using a needle valve. The flow control is estimated to be with 0.08 ml /min.

A capillary column (007-FFAP on fused silica) was used in the Varian 3300 GC. The following operating conditions were found to give good separation for all the chemicals:

Column temperature	30°C
Detector temperature	150°C
Injector temperature	150°C

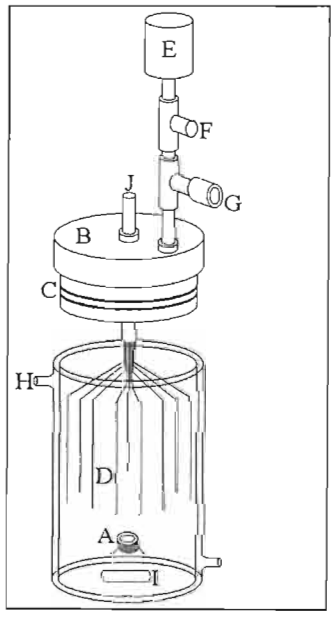

Figure 7-8: Dilutor cell used to measure infinite dilution activity coefficients by the inert gas stripping technique A - Liquid sample point; B - Teflon plug; C - O-rings; D - Capillaries for gas dispersion; E - Pressure transducer; F - Gas outlet; G - Relief-valve; H - Water jacket; I - Magnetic stirrer bar; J - Gas inlet

The new dilutor cell is shown in Figure 7-8. The height of the cell was specified once mass transfer of the solute into the gas was considered (see Appendix A and B). Thus the appropriate path length is achieved for bubbles rising through the liquid so that equilibrium is achieved between the gas and liquid phases. Appendix B shows that equilibrium in the cell is achieved

after a rise height of less than 3cm for bubble sizes of less than 2.5mm. A cell height of 10 cm was chosen as this provides a more than appropriate bubble rise height after considering the clearance of the capillaries and the liquid-level.

Provision is made for a liquid sample to be taken through a septum (A). As it was not necessary to sample the liquid in this study, a thermowell was fitted into the sample point so that the temperature could be measured. A Teflon plug (B) fits onto the top of the cell and a seal is made by means of two o-rings (C). Two threaded holes were bored into the plug. The hole in the centre is used for a length of ¼ in. stainless tubing (J), which contains the dispersion capillaries (D). The second hole is for the gas outlet.

The Sensotec pressure transducer (E) is installed on the gas outlet line (F). The transducer was calibrated using a similar procedure to that explained in Chapter 6 except that the cell was pressurised with nitrogen rather than evacuated with a pump. The response was found to be linear and is shown in Figure 7-9. Due to the glass cell being slightly pressurised a relief-valve (G) is installed for safety reasons (shown in Figure 7-8). The cell is contained in a water jacket (H) to ensure that the dilutor operates isothermally.

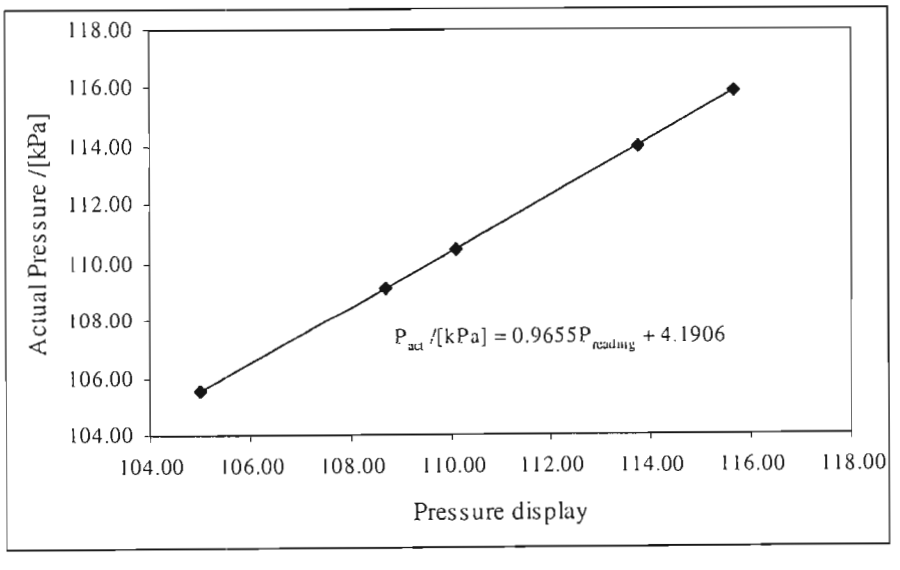

Figure 7-9: Plot to show the linear relationship of actual pressure with pressure displayed on the Sensotec display used in the inert gas stripping apparatus

7.3 Experimental difficulties

The cell (shown in Figure 7-2) was constructed from glass by an expert glassblower, P. Siegling. The plug, fitted onto the top of cell, is made from Teflon. Two threaded holes are drilled into the plug for the gas inlet and outlet lines. The pressure transducer is fitted on the gas

exit line, as is the relief valve. The seal between the plug and the cell is made with two o-rings. The set of stainless-steel capillaries used to disperse the gas ensures small bubble sizes and no coalescence of bubbles was observed. Coalescence was a problem experienced when using a sintered glass disk to disperse the gas.

The following problems were experienced during the experiments:

- Analysis of the gas.
  It was noted that previous researchers made use of GC's fitted with a flame ionisation detector (FID). The exit gas in this study was, however, originally directed to a Hewlett Packard gas chromatograph (Model 5890 Series II), fitted with a TCD, due to availability. Large sample sizes were necessary when using the TCD(thermal conductivity detector) and analysis was most unsatisfactory. The solution was to direct the gas to a Varian 3300 GC fitted with a FID. The improved detector sensitivity yielded better results.
- Leaks in the Teflon plug.
  It was required to remove the plug prior to each experiment to introduce the chemicals. The considerable weight of the transducer and the stainless-steel tubing, as well as removing the plug often, tended to damage the Teflon threads. The cell would leak as a result. Sealing the leaks proved difficult due to the non-stick nature of Teflon. Filling these leaks with Loctite and reducing the pressure in the cell to allow the leaks to seal was an effective solution.
- O-ring seals.
  The o-ring seals were effective during the earlier experiments. It did, however, become necessary to clamp the plug to the cell eventually.

7.4 Experimental procedure

1. The thermostatted water baths containing the heat exchange coils were allowed to reach their set-point temperatures.
2. The cold trap was filled with a mixture of acetone and ice and the transient lines between the cell, the gas sampling valve and the GC were heated to ensure no partial condensation.
3. The dilutor flask was filled with a known amount of solvent (gravimetrically).
4. A small quantity of solute was introduced into the cell such that the solute mole fraction is less than 10^{-3} (reason given in Chapter 4). It was not required to know this mole fraction exactly as discussed in Chapter 9.

5. The Teflon plug is fitted onto the cell and water at the experiment temperature was circulated through the jacket.
6. The magnetic stirrer was switched on and the inert gas was allowed to flow through the cell. The flow rate of the gas was measured with a soap film flow-meter and controlled with a needle valve. The flow rate was checked periodically during the experiment.
7. The gas sampling valve was set to the "fill" position and the stripping gas was allowed to flow through the apparatus for 15 minutes.
8. The sampling valve was set to the "inject" position for approximately 1 minute, then set back to "fill."
9. Step 8 was repeated periodically and the time noted when each injection was made. The time between injections depends on the GC run-times and on the chemicals being studied. For relatively non-volatile solutes, the time between injections must be large to allow for significant change in composition. The latter was not a problem in this study.
10. The experiment was stopped after sufficient measurements were made for the infinite dilution activity coefficient to be calculated. The gas flow was ceased and the transient lines were allowed to cool.
11. It is possible that the stripping gas flow rate is too large to allow the gas phase to reach equilibrium with the liquid. The experiment was repeated to ensure that the values of the infinite dilution activity coefficient obtained were not significantly different for various values of the flow rate as suggested by Li et al. (1993).

CHAPTER EIGHT

EXPERIMENTAL RESULTS

The VLE measurements made with the low-pressure recirculating still of Raal and Mühlbauer (1998) are presented in this Chapter. Previously unmeasured vapour pressure data for 2,3-pentanedione are presented, as are isobaric and isothermal data for cyclohexane with ethanol. The purpose of measuring data for this system was to demonstrate the accuracy of the apparatus and the experimental procedure. VLE data for previously unmeasured binary systems involving diacetyl and 2,3-pentandione measured at multiple isotherms and an isobar are also presented.

8.1. Vapour pressure measurements for 2,3-pentanedione

The vapour pressure measurements for 2,3-pentanedione are new data. The recirculating still of Raal and Mühlbauer (1998) was charged with a pure sample of 2,3-pentanedione and the boiling temperature was measured for various pressure set-points. The design of the still is based on the on a sophisticated ebulliometer (as discussed in Chapter 2). The still provided boiling temperatures for the other test chemicals (ethanol, cyclohexane, methanol, diacetyl and acetone) that compare very well with reliable literature data (refer to Table 9-1).

Table 8-1: Vapour Pressure Data for 2,3-Pentanedione

T /[°C]	P /[kPa]
58.69	15.37
65.23	20.36
70.58	25.35
74.98	30.35
79.00	35.34
82.59	40.33
85.70	45.32
88.74	50.21
91.54	55.21
93.94	60.20
96.29	65.19
98.46	70.18
100.65	75.27

The vapour pressure data for 2,3-pentanedione were correlated to the Antoine equation:

$$\ln P^{sat}[kPa] = A - \frac{B}{T[^{o}C] + C} \tag{8-1}$$

The constants in Eq. 8-1 are A = 13.771 B = 2756.639 C = 191.054

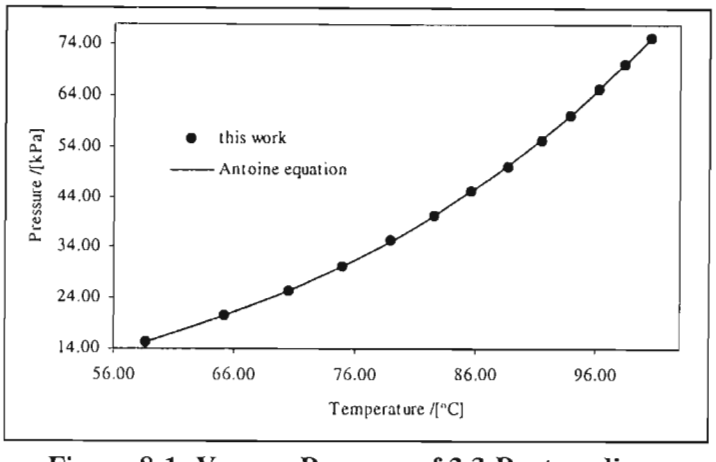

Figure 8-1: Vapour Pressure of 2,3-Pentanedione

8.2 VLE measurements for cyclohexane with ethanol

Isothermal measurements were made for the system at 40 °C. Isobaric data at 40 kPa were also measured. The measurements are listed in Table 8-2 and are presented in Figures 8-2 to 8-5, together with data sets measured by Joseph et al [2000] for comparison. The system displays an azeotrope and much care must be taken to produce accurate VLE. The measurements made in this study show excellent agreement with the literature set.

Table 8-2: VLE for cyclohexane(1) with ethanol(2) at 40 °C and 40 kPa

40 °C			40 kPa		
P /[kPa]	y1	x1	T /[°C]	y1	x1
17.85	0.000	0.000	56.52	0.000	0.000
20.14	0.110	0.012	50.25	0.280	0.043
27.43	0.373	0.061	47.73	0.363	0.074
32.13	0.486	0.121	46.11	0.425	0.095
35.02	0.542	0.196	43.52	0.518	0.173
36.32	0.576	0.276	42.28	0.568	0.264
37.12	0.597	0.387	41.89	0.581	0.326
37.52	0.620	0.652	41.70	0.593	0.378
37.32	0.633	0.789	41.60	0.619	0.480
36.82	0.651	0.893	41.64	0.619	0.762
37.12	0.638	0.836	41.97	0.641	0.878
36.92	0.646	0.879	42.55	0.666	0.928
36.22	0.666	0.922	44.08	0.716	0.973
24.70	1.000	1.000	52.54	1.000	1.000

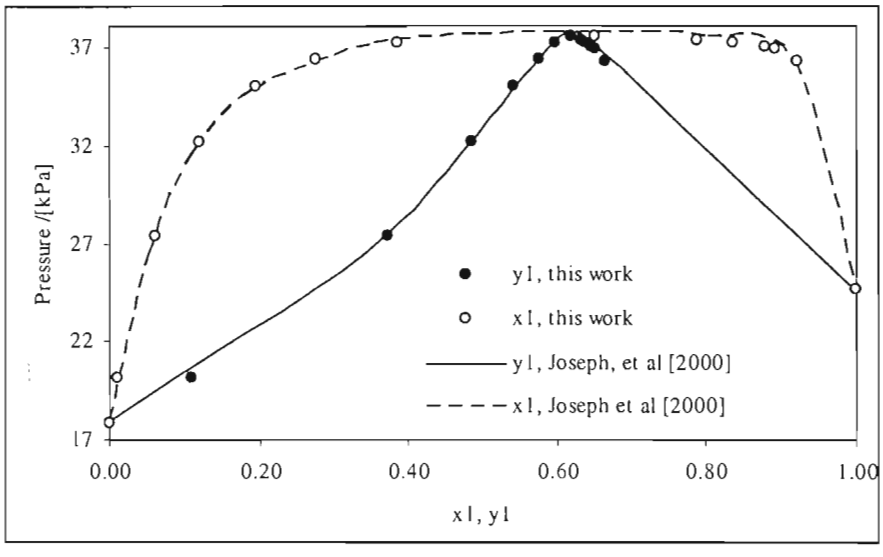

Figure 8-2: P-x-y diagram for cyclohexane(1) with ethanol(2) at 40 °C

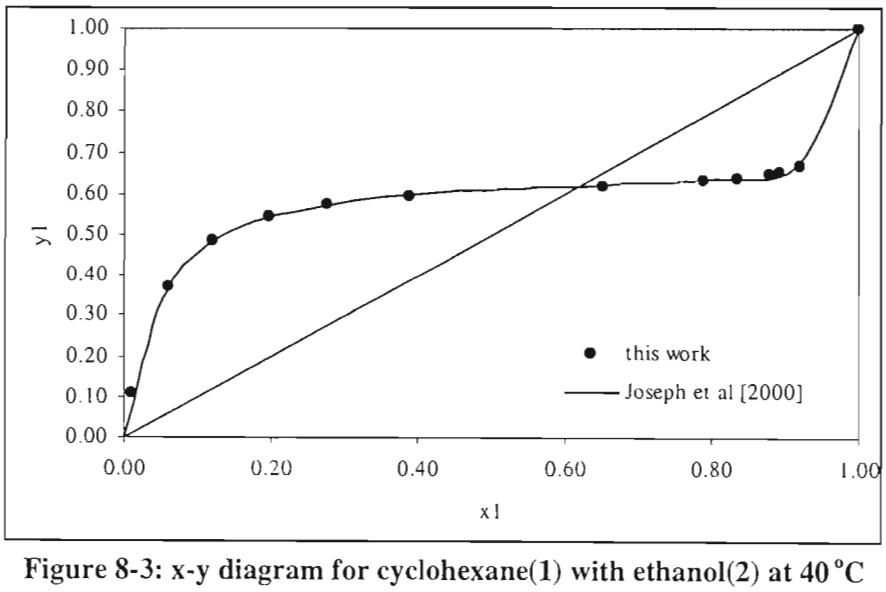

Figure 8-3: x-y diagram for cyclohexane(1) with ethanol(2) at 40 °C

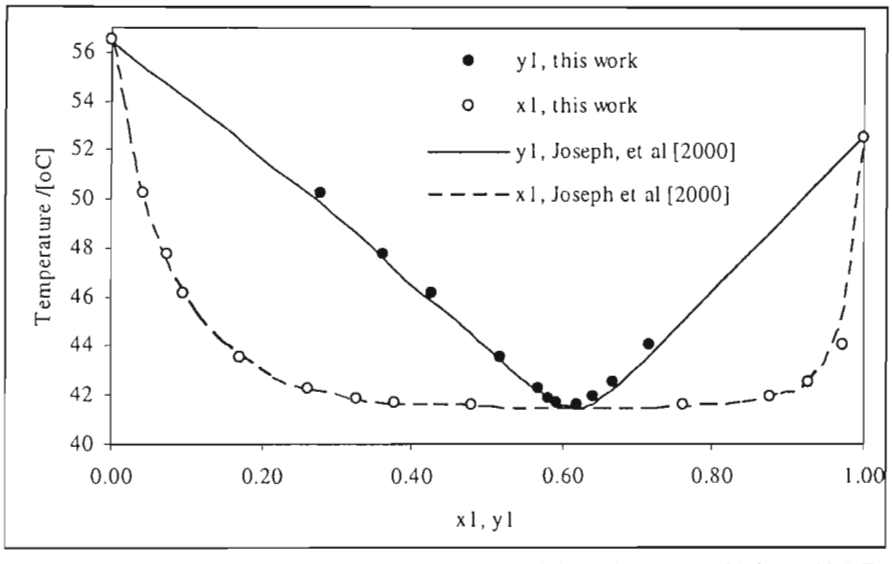

Figure 8-4: P-x-y diagram for cyclohexane(1) with ethanol(2) at 40 kPa

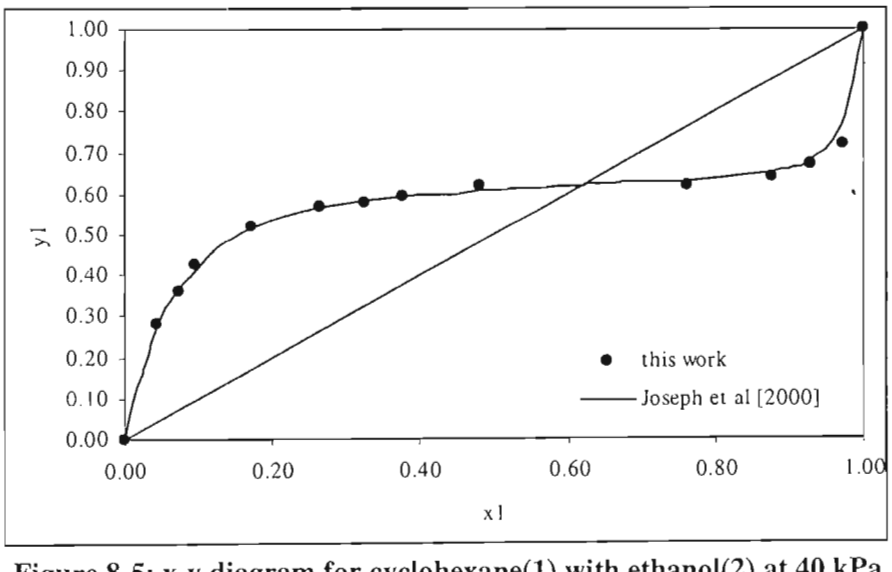

Figure 8-5: x-y diagram for cyclohexane(1) with ethanol(2) at 40 kPa

8.3 VLE Measurements for Acetone with Diacetyl

Isothermal measurements were made for the system at 30 °C, 40 °C and 50 °C. Isobaric data at 40 kPa were also measured. All four sets are new data. The measurements are listed in Tables 8-3 and 8-4 and are presented in Figures 8-6 to 8-13. As can be expected for mixtures of chemically similar substances (ketones), the VLE displays nearly ideal behaviour.

Table 8-3: VLE for acetone(1) with diacetyl(2) at 30 °C and 40 °C

30 °C			40 °C		
P /[kPa]	y1	x1	P /[kPa]	y1	x1
8.62	0.000	0.000	14.33	0.000	0.000
9.36	0.074	0.018	15.25	0.071	0.018
9.86	0.129	0.034	16.05	0.128	0.035
10.56	0.196	0.057	16.95	0.181	0.058
12.15	0.358	0.118	19.24	0.341	0.116
15.35	0.544	0.231	23.54	0.536	0.231
18.75	0.704	0.350	28.83	0.671	0.356
23.44	0.818	0.518	35.42	0.804	0.513
30.43	0.930	0.756	45.41	0.923	0.749
33.82	0.967	0.868	50.60	0.963	0.867
35.22	0.979	0.913	52.50	0.976	0.913
36.42	0.990	0.956	53.60	0.985	0.943
36.82	0.992	0.965	54.50	0.991	0.966
38.04	1.000	1.000	56.64	1.000	1.000

Table 8-4: VLE for acetone(1) with diacetyl(2) at 50 °C and 40 kPa

50 °C			40 kPa		
P /[kPa]	y1	x1	T /[°C]	y1	x1
22.77	0.000	0.000	63.52	0.000	0.000
23.74	0.061	0.018	60.96	0.152	0.052
24.84	0.114	0.035	58.46	0.267	0.101
26.23	0.175	0.061	54.17	0.446	0.189
29.73	0.318	0.121	50.05	0.595	0.297
35.82	0.506	0.228	46.07	0.715	0.413
43.01	0.670	0.357	42.56	0.809	0.530
52.20	0.795	0.519	39.39	0.879	0.649
66.08	0.914	0.754	36.58	0.930	0.768
73.17	0.959	0.868	34.61	0.962	0.857
75.77	0.974	0.912	33.03	0.983	0.931
77.76	0.985	0.943	32.55	0.989	0.956
79.06	0.991	0.967	32.22	0.994	0.973
81.65	1.000	1.000	32.01	0.996	0.983
			31.22	1.000	1.000

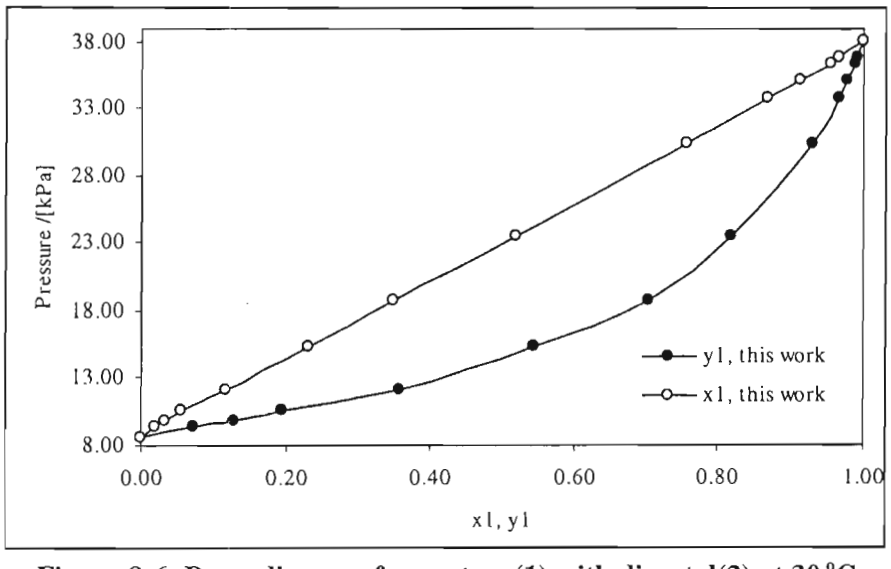

Figure 8-6: P-x-y diagram for acetone(1) with diacetyl(2) at 30 °C

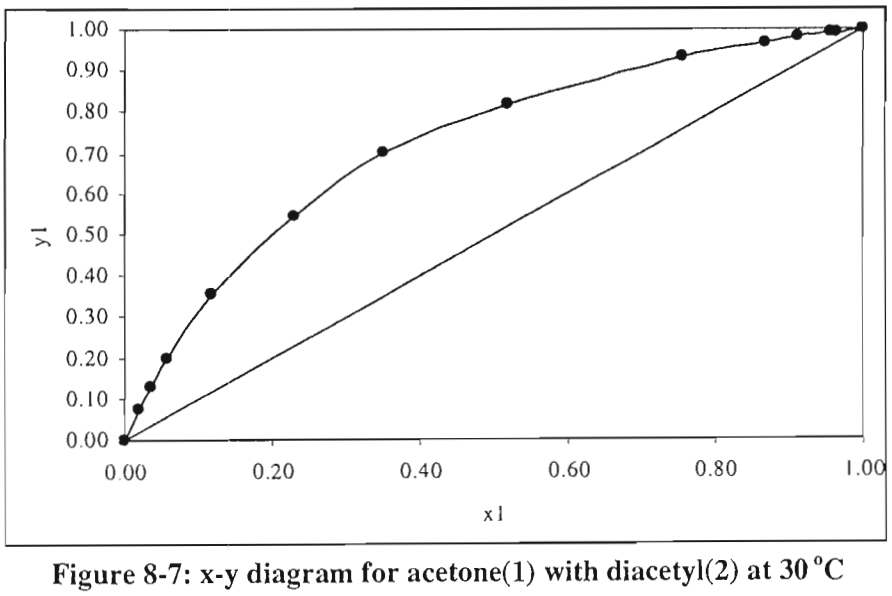

Figure 8-7: x-y diagram for acetone(1) with diacetyl(2) at 30 °C

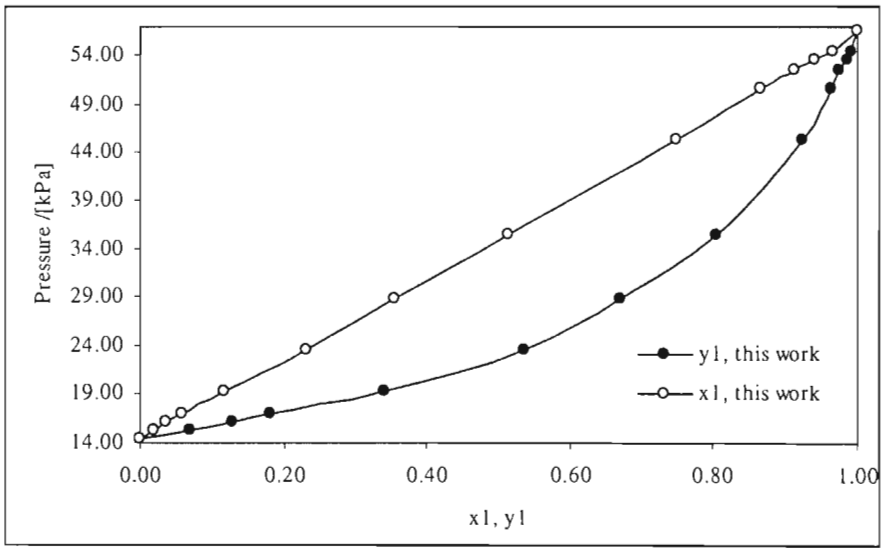

Figure 8-8: P-x-y diagram for acetone(1) with diacetyl(2) at 40 °C

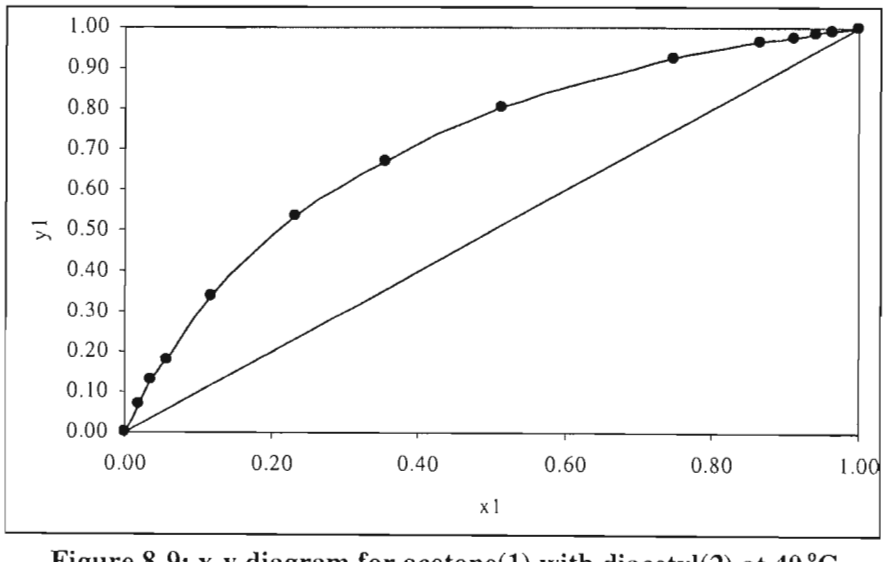

Figure 8-9: x-y diagram for acetone(1) with diacetyl(2) at 40 °C

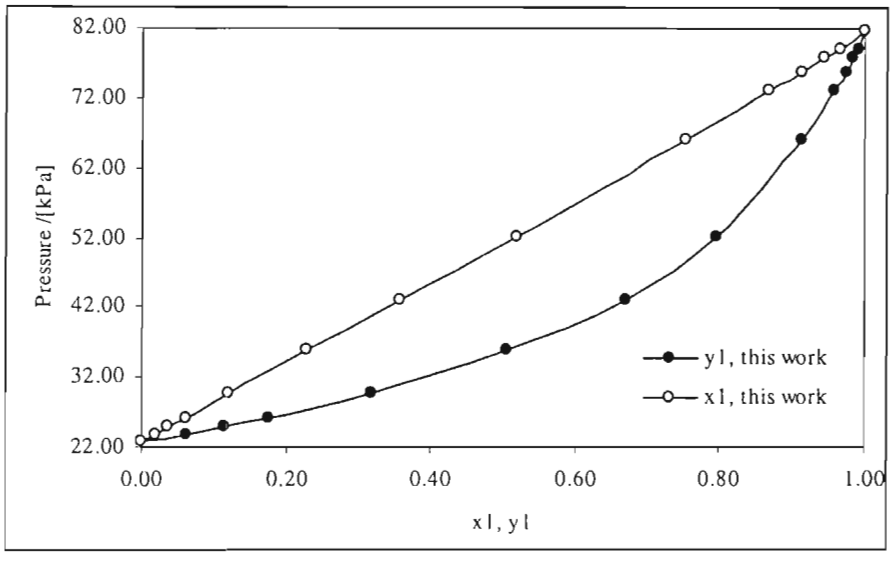

Figure 8-10: P-x-y diagram for acetone(1) with diacetyl(2) at 50 °C

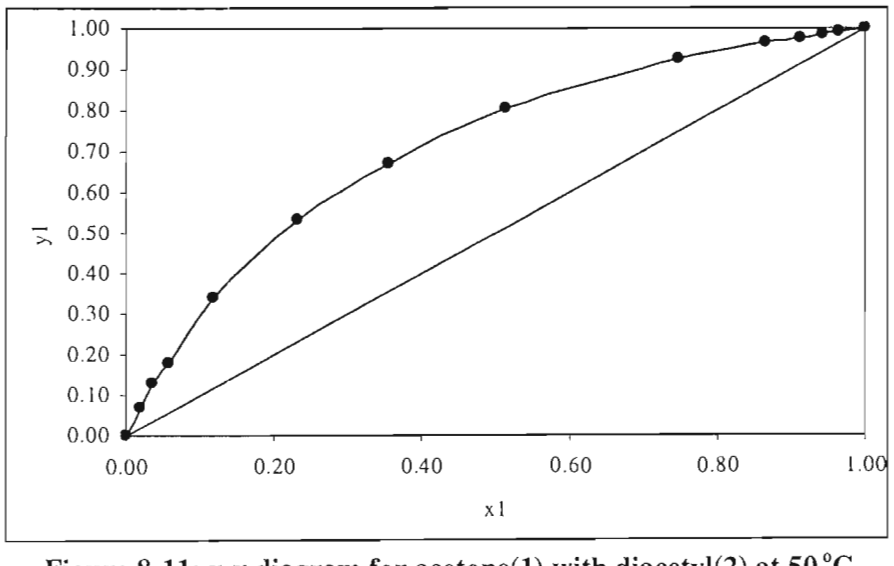

Figure 8-11: x-y diagram for acetone(1) with diacetyl(2) at 50 °C

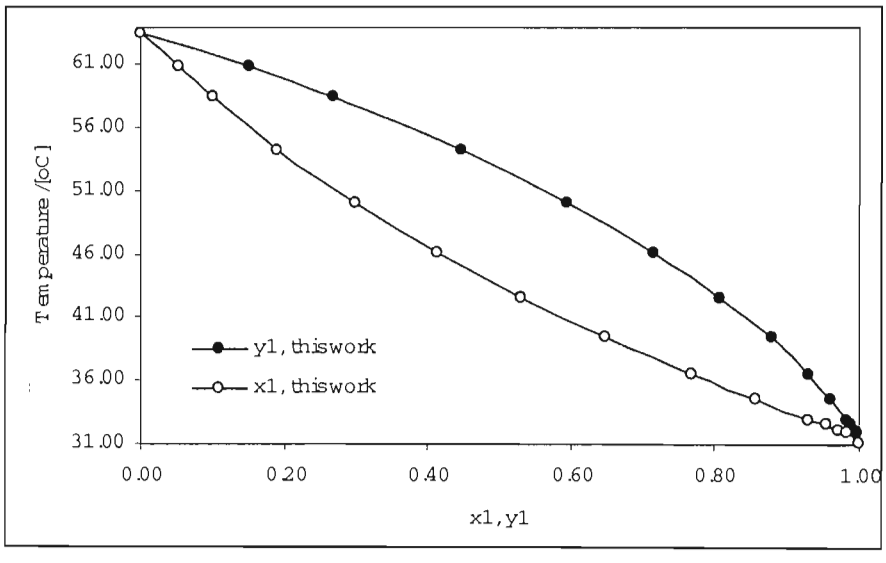

Figure 8-12: T-x-y diagram for acetone(1) with diacetyl(2) at 40 kPa

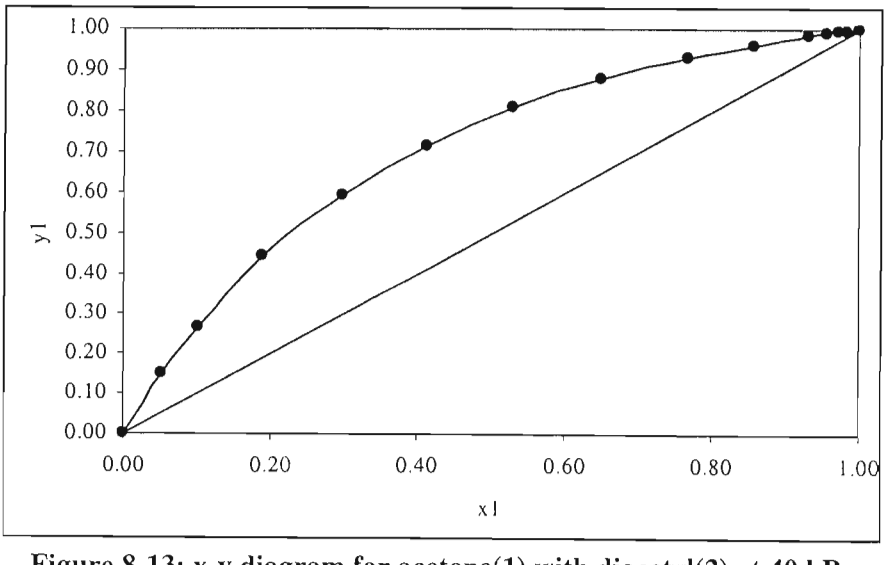

Figure 8-13: x-y diagram for acetone(1) with diacetyl(2) at 40 kPa

8.4 VLE measurements for Methanol with Diacetyl

Isothermal measurements were made for the system at 40 °C, 50 °C and 60 °C. Isobaric data at 40 kPa were also measured. All four sets are new data. The measurements are listed in Tables 8-5 and 8-6 and are presented in Figures 8-14 to 8-21.

Table 8-5: VLE for methanol(1) with diacetyl(2) at 313.15K and 323.15K

40 °C			50 °C		
P /[kPa]	y1	x1	P /[kPa]	y1	x1
14.33	0.000	0.000	22.77	0.000	0.000
17.15	0.205	0.072	26.93	0.209	0.070
18.95	0.323	0.125	30.13	0.325	0.119
21.54	0.447	0.198	34.02	0.445	0.191
24.04	0.577	0.301	38.32	0.550	0.282
26.33	0.653	0.395	42.11	0.644	0.400
28.83	0.724	0.532	46.01	0.722	0.533
31.03	0.791	0.666	49.40	0.787	0.669
32.63	0.858	0.781	51.90	0.855	0.782
34.32	0.940	0.918	54.10	0.939	0.914
34.72	0.968	0.957	54.40	0.964	0.956
35.02	0.980	0.973	54.99	0.986	0.984
35.32	0.989	0.985	55.69	1.000	1.000
35.52	1.000	1.000			

Table 8-6: VLE for methanol(1) with diacetyl(2) at 60 °C and 40 kPa

60 °C			40 kPa		
P /[kPa]	y1	x1	T /[°C]	y1	x1
34.76	0.000	0.000	63.52	0.000	0.000
41.51	0.219	0.070	59.04	0.225	0.071
45.91	0.326	0.116	55.45	0.375	0.138
52.30	0.448	0.191	53.38	0.471	0.193
58.99	0.552	0.282	49.74	0.602	0.320
64.88	0.644	0.399	47.99	0.669	0.423
70.67	0.724	0.533	46.39	0.734	0.540
75.77	0.791	0.668	45.28	0.789	0.651
79.56	0.858	0.784	43.93	0.874	0.816
82.26	0.940	0.916	43.36	0.928	0.901
82.96	0.968	0.959	43.10	0.955	0.940
83.45	0.980	0.973	42.92	0.972	0.964
83.75	0.989	0.986	42.89	0.979	0.975
84.72	1.000	1.000	42.84	0.986	0.982
			42.575	1.000	1.000

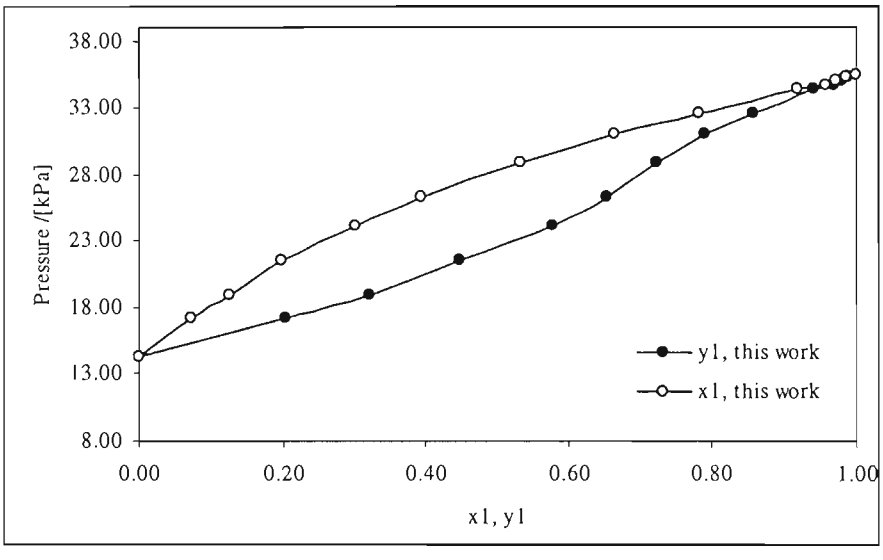

Figure 8-14: P-x-y diagram for methanol(1) with diacetyl(2) at 40 °C

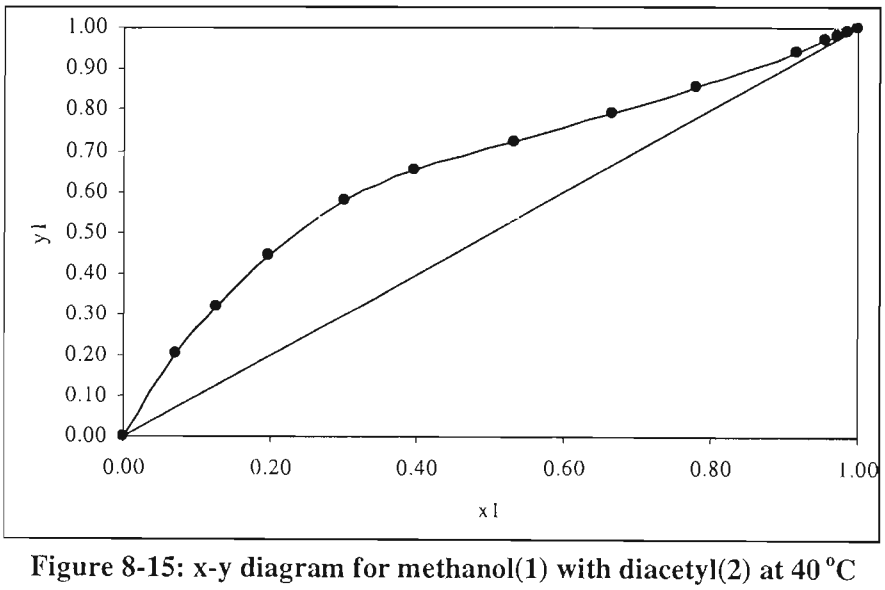

Figure 8-15: x-y diagram for methanol(1) with diacetyl(2) at 40 °C

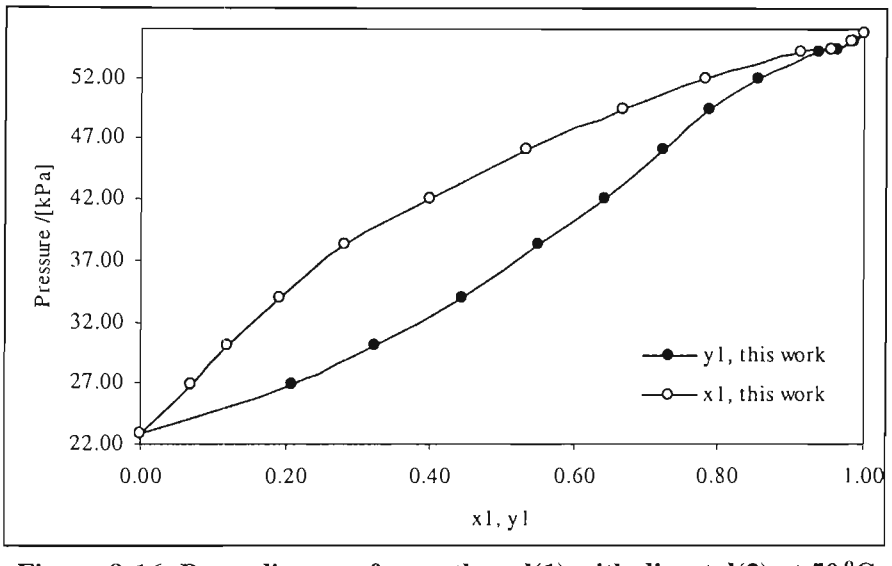

Figure 8-16: P-x-y diagram for methanol(1) with diacetyl(2) at 50 °C

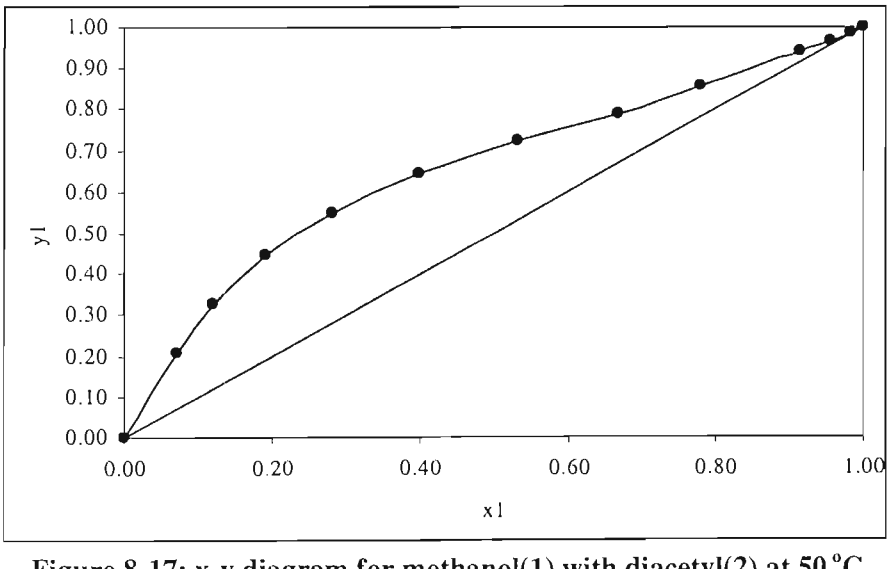

Figure 8-17: x-y diagram for methanol(1) with diacetyl(2) at 50 °C

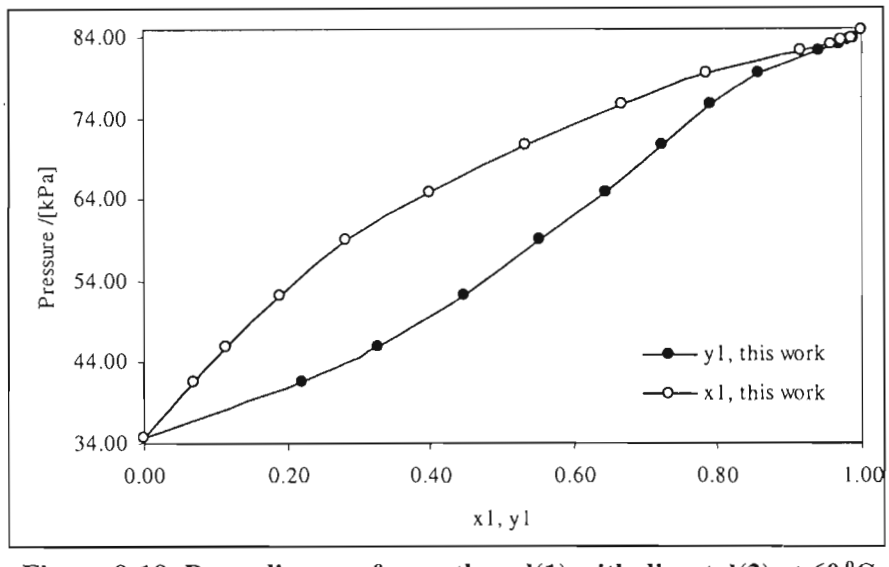

Figure 8-18: P-x-y diagram for methanol(1) with diacetyl(2) at 60 °C

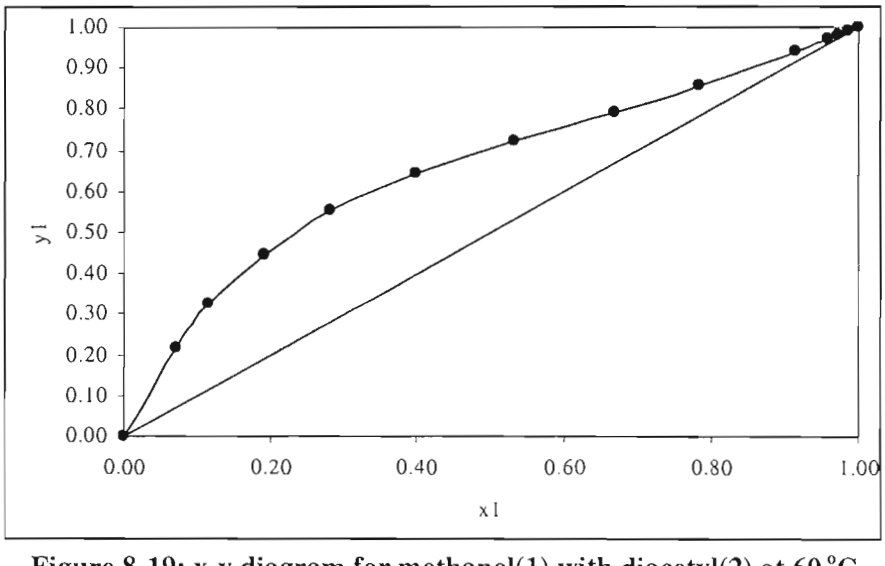

Figure 8-19: x-y diagram for methanol(1) with diacetyl(2) at 60 °C

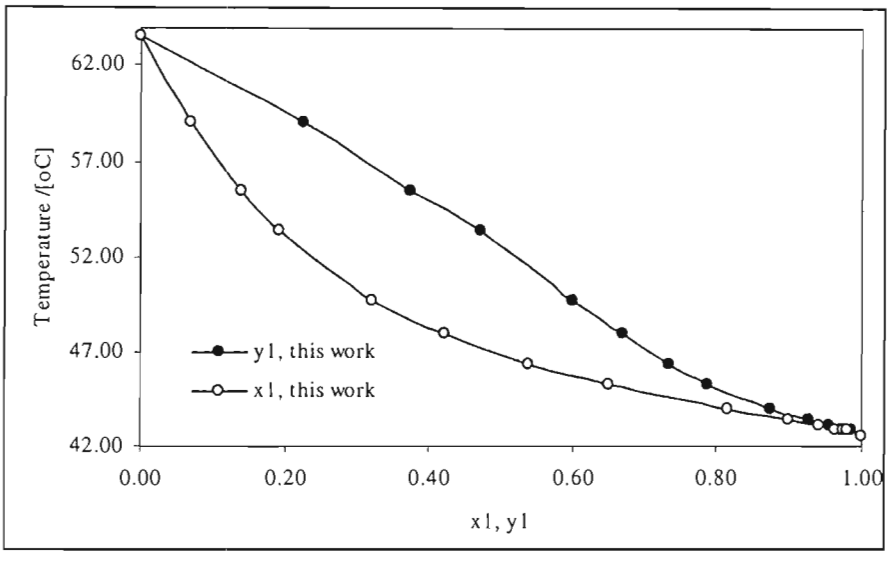

Figure 8-20: T-x-y diagram for methanol(1) with diacetyl(2) at 40 kPa

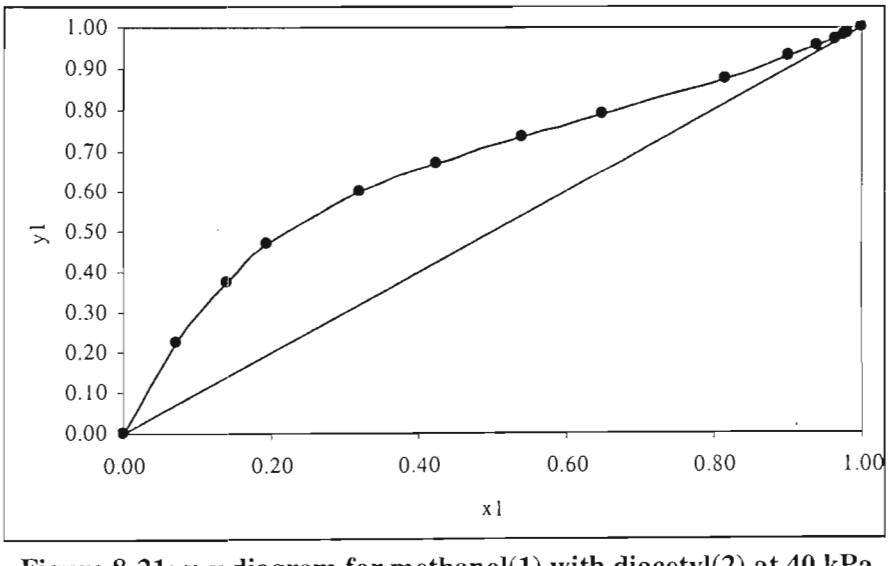

Figure 8-21: x-y diagram for methanol(1) with diacetyl(2) at 40 kPa

8.5 VLE measurements for Diacetyl with 2,3-Pentanedione

Isothermal measurements were made for the system at 60 °C, 70 °C and 80 °C. Isobaric data at 40 kPa were also measured. All four sets are new data. The measurements are listed in Tables 8-7 and 8-8 and are presented in Figures 8-22 to 8-29. As can be expected for mixtures of chemically similar substances (diketones), the VLE displays nearly ideal behaviour.

Table 8-7: VLE for diacetyl(1) with 2,3-pentanedione at 60 °C and 70 °C

60 °C			70 °C		
P /[kPa]	y1	x1	P /[kPa]	y1	x1
16.30	0.000	0.000	24.80	0.000	0.000
16.57	0.066	0.033	25.25	0.066	0.035
17.17	0.140	0.072	25.95	0.126	0.068
18.36	0.233	0.133	27.65	0.233	0.132
21.16	0.434	0.276	31.44	0.410	0.273
23.66	0.574	0.418	35.04	0.568	0.413
25.75	0.699	0.538	38.33	0.684	0.534
27.65	0.779	0.647	41.13	0.771	0.643
29.55	0.844	0.737	48.32	0.963	0.916
34.76	1.000	1.000	49.02	0.973	0.939
			51.20	1.000	1.000

Table 8-8: VLE for diacetyl(1) with 2,3-pentanedione at 80 °C and 40 kPa

80 °C			40 kPa		
P /[kPa]	y1	x1	T /[°C]	y1	x1
36.60	0.000	0.000	82.37	0.000	0.000
37.13	0.067	0.034	80.82	0.100	0.054
38.53	0.128	0.071	79.03	0.223	0.130
40.63	0.231	0.132	76.26	0.407	0.264
45.62	0.401	0.276	70.79	0.695	0.548
50.91	0.570	0.418	68.91	0.783	0.652
55.80	0.691	0.546	66.06	0.897	0.828
59.30	0.778	0.648	65.12	0.933	0.885
69.18	0.963	0.916	64.07	0.984	0.970
70.48	0.974	0.940	63.63	1.000	1.000
73.20	1.000	1.000			

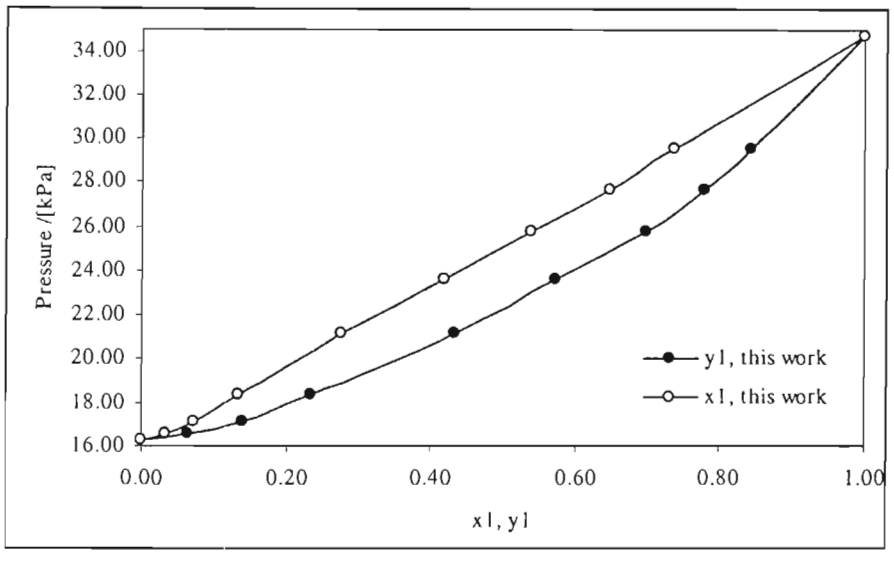

Figure 8-22: P-x-y diagram for diacetyl(1) with 2,3-pentanedione(2) at 60 °C

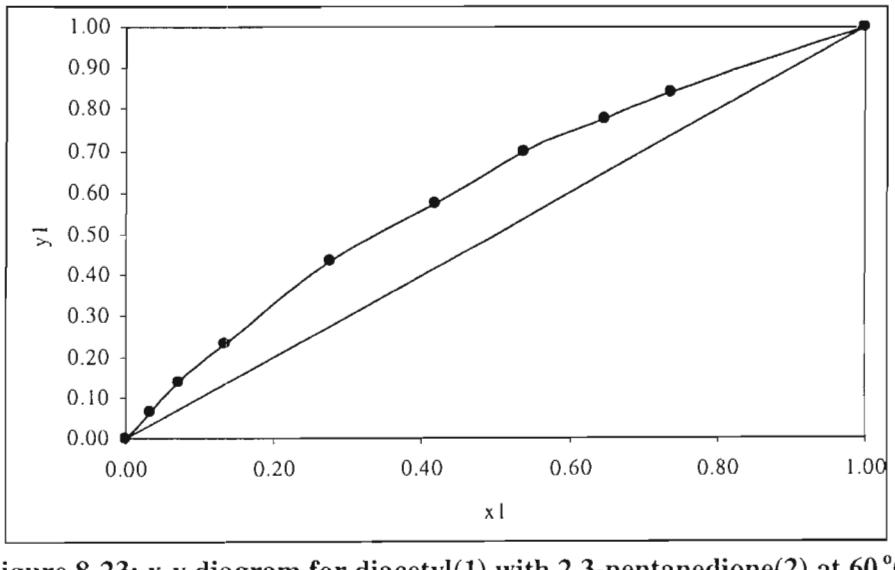

Figure 8-23: x-y diagram for diacetyl(1) with 2,3-pentanedione(2) at 60 °C

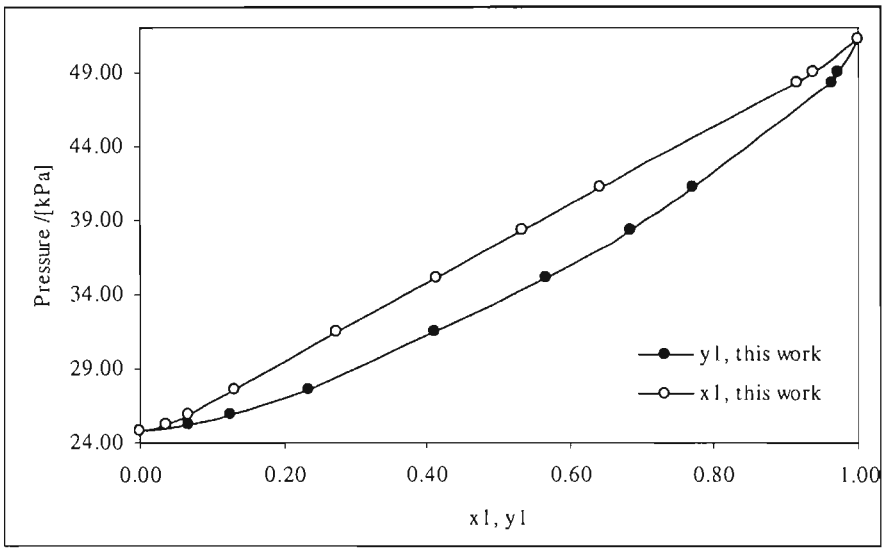

Figure 8-24: P-x-y diagram for diacetyl(1) with 2,3-pentanedione(2) at 70 °C

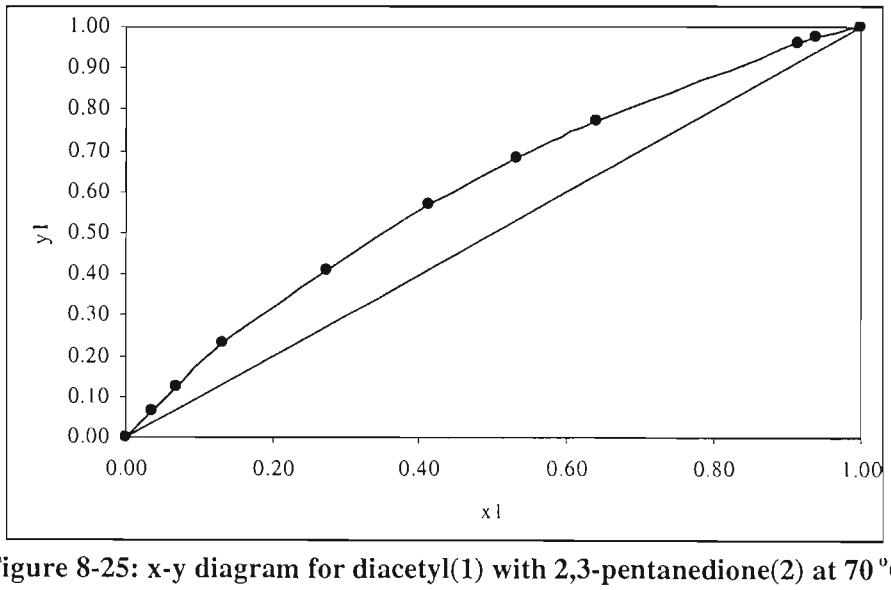

Figure 8-25: x-y diagram for diacetyl(1) with 2,3-pentanedione(2) at 70 °C

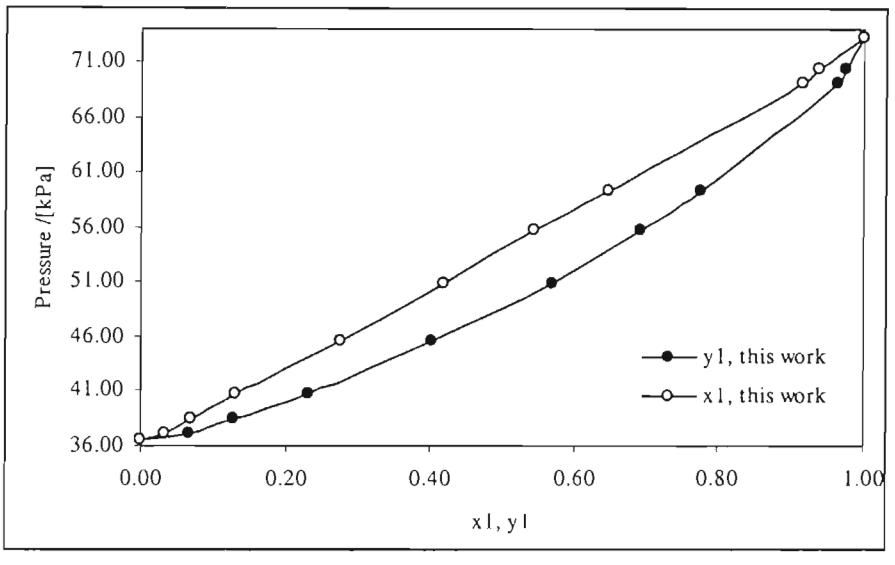

Figure 8-26: P-x-y diagram for diacetyl(1) with 2,3-pentanedione(2) at 80 °C

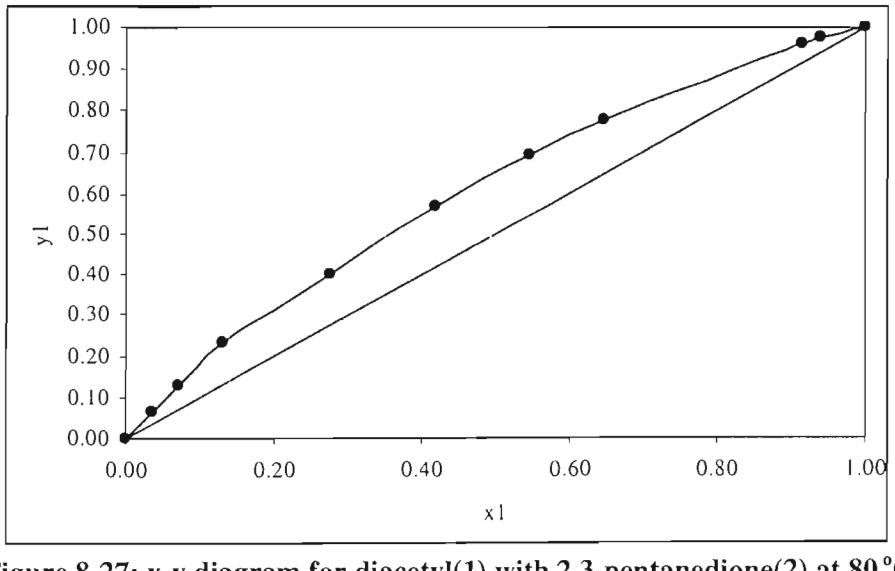

Figure 8-27: x-y diagram for diacetyl(1) with 2,3-pentanedione(2) at 80 °C

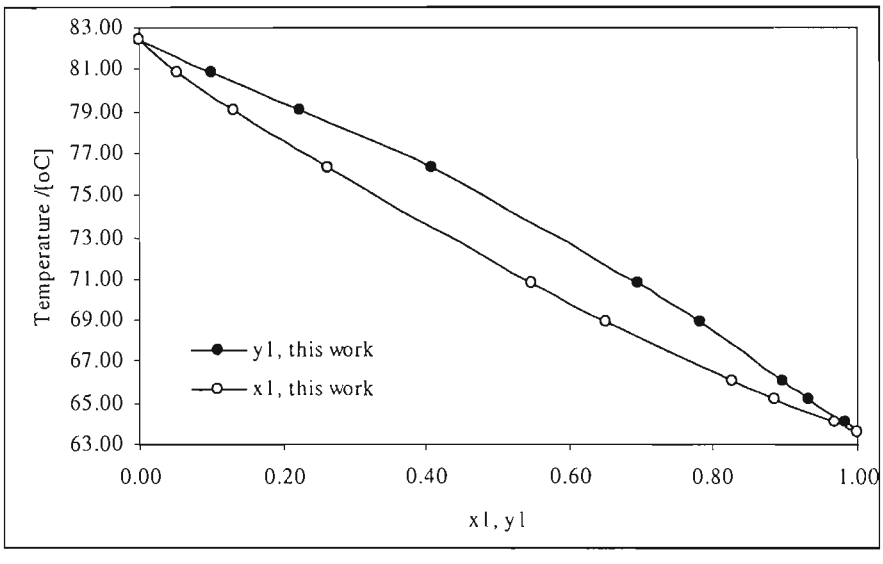

Figure 8-28: T-x-y diagram for diacetyl(1) with 2,3-pentanedione(2) at 40 kPa

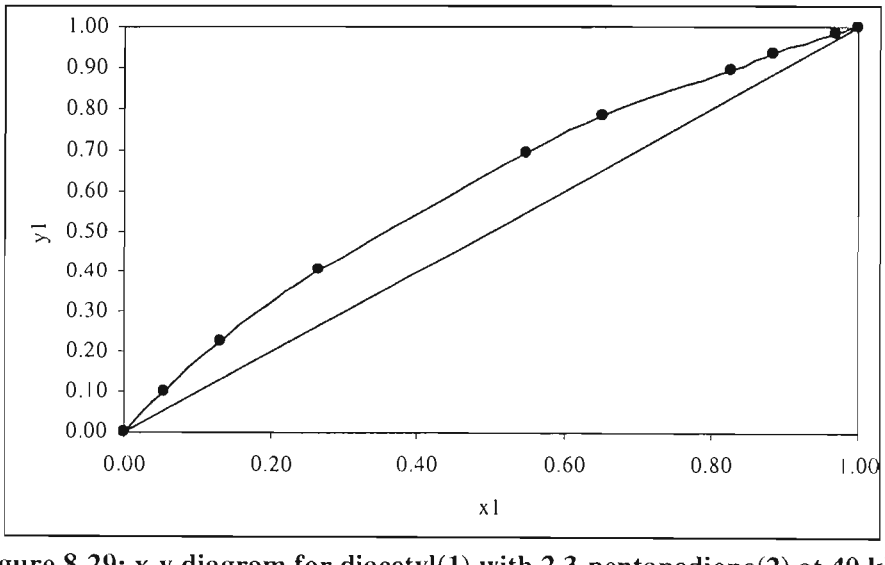

Figure 8-29: x-y diagram for diacetyl(1) with 2,3-pentanedione(2) at 40 kPa

8.6 VLE measurements for Acetone with 2,3-Pentanedione

Isothermal measurements were made for the system at 50 °C. Isobaric data at 30 kPa and 40 kPa were also measured. All three sets are new data. The measurements are listed in Tables 8-9 and 8-10 and are presented in Figures 8-30 to 8-35. As can be expected for mixtures of chemically similar substances (ketones), the VLE displays nearly ideal behaviour.

Table 8-9: VLE for acetone(1) with 2,3-pentanedione at 323.15K and 30 kPa

50 °C			30 kPa		
P /[kPa]	y1	x1	T /[°C]	y1	x1
10.30	0.000	0.000	74.79	0.000	0.000
11.48	0.108	0.016	71.43	0.028	0.139
13.97	0.322	0.053	69.11	0.048	0.222
22.76	0.614	0.179	65.01	0.089	0.387
31.44	0.768	0.300	62.61	0.123	0.468
44.92	0.880	0.496	50.90	0.281	0.727
57.10	0.944	0.665	42.41	0.425	0.857
77.37	0.993	0.945	36.32	0.577	0.931
80.07	0.997	0.976	24.38	1.000	1.000
81.90	1.000	1.000			

Table 8-10: VLE for acetone(1) with 2,3-pentanedione at 40 kPa

40 kPa		
T /[°C]	y1	x1
82.37	0.000	0.000
80.04	0.017	0.084
78.27	0.034	0.152
75.68	0.057	0.251
67.15	0.153	0.523
58.49	0.275	0.718
52.00	0.396	0.842
43.60	0.576	0.926
35.67	0.825	0.980
33.80	0.899	0.989
32.74	0.943	0.994
31.22	1.000	1.000

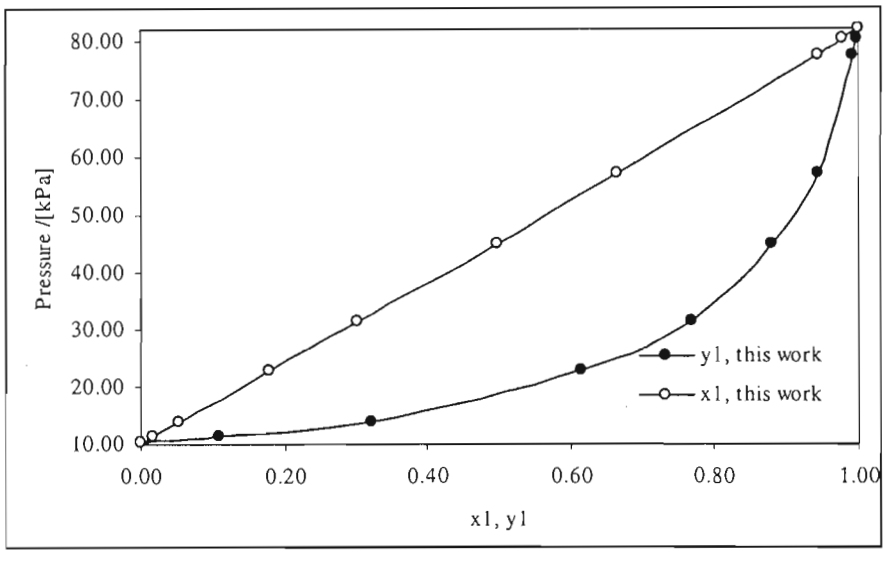

Figure 8-30: P-x-y diagram for acetone(1) with 2,3-pentanedione(2) at 50 °C

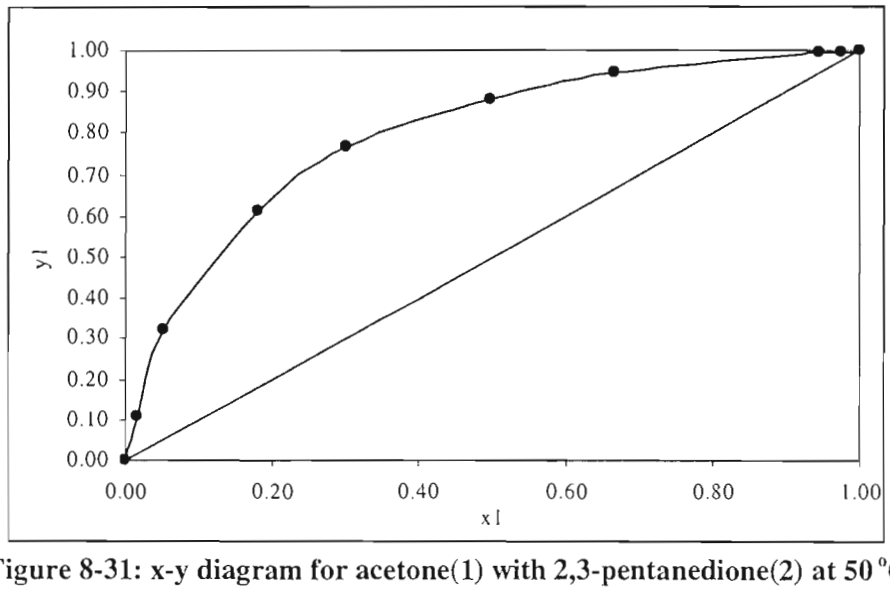

Figure 8-31: x-y diagram for acetone(1) with 2,3-pentanedione(2) at 50 °C

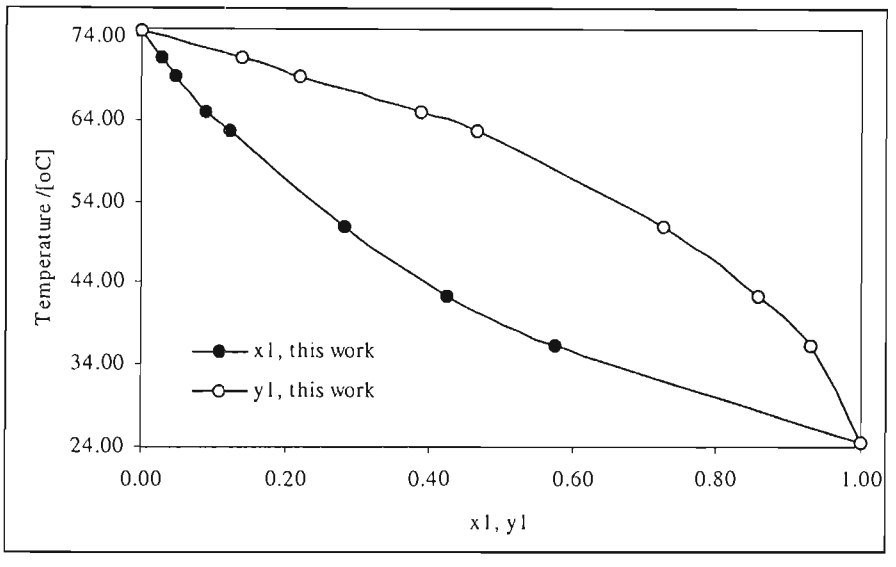

Figure 8-32: T-x-y diagram for acetone(1) with 2,3-pentanedione(2) at 30 kPa

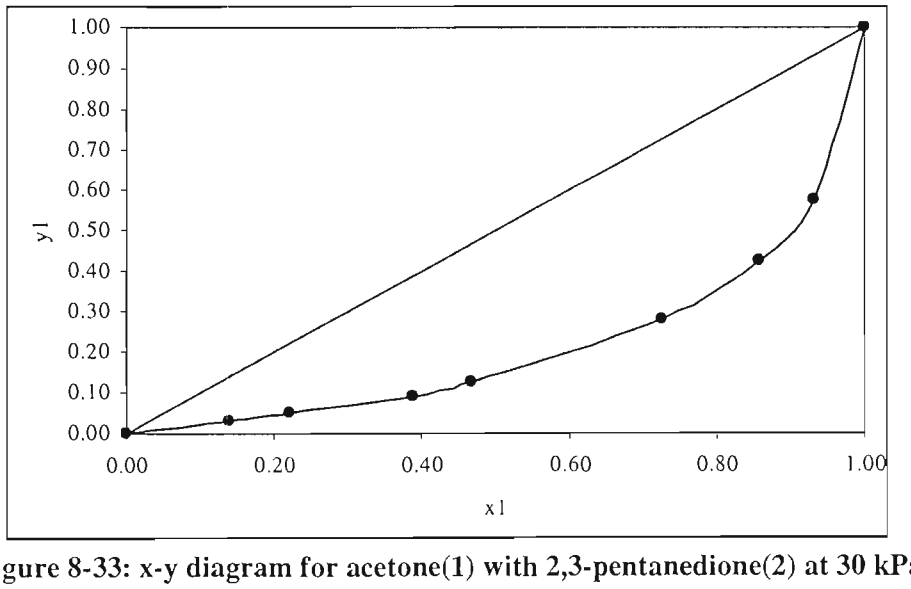

Figure 8-33: x-y diagram for acetone(1) with 2,3-pentanedione(2) at 30 kPa

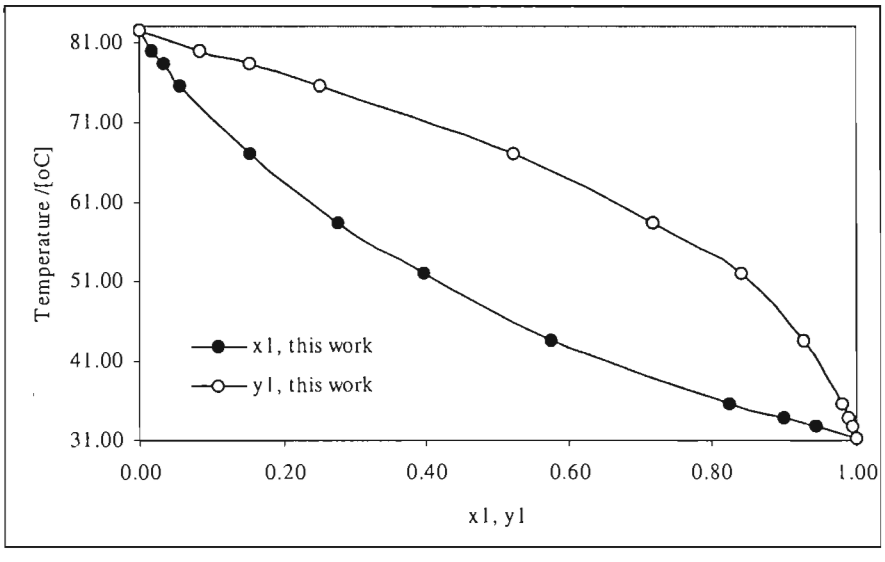

Figure 8-34: T-x-y diagram for acetone(1) with 2,3-pentanedione(2) at 40 kPa

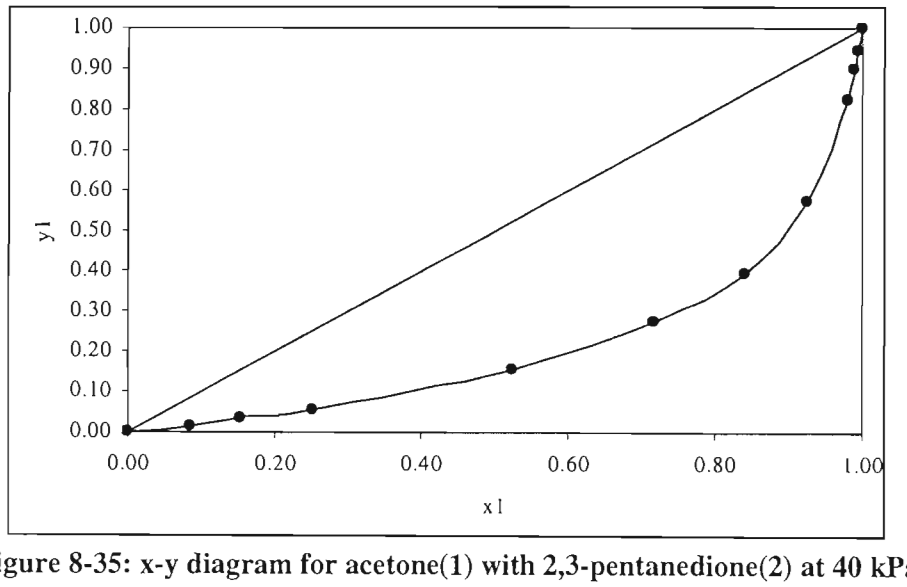

Figure 8-35: x-y diagram for acetone(1) with 2,3-pentanedione(2) at 40 kPa

CHAPTER 9

DISCUSSION

The major objectives of this study were:

1. The measurement of isobaric and isothermal vapour-liquid equilibria for the systems:
    - Acetone with diacetyl
    - Methanol with diacetyl
    - Diacetyl with 2,3-pentanedione
    - Acetone with 2,3-pentanedione
2. Thermodynamic treatment of the VLE data to judge the quality of the data and to enable interpolation and extrapolation of the data.
3. Measurement of the infinite dilution activity coefficients.

The results of each of the above three tasks will be discussed in this chapter.

9.1 Chemicals used in this study

The experiments require chemicals of high purity. GC analysis of all these chemicals showed no significant impurities. Measured vapour pressures compared well with those values available in literature as shown in Table 9-1. All the chemicals were used with no further purification.

Table 9-1: Purity of the chemicals used in this study

Chemical	Supplier	Assay mass %	GC Peak Area %	ΔT^* [°C]
Cyclohexane	Associated Chemical Enterprises	99+	99.851	0.06[a]
Ethanol	Merck Chemical & Laboratory Supplies (Pty) Ltd	>99.7	99.83	0.05[a]
Acetone	Rochelle Chemicals	min 99.5	99.968	0.04[a]
Methanol	Rochelle Chemicals	min 99.5	99.875	0.05[a]
Diacetyl	Illovo (Pty) Ltd	min 98.82	99.763	0.06[b]
2,3-Pentanedione	Illovo (Pty) Ltd	min 98.52	99.722	-

* Average absolute deviation of the measured temperature from literature

[a] Literature data sourced from Reid et al. (1988)

[b] Literature data sourced from Joseph et al. (2001)

The concern of a chemical reaction occurring between diacetyl and methanol is discussed by McGee (1999). The uncommon chemical reaction between a ketone and an alcohol, to form a thermally unstable hemiketal, does not occur to a significant extent. Professor TM Letcher, of the Chemistry Department of the University of Natal, suggested analysing an equal-volume mixture of diacetyl and methanol with a GLC apparatus (see Chapter 4). The injector, column and detector temperatures were set to ambient temperature to ensure that thermally unstable compounds can be detected. A ¼ in. stainless-steel column packed with hexadecane on a celite support was used. Numerous qualitative analysis of the mixture showed no peak other than diacetyl or methanol. The addition of acid, to a mixture that forms a hemiketal, results in the formation of a stable ketal and water. Neither water nor an additional component was detected when the mixture was acidified. The VLE data were smooth and the data reduction yielded a high degree of correlation and satisfies the requirements of the thermodynamic consistency tests (Section 9.3). Thus, the possibility of a reaction between diacetyl and methanol was excluded.

9.2 Low-pressure VLE measurements

The review of available methods for measuring low-pressure VLE, presented in Chapter 2, revealed that the vapour and liquid recirculating still is most appropriate for this study. The description of the low-pressure recirculating still of Raal and Mühlbauer (1998), used in this study, can be found in Chapter 2. A full description of the experimental procedure and pressure control is given in Chapter 6.

Kneisl et al. (1989) studied the slope and the extent of the plateau region for ebulliometer measurements of pure fluids. Kneisl et al. (1989) present the following equation to screen chemicals for study by the ebulliometric methods.

$$\log\left(\frac{dT}{dq}\right)_{\min} = -6.22 + 0.61\mu_D + 0.75\chi \qquad (9\text{-}1)$$

where

$\chi = 0$ for systems with only dipole-dipole interactions (e.g. n-alkanes and ketones).

$\chi = 1$ for fluids with hydrogen bonds or electronegative groups that can interact through a single site (e.g alcohols).

$\chi = 2$ for fluids with hydrogen bonds or electronegative groups that can interact through a multiple sites (e.g glycols).

μ_D is the dipole moment (refer to Section 3.7.2.1.2)

$\log\left(\frac{dT}{dq}\right)_{min}$ is the temperature change per unit heat input (units of μK /W) of the plateau region (see Chapter 2). The slope of the plateau region is the minimum value of the slope.

The operation of the still (and hence the accuracy of the vapour pressures measured) can be adversely affected by fluid properties. Kneisl et al. (1989) found the dipole moment and the type of molecular association to be most significant. These properties can be used to estimate the slope of the plateau region from Eq. 9-1. Kneisl et al. (1989) found that chemicals with large slopes are poorly behaved in an ebulliometer. These slopes can, therefore, be used to judge the suitability of ebulliometric methods for chemicals. Based on a number of substances studied, Kneisl et al. (1989) found that a value of 300 μK /W for the slope yields results precise to within ±0.005K. Methanol and ethanol were found to have the highest slopes in this study. As these slopes were less than 40 μK /W, the ebulliometric method is suitable for all these chemicals.

Prior to measuring VLE, vapour pressure measurements were made for all the chemicals used in this study. As mentioned in Section 9-1, the vapour pressures of diacetyl, acetone, cyclohexane, ethanol and methanol compared well with the available literature. The vapour pressure measurements for 2,3-pentanedione (shown in Table 8-1) are new data. The data are correlated to the Antoine equation (Eq. 8-1) and the resulting parameters are given in Chapter 8.

The first chemical system measured was cyclohexane with ethanol. This highly non-ideal system exhibits an azeotrope and presents a considerable challenge in accurate VLE measurement. Data sets of high quality are available in literature. One is, therefore, able to judge the capability of the VLE still to provide accurate data, as well as to test the experimental procedure used. Isothermal data measured at 40 °C are shown in Table 8-2, Figure 8-2 and Figure 8-3. Isobaric data at 40 kPa are shown in Table 8-2, Figure 8-4 and Figure 8-5. Both data sets compare well to the thermodynamically consistent data sets measured by Joseph et al. (2000). Thus, the accuracy of the apparatus and the correctness of the method are confirmed.

Data measured for the following systems are presented in Chapter 8:

- Acetone with diacetyl at 30 °C, 40 °C, 50 °C and 40 kPa.
  Shown in Table 8-3, Table 8-4 and Figures 8-6 to 8-13.

- Methanol with diacetyl at 40 °C, 50 °C, 60 °C and 40 kPa.
  Shown in Table 8-5, Table 8-6 and Figures 8-14 to 8-21.
- Diacetyl with 2,3-pentanedione at 60 °C, 70 °C, 80 °C and 40 kPa.
  Shown in Table 8-7, Table 8-8 and Figures 8-22 to 8-29.
- Acetone with 2,3-pentanedione at 50 °C, 30 kPa and 40 kPa.
  Shown in Table 8-9, Table 8-10 and Figures 8-30 to 8-35.

9.3 Reduction of the VLE data

The reduction of VLE data provides a framework for compact data storage and permits accurate interpolation and extrapolation of data. The Gamma-Phi approach to VLE is the preferred method for low-pressure computations. It was, therefore, the method used in this study. The Phi-Phi (or equation of state) approach is an alternative formulation. Descriptions and specific details of the applicability of the methods are given in Chapter 3.

The Gamma-Phi approach accounts for the vapour phase deviation from ideal gas behaviour using the fugacity coefficient. The fugacity coefficient was calculated from the truncated virial equation of state (two terms) as it provides satisfactory results for low-pressure computations. It was, therefore, unnecessary to use the more complex cubic equations of state discussed in Chapter 3. Second virial coefficients are required when using the two-term virial equation of state. A review of the available methods for calculating these coefficients (Chapter 3) revealed that the method of Hayden and O' Connell (1975) yields consistently good results for a variety of compounds. The method requires critical properties, dipole moments and the mean radius of gyration in order to predict the virial coefficients. These values (or methods to estimate them) are available in Reid et al. (1988). The values for the dipole moments and mean radius of gyration were calculated by the methods described in Chapter 3. The critical properties of diacetyl and 2,3-pentanedione (given Appendix B) were estimated by the Ambrose method (Reid et al., 1988).

The liquid phase departure from ideal solution behaviour is accounted for through the activity coefficient in the Gamma-Phi approach. The activity coefficient is represented by any of a large number of excess Gibbs energy models available (Chapter 3). The Wilson, NRTL and UNIQUAC models were used in this study, as they are most successful at correlating activity coefficients. The scheme shown in Figure 3-8 was used to reduce the data sets measured and the adjustable parameters of each of the models were computed. As the computations are iterative and complex, programs were written in Matlab to perform the calculations. The programs were

integrated with the non-linear regression scheme of Marquadt (1963) written by R Rawatlal (University of Natal – Durban).

9.3.1 Isothermal data

Van Ness and Abbott (1982) suggest that using only the pressure residual (discussed in Section 3.13.1) in the objective function yields the best fit to the models for low-pressure isothermal data. This was confirmed by Joseph (2001) and was found to be the case in this study. Best-fit models were found for each data set. The best-fit model correlations, for all the data sets, are given in Figures 9-1 to 9-20.

Although one particular model was found to yield the best correlation for each data set, all the models were found to yield satisfactory results. The parameters are given in Tables 9-3 to 9-6. The best-fit models were chosen on the basis of the percentage of the average absolute deviation of predicted pressure from the experimental value. These percentages can be seen to be much less than 1%, even in the worst case. The average absolute vapour composition residuals are also less than 0.01 mole fraction in every case.

Walas (1985) suggests that a value of 0.3 be used for the NRTL parameter α (see Chapter 3). In some cases it was found that a better fit was obtained by allowing α to be fitted by the data reduction procedure. This is consistent with the work of Joseph (2001). Table 9-2 shows the best fit excess Gibbs energy models for the isothermal data measured in this study.

Table 9-2: Best fit excess Gibbs energy models for the isothermal data

System		Best-fit model
Acetone+Diacetyl	30 °C	UNIQUAC
	40 °C	NRTL
	50 °C	UNIQUAC
Methanol+Diacetyl	40 °C	UNIQUAC
	50 °C	NRTL
	60 °C	UNIQUAC
Diacetyl+2,3-Pentanedione	60 °C	Wilson
	70 °C	Wilson
	80 °C	UNIQUAC
Acetone+2,3-Pentanedione	50 °C	Wilson

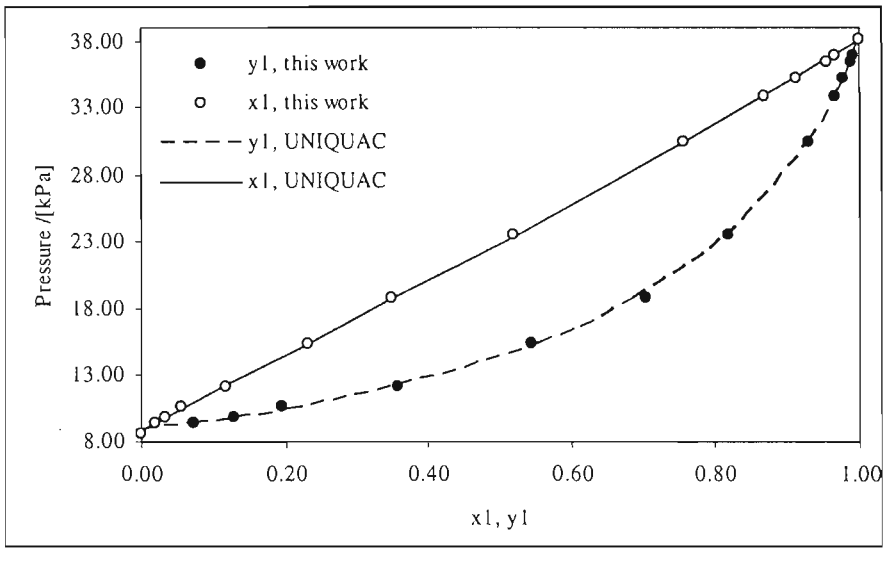

Figure 9-1: UNIQUAC model fit to P-x-y diagram for acetone(1) with diacetyl(2) at 30 °C

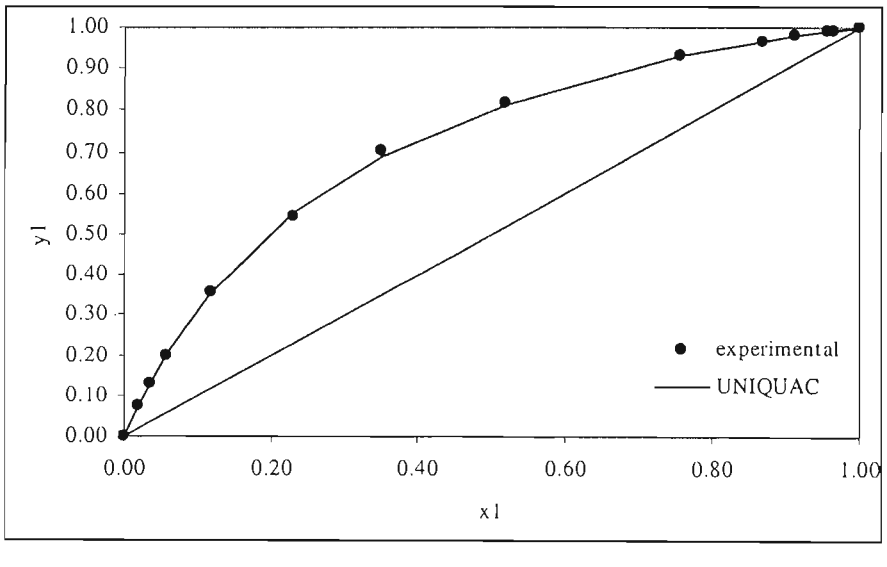

Figure 9-2: UNIQUAC model fit to x-y diagram for acetone(1) with diacetyl(2) at 30 °C

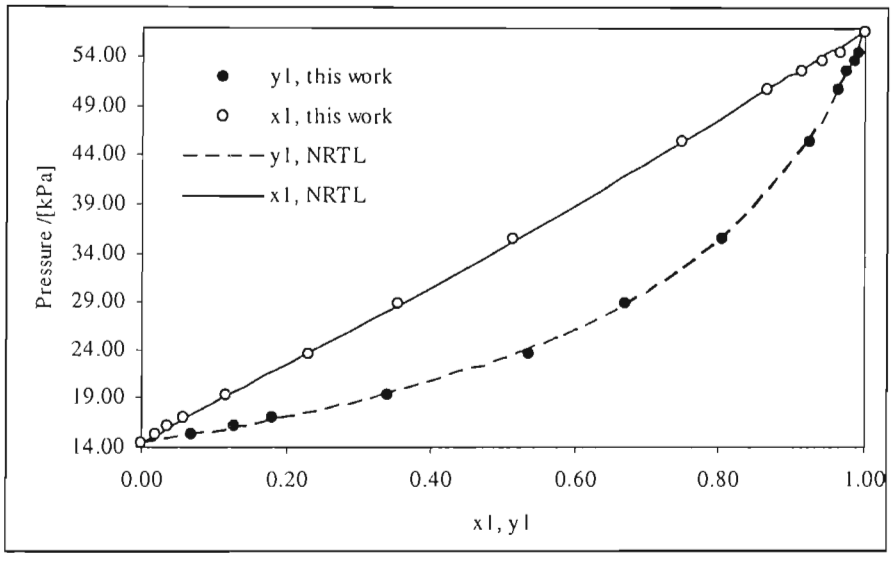

Figure 9-3: NRTL model fit to P-x-y diagram for acetone(1) with diacetyl(2) at 40 °C

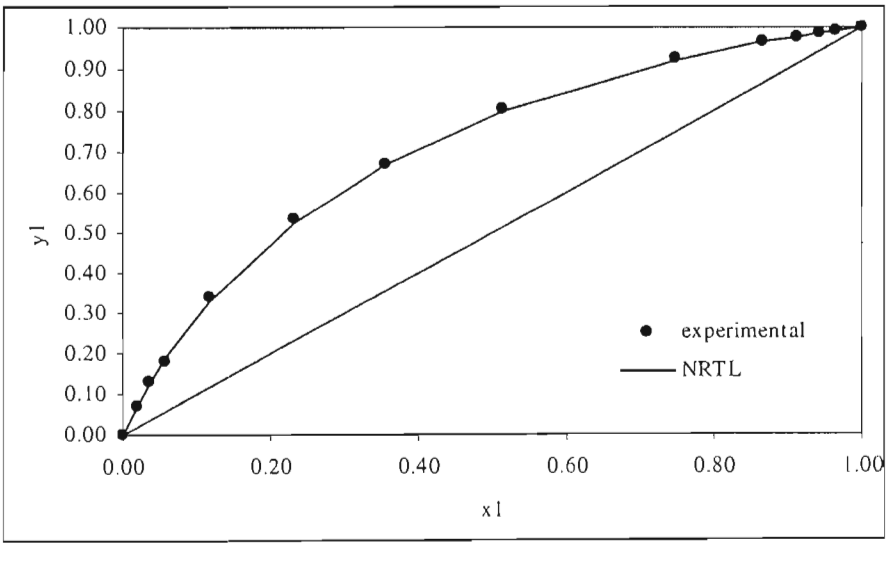

Figure 9-4: NRTL model fit to x-y diagram for acetone(1) with diacetyl(2) at 40 °C

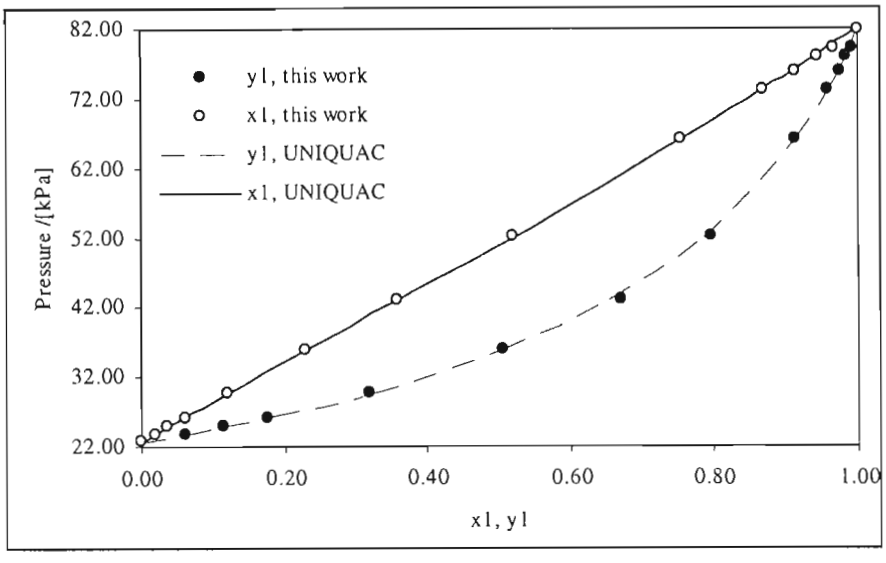

Figure 9-5: UNIQUAC model fit to P-x-y diagram for acetone(1) with diacetyl(2) at 50 °C

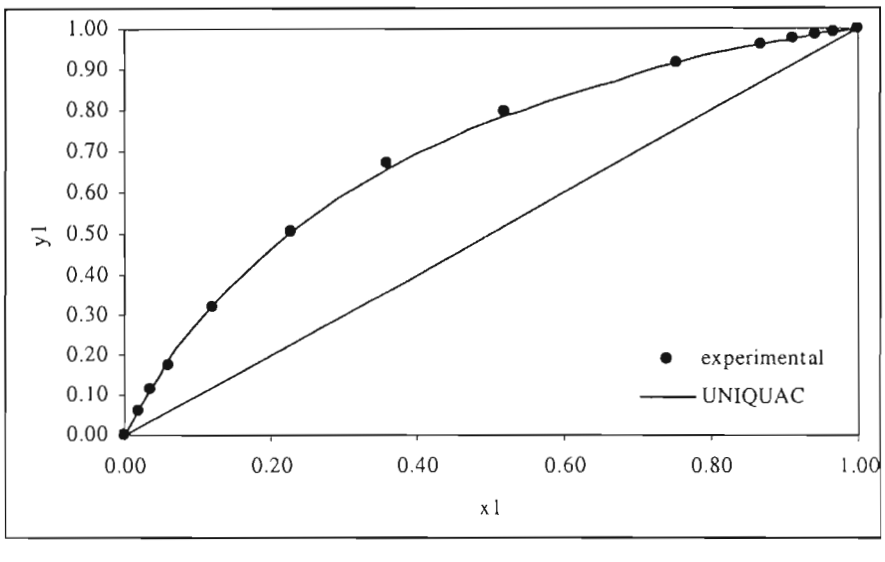

Figure 9-6: UNIQUAC model fit to x-y diagram for acetone(1) with diacetyl(2) at 50 °C

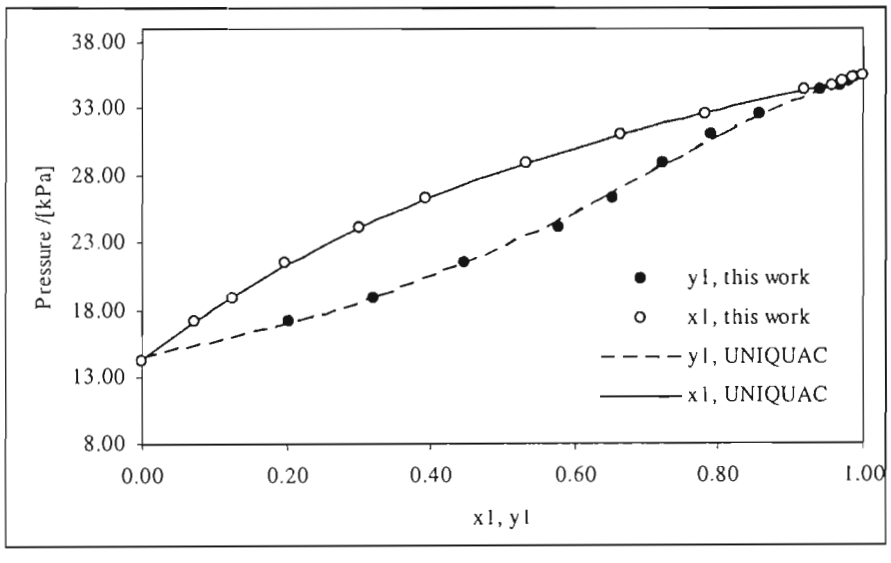

Figure 9-7: UNIQUAC model fit to P-x-y diagram for methanol(1) with diacetyl(2) at 40 °C

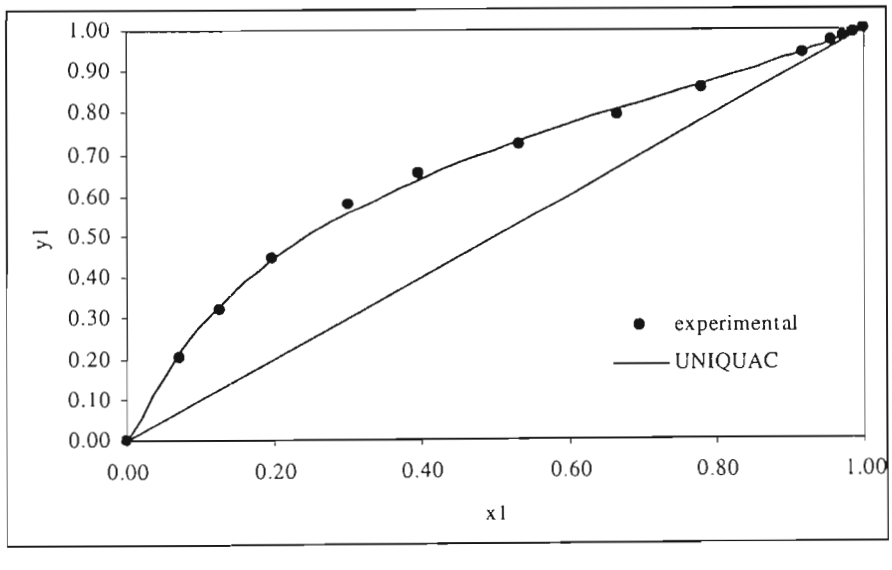

Figure 9-8: UNIQUAC model fit to x-y diagram for methanol(1) with diacetyl(2) at 40 °C

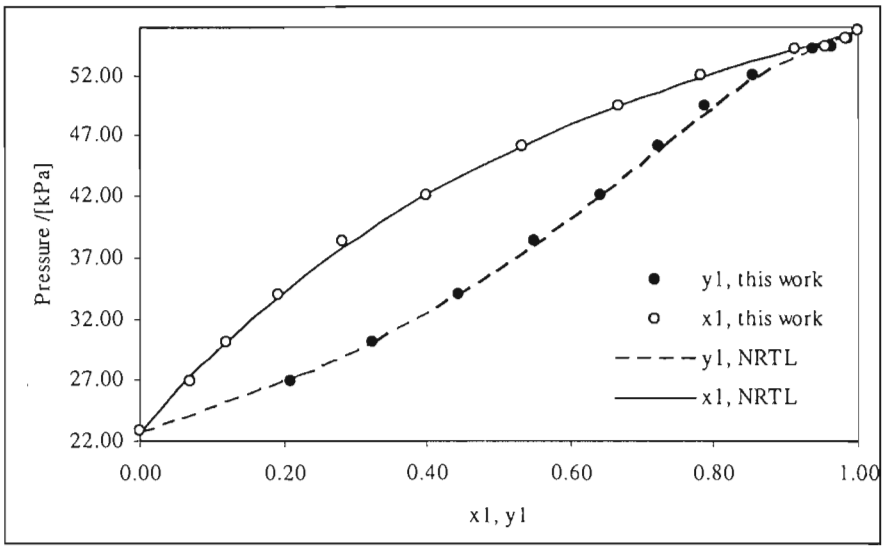

Figure 9-9: NRTL model fit to P-x-y diagram for methanol(1) with diacetyl(2) at 50 °C

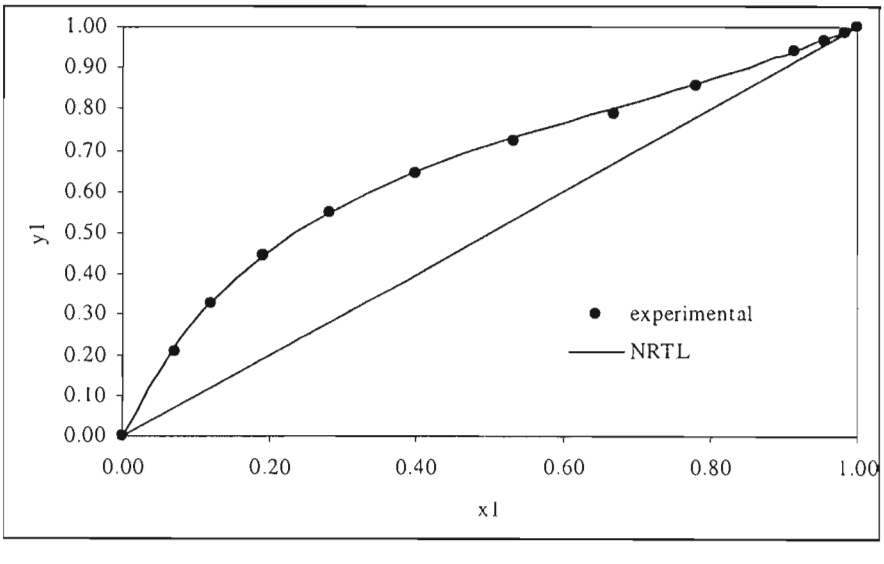

Figure 9-10: NRTL model fit to x-y diagram for methanol(1) with diacetyl(2) at 50 °C

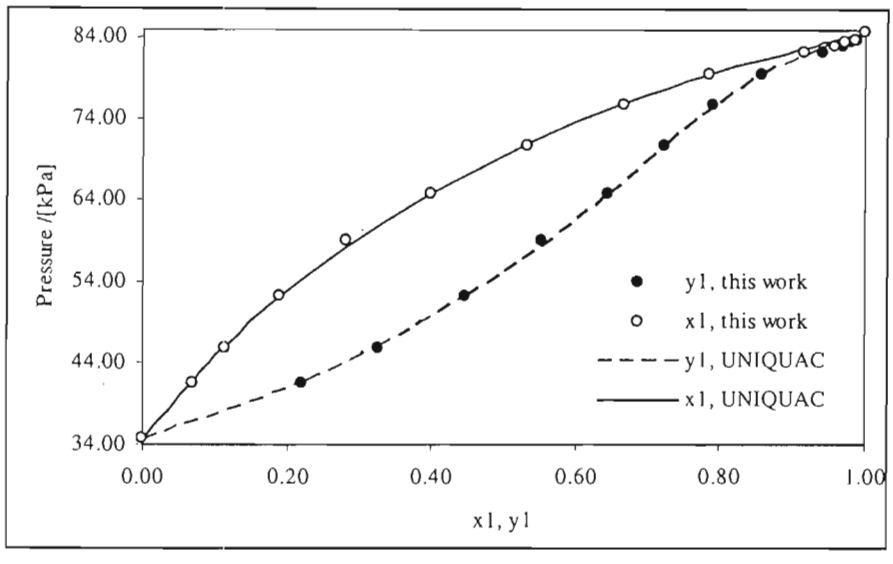

Figure 9-11: UNIQUAC model fit to P-x-y diagram for methanol(1) with diacetyl(2) at 60 °C

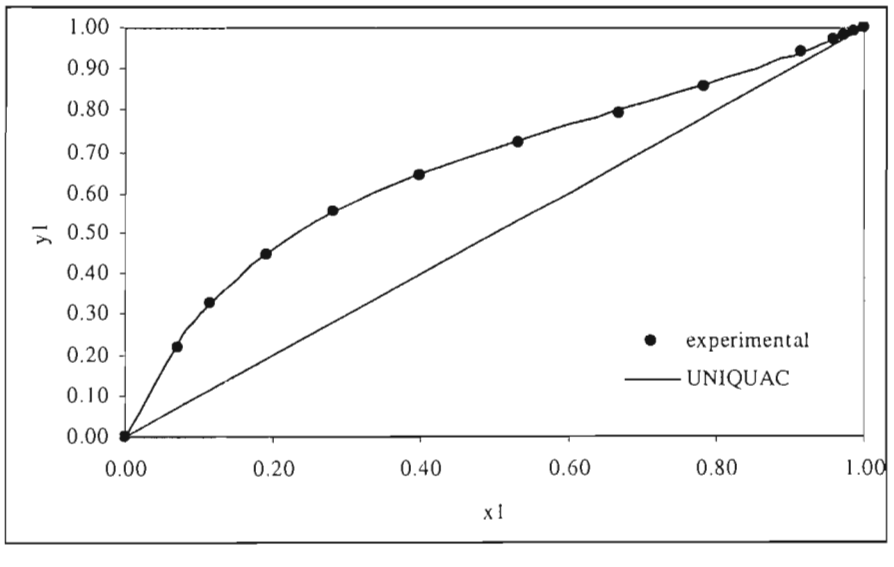

Figure 9-12: UNIQUAC model fit to x-y diagram for methanol(1) with diacetyl(2) at 60 °C

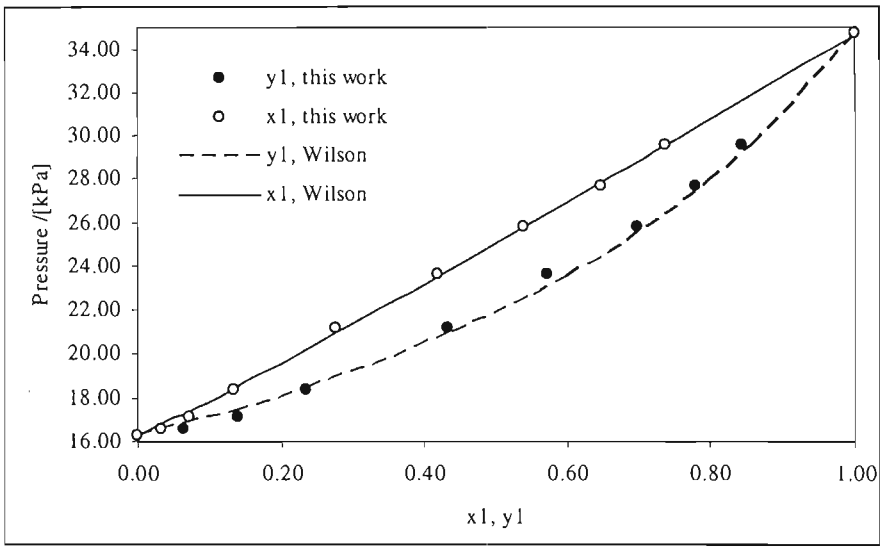

Figure 9-13: Wilson model fit to P-x-y diagram for diacetyl(1) with 2,3-pentanedione(2) at 60 °C

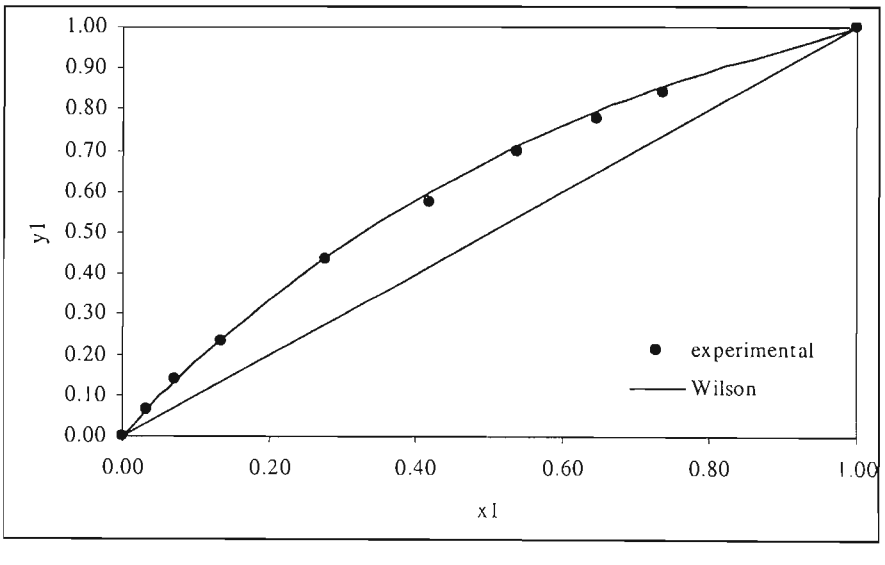

Figure 9-14: Wilson model fit to x-y diagram for diacetyl(1) with 2,3-pentanedione(2) at 60 °C

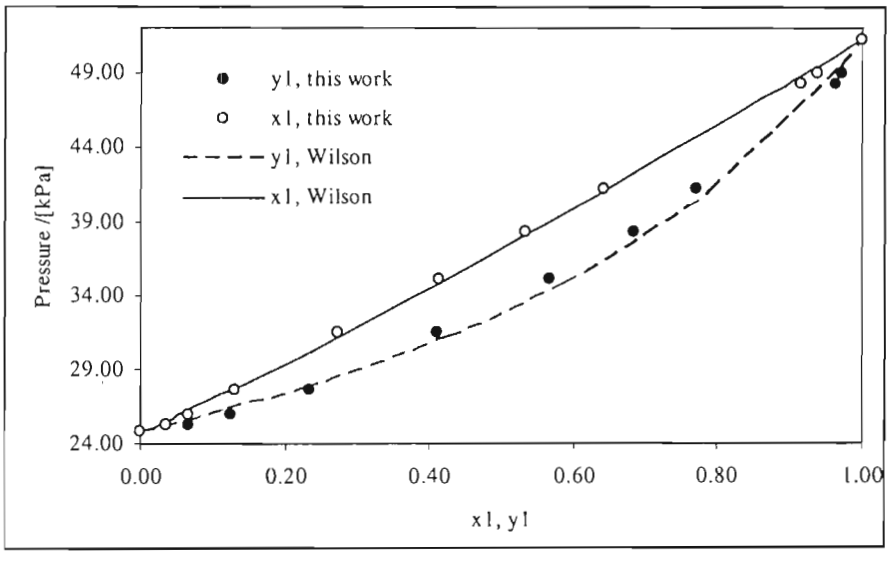

Figure 9-15: Wilson model fit to P-x-y diagram for diacetyl(1) with 2,3-pentanedione(2) at 70 °C

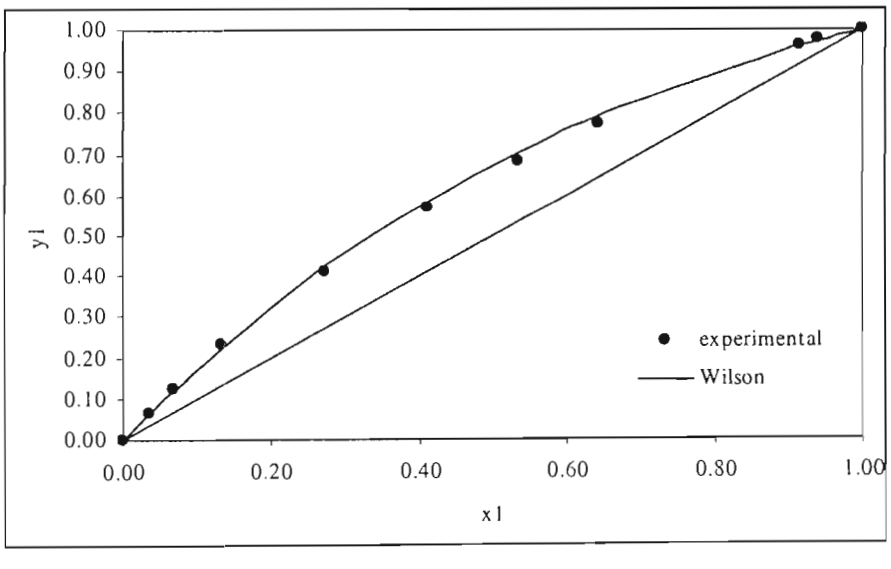

Figure 9-16: Wilson model fit to x-y diagram for diacetyl(1) with 2,3-pentanedione(2) at 70 °C

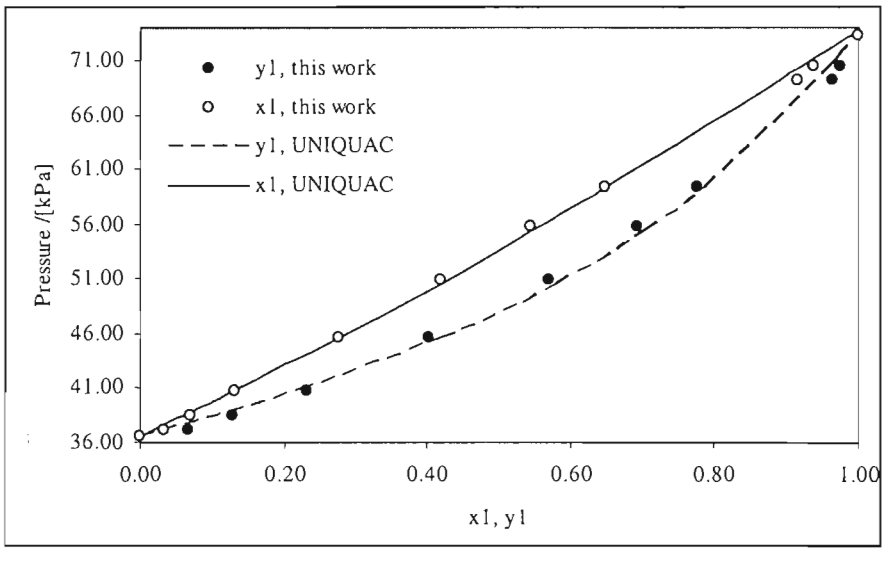

Figure 9-17: UNIQUAC model fit to P-x-y diagram for diacetyl(1) with 2,3-pentanedione(2) at 80 °C

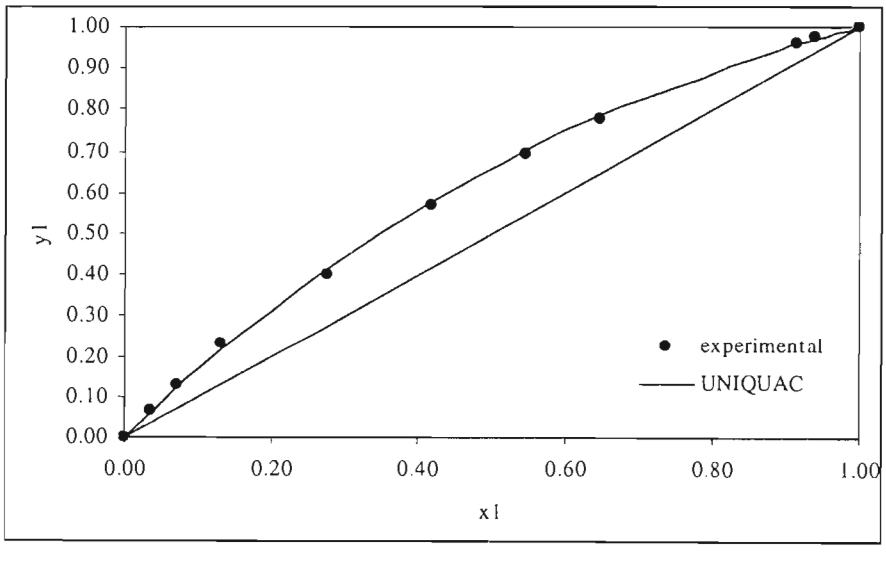

Figure 9-18: UNIQUAC model fit to x-y diagram for diacetyl(1) with 2,3-pentanedione(2) at 80 °C

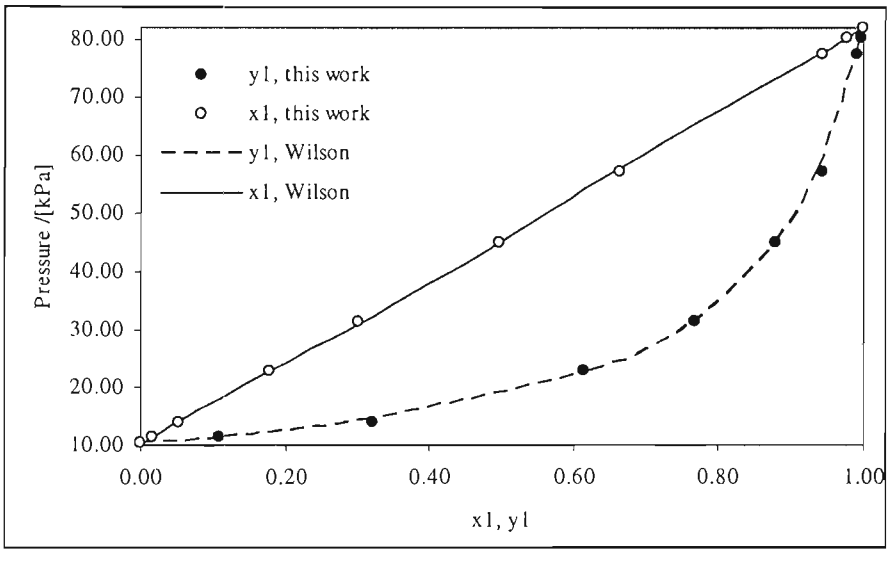

Figure 9-19: Wilson model fit to P-x-y diagram for acetone(1) with 2,3-pentanedione(2) at 50 °C

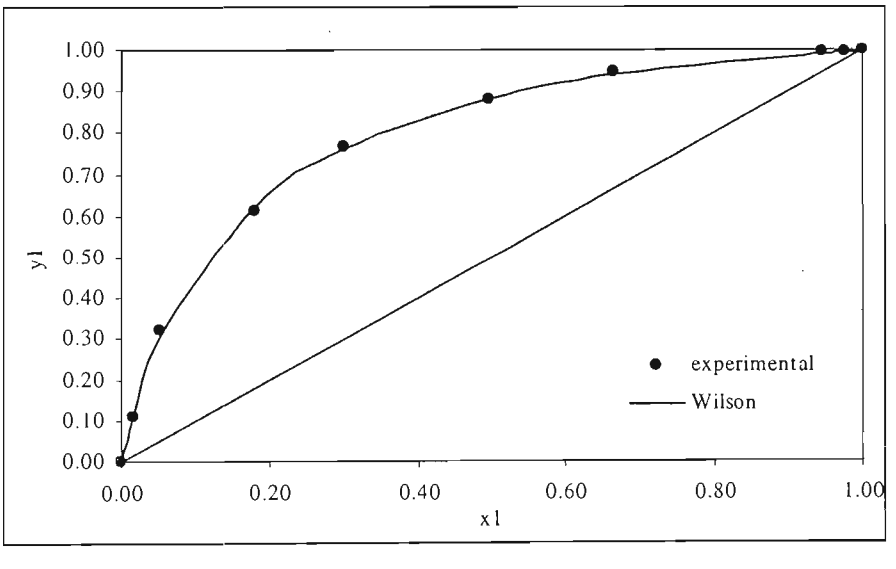

Figure 9-20: Wilson model fit to x-y diagram for acetone(1) with 2,3-pentanedione(2) at 50 °C

Table 9-3: Excess Gibbs energy model parameters regressed for the system acetone(1) + diacetyl(2)

Activity coefficient model		30 °C	40 °C	50 °C
UNIQUAC				
	u_{12}-u_{11} [J /mol]	-1051.989	-927.134	-1220.461
	u_{12}-u_{22} [J /mol]	1736.335	1535.946	2058.993
	$\delta P\%$	0.61	0.55	0.36
	δy	0.003	0.004	0.004
Wilson				
	λ_{12}-λ_{11} [J /mol]	-90.483	-43.520	16.481
	λ_{12}-λ_{22} [J /mol]	90.827	46.103	-16.000
	$\delta P\%$	0.86	0.72	0.72
	δy	0.003	0.004	0.003
NRTL				
	g_{12}-g_{11} [J /mol]	-2550.659	-2527.391	-2724.817
	g_{12}-g_{22} [J /mol]	3568.792	3476.265	3921.795
	α	0.3	0.3	0.3
	$\delta P\%$	0.73	0.52	0.54
	δy	0.003	0.003	0.005

Table 9-4: Excess Gibbs energy model parameters regressed for the system methanol(1) + diacetyl(2)

Activity coefficient model		40 °C	50 °C	60 °C
UNIQUAC				
	u_{12}-u_{11} [J /mol]	-1036.976	-1025.735	-1017.601
	u_{12}-u_{22} [J /mol]	3163.642	3382.082	3535.794
	$\delta P\%$	0.57	0.73	0.61
	δy	0.009	0.007	0.005
Wilson				
	λ_{12}-λ_{11} [J /mol]	2748.535	2893.198	3054.824
	λ_{12}-λ_{22} [J /mol]	-1322.138	-1186.200	-1157.412
	$\delta P\%$	0.59	0.74	0.73
	δy	0.009	0.007	0.005
NRTL				
	g_{12}-g_{11} [J /mol]	2780.543	2646.970	2878.722
	g_{12}-g_{22} [J /mol]	-1317.844	-938.333	-995.998
	α	0.089	0.119	0.109
	$\delta P\%$	0.58	0.73	0.71
	δy	0.009	0.007	0.005

Table 9-5: Excess Gibbs energy model parameters regressed for the system diacetyl(1) + 2,3-pentanedione(2)

Activity coefficient model		60 °C	70 °C	80 °C
UNIQUAC				
	u_{12}-u_{11} [J /mol]	1484.872	767.862	886.137
	u_{12}-u_{22} [J /mol]	-1237.009	-767.923	-885.832
	$\delta P\%$	0.53	0.61	0.66
	δy	0.008	0.008	0.008
Wilson				
	λ_{12}-λ_{11} [J /mol]	801.205	988.544	-1504.140
	λ_{12}-λ_{22} [J /mol]	-801.215	-978.958	1490.195
	$\delta P\%$	0.52	0.59	0.66
	δy	0.008	0.009	0.008
NRTL				
	g_{12}-g_{11} [J /mol]	8505.421	5491.949	-8981.612
	g_{12}-g_{22} [J /mol]	-7712.616	-5185.405	9987.226
	α	0.041	0.053	0.042
	$\delta P\%$	0.52	0.60	0.67
	δy	0.009	0.009	0.008

Table 9-6: Excess Gibbs energy model parameters regressed for the system acetone(1) + 2,3-pentanedione(2)

Activity coefficient model		50 °C
UNIQUAC		
	u_{12}-u_{11} [J /mol]	448.875
	u_{12}-u_{22} [J /mol]	-448.400
	$\delta P\%$	0.43
	δy	0.006
Wilson		
	λ_{12}-λ_{11} [J /mol]	3397.488
	λ_{12}-λ_{22} [J /mol]	-2557.570
	$\delta P\%$	0.50
	δy	0.005
NRTL		
	g_{12}-g_{11} [J /mol]	1955.294
	g_{12}-g_{22} [J /mol]	-1954.880
	α	0.008
	$\delta P\%$	0.38
	δy	0.006

9.3.2 Isobaric data

The adjustable parameters of the activity coefficient models are temperature dependent. Each point of an isobaric data set, therefore, has its own set of parameters for the excess Gibbs energy model. The discussion in Chapter 3 suggests that isobaric data can be reduced in the same way as isothermal data (i.e. ignoring the temperature dependence of the parameters). Models such as the Wilson equation are able to correlate the data satisfactorily over a modest temperature range. Rather than neglecting the temperature dependence in this study, the parameters were assumed to have the following relationship with temperature:

$$Parameter = Q_1 T^2 + Q_2 T + Q_3 \tag{9-2}$$

The coefficients, Q_i, were fitted during the regression. It must be noted that there is no theoretical basis to Eq. 9-2. The equation also introduces more parameters, which makes the data reduction more difficult. Initial guesses for the Q_i parameters must be close to the actual values to ensure convergence. The results of the isothermal measurements provided a good starting point and good fits were found for all the isobaric sets. The best-fit model correlations, for all the isobaric sets, are given in Figures 9-21 to 9-28.

Two isobars were measured for the acetone with 2,3-pentanedione system (viz. 30 kPa and 40 kPa). The 30 kPa was reduced for the Q_i parameters shown in Eq. 9-2 and the results were used to predict data for the 40 kPa isobar. These results correspond well with the experimental values as shown in Figures 9-29 and 9-30. The parameters for the excess Gibbs energy models are given in Tables 9-7 and 9-8. As advocated by Van Ness and Abbot (1982) using only the temperature residual in the objective function was found to yield the best results.

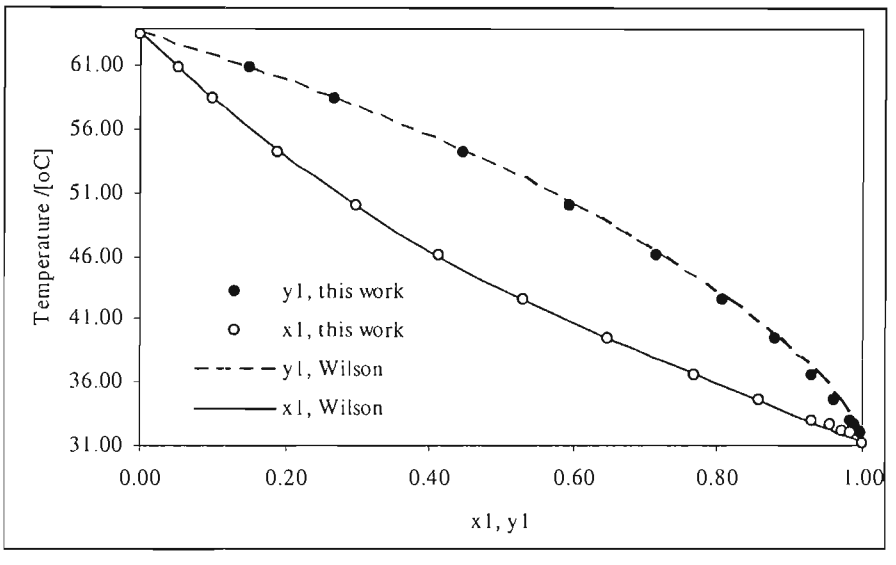

Figure 9-21: Wilson model fit to T-x-y diagram for acetone(1) with diacetyl(2) at 40 kPa

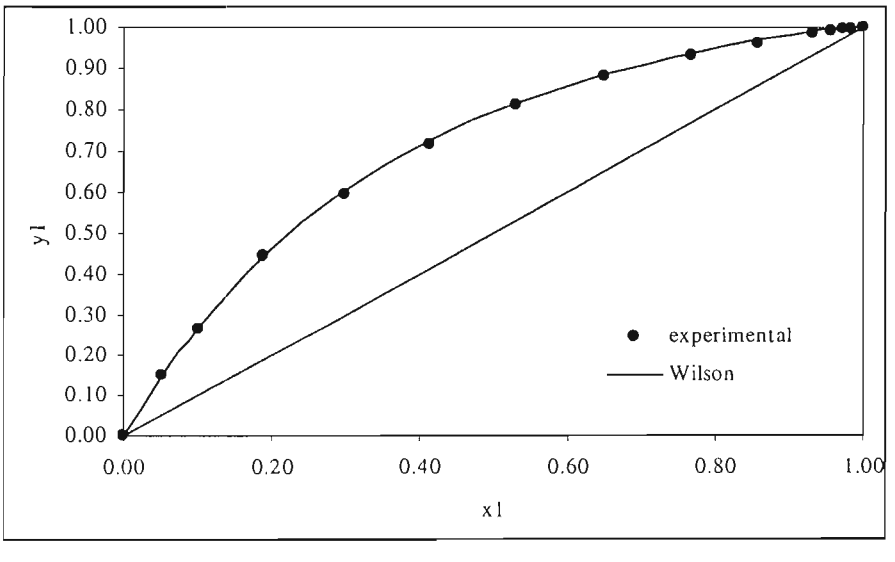

Figure 9-22: Wilson model fit to x-y diagram for acetone(1) with diacetyl(2) at 40 kPa

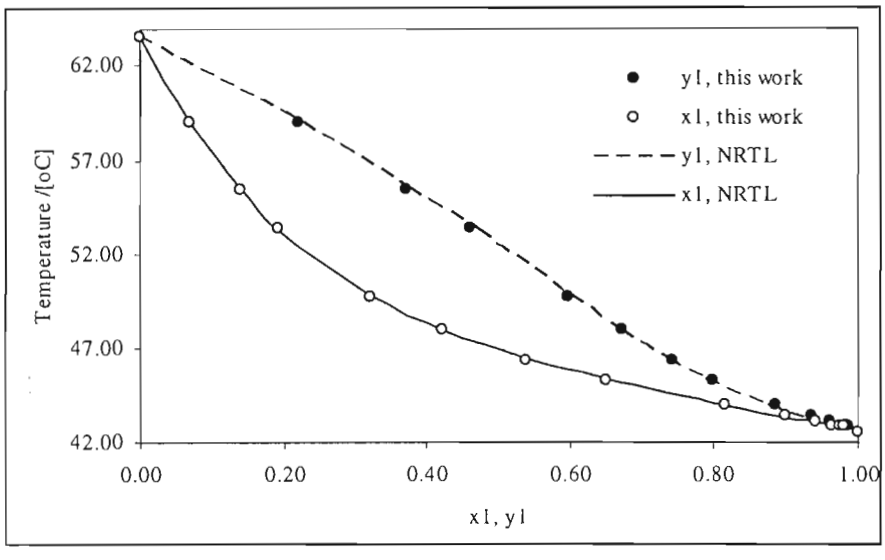

Figure 9-23: NRTL model fit to T-x-y diagram for methanol(1) with diacetyl(2) at 40 kPa

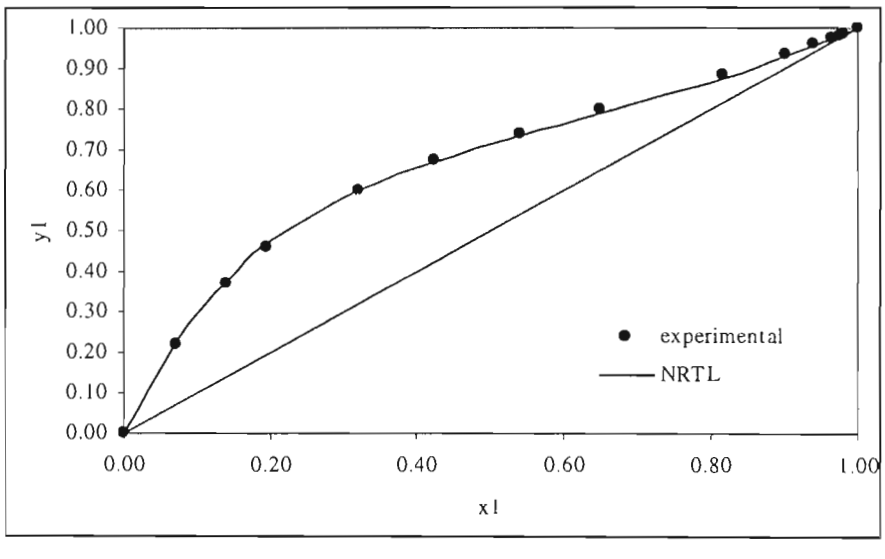

Figure 9-24: NRTL model fit to x-y diagram for methanol(1) with diacetyl(2) at 40 kPa

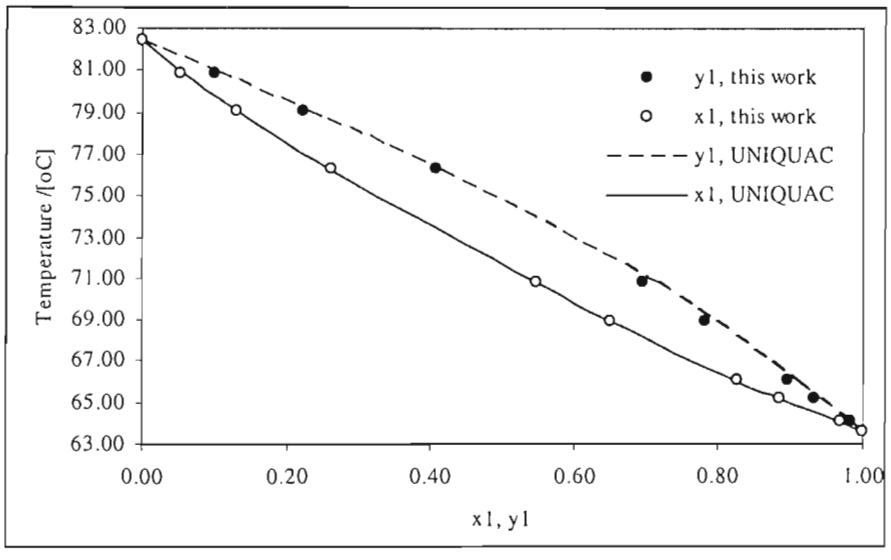

Figure 9-25: UNIQUAC model fit to T-x-y diagram for diacetyl(1) with 2,3-pentanedione(2) at 40 kPa

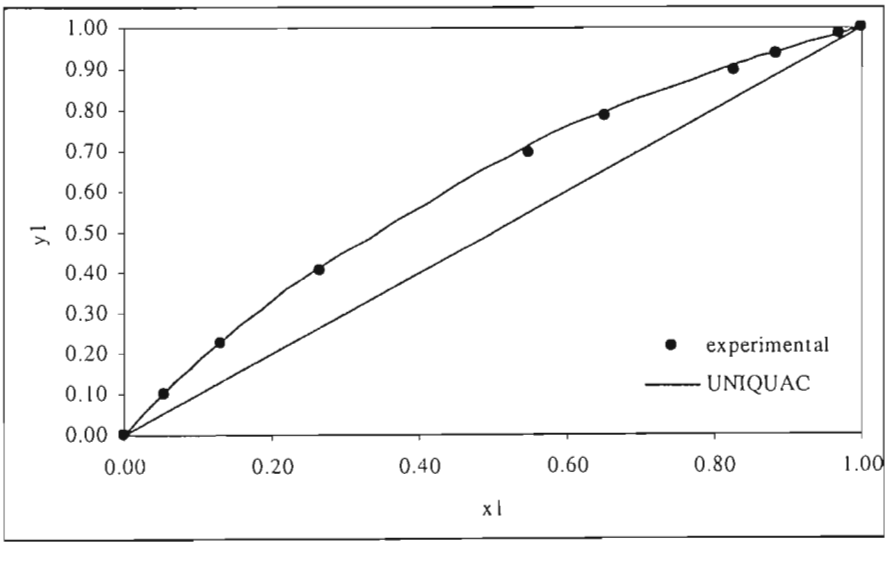

Figure 9-26: UNIQUAC model fit to x-y diagram for diacetyl(1) with 2,3-pentanedione(2) at 40 kPa

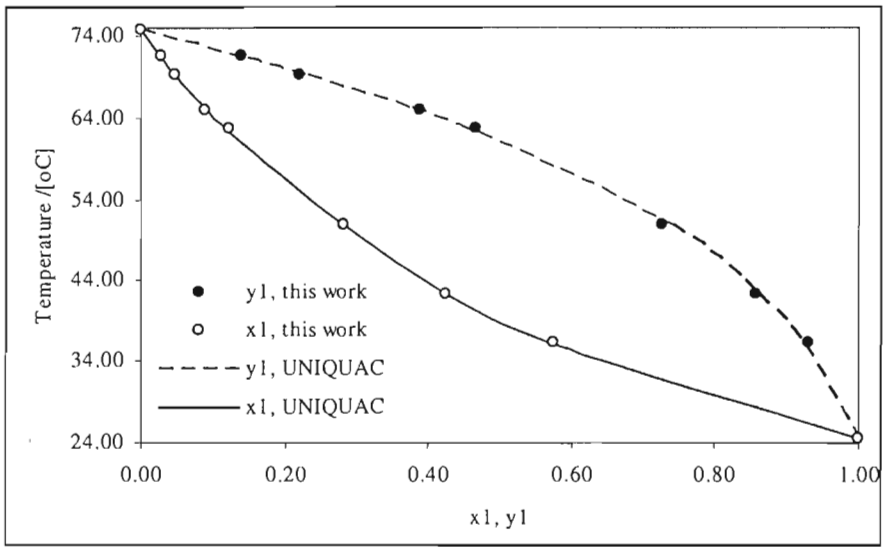

Figure 9-27: UNIQUAC model fit to T-x-y diagram for acetone(1) with 2,3-pentanedione(2) at 30 kPa

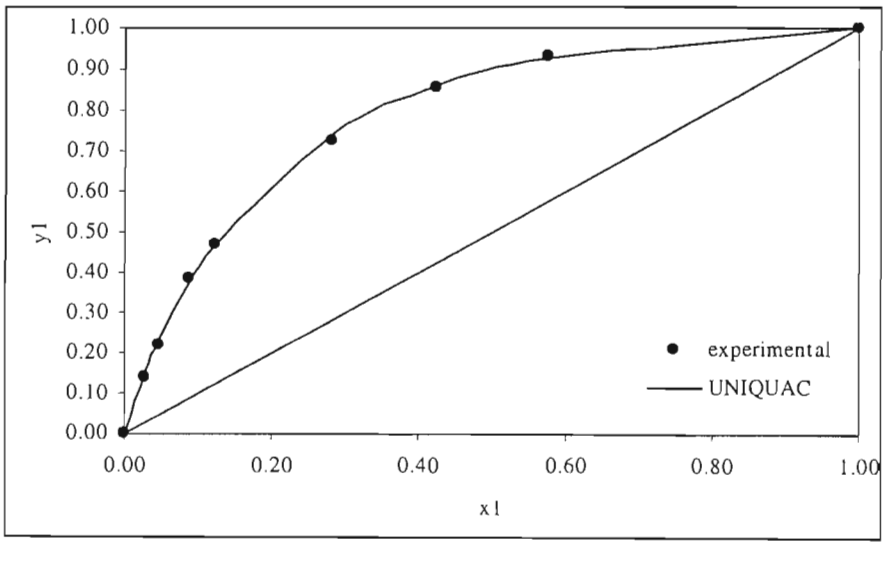

Figure 9-28: UNIQUAC model fit to x-y diagram for acetone(1) with 2,3-pentanedione(2) at 30 kPa

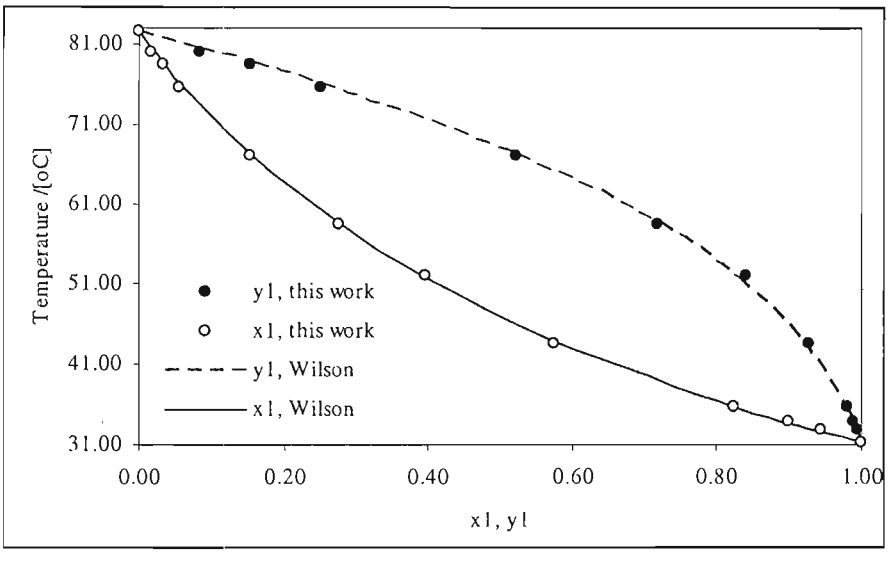

Figure 9-29: Wilson model prediction of T-x-y diagram for acetone(1) with 2,3-pentanedione(2) at 40 kPa

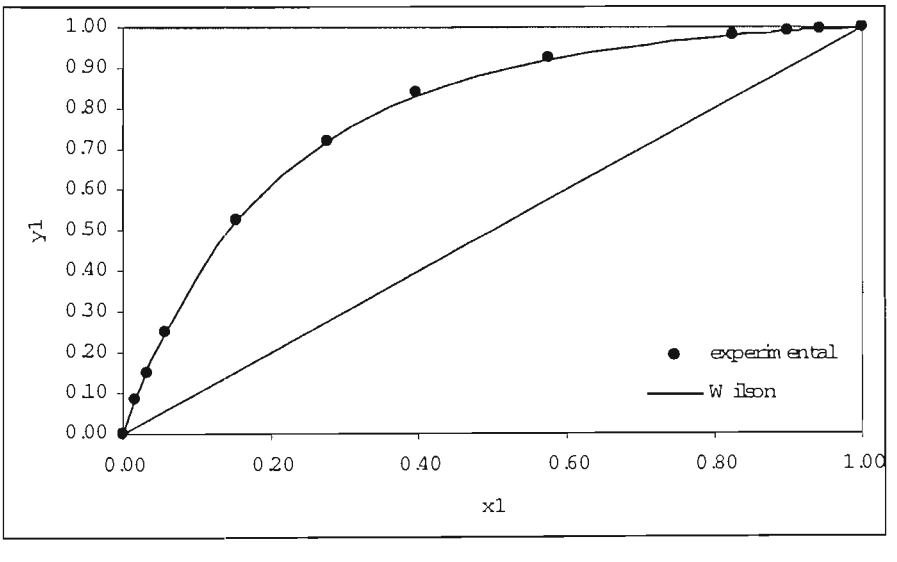

Figure 9-30: Wilson model prediction of x-y diagram for acetone(1) with 2,3-pentanedione(2) at 40 kPa

Table 9-7: Excess Gibbs energy model parameters regressed for the systems acetone(1) + diacetyl(2) and methanol(1) + diacetyl(2)

Activity coefficient model*			Acetone(1)+ Diacetyl(2) 40 kPa	Methanol(1)+ Diacetyl(2) 40 kPa
UNIQUAC				
	u_{12}-u_{11} [J /mol]	Q_1[a]	-2.089	-0.020
		Q_2[b]	1299.970	11.091
		Q_3[c]	-203954.246	-2932.178
	u_{12}-u_{22} [J /mol]	Q_1[a]	3.633	-0.434
		Q_2[b]	-2248.989	228.147
		Q_3[c]	351317.338	-23837.942
	$\delta T\%$		0.505	0.118
	δy		0.007	0.007
Wilson				
	λ_{12}-λ_{11} [J /mol]	Q_1[a]	-0.082	-0.658
		Q_2[b]	46.744	347.605
		Q_3[c]	-8301.521	-39248.159
	λ_{12}-λ_{22} [J /mol]	Q_1[a]	0.372	0.098
		Q_2[b]	-45.034	-44.293
		Q_3[c]	-18961.884	1747.150
	$\delta T\%$		0.378	0.133
	δy		0.004	0.007
NRTL				
	g_{12}-g_{11} [J /mol]	Q_1[a]	-1.036	1.925
		Q_2[b]	687.596	-1172.737
		Q_3[c]	-116973.527	180992.191
	g_{12}-g_{22} [J /mol]	Q_1[a]	2.408	-2.157
		Q_2[b]	-1659.381	1434.961
		Q_3[c]	289693.108	-239153.990
	α	Q_1[a]	0	0.000
		Q_2[b]	0	0.126
		Q_3[c]	0.3**	-23.847
	$\delta T\%$		0.541	0.098
	δy		0.005	0.005

*Parameters calculated from $Q_1T^2 + Q_2T + Q_3T$

**Fixed value of α used

[a] Units of [J /mol]

[b] Units of [J /mol /K]

[c] Units of [J /mol /K^2]

Table 9-8: Excess Gibbs energy model parameters regressed for the systems diacetyl(1) + 2,3-pentanedione(2) and acetone(1) + 2,3-pentanedione(2)

Activity coefficient model*			Diacetyl(1)+ 2,3-Pentanedione	Acetone(1)+ 2,3-Pentanedione(2)	
			40 kPa	30 kPa	40 kPa**
UNIQUAC					
	u_{12}-u_{11} [J /mol]	Q_1[a]	4.190	-2.000	-
		Q_2[b]	-2899.356	1298.409	-
		Q_3[c]	501026.971	-211413.245	-
	u_{12}-u_{22} [J /mol]	Q_1[a]	-2.917	3.471	-
		Q_2[b]	2034.113	-2258.232	-
		Q_3[c]	-353421.226	368125.821	-
	$\delta T\%$		0.047	0.358	0.442
	δy		0.009	0.005	0.005
Wilson					
	λ_{12}-λ_{11} [J /mol]	Q_1[a]	13.111	-0.082	-
		Q_2[b]	-8945.690	50.111	-
		Q_3[c]	1523702.815	-5687.572	-
	λ_{12}-λ_{22} [J /mol]	Q_1[a]	-13.418	0.055	-
		Q_2[b]	9082.986	-31.694	-
		Q_3[c]	-1533856.840	2675.500	-
	$\delta T\%$		0.125	0.572	0.334
	δy		0.008	0.005	0.003
NRTL					
	g_{12}-g_{11} [J /mol]	Q_1[a]	63.238	-1.097	-
		Q_2[b]	-42502.067	684.545	-
		Q_3[c]	7135576.603	-109209.720	-
	g_{12}-g_{22} [J /mol]	Q_1[a]	-57.314	2.678	-
		Q_2[b]	38446.570	-1667.772	-
		Q_3[c]	-6441660.000	263327.656	-
	α	Q_1[a]	0.000	0.000	-
		Q_2[b]	0.078	0.078	-
		Q_3[c]	-13.372	-12.983	-
	$\delta T\%$		0.148	0.484	0.948
	δy		0.009	0.006	0.011

*Parameters calculated from $Q_1T^2 + Q_2T + Q_3T$

**Values predicted from the 30 kPa parameters

[a] Units of [J /mol]

[b] Units of [J /mol /K]

[c] Units of [J /mol /K^2]

9.3.3 Thermodynamic consistency tests

The traditional area test for thermodynamic consistency of Redlich and Kister (1948) was not performed for reasons given in Chapter 3. The stringent point test of Van Ness (Van Ness and Abbott, 1982) and the more recent direct test (Van Ness, 1995) were used in this study. The merits and procedure for these tests are discussed in Chapter 3.

9.3.3.1 Point test

The test requires that isothermal data be reduced using an objective function based on the pressure residual only. For isobaric data, only the temperature residual must be used in the objective function. In doing so, the systematic errors are transferred to the vapour composition residual. For a thermodynamically consistent set, the vapour composition residual scatters randomly about the x-axis across the composition range. Furthermore, the average absolute deviation of the vapour composition must be below 0.01 mole fraction. These values are shown to be less than 0.01 for all the measured sets (Tables 9-2 to 9-5 and Tables 9-7 and 9-8). A plot of the vapour composition residual (δy), for the system acetone(1) with diacetyl(2), across the composition range is shown in Figure 9-31. The residuals scatter randomly about the x-axis for this system, thus satisfying the requirement of the consistency test. Plots for the rest of the data are given in Appendix E. The 50 °C and 60 °C isotherms for the methanol with diacetyl systems shows a negative bias, as does the 40 kPa isobar for the system diacetyl with 2,3-pentanedione. The average absolute residuals are however, within the required value of 0.01.

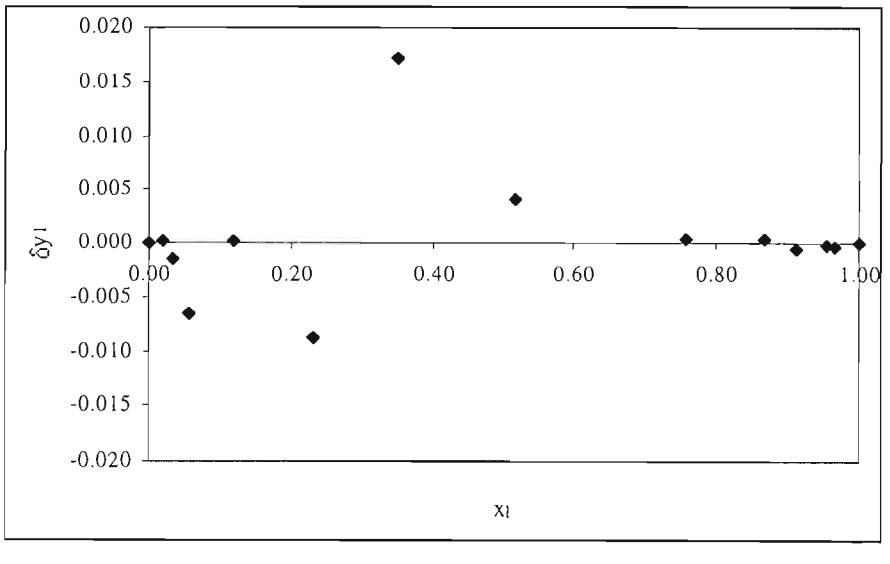

Figure 9-31: Point test of consistency for acetone(1) with diacetyl(2) at 30 °C

9.3.3.2 Direct test

The direct test for thermodynamic consistency was presented by Van Ness (1995). The formulation is such that the method directly measures deviations of experimental data from the Gibbs-Duhem equation. The data must be regressed using an objective function based on the excess Gibbs energy residual (see Chapter 3). The residual, $\delta\ln(\gamma_1/\gamma_2)$, scatters randomly about the x-axis, across the composition range, for thermodynamically consistent data. Figure 9-32 shows that this requirement is satisfied for the system acetone with diacetyl at 30 °C. Plots for the other data sets are given in Appendix F. The results are similar to those of the point test. The 50 °C and 60 °C isotherms for the system methanol and diacetyl show a bias (positive, for this test). The 40 kPa measurements for the diacetyl with 2,3-pentanedione system also show a positive bias. Van Ness (1995) proposes a scale by which the quality of VLE data can be judged. The scale is in terms of the root mean square (RMS) of the residual $\delta\ln(\gamma_1/\gamma_2)$. The larger the RMS value of this residual, the greater is the departure of the measurements from the Gibbs-Duhem equation. The scale is given in Table 3-1 of Chapter 3. The index ranges from 1 (data of the highest quality) to 10 (data of poor quality). The VLE measurements made in this study were found to rate, at worst, 3 on the Van Ness scale (even for the systems that showed a bias). The results of the direct test are given in Table 9-9.

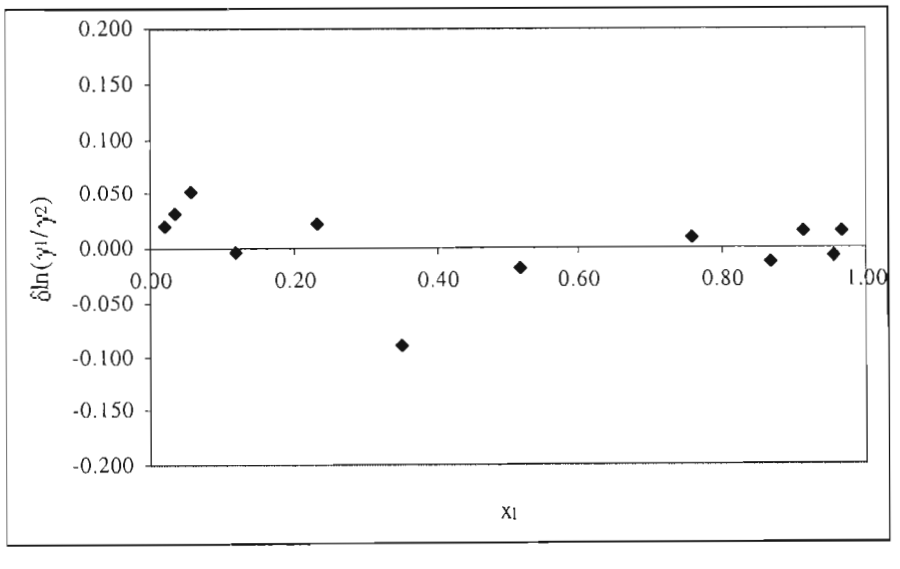

Figure 9-32: Direct test of consistency for acetone(1) with diacetyl(2) at 30 °C

Table 9-9: Results of the Van Ness (1995) direct test for thermodynamic consistency

System		Index
Acetone+Diacetyl	30 °C	2
	40 °C	2
	50 °C	2
	40 kPa	3
Methanol+Diacetyl	40 °C	3
	50 °C	3
	60 °C	3
	40 kPa	3
Diacetyl+2,3-Pentanedione	60 °C	3
	70 °C	3
	80 °C	3
	40 kPa	3
Acetone+2,3-Pentanedione	50 °C	3
	30 kPa	3

9.4 Measurement of infinite dilution activity coefficients

The inert gas stripping technique was used to measure the infinite dilution activity coefficients in this study. The apparatus and theory of the inert gas stripping method are described in Chapters 5 and 7. It is important that the height of the dilutor cell be sufficiently large to allow the stripping gas to be in equilibrium with the liquid in the cell. The mass transfer considerations to ensure that the height is appropriately specified are presented in Appendix D and discussed in Chapter 7. Difficulties experienced during the experiments are also discussed in Chapter 7.

It was required that the following infinite dilution activity coefficients be measured:

- Acetone in diacetyl.
- Methanol in diacetyl.
- Diacetyl in 2,3-pentanedione.
- Acetone in 2,3-pentanedione.

The development of the equations used to calculate the infinite dilution activity coefficient from the inert gas stripping method can be found in Chapter 5. Eq. 5-17 describes the case of a

volatile solvent and includes the correction of Duhem and Vidal (1978). As pressure and temperature are constant, Eq. 5-17 is a linear relationship:

$$\alpha = \varepsilon\beta$$

where

$$\alpha = \ln\frac{A}{A_0} \qquad \varepsilon = \frac{1}{1+\dfrac{\gamma_{sol}^{\infty} P_{sol}^{sat} V_G}{N_0 RT}} \frac{\gamma_{sol}^{\infty} P_{sol}^{sat}}{P_S^{sat}} - 1 \qquad \beta = \ln\left(1 - \frac{P_S^{sat}}{P - P_S^{sat}} \frac{PD}{N_0 RT} t\right)$$

Plotting α vs β yields a straight line which passes through the origin and the gradient, ε, is used to calculate the infinite dilution activity coefficient.

The first chemical system measured was acetone in methanol. This provided a good test system as values for the infinite dilution activity coefficient are available in literature. Bao and Han (1995) advocate the use of the single-cell technique for this type of system (volatile solute in an alcohol). Figure 9-33 shows the plot used to calculate the infinite dilution activity coefficient for acetone in methanol at 25 °C. A value of 2.36 was obtained, which is in fair agreement with Bao and Han (1995) who measured a value of 2.28 using the inert gas stripping technique.

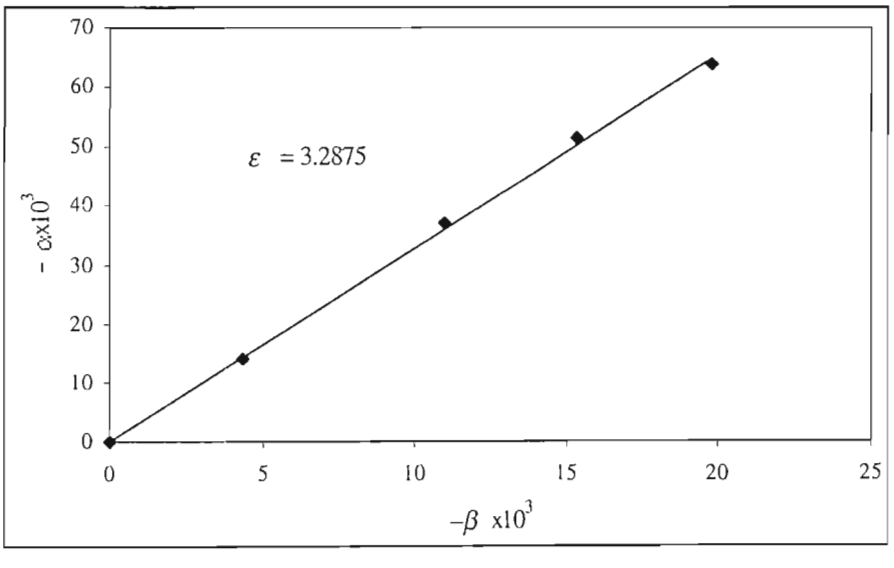

Figure 9-33: Plot used to calculate the infinite dilution activity coefficient by the inert gas stripping method for acetone in methanol

The plots used to calculate the infinite dilution activity coefficient for the systems involving diacetyl and 2,3-pentanedione (mentioned earlier in Section 9.4) can be found in Appendix E.

The measured values of the infinite dilution activity coefficient are shown in Table 9-10. All the systems had vapour corrections (Φ) close to unity, therefore, applying the modified Raoult's law when developing Eq. 5-17 was valid. The VLE data measured for the following systems showed no significant departure from Raoult's Law (see Chapter 3):

- Acetone with diacetyl.
- Acetone with 2,3-pentanedione.
- Diacetyl with 2,3-pentanedione.

These systems displayed nearly ideal behaviour, as can be expected for mixtures of similar chemicals at low-pressure. The infinite dilution activity coefficients are, therefore, close to 1. The methanol in diacetyl system, however, yielded a value of 1.32. It was noted that all these values are low enough to ignore the Duhem and Vidal (1978) correction. Indeed, Eqs. 5-17 and 5-15 yield values not significantly different. The correction is more crucial for systems such as benzene in water, where the infinite dilution activity coefficient is several orders of magnitude larger (Duhem and Vidal, 1978).

Table 9-10: Infinite dilution activity coefficients measured by the inert gas stripping method

System		Temperature	γ^{∞}
Solute	Solvent		
Acetone	Diacetyl	30 °C	1.04
Methanol	Diacetyl	40 °C	1.33
Diacetyl	2,3-Pentanedione	60 °C	1.01
Acetone	2,3-Pentanedione	50 °C	1.02

CHAPTER 10

CONCLUSION

The objective of this study was to investigate the phase equilibrium behaviour of systems involving diacetyl and 2,3-pentanedione. The conclusions of the study are presented in this chapter.

1. A survey of recent journal articles was made to determine the popular methods for low-pressure VLE measurements. The survey suggested the vapour and liquid recirculating method to be most popular. A review of these methods found the low-pressure apparatus of Raal and Mühlbauer (1998) to be most appropriate. This was, therefore, the apparatus used in this study. Isothermal operation of the still was achieved by manually adjusting the pressure set-point of the pressure controller by trial and error until the experimental temperature was achieved. The accuracy of the apparatus and method were tested by measuring the highly demanding binary system cyclohexane with ethanol. These measurements compared very well with reliable literature.

2. Previously unmeasured vapour pressure measurements were made for 2,3-pentanedione. All the VLE measurements made (except for the test system) are new data. The following systems showed nearly ideal behaviour (small deviations from Raoult's law):

    - Acetone with diacetyl at 30 °C, 40 °C, 50 °C and 40 kPa
    - Diacetyl with 2,3-pentanedione at 60 °C, 70 °C, 80 °C and 40 kPa
    - Acetone with 2,3-pentanedione at 50 °C, 30 kPa and 40 kPa

    This was expected as these are mixtures of similar chemicals (ketones). Measurements were also made for methanol with diacetyl at 40 °C, 50 °C, 60 °C and 40 kPa. The system displayed nearly ideal behaviour in the vapour phase (typical for low-pressure data) but did deviate from Raoult's law.

3. A review of the use of solution thermodynamics to interpolate and extrapolate low-pressure VLE data and to judge the quality of the measurements was made. The data were reduced using the Gamma-Phi approach to VLE. The vapour correction term was calculated from the truncated (two-term) virial equation of state. The second virial coefficients were

calculated using the Hayden and O' Connell (1975) method. The data were correlated to the Wilson, NRTL and UNIQUAC excess Gibbs energy models. Temperature dependent parameters are given for the isobaric sets. Best-fit models are proposed, although all the models were found to fit well.

4. The parameters reduced from the 30 kPa measurements, for acetone with 2,3-pentanedione, were used accurately to predict data at 40 kPa.

5. The stringent point test (Van Ness and Abbott, 1982) and the direct test (Van Ness, 1995) were used to test for thermodynamic consistency. All the data sets were found to fulfil the requirements of these tests. Van Ness (1995) proposes a scale by which the quality of data can be judged. The scale ranges from "1" for a perfectly consistent data set to "10" for a completely unacceptable set. The measured data in this study were found to be rated at worst "3."

6. The various methods for measuring infinite dilution activity coefficients were reviewed. The inert gas stripping technique was found to be accurate and versatile. Richon et al. (1980) suggest how mass transfer considerations can be used to ensure that the dilutor flask height is sufficiently large to ensure that the exiting gas phase is in equilibrium with the liquid. These computations were made and the apparatus was assembled. Although some difficulties (related to the plug fitted onto the dilutor flask) were encountered (and resolved), activity coefficients at infinite dilution were measured for the following systems:

    - Acetone in diacetyl at 30 °C
    - Methanol in diacetyl at 40 °C
    - Diacetyl in 2,3-pentanedione at 60 °C
    - Acetone in 2,3-pentanedione at 50 °C

CHAPTER 11

RECOMMENDATIONS

During the course of this study, some areas were noted as having potential for improvement. The recommendations given in this chapter are related to the method of temperature control in the VLE still and the construction of the dilutor flask plug.

In order to achieve isothermal operation of the VLE still, the pressure in the still was adjusted manually by changing the pressure controller set-point. This trial and error method is labour-intensive and tedious. Joseph et al. (2001) made use of a pair of computer-controlled solenoid valves to operate the still isothermally. One valve opens the still to the atmosphere and the other to a vacuum pump. The computer interface accepts a temperature set-point and the computer manipulates the valves to achieve this temperature. Joseph et al. (2001) state temperature control to vary from 0.01 K to 0.05 K. The solution is cost-effective and will improve data productivity.

The difficulties experienced during the inert gas stripping experiments were mainly related to the Teflon plug fitted onto the dilutor flask.

- As discussed in Chapter 7, the weight of the fittings and the pressure transducer tended to damage the soft Teflon threads when removing the plug. Sealing these leaks was most problematic due to the non-stick property of Teflon. Filling the leaks with Loctite proved to be an effective, although temporary solution. It is suggested that the dilutor flask designs of Richon et al. (1980) and Bao and Han (1995) be considered for future work.
- The seal between the Teflon plug and the dilutor flask was made by a pair of o-rings. It did, however, become necessary to clamp the plug onto the cell during the experiments. The dilutor flask design of Richon et al. (1980) uses a threaded plug that screws onto the top of the flask. This method was also used in the more recent work of Bao and Han (1995) and seems to be a more effective solution.

Li et al. (1993) advocate the use of a sintered glass disk to disperse the inert gas (as used originally by Leroi et al., 1977). The results of this study are consistent with those of Richon et

al. (1980) who suggest that using capillaries to disperse the inert gas reduces the occurrence of bubble coalescence.

There are many variations to the inert gas stripping technique, such as pre-saturation of the inert gas with solvent or the exponential saturation method. The method can also be used to measure properties other than the infinite dilution activity coefficient, such as VLE data or Henry's constants. These variations are slight modifications of the basic inert gas stripping technique. The applicability of the method can, therefore, be extended at a small expense.

REFERENCES

Abbott, MM, (1986), "Low Pressure Phase Equilibria: Measurement of VLE," *Fluid Phase Equilibria*, Vol. 29, Pg. 193-207.

Abrams, DS and Prausnitz, JM, (1975), "Statistical Thermodynamics of Liquid Mixtures: A New Expression for the Excess Gibbs Energy of Partly or Completely Miscible Systems," ," *American Institute of Chemical Engineers Journal*, Vol. 21, Pg. 116-128.

Alessi, P, Fermeglia, M and Kikic, I, (1986), "A Differential Static Apparatus for the Investigation of the Infinitely Dilute Region," *Fluid Phase Equilibria*, Vol. 29, Pg. 249-256.

Alessi, P, Fermeglia, M and Kikic, I, (1991), "Significance of Dilute Regions," *Fluid Phase Equilibria*, Vol. 70, Pg. 239-250.

Altsheler, WB, Unger, ED and Kolachov, P, (1951), "Improved Still for Liquid-Vapor Equilibria Data on Systems: Ethanol-Water and Acetic Acid-Water," *Industrial and Engineering Chemistry*, Vol. 43, Pg. 2559-.

Bao, J-B and Han, S-J, (1995), "Infinite Dilution Activity Coefficients for Various Types of Systems," *Fluid Phase Equilibria*, Vol. 112, Pg. 307-316.

Barker, C, (1953), "Determination of Activity Coefficients from Total Pressure Measurements," *Australian Journal of Chemistry*, Vol. 6, Pg. 207-210.

Black, C, (1958), "Phase Equilibria in Binary and Multicomponent Systems," *Industrial and Engineering Chemistry*, Vol. 50, Pg. 403-412

Brown, I, (1952), "Liquid-Vapour Equilibria. III. The Systems Benzene-n-Heptane, n-Hexane-Chlorobenzene and Cyclohexane-Nitrobenzene," *Australian Journal of Scientific Research*, Vol. 5, Pg. 530-540.

Cheh, HY and Tobias, CW, (1968), "Mass Transfer to Spherical Drops or Bubbles at High Reynolds Number," *Industrial and Engineering Chemistry Fundamentals*, Vol. 7, No. 1, Pg. 48-52.

Cottrell, FG, (1919), "On the Determination of Boiling Points of Solutions," *Journal of the American Chemical Society*, Vol. 41, Pg. 721-728.

Doležal, B and Holub, R, (1985), "Approximate Relations for Determining the Activity Coefficient at Very Low Concentration by the Method of Variation of Solute Concentration," *Collection of Czechoslovak Chemical Communications*, Vol. 50, Pg. 704-711.

Doležal, B, Popl, M and Holub, R, (1985), "Determination of the Activity Coefficient at Very Low Concentration by the Inert Gas Stripping Method," *Journal of Chromatography*, Vol. 207, Pg. 193-201.

Duhem, P and Vidal, P, (1978), "Short Communication: Extension of the Dilutor Method to Measurement of High Activity Coefficients at Infinite Dilution," *Fluid Phase Equilibria*, Vol. 2, Pg. 231-235.

Dvorak, K and Boublik, T, (1963), "Liquid-vapour Equilibria. XXIX. Measurement of Equilibrium Data in Systems with High Equilibrium Ratio of Components," *Collection of Czechoslovak Chemical Communications*, Vol. 28, Pg. 1249-1255.

Fowlis, IA and Scott, RPW, (1963), "A Vapour Dilution System for Detector Calibration," *Journal of Chromatography*, Vol. 11, Pg. 1-10.

Fredenslund A, Gmehling, J, Michelson, ML, Rasmussen, P and Prausnitz, JM, (1977a), "Computerized Design of Multicomponent Distillation Columns Using the UNIFAC Group Contribution Method for Calculation of Activity Coefficients," *Industrial and Engineering Chemistry: Process Design and Development*, Vol. 16, Pg. 450-462.

Fredenslund, A, Gmehling, J and Rasmussen, P, (1977b), "Vapour-Liquid Equilibria Using UNIFAC: A Group Contribution Method," Amsterdam: Elsevier, North Holland.

Fredenslund, A, Jones, JL and Prausnitz, JM, (1975), "Group Contribution Method for the Estimation of Activity Coefficients in Non-Ideal Solutions," *American Institute of Chemical Engineers Journal*, Vol. 21, Pg. 1086.

Gautreaux, MF and Coates, J, (1955), "Activity Coefficients at Infinite Dilution," *American Institute of Chemical Engineers Journal*, Vol. 1, No. 4, Pg. 496-500.

Gibbs, RE and Van Ness, HC, (1972), "Vapor-Liquid Equilibria from Total-Pressure Measurements. A New Apparatus," *Industrial and Engineering Chemistry Fundamentals*, Vol. 11, Pg. 410-413.

Gillespie, DTC, (1946), "Vapor-liquid Equilibrium for Miscible Liquids," *Industrial and Engineering Chemistry, Analytical Edition*, Vol. 18, Pg. 575-577.

Hála, E, Pick, J, Fried, V and Vilím, O, (1957), "Vapour-Liquid Equilibrium," Pergamon Press, New York.

Hayden, JG and O' Connell, JP, (1975), "A Generalized Method for Predicting Second Virial Coefficients," *Industrial and Engineering Chemistry: Process Design and Development,"* Vol. 14, Pg. 209-215.

Heertjes, PM, (1960), "Determination of Vapour-Liquid Equilibria of Binary Systems," *Chemical and Process Engineering*, Vol. 41, Pg. 385-386.

Hovorka, Š and Dohnal, V, (1999), "Exponential Saturator: A Novel Gas-Liquid Partitioning Technique for Measurement of Large Limiting Activity Coefficients," *Industrial and Engineering Chemistry Research*, Vol. 38, Pg. 2036-2043.

Howell, WJ, Karachewski, AM, Stephenson, KM, Eckert, CA, Park, JH, Carr, PW and Ruttan, SC, (1989), "An Improved MOSCED Equation for the Prediction and Application of Infinite Dilution Activity Coefficients," *Fluid Phase Equilibria*, Vol. 52, Pg. 151-160.

Hradetzky, G, Wobst, M, Vopel, H and Bittrich, H-J, (1990), "Measurement of Activity Coefficient in Highly Dilute Solutions Part I," *Fluid Phase Equilibria*, Vol. 54, Pg. 133-145.

J, Crank, (1956), "The Mathematics of Diffusion," Oxford University Press, Oxford.

Jones, CA, Schoenborn, EM and Colburn, AP, (1943), "Equilibrium Still for Miscible Liquids," *Industrial and Engineering Chemistry*, Vol. 35, Pg. 666-672.

Joseph, MA, (2001), "Computer-Aided Measurement of Vapour-Liquid Equilibria in a Dynamic Still at Sub-Atmospheric Pressures," MSc. Eng. Thesis, University of Natal.

Joseph, MA, Ramjugernath, D and Raal, JD, (2001), "Phase Equilibrium Properties for Binary Systems with Diacetyl from a Computer Controlled Vapour-Liquid Equilibrium Still," *Fluid Phase Equilibria*, Vol. 182, Pg. 157-176.

Joseph, MA, Ramjugernath, D and Raal, JD, (2002), "Computer-Aided Measurement of Vapour-Liquid Equilibria in a Dynamic Still at Sub-Atmospheric Pressures," *Developments in Chemical Engineering and Mineral Processing*, Vol. 10, No. 5-6, Pg. 615-638.

Jourdain, F, (2000), "Inert Gas Stripping Technique for the Determination of Activity Coefficients at Infinite Dilution," Communication to Profs. JD Raal and D Ramjugernath, University of Natal.

Kneisl, P, Zondlo, JW and Whiting, WB, (1989), "The Effect of Fluid Properties on Ebulliometer Operation," *Fluid Phase Equilibria*, Vol. 46, Pg. 85-94.

Kreglewski, A, (1969), "Second Virial Coefficients of Real Gases," *Journal of Physical Chemistry*, Vol. 73, Pg. 608-615.

Lee, BI and Kesler, (1975), MG, "A Generalized Thermodynamic Correlation Based on Three-Parameter Corresponding States," *American Institute of Chemical Engineers Journal*, Vol. 21, Pg. 510-527.

Lee, SC, (1931), "Partial Pressure Isotherms," *Journal of Physical Chemistry*, Vol. 35, Pg. 3558-3582.

Legret, D, Desteve, J, Richon, D and Renon, H, (1983), "Vapor-Liquid Equilibrium Constants at Infinite Dilution Determined by a Gas Stripping Method: Ethane, Propane, n-Butane, n-Pentane in the Methane-n-Decane System," *American Institute of Chemical Engineers Journal*, Vol. 29, No. 1, Pg. 137-144.

Leroi, J-C, Masson, J-C, Renon, H, Fabries, J-F and Sannier, H, (1977) "Accurate Measurement of Activity Coefficients at Infinite Dilution by Inert Gas Stripping and Gas Chromatography," *Industrial and Engineering Chemistry Process Design and Development*, Vol. 16, No. 1, Pg. 139-144.

Letcher, TM, (1978), "Activity Coefficients at Infinite Dilution Using GLC," *Chemical Thermodynamics: A Specialist Periodical Report*, Vol. 2, Chapter 2, Edited by McGlashan, ML, Chemical Society London.

Li, H, Han S and Teng, Y, (1995), "Bubble Point Measurement for Systems Chloroform-Ethanol-Benzene by Inclined Ebulliometer," *Fluid Phase Equilibria*, Vol. 113, Pg. 185-195.

Li, J and Carr, PW, (1993), "Measurement of Water-Hexadecane Partition Coefficients by Headspace Chromatography and Calculation of Limiting Activity Coefficients in Water," *Analytical Chemistry*, Vol. 65, Pg. 1443-1450.

Maher, PJ and Smith, BD, (1979), "A New Total Pressure Vapour-Liquid Equilibrium Apparatus. The Ethanol + Aniline System at 313.15K, 350.81K and 386.67K," *Journal of Chemical and Engineering Data*, Vol. 24, Pg. 16-22.

Malanowski, S, (1982), "Experiemental Methods for Vapour-Liquid Equilibria. Part I. Circulation Methods," *Fluid Phase Equilibria*, Vol. 8, Pg. 197-219.

Marquardt, DW, (1963), "An Algorithm for Least-Squares Estimation of Non-Linear Parameters," *Journal of the Society of Industrial and Applied Mathematics*, Vol. 11, Pg. 431-441.

Martin, HW, (1964), "Scale-Up Problems in a Solvent-Water Fractionator," *Chemical Engineering Progress*, Vol. 60, No. 10, Pg. 50-54.

McClellan, AL, (1963), "Tables of Experimental Dipole Moments," WH Freeman, San Francisco.

McGee, JJ, (1999), "An investigation into the formation and reactions of diacetyl," M.Sc. Thesis, University of Natal.

Mixon, FO, Gumowski, B and Carpenter, BH,(1965), "Computation of Vapor-Liquid Equilibrium from Solution Vapour Pressure Measurements," *Industrial and Engineering Chemistry Fundamentals*, Vol. 4, Pg. 455-459.

Miyamoto, S, Nakamura, S, Iwai, Y and Arai, Y (2000), "Measurement of Isothermal Vapour-Liquid Equilibria for Hydrocarbon + Monocarboxylic Acid Binary Systems by a Flow-type Apparatus," *Journal of Chemical and Engineering Data*, Vol. 45, Pg. 857-861.

Moollan, WC, (1996), "The determination of activity coefficients at infinite dilution," Ph.D. Thesis, University of Natal.

Nothnagel, KH, Abrams, DS and Prausnitz, JM, (1973), "Generalized Correlation for the Fugacity Coefficients in Mixtures at Moderate Pressures," Industrial and Engineering Chemistry: Process Design and Development, Vol. 12, No. 1, Pg. 25-35.

O' Connell, JP and Prausnitz, JM, (1967), "Empirical Correlation of Second Virial Coefficients for Vapor-Liquid Equilibrium Calculations," *Industrial and Engineering Chemistry: Process Design and Development,"* Vol. 6, No. 2, Pg. 245-250.

Othmer, DF, (1928), "Composition of Vapors from Boiling Binary Solutions. Improved Equilibrium Still," *Industrial and Engineering Chemistry*, Vol. 20, Pg. 743-766.

Othmer, DF, (1948), "Composition of Vapors from Boiling Binary Solutions. Improved Equilibrium Still," *Analytical Chemistry*, Vol. 20, Pg. 763-766.

Ovečková, J, Surový, J and Graczová, E, (1991), "A Modified Method for Vapour-Liquid Equilibria Measurement by Inert Gas Stripping," *Fluid Phase Equilibria*, Vol. 68, Pg. 163-172.

Palmer, DA, (1987), "Handbook of Applied Thermodynamics," CRC Press, Inc., Florida

Peng, DY, and Robinson, DB, (1976), "A New Equation of State," *Industrial and Engineering Fundamentals*, Vol. 15, Pg. 59-64.

Perry, RH and Green, DW, (1998), "Perry's Chemical Engineers' Handbook," 7th edition, McGraw-Hill, New York.

Pitzer, KS and Brewer, L, (1961), "Thermodynamics," McGraw-Hill, New York.

Pitzer, KS and Curl, RF Jr., (1957), "The Volumetric and Thermodynamic Properties of Fluids: Empirical Equation for the Second Virial Coefficient," *Journal of the American Chemical Society*, Vol. 79, Pg. 2369-2370.

Prausnitz, JM, Anderson, TF, Grens, EA, Eckert, CA, Hsieh and O' Connell, JP, (1980), "Computer Calculations for Multicomponent Vapor-Liquid and Liquid-Liquid Equilibria," Prentice-Hall, Englewood Cliffs, New Jersey.

Prausnitz, JM, Ruediger, NL and de Azevedo, EG, (1986), "Molecular Thermodynamics of Fluid-Phase Equilibria," 2nd Edition, Prentice-Hall, Englewood Cliffs, New Jersey.

Raal, JD and Mühlbauer, AL, (1998), "Phase Equilibria: Measurement and Computation," Taylor and Francis, Bristol PA.

Raal, JD and Ramjugernath, D, (2001), "Rigorous Characterization of Static and Dynamic Apparatus for Measuring Limiting Activity Coefficients," *Fluid Phase Equilibria*, Vol. 187-188, Pg. 473-487.

Raal, JD, (2000), "Characterization of Differential Ebulliometers for Measuring Activity Coefficients," *American Institute of Chemical Engineers Journal*, Vol. 46, No. 1, Pg. 210-220.

Raal, JD, (2003), "Experimental Thermodynamics," Vol. 7, Chapter 2a, Elsevier, In Press.

Redlich, O and Kister, AT, (1948), "Algebraic Representation of Thermodynamic Properties and the Classification of Solutions," *Industrial and Engineering Chemistry*, Vol. 40, Pg. 345-348.

Redlich, O and Kwong, JNS, (1949), "On the Thermodynamics of Solutions. V. An Equation of State. Fugacities of Gaseous Solutions," *Chemical Reviews* Vol. 44, Pg. 233-244.

Reid, RC, Prausnitz, JM and Poling, BE, (1988)), "Properties of Gases and Liquids," McGraw-Hill, New York.

Renon, H and Prausnitz, JM, (1968), "Local Composition in the Thermodynamic Excess Functions for Liquid Mixtures," ," *American Institute of Chemical Engineers Journal*, Vol. 14, Pg. 135-144.

Richon, D and Renon, H, (1980), "Infinite Dilution Henry's Constants of Light Hydrocarbons in n-Hexadecane, n-Octadecane and 2,2,4,4,6,8,8-Heptamethylnonane by Inert Gas Stripping," *Journal of Chemical and Engineering Data*, Vol. 25, Pg. 59-60.

Richon, D, Antoine, P and Renon, H, (1980), "Infinite Dilution Activity Coefficients of Linear and Branched Alkanes from C_1 to C_9 in n-Hexadecane by Inert Gas Stripping," *Industrial and Engineering Chemistry Process Design and Development*, Vol. 19, Pg. 144-147.

Richon, D, Sorrentino, F and Voilley, A, (1985), "Infinite Dilution Activity Coefficients by the Inert Gas Stripping Method: Extension to the Study of Viscous and Foaming Mixtures," *Industrial and Engineering Chemistry Process Design and Development*, Vol. 24, Pg. 1160-1165.

Ritter, JJ and Adams, NK, (1976), "Exponential Dilution as a Calibration Technique," *Analytical Chemistry*, Vol. 48, Pg. 612-619.

Rogalski, M and Malanowski, S, (1980), "Ebulliometers modified for the Accurate Determination of Vapour-Liquid Equilbrium," *Fluid Phase Equilibria*, Vol. 5, Pg. 97-112.

Rose, A and Williams, ET, (1955), "Vapor-Liquid Equilibrium Self Lagging Stills. Design and Evaluation," *Industrial and Engineering Chemistry*, Vol. 47, Pg. 1528-1533.

Sayegh, SG and Vera, JH, (1980), "Model-free Methods for Vapor-Liquid Equilibria Calculations: Binary Systems," *Chemical Engineering Science*, Vol. 35, Pg. 2247-2256.

Scatchard, G, Raymond, CL and Gillman, HH, (1938), "Vapour-Liquid Equilibrium. I. The Apparatus for the study of systems with volatile components," *Journal of the American Chemical Society*, Vol. 60, Pg. 1275-1287.

Slattery, JC and Bird, RB, (1958), "Calculation of the Diffusion Coefficient of Dilute Gases and the Self-Diffusion Coefficient of Dense Gas," *American Institute of Chemical Engineers Journal*, Vol. 4, No. , Pg. 137-142.

Smith, JM, Van Ness, HC and Abbott, MM, (1996), "Introduction to Chemical Engineering Thermodynamics," McGraw-Hill, New York.

Soave, (1972), "Equilibrium Constants from a Modified Redlich-Kwong Equation of State," *Chemical Engineering Science,* Vol. 27, Pg. 1197-1203.

Tsonopoulos, C, (1974), "An Empirical Correlation of Second Virial Coefficients," *American Institute of Chemical Engineers Journal*, Vol. 20, Pg. 263-272.

Van Ness, HC and Abbott, MM, (1982), "Classical Thermodynamics of Non Electrolyte Solutions: With Applications to Phase Equilibria," McGraw-Hill, New York.

Van Ness, HC, (1995), "Thermodynamics in the Treatment of Vapor /Liquid Equilibrium (VLE) Data," *Pure and Applied Chemistry*, Vol. 67, Pg. 859-872.

Walas, SM, (1985), "Phase Equilibria in Chemical Engineering," Butterworth Publishers, Boston.

Washburn, R and Read, JW, (1919), "The Laws of "Concentrated" Solutions. VI. The General Boiling Point Law," *Journal of the American Chemical Society*, Vol. 41, Pg. 729-741.

Weidlich, U and Gmehling, J, (1985), "Extension of UNIFAC by Headspace Chromatography," *Journal of Chemical and Engineering Data*, Vol. 30, Vol. 95-101.

Wilke, CR and Chang, P, (1955), "Correlation of Diffusion Coefficients in Dilute Solutions," *American Institute of Chemical Engineers Journal*, Vol. 1, No. 2, Pg. 264-269.

Wobst, M, Hradetzky, G and Bittrich, H-J, G (1992), "Measurement of Activity Coefficient in Highly Dilute Solutions Part II," *Fluid Phase Equilibria*, Vol. 77, Pg. 297-312.

Wong, and Sandler, (1992), "A Theoretically Correct Mixing Rule for Cubic Equations of State," *American Institute of Chemical Engineers Journal*, Vol. 38, Pg. 671-680.

Yerazunis, S, Plowright, JD, and Smola, FM, (1964), "Vapor-Liquid Equilibrium Determination by a New Apparatus," *American Institute of Chemical Engineers Journal*, Vol. 10, Pg. 660-665.

Yu, Y-X, Liu, J-G and Gao, G-H, (1999), "Isobaric Vapor-Liquid Equilibria for Three Aromatic Hydrocarbon-tetraethylene Glycol Binary Mixtures," *Fluid Phase Equilibria*, Vol. 157, Pg. 299-307.

APPENDIX A

BIBLIOGRAPHY

VLE data sets, published between September 1999 and September 2002 in the following journals, were considered in the survey presented in Chapter 2:

- *Fluid Phase Equilibria*
- *Journal of Chemical and Engineering Data*
- *Journal of Chemical Thermodynamics*

The purpose was to gauge the popularity of the various methods available for the measurement of VLE. Articles containing VLE data of the following type were noted (as these were the parameters of the measurements required by this study):

- Non-reacting binary systems.
- Temperature range from 303.15K to 493.15K.
- System pressures up to atmospheric.

The *Journal of Chemical Thermodynamics* was excluded as the number of relevant articles published during this period was small compared to the other two journals considered. The results of the review are presented in Chapter 2 and this appendix is a bibliography to the review.

A.1 *Fluid Phase Equilibria*

1. Seiler, M, Arlt, W, Kautz, H, and Frey, H, (2002), Vol. 201, Iss. 2, Pg. 359-379.
2. Ussi-Kyyny, P, Pokki, J-P, Laakonen, Aittamaa, J and Luikkonen, S, (2002), Vol. 201, Iss. 2, Pg. 343-358.
3. Rodríguez, A, Canosa, J, Domíguez, A and Tojo, J, (2002), Vol. 201, Iss. 1, Pg. 187-201.
4. Prasad, TEA, Kumar, AS and Prasad, DHL, (2002), Vol. 201, Iss. 1, Pg. 47-55.
5. Park, S-J, Han, KJ and Gmehling, J, (2002), Vol. 200, Iss. 2, Pg. 399-409.
6. Chaudhari, SK, (2002), Vol 200, Iss. 2, Pg. 329-336.

7. Asensi, JC, Moltó, J, del Mar Olaya, M, Ruiz, F and Gomis, V, (2002), Vol. 200, Iss. 2, Pg. 287-293.
8. del Río, A, Coto, B, Pando, C and Renuncio, JAR, (2002), Vol. 200, Iss. 1, Pg. 41-51.
9. Duce, C, Tinè, MR, Lepori, L and Matteoli, (2002), Vol. 199, Iss. 1-2, Pg. 197-212.
10. Batiu, I, (2002), Vol 198, Pg. 111-121.
11. Rodríguez, A, Canosa, J, Domíguez, A and Tojo, J, (2002), Vol. 198, Pg. 95-109.
12. Hiaki, T, Nanao, M, Urata, S and Murata, J, (2002), Vol. 194-197, Pg. 969-979.
13. Loras, S, Aucejo, A and Muñoz, R, (2002), Vol. 194-197, Pg. 957-968.
14. Park, S-J, Han, K-J, Choi, M-J and Gmehling, J, (2002), Vol. 193, Iss. 1-2, Pg. 109-121.
15. Du, T-B, Tang, M and Chen, Y-P, (2001), Vol. 192, Iss. 1-2, Pg. 71-83.
16. Artigas, H, Lafuente, C, Martín, S, Miñones, J Jr. and Royo, FM, (2001), Vol. 192, Iss. 1-2, Pg. 49-61.
17. Yu, Y-X, He, M-Y, Gao, G-H and Li, Z-C, (2001), Vol. 190, Iss. 1-2, Pg. 61-71.
18. Wang, C, Li, H, Zhu, L and Han, S, (2001), Vol. 189, Iss. 1-2, Pg. 119-127.
19. Bernatová, S and Wichterle, I, (2001), Vol. 189, Iss. 1-2, Pg. 111-118.
20. del Río, A, Coto, B, Pando, C and Renuncio, JAR, (2001), Vol. 187-188, Pg. 299-310.
21. Alonso, C, Montero, EA, Chamorro, CR, Sergovia, JJ, Martín, MC and Villamañán, MA, (2001), Vol. 182, Pg. 241-255.
22. Chamorro, CR, Segovia, JJ, Martín, MC and Villamañán, MA, (2001), Vol. 182, Pg. 229-239.
23. Hiaki, T, Nanao, M, Urata, S and Murata, J, (2001), Vol. 182, Pg. 189-198.
24. Resa, JM, González, C, de Landaluce, SO, Lanz, J and Fanega, M, (2001), Vol 182, Pg. 177-187.
25. Joseph, MA, Raal, JD and Ramjugernath, D, (2001), Vol. 182, Pg. 157-176.
26. Park, S-J, Kim, H-H, Won, DB, Lee, SB and Choi, M-J, (2002), Vol. 180, Pg. 361-373.
27. Bernatová, S and Wichterle, I, (2001), Vol 180, Pg. 235-245.
28. Rhodes, JM, Griffin, TA, Lazzaroni, MJ, Bhethanabotla, VR and Campbell, SW, (2001), Vol. 179, Pg. 217-229.
29. Hwang, S-M, Lee, M-J and Lin, H-m, (2001), Vol. 178, Pg. 209-233.
30. Tu, C-H, Wang, W-F, Hsian, H-y and Chou, Y-T, (2000), Vol. 175, Nos. 1-2, Pg. 139-152.
31. Loras, S, Aucejo, A, Muñoz, R and de la Torre, J, (2000), Vol. 175, Nos. 1-2, Pg. 125-138.
32. Chen, C-C, Chang, C-mJ Yang, P-w, (2000), Vol. 175, Nos. 1-2, Pg. 107-115.
33. Hiaki, T and Nanao, M, (2000), Vol. 174, Nos. 1-2, Pg. 81-91.
34. Zhenghong, G, Zhonglong, M and Qin, CLW, (2000), Vol. 173, Nos. 2, Pg. 253-261.
35. Hwang, S-M, Lee, M-G and H-m, Lin, (2000), Vol. 172, No. 2, Pg. 183-196.

36. Ortega, J, Gonzalez, C, Pena, J and Galvan, S, (2000), Vol. 170, No. 1, Pg. 87-111.
37. Li, J, Chen, C and Wang, J, (2000), Vol. 169, No. 1, Pg. 75-84.
38. Al-Hayan, MNM and Newsham, DMT, Vol. 168, No. 2, Pg. 259-266.
39. Kammerer, K, Oswald, G, Rezanova, E, Silkenbaumer, D and Lichenthaler, RN, (2000), Vol. 167, No. 2, Pg. 223-241.
40. Al-Hayan, MNM and Newsham, DMT, (1999), Vol. 166, No. 1, Pg. 91-100.
41. Krishnaiah, A, Reddy, KVR, Devarajulu, T and Ramakrishna, M, (1999), Vol. 165, No. 1, Pg. 59-66.
42. Domnguez, M, Cea, P, López, CM, Royo, FM and Urieta, JS, (1999), Vol 164, No. 2, Pg. 195-207.
43. Fernandez, J, Garriga, R, Velasco, I and Otn, S, (1999), Vol. 163, No. 2, Pg. 231-242.
44. Wen, T-Y, Tang, M and Chen, Y-P, (1999), Vol. 163, No. 1, Pg. 99-108.

A.2 *Journal of Chemical and Engineering Data*

1. Rodríguez, A, Canosa, J, Domínguez, A and Tojo, J, (2002), Vol. 47, No. 5, Pg. 1098-1102.
2. Resa, JM, González, C, de Landulce, SO and Lanz, J, (2002), Vol. 47, No. 5, Pg. 1123-1127.
3. Díaz, C and Tojo, J, (2002) Vol. 47, No. 5, Pg. 1154-1158.
4. Loras, S, Aucejo, A, Montón, JB, Wisniak, J and Segura, H, (2002), Vol. 47, No. 5, Pg. 1256-1262.
5. Bolun, Y and Wang, H, (2002), Vol. 47, No. 5, Pg. 1324-1329.
6. Sanz, MT, Calvo, B, Beltrán, S and Cabezas, JL, (2002), Vol. 47, No. 4, Pg. 1003-1006.
7. Díaz, C, Domínguez, A and Tojo, J, (2002), Vol. 47, No. 4, Pg. 867-871.
8. Prasad, TEV, Mythili, R, Nirmala, GS and Prasad, DHL, (2002), Vol. 47, No. 4, Pg. 816-817.
9. Harris, RA, Ramjugernath, D, Letcher, TM and Raal, JD, (2002), Vol. 47, No. 4, Pg. 781-787.
10. Antosik, M, Fraś, Z and Malanowski, S, (2002), Vol. 47, No. 4, Pg. 757-760.
11. Wilding, VW, Adams, KL, Carmichael, AE, Hull, JB, Jarman, TC and Marshall, TL, (2002), Vol. 47, No. 4, Pg. 740-747.
12. Wilding, VW, Adams, KL, Carmichael, AE, Hull, JB, Jarman, TC, Jenkins, KP, Marshall, TL and Wilson, HL, (2002), Vol. 47, No. 4, Pg. 739-739.
13. Gu, F, Wang, L and Wu, Z, (2002), Vol. 47, No. 4, Pg. 643-647.
14. Sewnarain, R, Ramjugernath, D and Raal, JD, (2002), Vol. 47, No. 3, Pg. 603-607.
15. Świątek, BE and Malanowski, S, (2002), Vol. 47, No. 3, Pg. 478-481.

16. Resa, JM, González, C, de Landaluce, SO and Lanz, J, (2002), Vol. 47, No. 3, Pg. 435-440.
17. Domínguez, M, Martín, S, Artigas, H, López, CM and Royo, FM, (2002), Vol. 47, No. 3, Pg. 405-410.
18. Pokki, J-P, Uusi-Kyyny, P, Aittamaa, J and Liukkonen, S, (2002), Vol. 47, No. 2, Pg. 371-375.
19. Kodama, D, Tanaka, H and Kato, M, (2002), Vol. 47, No. 1, Pg. 91-92.
20. del Mar Olaya, M, Gomis, V, Moltó, J andRuiz, F, (2002), Vol. 47, No. 1, Pg. 65-67.
21. Vercher, E, Vázquez, I and Martínez-Andreu, A, (2001), Vol. 46, No. 6, Pg. 1584-1588.
22. Chamorro, CR, Segovia, JJ, Martín, MC and Villamañán, MA, (2001), Vol. 46, No. 6, Pg. 1574-1579.
23. Loras, S, Aucejo, A, Montón, JB, Wisniak, J and Segura, H, (2001), Vol. 46, No. 6, Pg. 1351-1356.
24. Resa, JM, González, C, de Landaluce, SO and Lanz, J, (2001), Vol. 46, No. 5, Pg. 1338-1343.
25. Prasad, TEV, Satyakishore, P, Ramserisj, GV and Prasad, DHL, (2001), Vol. 46, No. 5, Pg. 1266-1268.
26. Uusi-Kyyny, P, Pokki, J-P, Aittamaa, J and Liukkonen, S, (2001), Vol. 46, No. 5, Pg. 1244-1248.
27. Zhu, L, Li, H, Wang, C and Han, S, (2001), Vol. 46, No. 5, Pg. 1231-1234.
28. Miyamoto, S, Nakamura, S, Iwai, Y and Arai, Y, (2001), Vol. 46, No. 5, Pg. 1225-1230.
29. del Rio, A, Horstmann, S, Renuncio, JAR and Gmehling, J, (2001), Vol. 46, No. 5, Pg. 1181-1187.
30. Tochiga, K, Satou, T, Kurihara, K, Ochi, K, Yamamoto, H, Mochizuki, Y and Sako, T, (2001), Vol. 46, No. 4, Pg. 913-917.
31. Ortega, J, González, C and Galván, S, (2001), Vol. 46, No. 4, Pg. 904-912.
32. Albert, M, Hahnenstein, I, Hasse, H and Maurer, G, (2001), Vol. 46, No. 4, Pg. 897-903.
33. Luo, H-P, Zhou, J-H, Xiao, W-D and Zhu, K-H, (2001), Vol. 46, No. 4, Pg. 842-845.
34. Uusi-Kyyny, P, Pokki, J-P, Aittamaa, J and Liukkonen, S, (2001), Vol. 46, No. 3, Pg. 754-758.
35. Uusi-Kyyny, P, Pokki, J-P, Aittamaa, J and Liukkonen, S, (2001), Vol. 46, No. 3, Pg. 686-691.
36. Sanz, MT, Blanco, B, Beltrán, Cabezaz, JL and Coca, J, (2001), Vol. 46, No. 3, Pg. 635-639.
37. Martínez, S, Garriga, R, Pèrez, P and Gracia, M, (2001), Vol. 46, No. 3, Pg. 535-540.

38. Segura, H, Wisniak, J, Galindo, G and Reich, R, (2001), Vol. 46, No. 3, Pg. 511-515.
39. Segura, H, Wisniak, J, Galindo, G and Reich, R, (2001), Vol. 46, No. 3, Pg. 506-510.
40. Prasad, TEV, Naidu, BRP, Madhukiran, D and Prasad, DHL, (2001), Vol. 46, No. 2, Pg. 414-416.
41. Miyamoto, S, Nakamura, S, Iwai, Y and Arai, Y, Vol. 46, No. 2, Pg. 405-409.
42. Horstmann, S, Gardeler, H, Fischer, K, Köster, F and Gmehling, J, (2001), Vol. 46, No. 2, Pg. 337-345.
43. Rolemberg, MP Krähenbühl, MA, (2001), Vol. 46, No. 2, Pg. 256-260.
44. Everson, RC Jansen, W, (2001), Vol. 46, No. 2, Pg. 247-250.
45. Wisniak, J, Yardeni, B, Sling, T and Segura, H, (2001), Vol. 46, No. 2, Pg. 223-228.
46. Kirss, H, siimer, E, Kuus, M and Kudryavtseva, L, (2001), Vol. 46, No. 1, Pg. 147-150.
47. Muñoz, LAL and Krähenbühl, MA, (2001), Vol. 46, No. 1, Pg. 120-124.
48. Chyliński, K, Fraś, Z Malanowski, S, (2001), Vol. 46, No. 1, Pg. 29-33.
49. Arce, A, Rodil, E and Soto, A, (2000), Vol. 45, No. 6, Pg. 1112-1115.
50. Gabaldón, C, Martinez-Soria, V, Marzal, P and Montón, JB, (2000), Vol. 45, No. 5, Pg. 882-886.
51. Resa, JM, González, C, de Landaluce, SO, and Lanz, J, (2000), Vol. 45, No.5, Pg. 867-871.
52. Miyamoto, S, Nakamura, S, Iwai, Y and Arai, Y, (2000), Vol. 45, No. 5, Pg. 857-861.
53. Carmona, FJ, González, JA, de la Fuente, IG, Cobo, JC, Bhethanabotla, VR and Campbell, SW, (2000), Vol. 45, No. 4, Pg. 699-703.
54. Segura, H, Reich, R, Galindo and G, Wisniak, (2000), Vol. 45, No. 4, Pg. 600-605.
55. Yu, Y-X, Liu, J-G and Gao, G-H, (2000), Vol. 45, No. 4, Pg. 570-574.
56. Hiaki, T and Tatsuhana, K, (2000), Vol. 45, No. 4, Pg. 564-569.
57. Gu, F and Fang, W, (2000), Vol. 45, No. 2, Pg. 288-291.
58. Hofman, T, Sporzyński, A and Gołdon, A, (2000), Vol. 45, No. 2, Pg. 169-172.
59. Giles, NF and Wilson, GM, (2000), Vol. 45, No. 2, Pg. 146-153.
60. Kodama, D, Tanaka, H and Kato, M, (1999), Vol. 44, No. 6, Pg. 1252-1253.
61. Mun, S and Lee, H, (1999), Vol. 44, No. 6, Pg. 1231-1234.
62. Loras, S, Aucejo, A and Muñoz, R, (1999), Vol. 44, No. 6, Pg. 1169-1174.
63. Loras, S, Aucejo, A, Muñoz, R, Ordoñez, LM, (1999), Vol. 44, No. 6, Pg. 1163-1168.
64. Montón, JB, de la Torre, J, Burguet, MC, Muñoz, R and Loras, S, (1999), Vol. 44, No. 6, Pg. 1158-1162.
65. Horstmann, S, Gardeler, H, Bölts, R, Zudkevitch, Gmehling, J, (1999), Vol. 44, No. 5, Pg. 959-964.
66. Segura, H, Reich, R, Galindo, G and Wisniak, J, (1999), Vol. 44, No. 5, Pg. 912-917.

APPENDIX B

PHYSICAL PROPERTIES OF THE CHEMICALS STUDIED

Physical properties are required to perform the data reduction procedure described in Chapter 3. The method of Hayden and O' Connell (1975), to calculate second virial coefficients (Chapter 3), for example requires critical properties, dipole moments and the mean radius of gyration. The critical properties and dipole moments of acetone and methanol are given in Reid et al. (1988). The mean radius of gyration for acetone and methanol can be found in Prausnitz et al. (1980).

The required values for 2,3-pentanedione and diacetyl are not available in literature and must be estimated. The Ambrose method (as suggested by Reid et al., 1988) was used to estimate critical properties. The computation of the critical properties were performed by Y Nannoolal (Thermodynamic Research Unit, University of Natal). The dipole moments were calculated using molecular mechanics (by the simulation package CS Chem3D Ultra v6.0, CambridgeSoft.com). Hayden and O' Connell (1975) suggest that the mean radius of gyration can be estimated from the Parachor if values are not available (Chapter 3). The estimated parameters are given in Table B-1.

Table B-1: Physical properties of 2,3-pentanedione, diacetyl, methanol and acetone as required for the thermodynamic treatment of the VLE measurements

	2,3-Pentanedione	Diacetyl	Methanol	Acetone
Pc /[bar]	40.07	45.9	80.9	47
Tc /[K]	616.6	536.1	512.6	508.1
Vc /[cm^3 /mol]	315.38	271.5	118	209
R_D /[Å]	3.5665	3.184	1.536	2.74
μ_D /[debye]	0.122	0.011	1.7	2.9

APPENDIX C

CALIBRATION OF GAS CHROMATOGRAPH DETECTOR RESPONSE

The procedure used to calibrate the gas chromatograph detector is described in Chapter 6 and the GC specifications and operating conditions are given in Figure 6-1. The results are presented in Figures C-1 to C-8.

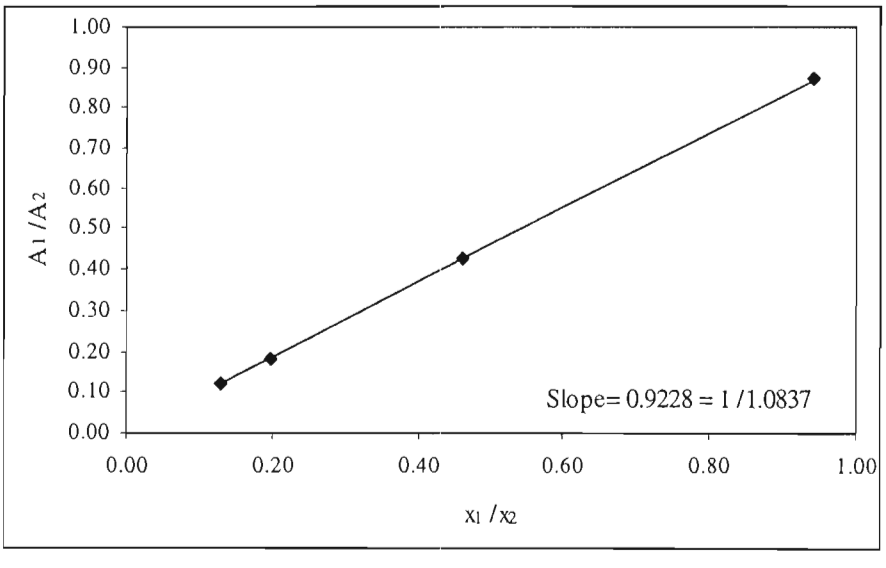

Figure C-1: Calibration of GC detector response for acetone(1) with diacetyl(2)

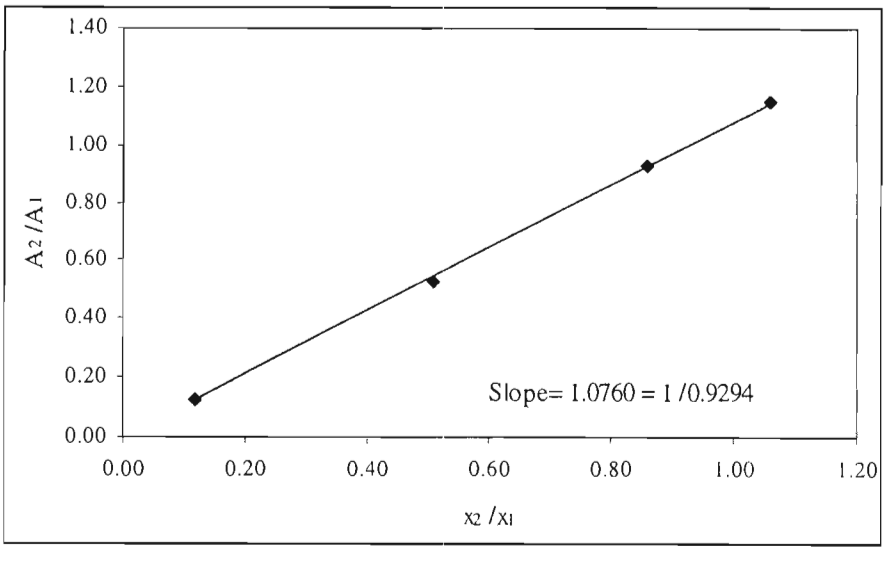

Figure C-2: Calibration of GC detector response for acetone(1) with diacetyl(2)

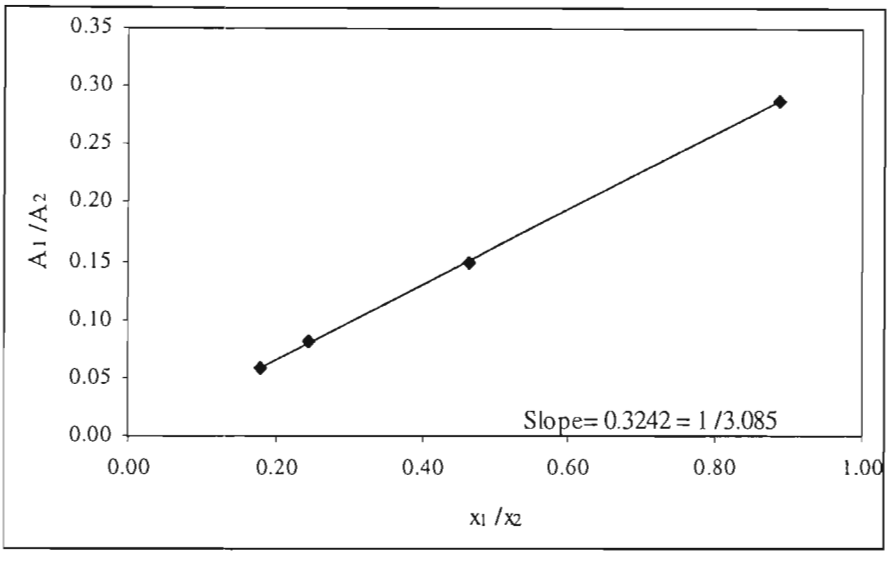

Figure C-3: Calibration of GC detector response for methanol(1) with diacetyl(2)

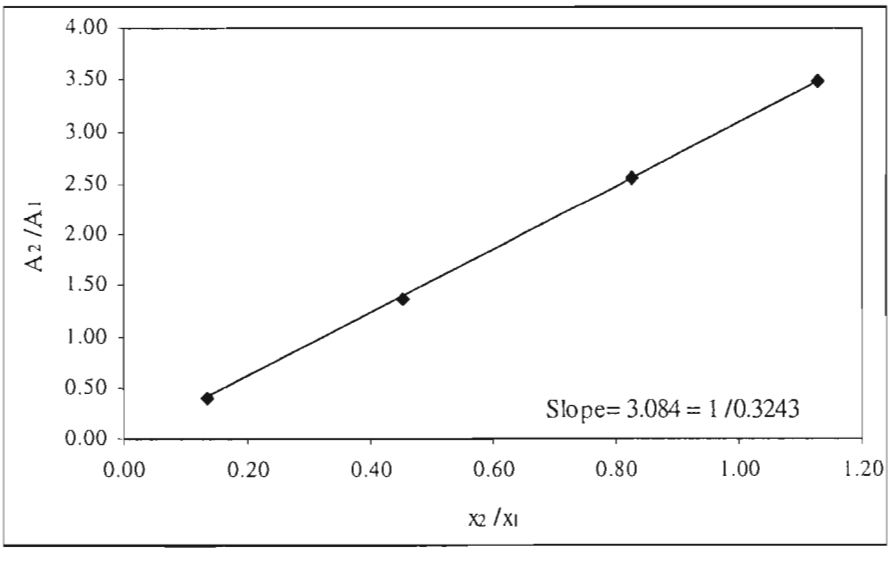

Figure C-4: Calibration of GC detector response for methanol(1) with diacetyl(2)

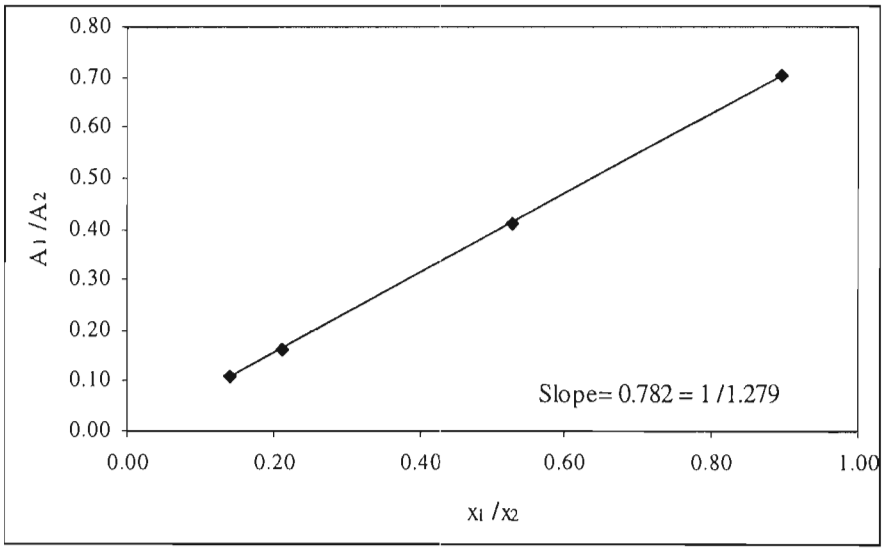

Figure C-5: Calibration of GC detector response for acetone(1) with 2,3-pentanedione(2)

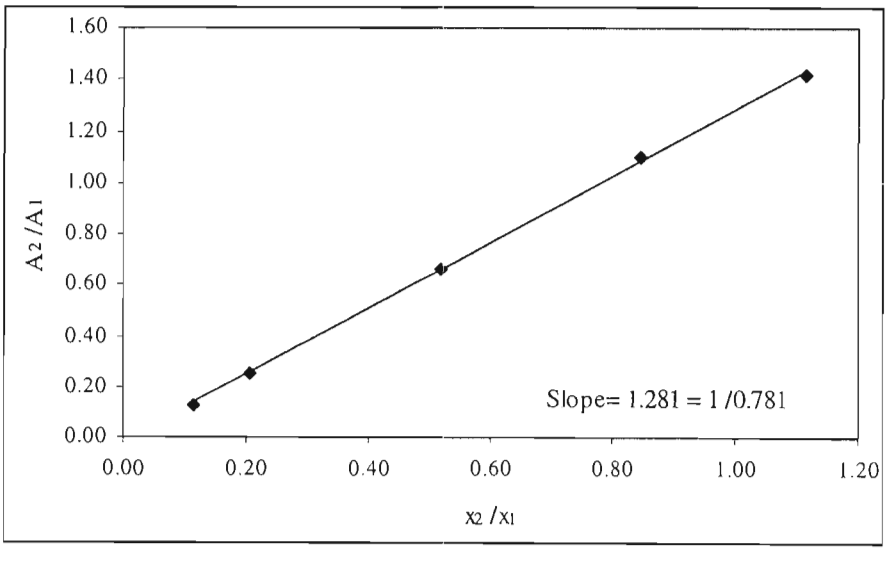

Figure C-6: Calibration of GC detector response for acetone(1) with 2,3-pentanedione(2)

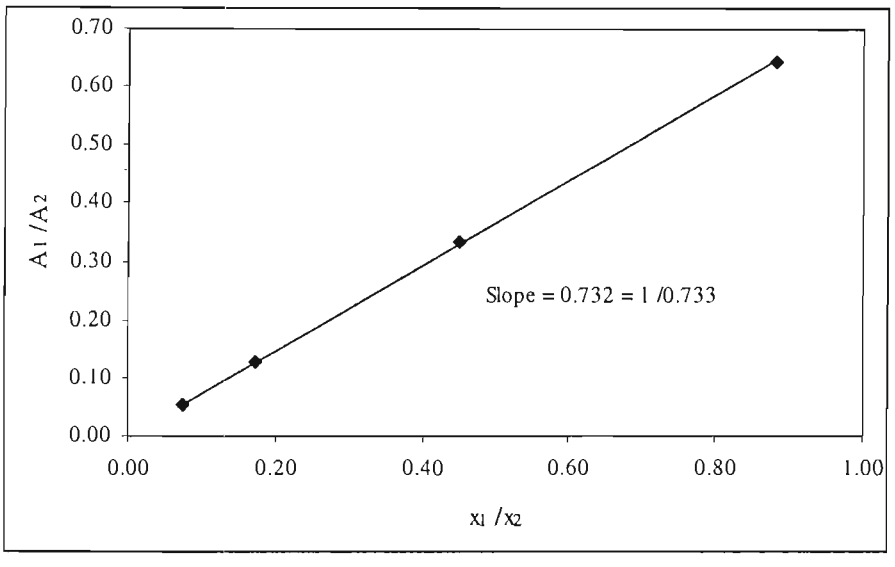

Figure C-7: Calibration of GC detector response for diacetyl(1) with 2,3-pentanedione(2)

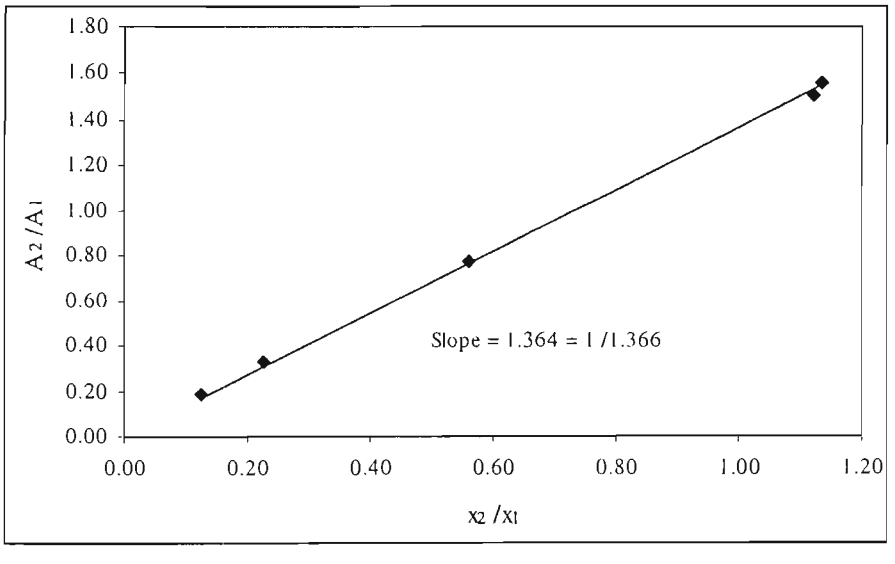

Figure C-8: Calibration of GC detector response for diacetyl(1) with 2,3-pentanedione(2)

APPENDIX D

MASS TRANSFER CONSIDERATIONS IN THE GAS STRIPPING CELL

Effective gas-liquid contact is essential for accurate results when using the inert gas stripping technique. The inert gas is introduced at the bottom of the cell and allowed to bubble through the liquid mixture. Figure D-1 shows a typical bubble rising through the bulk liquid. The process of solute stripping is essentially:

1. Mass transfer of the solute from the bulk liquid into the two-phase region surrounding the gas bubble.
2. Transfer of the solute into the gas bubble, which is a diffusion process.

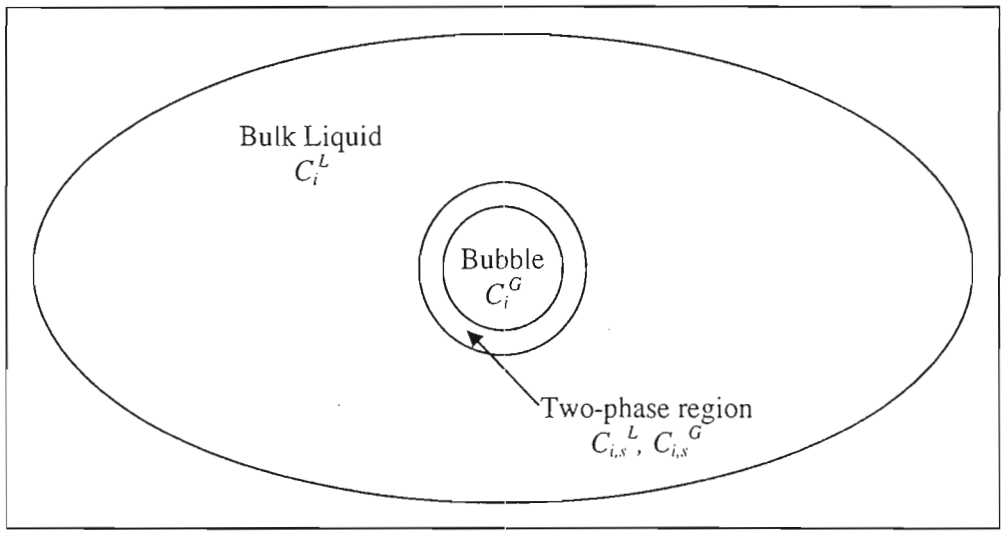

Figure D-1: A typical bubble rising through the liquid in the dilutor cell

Richon et al. (1980) developed the above model in order to calculate the optimal cell height. The development was subject to the following assumptions:

- The diffusion of solute into the bubble is very quick.
- Vapour-liquid equilibrium exists in the two phase region and is described by the modified Raoult's Law.
- Bubbles are perfectly spherical.
- The stripping gas is insoluble in the solvent.

It is difficult to justify the assumption of fast diffusion of the solute into the bubble at this stage. Its validity will, however, be tested.

D.1 Solute mass transfer to the bubble

Performing the solute material balance:

$$Accumulation = Input - Output$$

$$\frac{dn_i}{dt} = 4\pi R_b^2 k_L \left(C_i^L - C_{i,s}^L\right) \tag{D-1}$$

Since

$$C_{i,s}^L = x_i \frac{\rho^L}{M^L} \text{ and } C_{i,s}^G = y_i \frac{\rho^G}{M^G}$$

$$C_{i,s}^L = \frac{x_i}{y_i} \frac{\rho^L}{M^L} \frac{M^G}{\rho^G} C_{i,s}^G \tag{D-2}$$

The modified Raoult's Law (Eq. 3-79) as applied to the solute in infinite dilution:

$$x_i \gamma_i^{\infty} P_i^{sat} = y_i P$$

Therefore Eq. D-2 becomes:

$$C_{i,s}^L = \frac{P}{\gamma_i^{\infty} P_i^{sat}} \frac{\rho^L}{M^L} \frac{M^G}{\rho^G} C_{i,s}^G \tag{D-3}$$

The number of moles transferred from the liquid phase at any given time is:

$$n_i = x_i n_{tot} = C_i^G \frac{M^G}{\rho^G} \frac{PV_b}{RT} \tag{D-4}$$

Taking the derivative of Eq. D-4:

$$\frac{dn_i}{dt} = \frac{M^G}{\rho^G}\frac{PV_b}{RT}\frac{dC_i^G}{dt} \tag{D-5}$$

Since the diffusion into the bubble is fast:

$$C_{i,s}^G(t) = C_i^G(t) \tag{D-6}$$

Combining Eqs. D-1, D-3, D-5 and D-6

$$\frac{dC_{i,s}^G}{\left(C_i^L - AC_{i,s}^G\right)} = \frac{3}{R_b}k_L\frac{\rho^G}{M^G}\frac{RT}{P}dt \tag{D-7}$$

Integration of 7 between 0 and $C_i^G(t)$ and replacing t with $\frac{h}{u^\infty}$

$$\frac{AC_i^G(t)}{C_i^L} = 1 - \exp\left(-\frac{3}{R_b}\frac{\rho^L}{M^L}k_L\frac{RT}{\gamma_i^\infty P_i^{sat}}\frac{h}{u^\infty}\right) = \tau_L \tag{D-8}$$

$\tau_L = \frac{C_{i,s}^L}{C_i^L} \rightarrow 1$ at equilibrium. Thus Eq. D-8 can be used to calculate the appropriate path length for a bubble rising through the liquid and therefore the cell height (Richon et al., 1980). It also allows one to judge the sensitivity of the approach for equilibrium to variables such as bubble size. These will be discussed shortly.

Eq. D-8 is only valid if the assumption that diffusion of the solute into the bubble is quick, is true. To test this assumption a similar relationship to Eq. D-8 was formulated for diffusion into the bubble.

D.1.1 Bubble rise velocity

The following equation given in Richon et al. (1980) was used to calculate the bubble rise velocity (u^∞):

$$\left(u^{\infty}\right)^{1.4} = 7.2\times10^{-2}\eta_L^{-0.6}d_b^{1.6}g \tag{D-9}$$

Perry and Green (1998) suggest that Stokes law may be applied to small spherical bubbles rising through a fluid. Stokes law was also used in this study and the results for u^{∞} were found to be similar to those when Eq. D-9 was used.

D.1.2 Mass transfer coefficient

The mass transfer coefficient (k_L) was evaluated from the correlation of Cheh and Tobias (1968) which may be applied to bubbles rising steadily through a liquid. The correlation may be written as:

$$Nu = \sqrt{\frac{3}{4\pi}} IPe^{\frac{1}{2}}$$

Therefore:

$$k_L = \sqrt{\frac{3}{4\pi}} Iu^{\infty}\left(\frac{D_{ij}^L}{d_b}\right)^{\frac{1}{2}} \tag{D-10}$$

Where:

$$I = \int_0^{\pi} \frac{F(\theta)}{\left[\int F(\theta)d\theta - \left(\int F(\theta)d\theta\right)_{\theta=0}\right]^{\frac{1}{2}}} d\theta \tag{D-11}$$

$$\text{and } F = \sin^3\theta\left[1 - \frac{8}{3}\sqrt{\frac{1}{\pi\,\mathrm{Re}}}\Phi\cos ec^2\theta(1-\cos\theta)(2+\cos\theta)^{\frac{1}{2}}\right] \tag{D-12}$$

$$\text{where } \Phi \equiv \frac{1+\frac{3}{2}\frac{\mu_i}{\mu_0}}{\left(1+\frac{\rho_i\eta_i}{\rho_o\eta_o}\right)^{\frac{1}{2}}}$$

$$\text{and } \mathrm{Re} = \frac{d_b u^{\infty} \rho_L}{\eta_L}$$

Substituting Eq. D-12 into Eq. D-11:

$$I = \int_0^{\pi} \frac{\sin^3\theta\left[1-\alpha\cos ec^2\theta(1-\cos\theta)(2+\cos\theta)^{\frac{1}{2}}\right]}{\frac{1}{3}\sin^2\theta\cos\theta - \frac{3}{2}\cos\theta + 2\alpha(2+\cos\theta)^{\frac{3}{2}} - \frac{2}{5}\alpha(2+\cos\theta)^{\frac{5}{2}} - \frac{3}{2} + \frac{12}{5}\sqrt{3}} d\theta \quad \text{(D-13)}$$

Where

$$\alpha = \frac{8}{3}\sqrt{\frac{1}{\pi\,\mathrm{Re}}}\Phi$$

I was evaluated numerically using the trapezoidal method for integration and k_L was, therefore, calculated from Eq. D-10 once the liquid diffusion coefficient (D_{ij}^{L}) is evaluated (discussed shortly).

D.1.2.1 Liquid diffusion coefficient (D_{ij}^{L})

Reid et al. (1988) present many methods for estimating the liquid diffusion coefficient. The Wilke and Chang (1955) method is an older method but applies to dilute solutions. The method is an empirical modification to the Stokes-Einstein equation formulated for large spherical particles diffusing in a dilute solution. The values for D_{ij}^{L} required for calculating k_L were therefore estimated by this method.

$$D_{ij}^{L} = \frac{7.4\times10^{-8}(\phi M_j T)}{\eta_j V_i^{0.6}} \quad \text{(D-14)}$$

$\phi = 1$ for non-associating compounds

$\phi = 2.6$ for H_2O

$\phi = 1.9$ for methanol

$\phi = 1.5$ for ethanol

and V_i is the molar volume of the solute at its normal boiling temperature.

D.1.3 Liquid density (ρ_L)

The liquid density was estimated using Eq. 3-41, the Rackett equation (Smith et al., 1998) as discussed in the VLE data regression section. The liquid molar volumes are readily converted to densities. Liquid molar volumes may also be calculated from cubic equations of state (discussed in Chapter 3).

D.1.4 Vapour and gas density (ρ_V and ρ_G)

Both the vapour and gas densities were estimated using the Redlich Kwong equation of state (Eq. 3-58) (Smith et al., 1998):

$$V - b = \frac{RT}{P} - \frac{a(V-b)}{T^{\frac{1}{2}} PV(V+b)}$$

The solution to Eq. 3-58 for V (molar volume) is iterative and initial guesses for its value were calculated from the ideal gas law. Once again the molar volumes may readily be converted to densities. The ideal gas law will have suited the purpose of this study (as the measurements are made at moderate pressures), however a cubic equation of state allows for greater generality (e.g. extension to measurements at higher pressure).

D.1.5 Liquid viscosity (η_L)

Reid et al. (1988) list three methods for estimating liquid viscosity, viz. the methods of:

- Orrick and Erbar
- Van Velzen, Cardozo and Langenkamp
- Przezdziecki and Sridhar

Reid et al. (1988) also present a comparison of the three methods for various chemicals. The Van Velzen, Cardozo and Langenkamp method yielded the lowest percentage error for acetone and was used in this study. The basic equation is:

$$\log \eta_L = B\left(T^{-1} - T_a^{-1}\right) \qquad \text{(D-15)}$$

Eq. D-15 gives the viscosity in *cP* and T_0 is a parameter obtained through group contributions. The reader is referred to Reid et al. (1988) for tables for these group contributions.

D.1.6 Vapour and gas viscosity (η_V and η_V)

Reid et al. (1988) list three methods for estimating low pressure gas viscosity, viz. the methods of:

- Chung et al.
- Lucas
- Reichenberg

Reid et al. (1988) state that any of the above mentioned methods can be expected to yield results with errors of 0.5% to 1.5% for non-polar chemicals. Both the Reichenberg method and that of Chung et al. require data that may not be readily available. The disadvantage of the Lucas method is that it is not suitable for highly associating compounds such as organic acids. As those compounds are outside the scope of this study it was decided to use the Lucas method. The equations are:

$$\eta\xi = \left[0.807T_r^{0.618} - 0.357\exp(-0.449T_r) + 0.34\exp(-4.058T_r) + 0.018\right]F_P^0 F_Q^0 \qquad \text{(D-16)}$$

Where

$$\xi = 0.176\left(\frac{T_c}{M^3 P_c^4}\right)^{\frac{1}{6}}$$

$$F_P^0 = 1 \qquad 0 \le \mu_r \le 0.022$$

$$F_P^0 = 1 + 30.55(0.292 - Z_c)^{1.72} \qquad 0.022 \le \mu_r \le 0.075$$

$$F_P^0 = 1 + 30.55(0.292 - Z_c)^{1.72}\left|0.96 + 0.1(T_r - 0.7)\right| \qquad \mu_r \ge 0.075$$

The reduced dipole moment $\mu_r = 52.46\dfrac{\mu^2 P_c^2}{T_c^2}$

$F_Q^0 = 1$ for all gases besides He, H_2 and D_2

$$F_Q^0 = 1.22Q^{0.15}\left\{1+0.00385\left[(T_r-12)^2\right]^{\frac{1}{M}} sign(T_r-12)\right\}$$

where Q(He) = 1.38, $Q(H_2)$ = 0.76 and $Q(D_2)$ = 0.52.

D.2 Solute Diffusion into the bubble

The approach used by Richon et al. (1980) to describe solute diffusion into the bubble is given here briefly. Crank (1956) gives the relationship for the solute concentration in a bubble assuming that there are no convective movements stirring the bubble:

$$C_i^G(r,t) = C_{i,s}^G\left[1+\frac{2R_b}{\pi r}\sum_{l=1}^{\infty}\frac{(-1)^l}{l}\sin\frac{l\pi r}{R_b}\exp\left(-\frac{D_{ij}^G l^2\pi^2 t}{R_b^2}\right)\right] \qquad \text{(D-17)}$$

In order to define a similar quantity to τ_L to judge the approach to equilibrium in the diffusion step we write the expression for the instantaneous mass of solute in the bubble:

$$G(t) = 4\pi M_i\int_0^{R_b} r^2 C_i^G(r,t)dr \qquad \text{(D-18)}$$

As $t\rightarrow\infty$, the system tends to equilibrium and:

$$C_i^G(r) = C_{i,s}^G \quad \text{for all } r$$

At equilibrium Eq. D-18 becomes:

$$G^{\infty} = \frac{4}{3}\pi R_b^3 M_i C_{i,s}^G$$

τ_G may now be defined to judge the approach to equilibrium:

$$\tau_G = \frac{G(t)}{G^{\infty}} = \frac{3}{R_b^3}\int_0^{R_b} r^2 C_i^G(r,t)dr \qquad \text{(D-19)}$$

Substituting Eq. D-17 into Eq. D-19 and performing the integration

$$\tau_G = 1 - \frac{6}{\pi^2}\sum_{l=1}^{\infty}\frac{1}{l^2}\exp\left(-\frac{D_{ij}^G l^2 \pi^2 h}{R_b^2 u^\infty}\right) \tag{D-20}$$

In order to evaluate Eqs. D-8 and D-20 it is necessary for certain quantities to be known, such as the physical property density. As the calculations were numerous it was decided to perform them using a computer program and making the code generic. The same program may then be applied to various chemical systems by changing certain parameters in the code. These parameters were calculated using recommended correlations such as those found in Reid et al. (1988). Each shall be discussed briefly in the following sections.

Strictly, these properties should be evaluated for a chemical mixture, vapour density for example should be evaluated for a mixture of both solute and solvent. The objective of this exercise is, however, to generate a qualitative illustration of the system behaviour and to gauge the sensitivity of the experiment to certain parameters. The sensitivity of the results is discussed in Chapter 7. The physical properties, density and viscosity, were calculated for the pure components only. This is a good estimate for the liquid phase properties. The "worst case" value was used for the vapour properties.

D.2.1 Vapour diffusion coefficient (D_{ij}^G)

The diffusion coefficient of the solute (i) in the gas (j) was estimated by the method of Slattery and Bird (1958) in the study by Richon et al. (1980). Reid et al. (1988) suggest that the method of Fuller be used as it yielded the smallest percentage results in their study. Atomic diffusion volumes are required for this estimation, which may be found in Reid et al. (1988). The diffusion coefficient is calculated from:

$$D_{ij}^G = \frac{0.00143T^{1.75}}{PM_{ij}^{\frac{1}{2}}\left[\left(\sum u\right)_i^{\frac{1}{3}} + \left(\sum u\right)_j^{\frac{1}{3}}\right]^2} \tag{D-21}$$

where

$M_{ij} = 2\left[\left(\frac{1}{M_i}\right) + \left(\frac{1}{M_j}\right)\right]^{-1}$ and $\left(\sum u\right)_i$, $\left(\sum u\right)_j$ are the atomic diffusion volumes.

APPENDIX E

RESULTS OF VAN NESS POINT TEST FOR THERMODYNAMIC CONSISTENCY OF VLE DATA

The point test of Van Ness and Abbott (1982), described in Chapter 3, is a thermodynamic consistency test. The vapour composition residuals (required to perform this test) are given in Figures E-1 to E-13 for all the measured VLE.

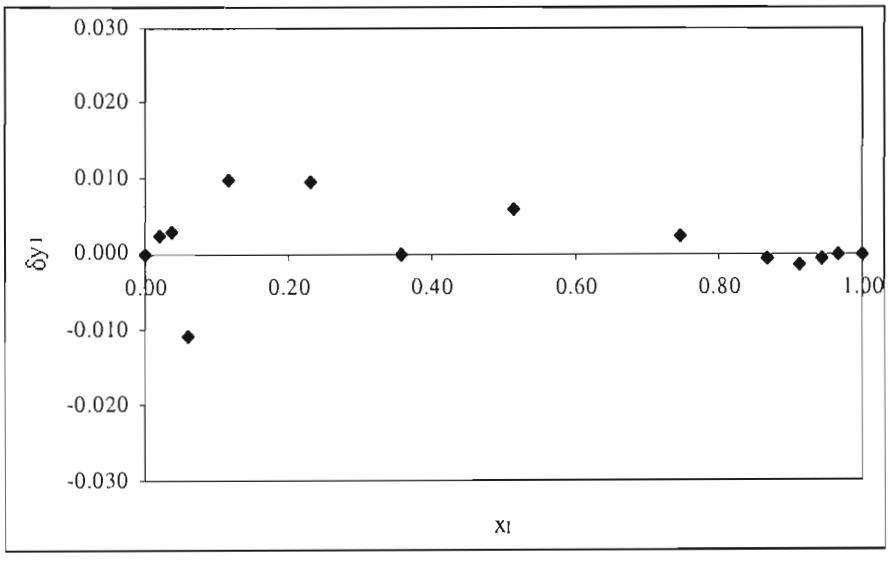

Figure E-1: Point test of consistency for acetone(1) with diacetyl(2) at 40°C

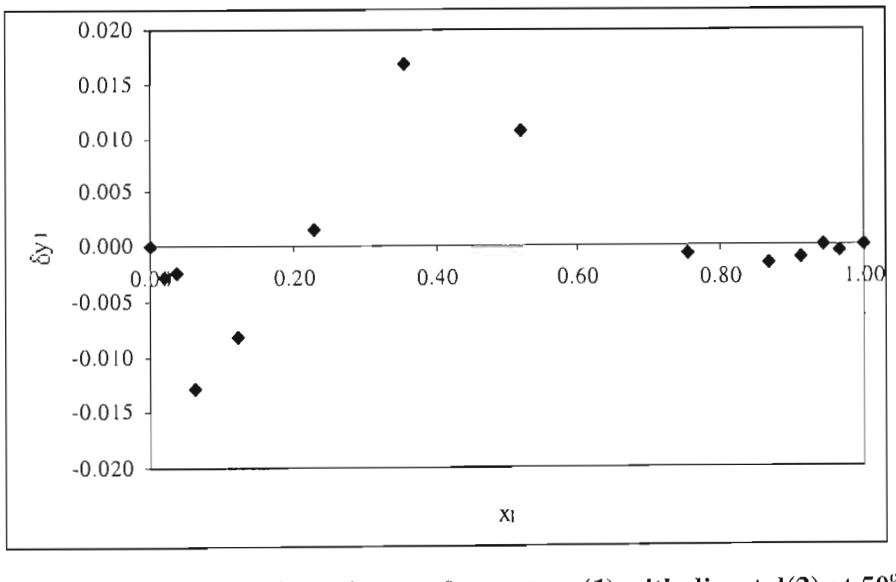

Figure E-2: Point test of consistency for acetone(1) with diacetyl(2) at 50°C

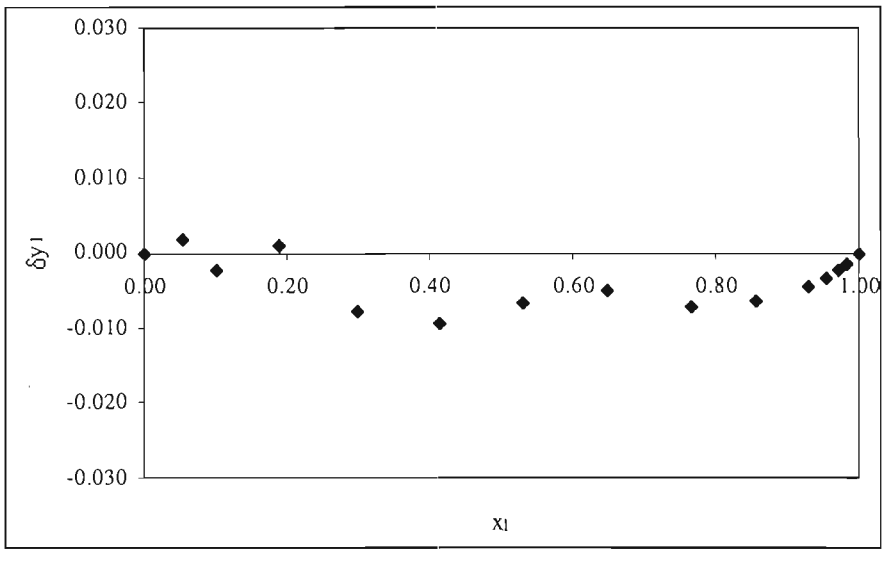

Figure E-3: Point test of consistency for acetone(1) with diacetyl(2) at 40kPa

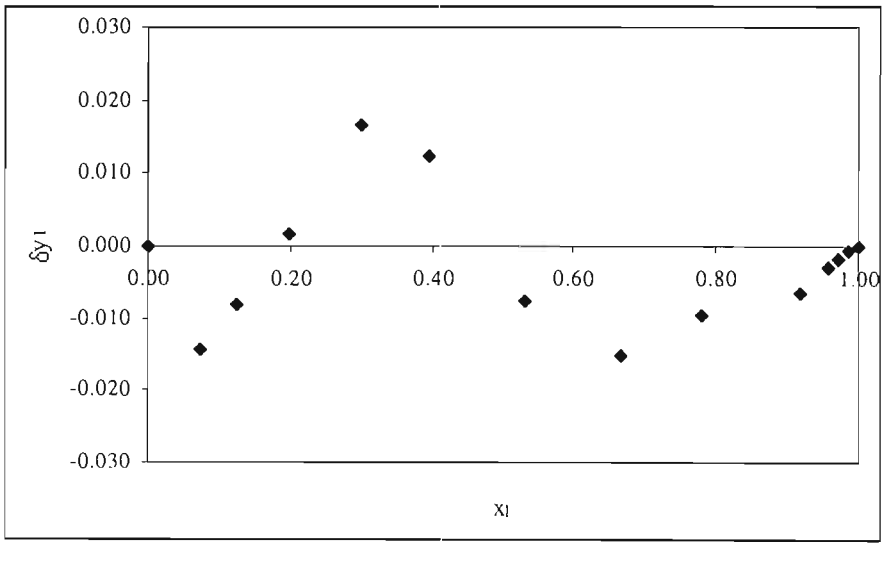

Figure E-4: Point test of consistency for methanol(1) with diacetyl(2) at 40°C

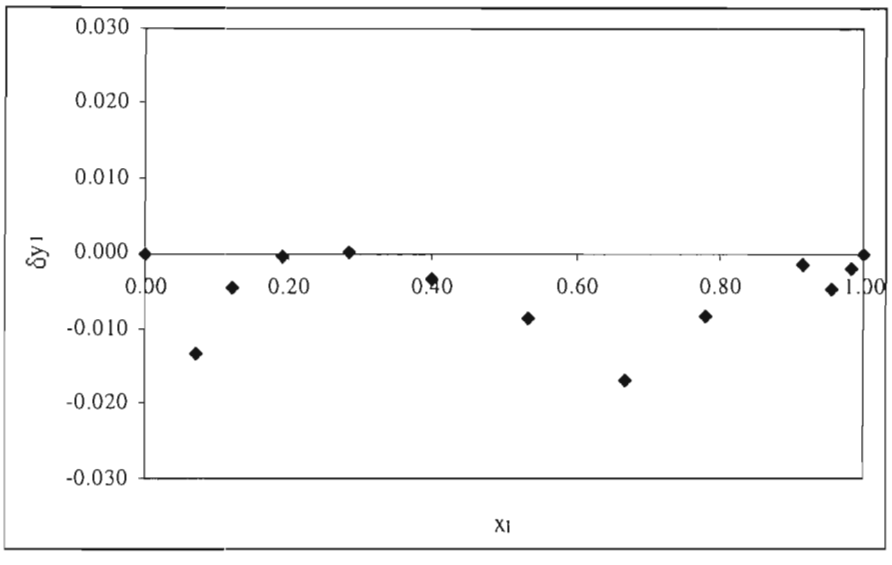

Figure E-5: Point test of consistency for methanol(1) with diacetyl(2) at 50°C

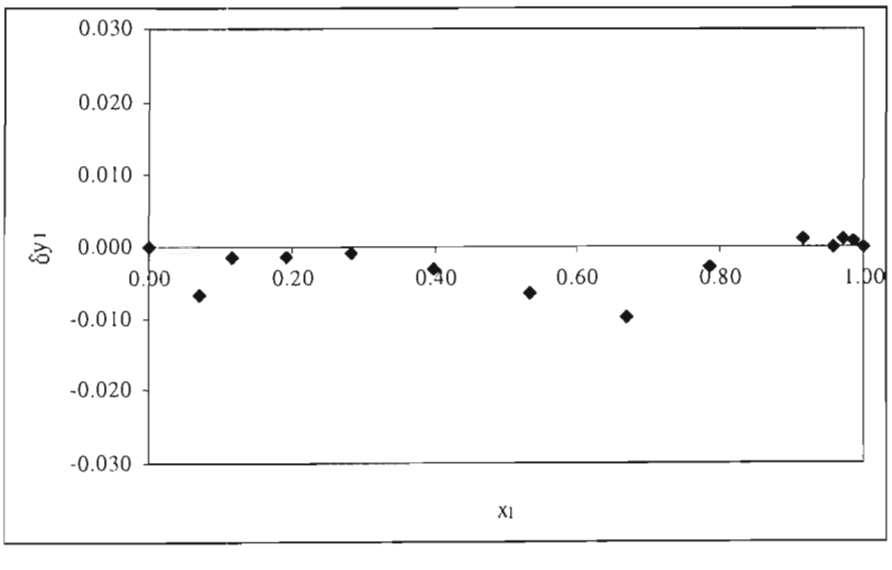

Figure E-6: Point test of consistency for methanol(1) with diacetyl(2) at 60°C

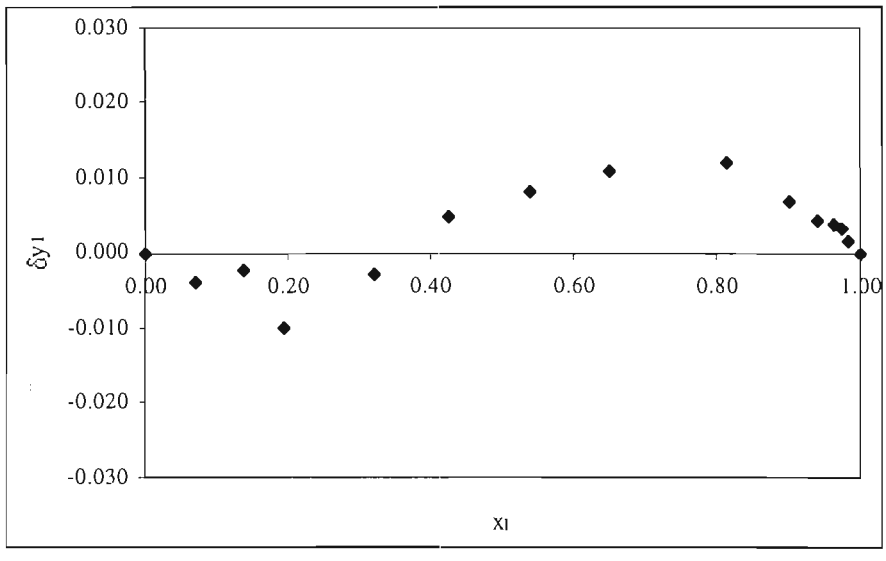

Figure E-7: Point test of consistency for methanol(1) with diacetyl(2) at 40kPa

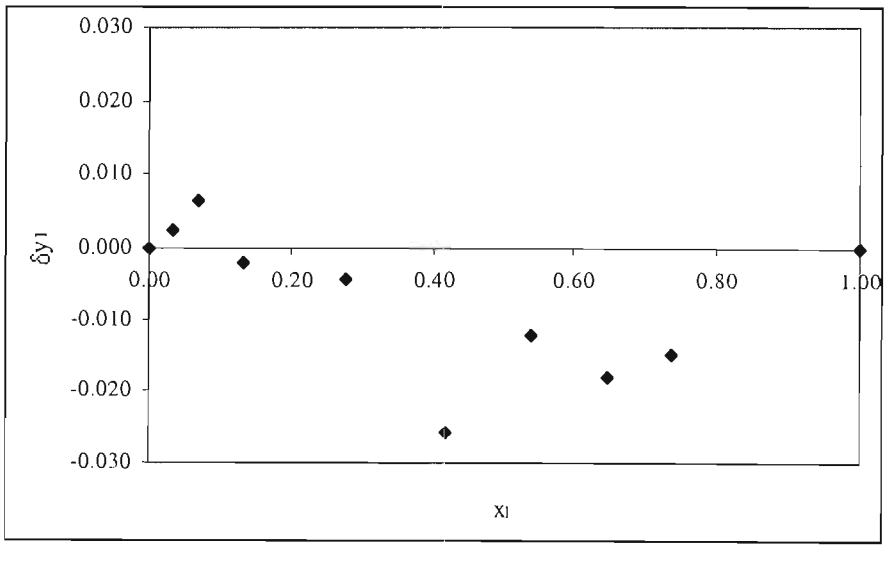

Figure E-8: Point test of consistency for diacetyl(1) with 2,3-pentanedione(2) at 60°C

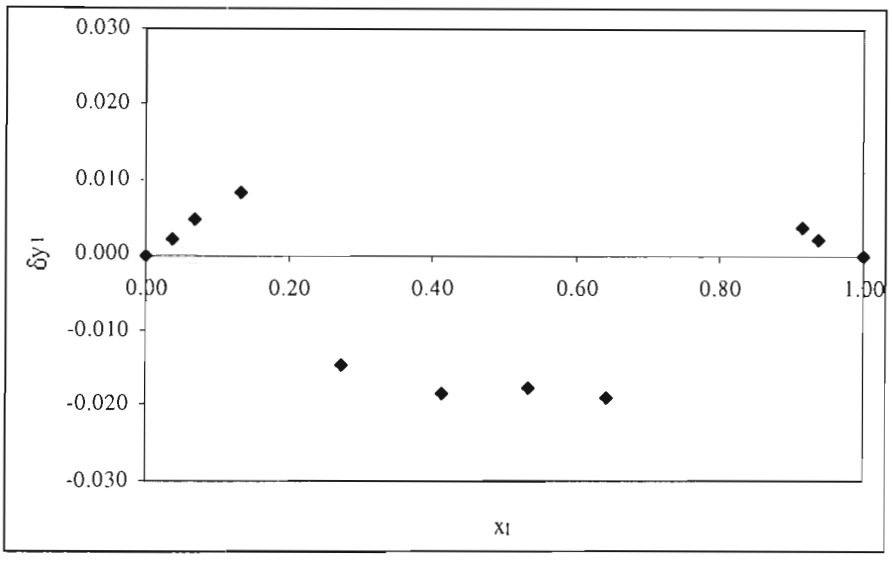

Figure E-9: Point test of consistency for diacetyl(1) with 2,3-pentanedione(2) at 70°C

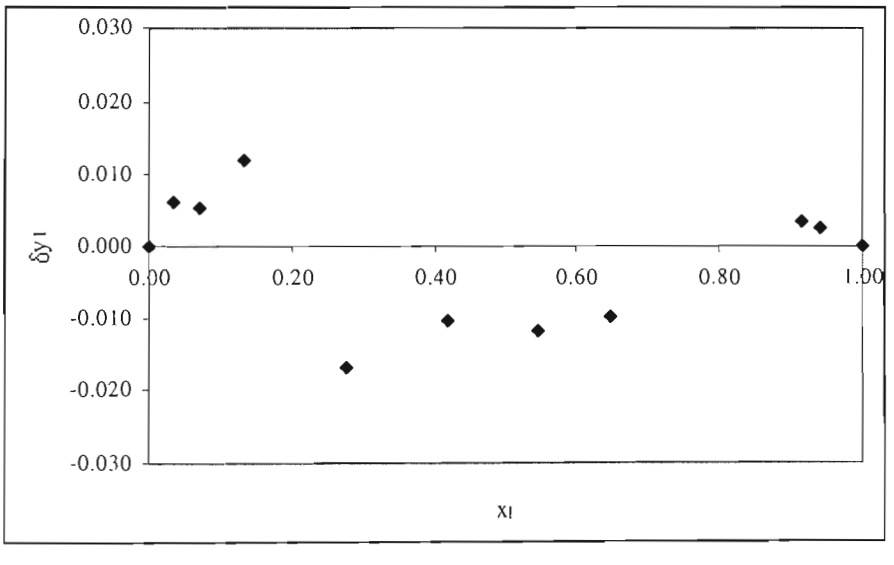

Figure E-10: Point test of consistency for diacetyl(1) with 2,3-pentanedione(2) at 80°C

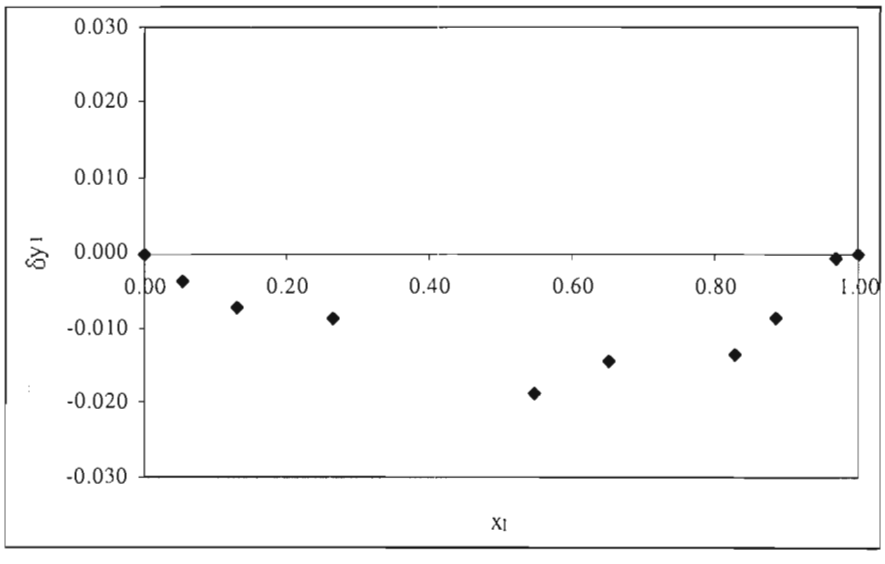

Figure E-11: Point test of consistency for diacetyl(1) with 2,3-pentanedione(2) at 40kPa

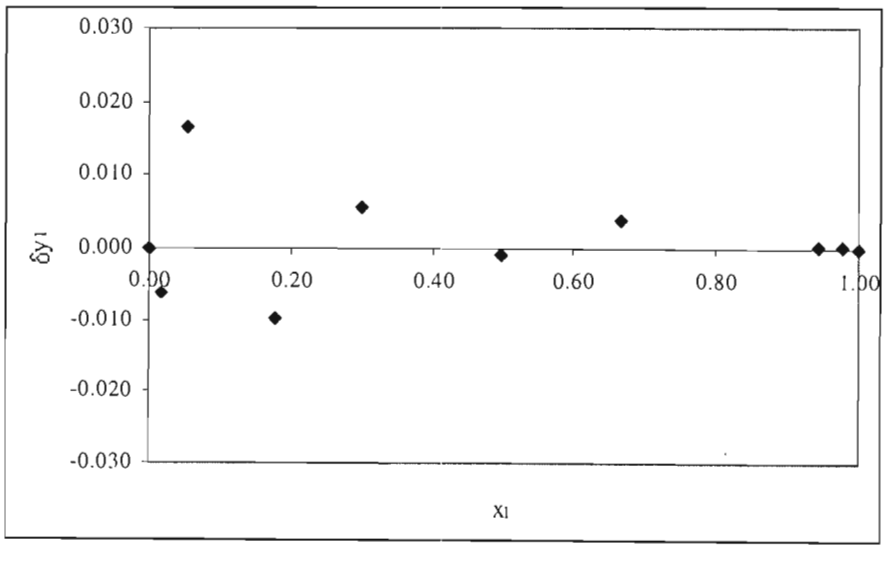

Figure E-12: Point test of consistency for acetone(1) with 2,3-pentanedione(2) at 50°C

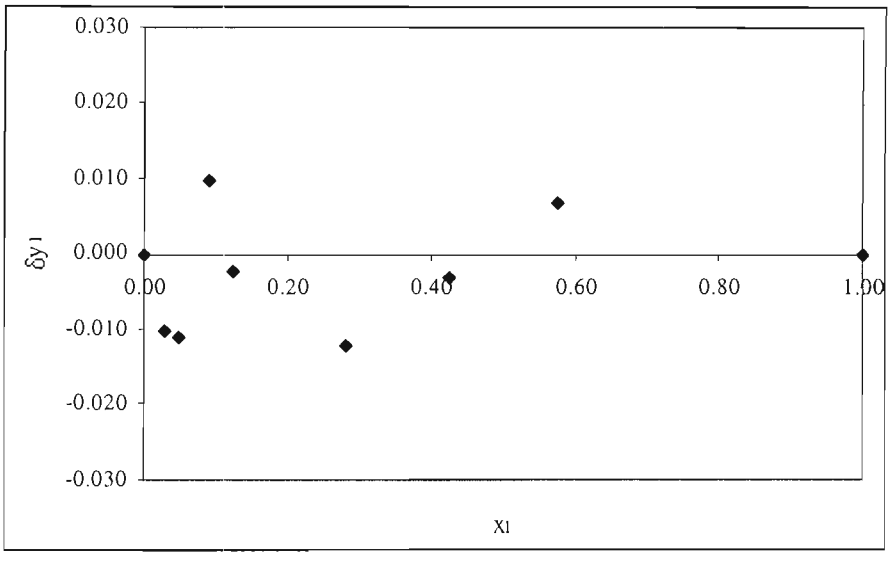

Figure E-13: Point test of consistency for acetone(1) with 2,3-pentanedione(2) at 30kPa

APPENDIX F

RESULTS OF VAN NESS DIRECT TEST FOR THERMODYNAMIC CONSISTENCY OF VLE DATA

The direct test of Van Ness (1995), described in Chapter 3, is a thermodynamic consistency test that directly measures the deviation of VLE data from the Gibbs-Duhem equation. The ratios of the activity coefficient residual (required to perform the test) are given in Figures F-1 to F-13 for all the measured VLE.

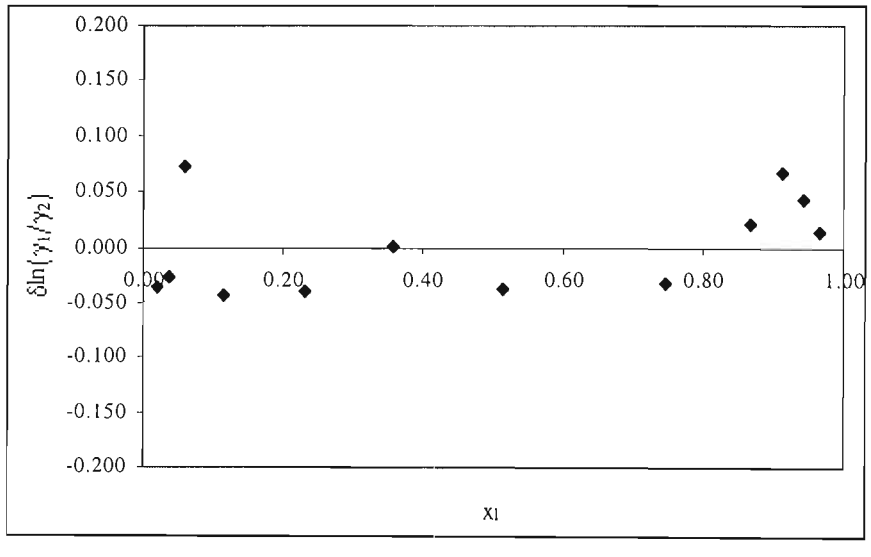

Figure F-1: Direct test of consistency for acetone(1) with diacetyl(2) at 40°C

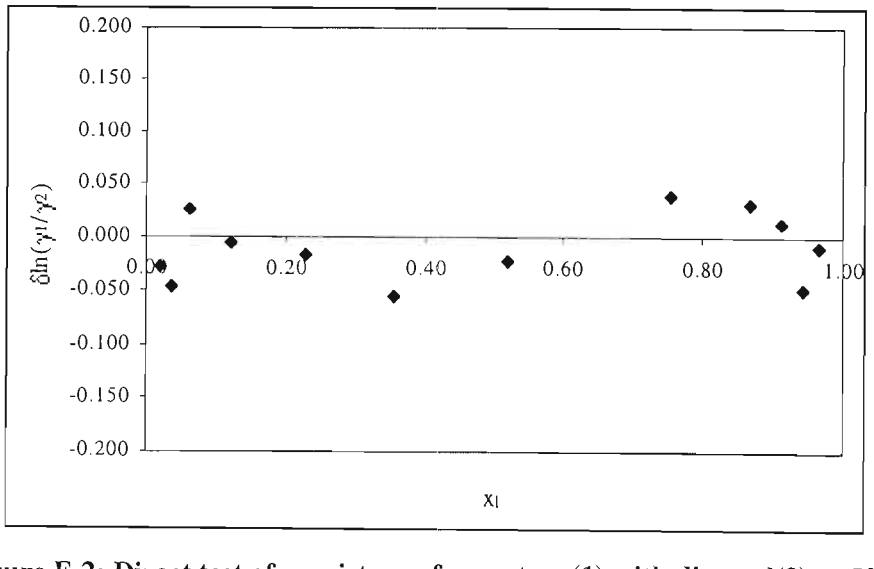

Figure F-2: Direct test of consistency for acetone(1) with diacetyl(2) at 50°C

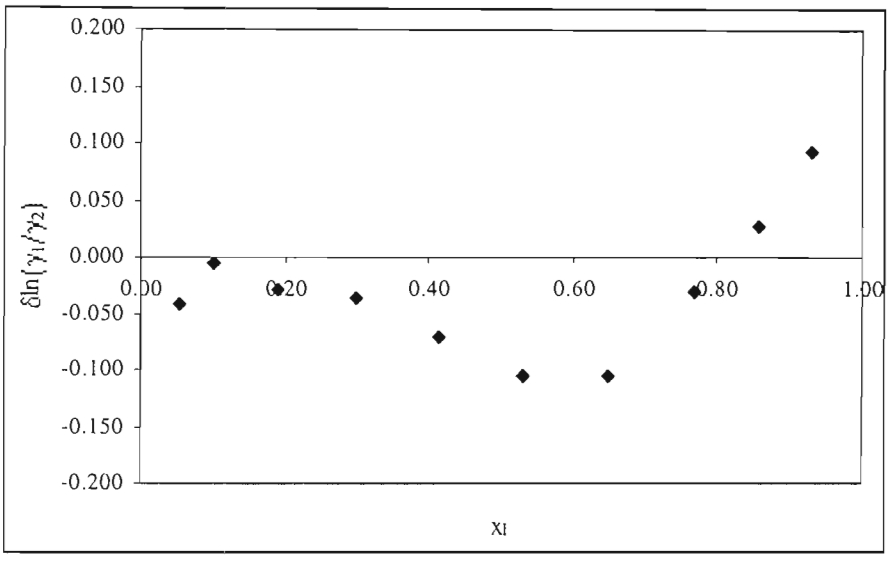

Figure F-3: Direct test of consistency for acetone(1) with diacetyl(2) at 40kPa

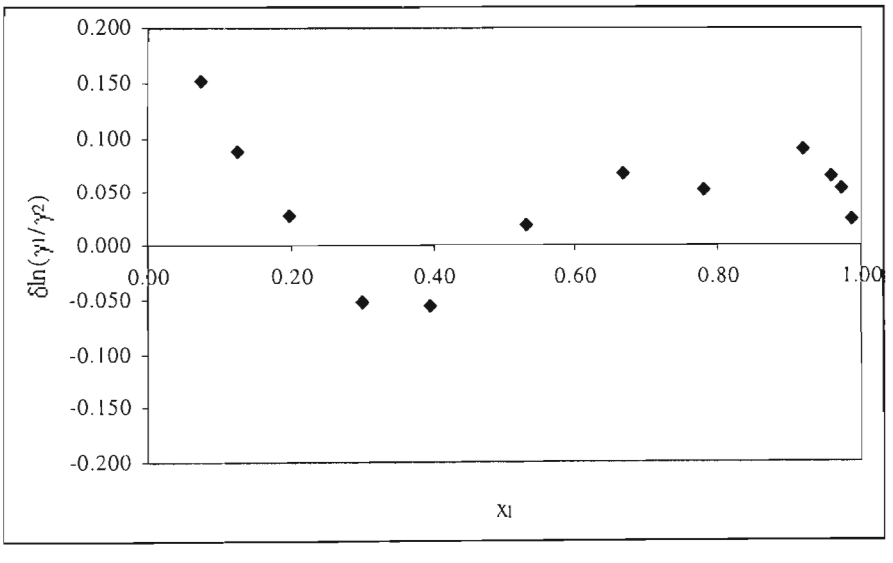

Figure F-4: Direct test of consistency for methanol(1) with diacetyl(2) at 40°C

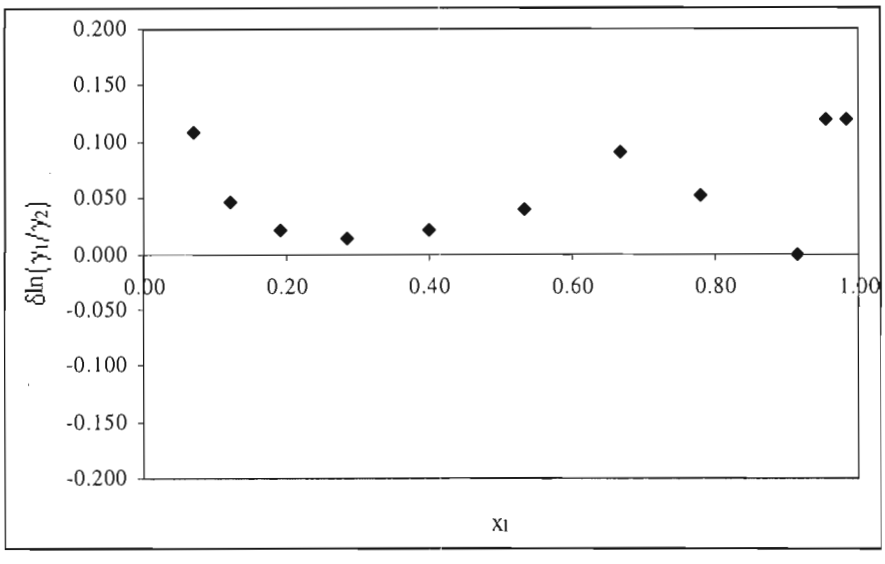

Figure F-5: Direct test of consistency for methanol(1) with diacetyl(2) at 50°C

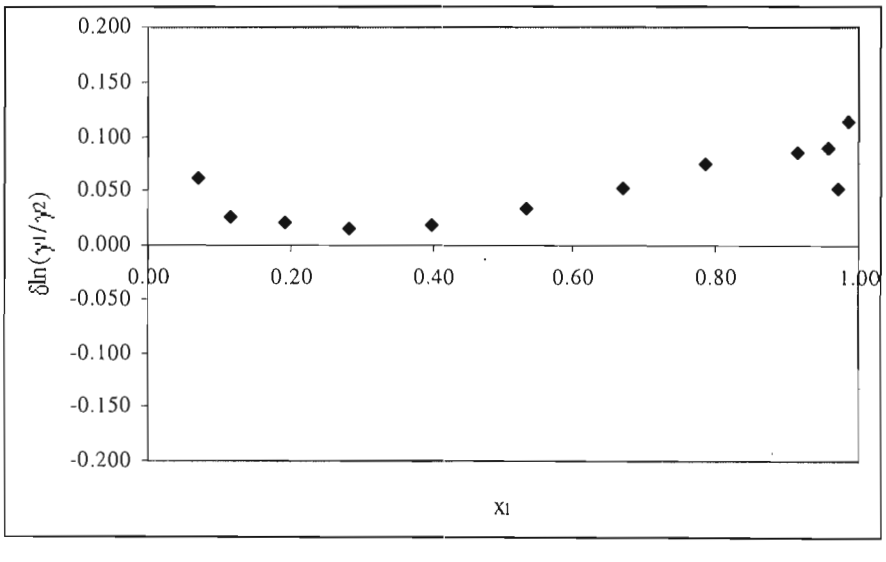

Figure F-6: Direct test of consistency for methanol(1) with diacetyl(2) at 60°C

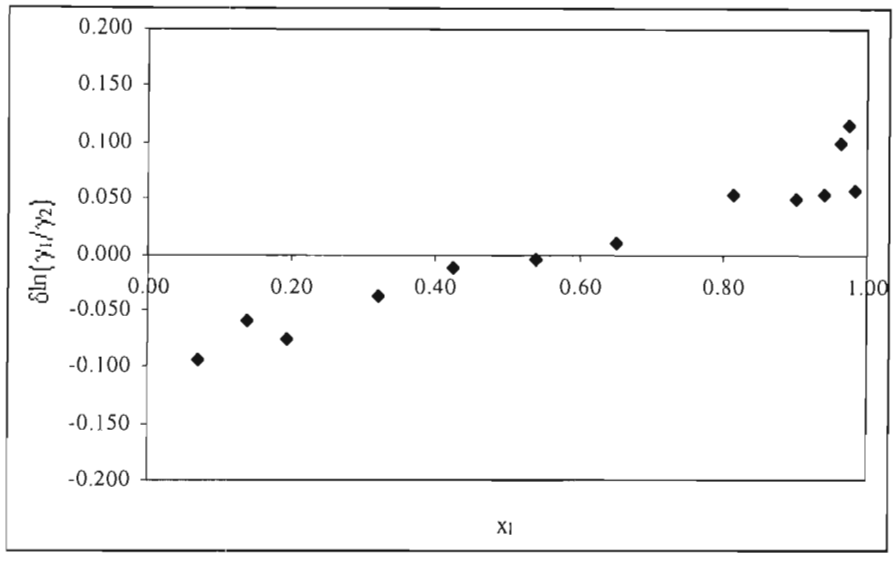

Figure F-7: Direct test of consistency for methanol(1) with diacetyl(2) at 40kPa

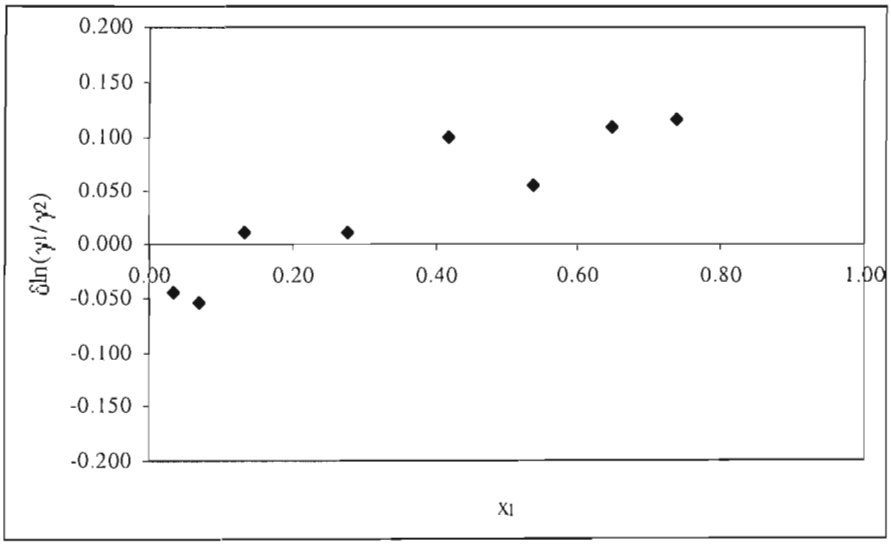

Figure F-8: Direct test of consistency for diacetyl(1) with 2,3-pentanedione(2) at 60°C

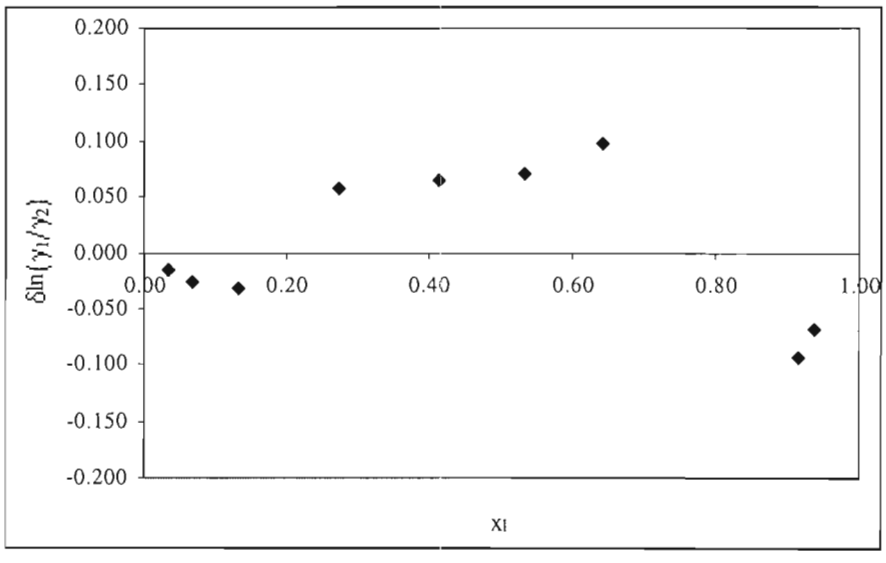

Figure F-9: Direct test of consistency for diacetyl(1) with 2,3-pentanedione(2) at 70°C

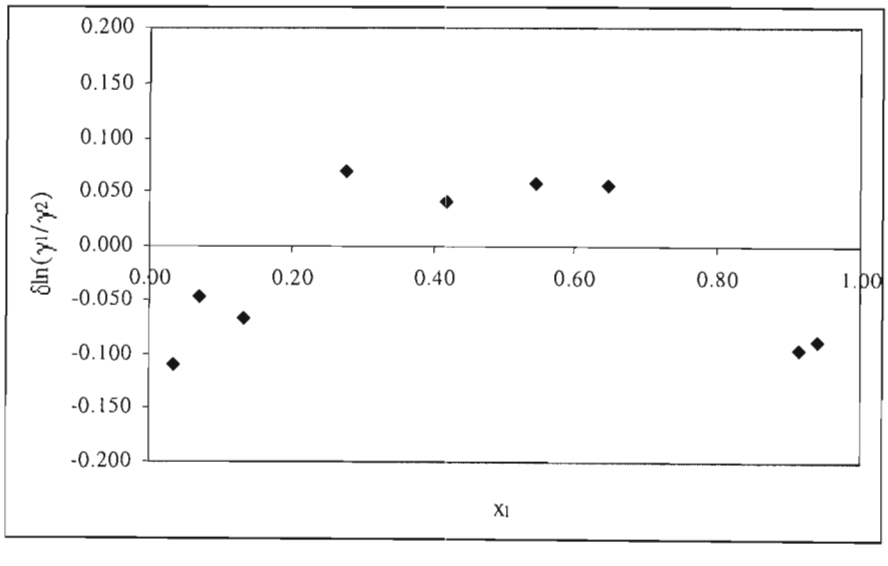

Figure F-10: Direct test of consistency for diacetyl(1) with 2,3-pentanedione(2) at 80°C

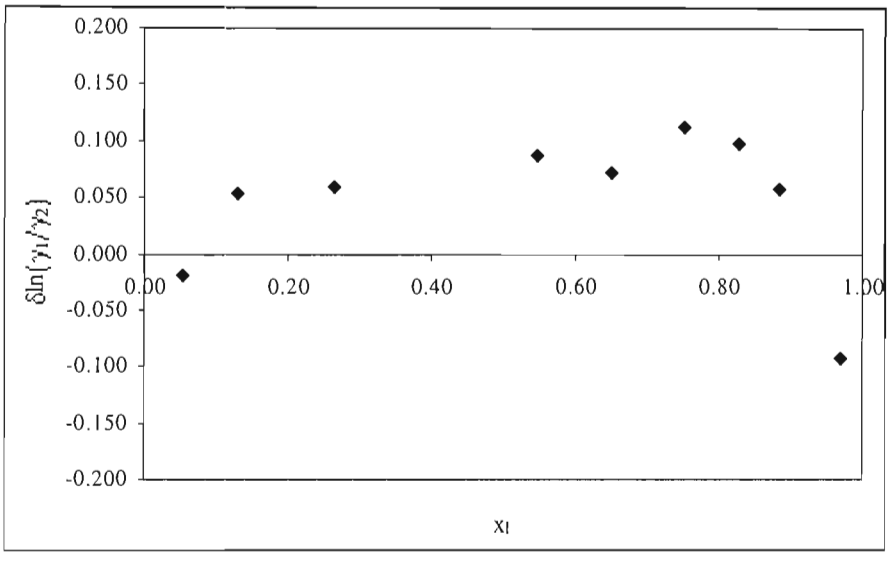

Figure F-11: Direct test of consistency for diacetyl(1) with 2,3-pentanedione(2) at 40kPa

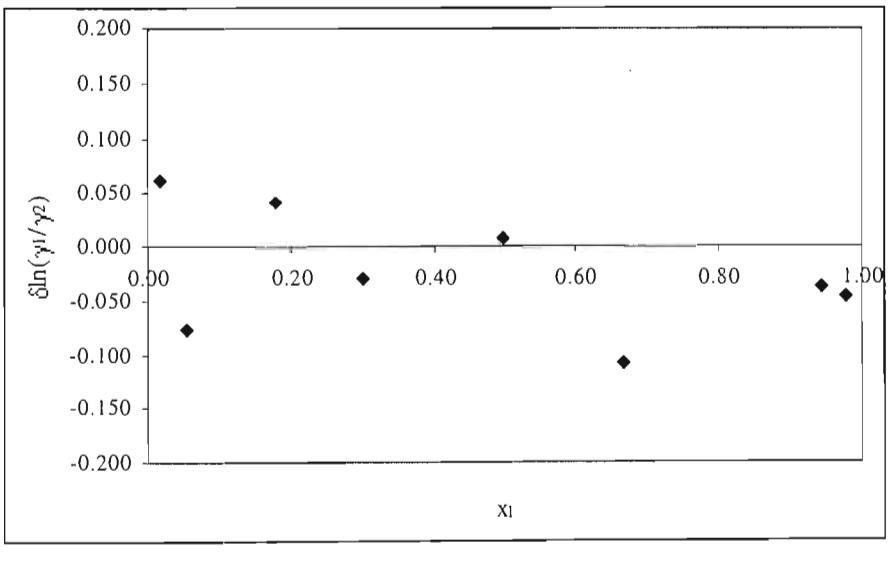

Figure F-12: Direct test of consistency for acetone(1) with 2,3-pentanedione(2) at 50°C

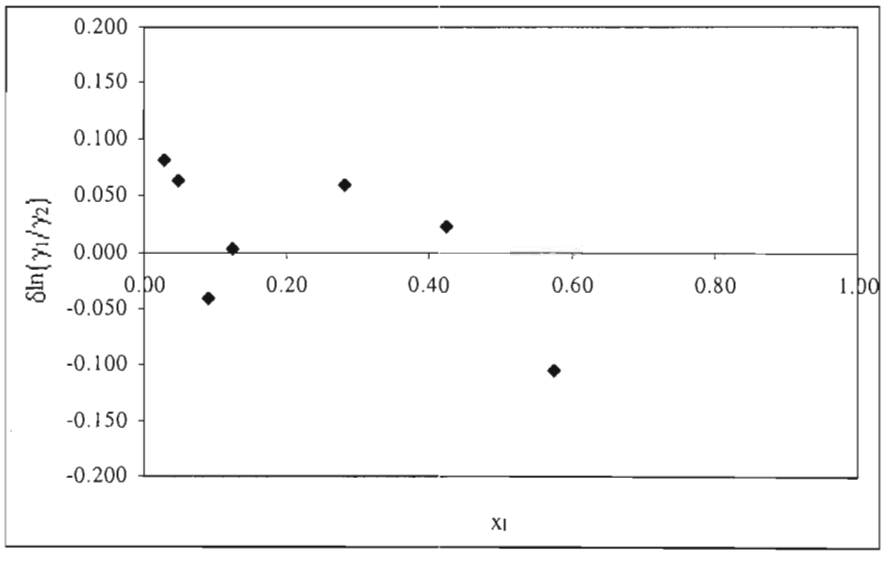

Figure F-13: Direct test of consistency for acetone(1) with 2,3-pentanedione(2) at 30kPa

APPENDIX G

GRAPHS USED TO CALCULATE THE INFINITE DILUTION ACTIVITY COEFFICIENTS

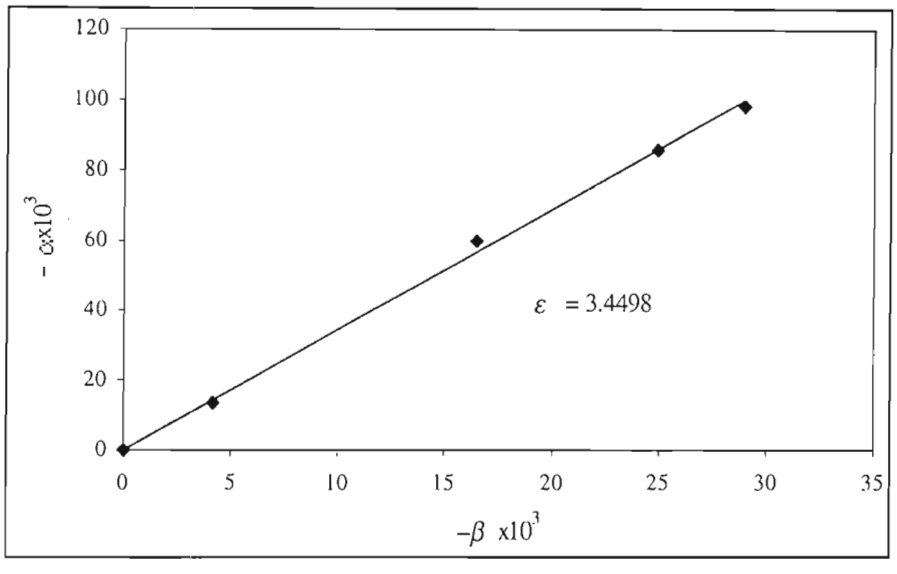

Figure G-1: Plot used to calculate the infinite dilution activity coefficient by the inert gas stripping method for acetone in diacetyl

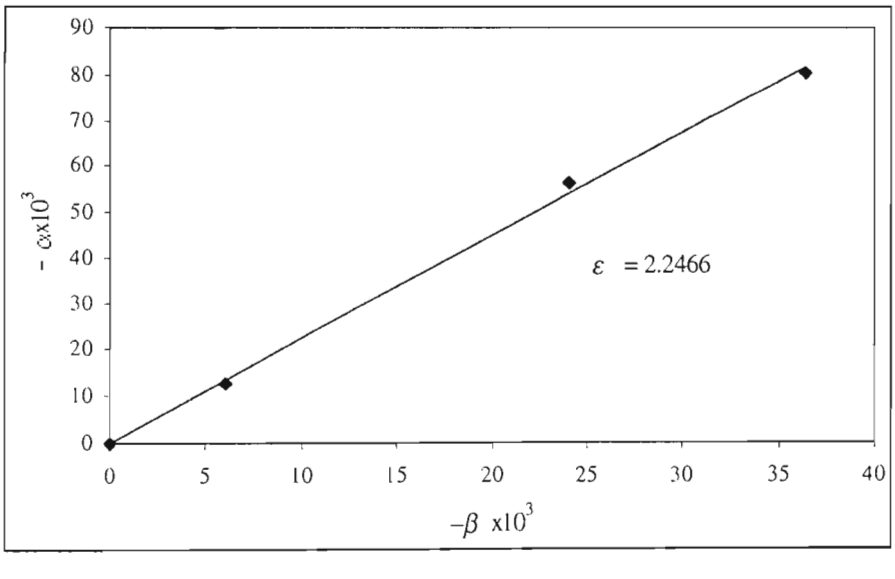

Figure G-2: Plot used to calculate the infinite dilution activity coefficient by the inert gas stripping method for methanol in diacetyl

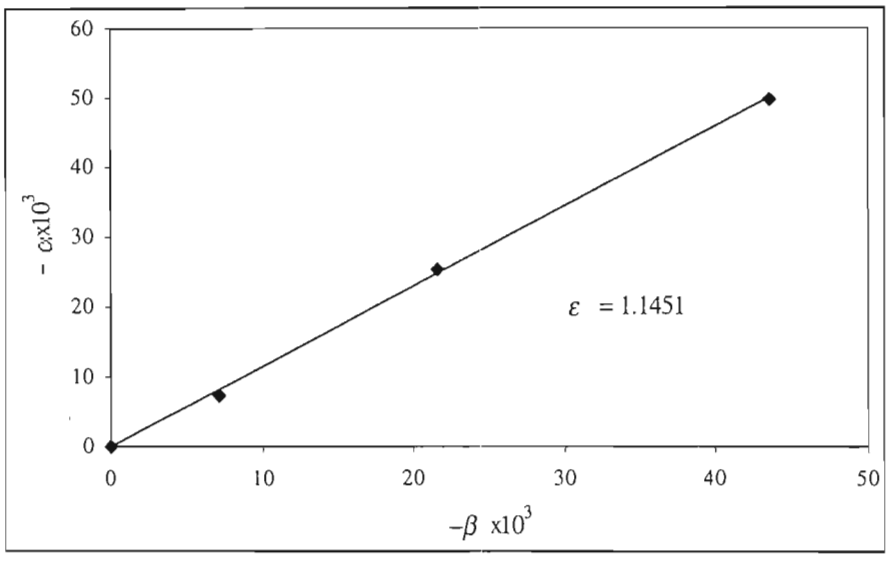

Figure G-3: Plot used to calculate the infinite dilution activity coefficient by the inert gas stripping method for diacetyl in 2,3-pentanedione

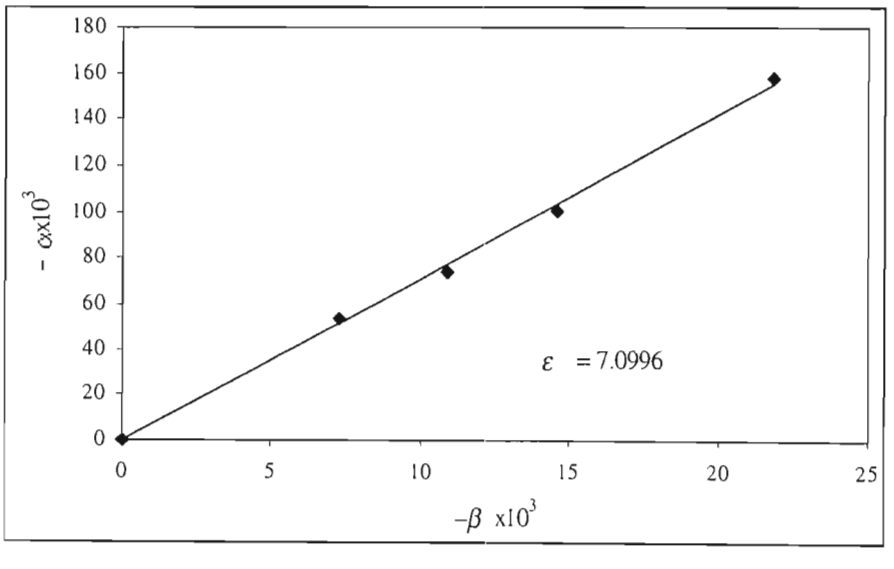

Figure G-4: Plot used to calculate the infinite dilution activity coefficient by the inert gas stripping method for acetone in 2,3-pentanedione